

Doctoral thesis

Doctoral theses at NTNU, 2021:16

Jelena Živković

Ductility and brittleness of lightweight aggregate concrete structures

NTNU
Norwegian University of Science and Technology
Thesis for the Degree of
Philosophiae Doctor
Faculty of Engineering
Department of Structural Engineering



Norwegian University of
Science and Technology

Jelena Živković

Ductility and brittleness of lightweight aggregate concrete structures

Thesis for the Degree of Philosophiae Doctor

Trondheim, January 2021

Norwegian University of Science and Technology
Faculty of Engineering
Department of Structural Engineering



Norwegian University of
Science and Technology

NTNU

Norwegian University of Science and Technology

Thesis for the Degree of Philosophiae Doctor

Faculty of Engineering
Department of Structural Engineering

© Jelena Živković

ISBN 978-82-471-9919-0 (printed ver.)
ISBN 978-82-471-9709-7 (electronic ver.)
ISSN 1503-8181 (printed ver.)
ISSN 2703-8084 (online ver.)

IMT-report 2021:16

Doctoral theses at NTNU, 2021:16

Printed by NTNU Grafisk senter

*The most beautiful experience we can have is the mysterious.
It is the fundamental emotion that stands at the cradle of true art and true science.*

Albert Einstein

Preface

This doctoral thesis was submitted to the Norwegian University of Science and Technology (NTNU) in Trondheim for the degree of Philosophiae Doctor (PhD).

The thesis is the product of an industrial PhD project under the DaCS (Durable advanced Concrete Solutions – Design and construction for coastal and arctic regions) project, work package 4: Ductile durable lightweight aggregate concrete. The DaCS project (Project number: 245645) is funded by the Norwegian Research Council; the project owner is Kværner AS, and the project partners are Axion AS (Stalite), AF Gruppen Norge AS, Concrete Structures AS, Mapei AS, Multiconsult AS, NorBetong AS, Norcem AS, NPRA (Statens Vegvesen), Norges Teknisk-Naturvitenskapelige Universitet (NTNU), SINTEF Byggforsk, Skanska Norge AS, Unicon AS, and Veidekke Entreprenør AS. The project started in September 2015, and the thesis was submitted in October 2020.

All the research was carried out at the department of Structural Engineering at NTNU in Trondheim, Norway. For one of the experiments, lightweight aggregate concrete was prepared and transported from a stationary plant, NorBetong AS at Heimdal in Trondheim.

The academic supervisors from NTNU were Professor Jan Arve Øverli as main supervisor, and Professor Terje Kanstad as co-supervisor. The industrial co-supervisor and consultant was Hans Stemland (Sintef/NTNU).

Trondheim, October 2020

Jelena Živković

Acknowledgements

To my childhood that determined my life vocation and path

Maybe it can sound a bit weird how one woman can feel so much passion for concrete and engineering science but that is the complete truth dating back to childhood. We had a lot of construction works in the yard and as a child I loved to play with sand, cement and water, spending hours and hours inventing new shapes and constructions. So, I say, “*Leave the kids playing in sand and this world will for sure have more engineers*”.

Confucius said, “*Choose a job you love, and you will never have to work a day in your life*”, which is completely true in my case. I do not know about the future, but I now recognize that I have just enjoyed the last four or five years at NTNU and did not work at all. I am very grateful that I got this chance to increase and confirm my knowledge in the field of concrete science at NTNU, one of the world's best universities with the best facilities and laboratories and the many nice people who work there.

Many people and companies have contributed to this PhD project:

My supervisors, Jan Arve Øverli and Terje Kanstad

First, thank you for the courage to choose me among all the other candidates and having me here at NTNU in this position.

Thank you, Jan, for your patient guidance and giving me the freedom to explore the things I felt passionate about, to choose and collaborate with other colleagues, and for your unconditional support in every situation. You taught me how to become a researcher, but also about life, priorities and important decisions. I am pleased to have you as a boss, and it has been very easy and enjoyable working with you.

Thank you, Terje, for the nice chats, your enormous patience, support, and extreme motivation in every situation. Your positive attitude and nice energy have always made me smile even when facing an unsolvable problem.

My consultant and co-supervisor Hans Stemland

I am honoured to have got to know you, Hans, and to have the opportunity to work with “en gammel mann” full of knowledge, who gave me the best advice and showed me the best literature. Your sense of humour is amazing, and you find the funny side of even difficult situations and it was really a pleasure to work and smile with you.

Kjell Tore Fosså leader of the DaCS project

First, thank you for starting this project that I have been a part of, and your amazing leadership. You are one of the most professional people I have ever met in my life, and you have been present and available at every moment of my project. Thank you for the helpful discussions, your enormous support, recommendations and help with the experimental set-up and in the organization of the LWAC Workshop.

The Norwegian Research Council and to all the DaCS companies

I would like to thank the Norwegian Research Council, Kværner AS, Axion AS (Stalite), AF Gruppen Norge AS, Concrete Structures AS, Mapei AS, Multiconsult AS, NorBetong AS, Norcem AS, NPRA (Statens Vegvesen), Norwegian University of Science and Technology (NTNU), SINTEF Byggeforsk, Skanska Norge AS, Unicon AS, and Veidekke Entreprenør AS for financing this PhD project.

Egil Fagerholt (Institute for materials and structures, NTNU), creator of the DIC tool eCorr.exe

Thank you for your help in setting up and conducting the experiments and following analyses. Thank you for making your amazing software, for teaching me and my students how to use it, and for your support all the way.

Steinar Seehuus, Gøran Loraas and Ove Loraas and the other boys from NTNU lab

I would also like to thank you all for your enormous patience and help with setting up and running the huge experimental work at the concrete laboratory and testing hall in the Department of Structural Engineering.

My Master students: Jon Myhre Sakshaug, Christian Lund, Simon André Petersen, Henrik Nesje Johannesen, Jonas Andås Belayachi, Khaled Bastami, Aleksander Hammer, and Håvard Lauvsland

Thank you all for your help with the enormous experimental work. You were reliable support in the lab, kept the mood up even when something did not go “according to plan”, and you created nice and positive energy, so it was very enjoyable to work with all of you. I hope you learned from me just as much as I learned from you.

My office mates Andrei Shpak, Elisabeth Leite Skare, Kathrine Stemland, Pamela Zuschlag and Evgeny Ramenskiy

I am so happy to have got to know you all and share an office with you. Thank you for all our nice chats, surprises, and your great energy. Even on my bad days, I always smile and feel great with you.

To all my concrete colleagues

Andres, Assis, Daniel, Stefan, Alisa, Elena, Karla, Guzel, Anja, Alessia, Reignard, Morten, Gilles, Tobias, Mette, Klaartje, Max, Barbara, Magda, Simen, Sara, Nick, and Muhammad Zohaib. Thank you all for making the concrete knowledge base in Norway and for making the best working environment.

Seyed Mohammad Javad Razavi and Filippo Berto, my colleagues from Department of Mechanical and Industrial Engineering

Thank you for your great collaboration in the fracture energy experimental programme. You are real professionals and wonderful colleagues and friends. I was very happy to get to know you both and work with you.

Thanks to all my PhD colleagues and people who work in the Structural Engineering Department.

To my friends in Trondheim that made all this time enjoyable

Thank you Bojana, Milica and Antonio for your support, good discussions, always nice get-togethers, and the wonderful time that we spent together with our kids. You have taken the same road and have been able to understand me best in each life situation. I am so happy to have you as my friends.

Dragan, the best economist I know and an amazing colleague: thank you for all our nice chats and your support in each life situation.

Vera: thank you for taking care of my kids whenever I needed, your unconditional support and warm mother hugs.

Arianna: thank you for your good collaboration throughout the project, but also for wonderful moments with our girls. You are a brave woman and a wonderful friend, and I am very happy that this PhD project brought us together.

The list of my Trondheim friends is very long; thank you all for wonderful times and memories.

To all my family and friends from Bosnia and Serbia

You have always been there on my side and I am so happy to have you all.

To my cousin Jana

We grew up together and we share so many memories of nice moments, and as we always conclude, kilometres are no obstacle for someone close to your heart. I am so happy to have you as my best friend and so proud because you have achieved so much and will soon defend your thesis.

And last but not least, thank you to the most important persons in my life

To my brother Vladan

Following you, sharing life and the same vocation is the nicest thing I can do in my life. You are and you have always been my enormous support and the role model that I followed because you are the best and most dedicated researcher I know. I am forever happy because you are my brother and my best friend.

To my parents "Hvala mama i tata"

Thank you for giving me a base, wings and enormous support all my life. You have been and you are the best parents I can ever imagine.

To my husband Sinisa and my kids Katarina and Stefan

You are my base, my heart and my inexhaustible source of energy and my inspiration. Dear Sinisa, because of me you came to Norway, sacrificed your career because of mine, and followed me faithfully on this journey giving me enormous support all the time. I will be forever thankful for your patience, love and unconditional support. I am happy having you as a life companion. Now it is my turn to repay the favour and I am looking forward to that. Kaca, Stefo and Sinki, we managed this all together!

Jelena

Abstract

Lightweight aggregate concrete (LWAC) has been used in construction since ancient Greek and Roman times, for more than two thousand years. With its low density, it was mainly used to reduce the weight of the structures. LWAs were eventually manufactured and used more widely after 1917. Nevertheless, the use of LWAC in structural applications is very limited compared to normal weight concrete (NWC) even nowadays. The main concerns are its more brittle post-peak behaviour, especially in compression, its uncontrolled crack propagation, and its reduced ductility.

The main objective of the research for this thesis was to study the factors influencing LWAC's compressive ductility, so it can provide the safe and reliable structures which are vital to making LWAC a more competitive material. Most material models and design codes treat LWAC as one material, irrespective of the type of lightweight aggregate. While some aggregates do indeed have a brittle structural response, other aggregates behave much more like normal weight concrete. The lightweight concrete used in this study, with Stalite as aggregate, is therefore compared to the design codes and material models to see if they compare it unfavourably to NWC.

The research included experimental work and a comparisons part. The experimental part included a series of stress-strain gradient tests on small concrete prisms to obtain the design parameters used later in the main experimental programme. The large-scale beam experimental programme was created to capture the confinement effect. This programme involved loading six over-reinforced beams in four-point bending. The geometry of the beams was 210x550x4500 mm (width x height x length), allowing a large compressive area of one metre between loading points. The main testing parameters we varied were the spacing of transverse reinforcement (stirrups), the amount of longitudinal compressive reinforcement, and the thickness of concrete cover. The test results were used in numerical analysis of the current material models to verify or obtain guidance for appropriate material models for structural LWAC behaviour in compression.

Compressive confinement and ductility were most influenced by the spacing of transverse reinforcement, while load capacity was determined jointly by the amount of longitudinal compressive reinforcement and the stirrup spacing. Analyses of the compressed part of the cross section with existing material models showed they can be used as a basis for obtaining a better

description of LWAC in compression. However, the type of aggregate needs to be included in the models.

To test brittleness, crack propagation, and shear resistance, another large-scale beam test programme was created involving five beams. The main test parameters were the shear span ratio (a/d) and the amount of shear reinforcement. The results indicate that existing design codes underestimate the ultimate strains and shear capacity of lightweight concrete.

In summary, by using appropriate reinforcement detailing it is possible to increase the ductility of LWAC structures and achieve responses close to the response of NWC structures. Bearing in mind the major advantages of LWAC, which are reduced weight and a high strength-to-weight ratio compared to conventional concrete, structural applications of LWAC should be increased significantly.

Keywords: lightweight aggregate concrete, testing in compression, strain level, centric loading, eccentric loading, stress gradients, shear, bending, confinement, ductility, transversal reinforcement, longitudinal reinforcement, concrete cover.

Table of contents

Preface.....	I
Acknowledgements.....	II
Abstract.....	V
Table of contents.....	VII
Structure of the doctoral thesis	VIII
List of appended papers in Part II.....	IX
Other publications.....	X
Declaration of authorship	XII
Abbreviations	XIII
Part I – Extended Summary.....	1
1. Introduction	1
2. Background.....	3
3. Experimental approach	11
3.1. Overview of the various concrete mixes and technology used in experiments.....	12
3.2. Small-scale experimental programme	14
3.2.1. Fracture energy.....	14
3.2.2. Effect of loading rate on the fracture energy	17
4. Summary of papers	20
4.1. The context of work	20
4.2. Paper I.....	21
4.3. Paper II	22
4.4. Paper IIa.....	23
4.5. Paper III.....	23
5. Conclusions.....	24
6. Future research.....	27
7. References.....	28
Part II – Appended papers.....
Annex A – Conference papers.....
Annex B – Database and supplementary information

Structure of the doctoral thesis

The thesis is written as a collection of papers with a general introduction.

Part I is the general introduction and highlights the research significance and framework, the main objectives and limitations, and summarizes the appended papers, and the main outcomes and conclusions.

Part II consists of four appended papers, of which two have been published in an international peer-reviewed scientific journal, one is under review at another international peer-reviewed scientific journal, and one has been published in the proceedings of a conference.

In addition, there are two annexes, which summarizes conference papers and the main results from experimental work.

List of appended papers in Part II

The PhD thesis includes the following scientific journal papers and one conference publication.

Appended journal publications:

- I **Failure of Lightweight Aggregate Concrete in Compression under Stress Gradients**
Jelena Zivkovic, Jan Arve Øverli
Published in Nordic Concrete Research, 2019, Vol. 60, Issue 1, 51–66
DOI: 10.2478/ncr-2019-0011

- II **Confinement in Bending of High-Strength Lightweight Aggregate Concrete Beams**
Jelena Zivkovic, Jan Arve Øverli
Submitted to Engineering Structures (October 2020)

- III **Behaviour and Capacity of Lightweight Aggregate Concrete Beams with and without Shear Reinforcement**
Jelena Zivkovic, Jan Arve Øverli
Published in Nordic Concrete Research, 2017, Vol. 57, Issue 2, 59–72
ISBN: 978-82-8208-058-3

Appended conference publication:

- Ila **Ultimate compressive strain in lightweight aggregate concrete beams**
Jelena Zivkovic, Jan Arve Øverli
Published in Proceedings of the 12th fib International PhD Symposium in Civil Engineering Materials (July 2020), Prague, Czech Republic, 2018, ISBN 978-80-01-06401-6. pp. 829–836

Other publications

Conference publications:

Shear capacity of lightweight concrete beams without shear reinforcement

Jelena Zivkovic, Jan Arve Øverli

Proceedings of the Eleventh High Performance Concrete (11th HPC) & The Second Concrete Innovation Conference (2nd CIC), Tromsø, Norway, March 6th – 8th 2017

Norwegian Concrete Association / Tekna 2017 ISBN 978-82-8208-054-5

Material properties of high performance structural lightweight concrete

Reid W. Castrodale, Jelena Zivkovic, Rolf Valum

Proceedings of the Eleventh High Performance Concrete (11th HPC) & The Second Concrete Innovation Conference (2nd CIC), Tromsø, Norway, March 6th – 8th 2017

Norwegian Concrete Association / Tekna 2017 ISBN 978-82-8208-054-5

Shear capacity of lightweight aggregate concrete beams without shear reinforcement

Jelena Zivkovic, Jan Arve Øverli

Proceedings of the XXIII Nordic Concrete Research Symposium, Aalborg, Denmark, August 21st – 23rd 2017.

Norsk Betongforening 2017 ISBN 978-82-8208-056-9

Strain level and cracking of the lightweight aggregate concrete beams

Jelena Zivkovic, Jan Arve Øverli

Proceedings of the 12th Nordic mini seminar: Crack width calculation methods for large concrete structures. Oslo, Norway, August 29th – 30th 2018.

Norsk Betongforening 2017 ISBN 978-82-8208-057-6

Confinement in Bending of Lightweight Aggregate Concrete Beams

Jelena Zivkovic, Jan Arve Øverli

Proceedings of the 5th International fib Congress – Melbourne, Australia, October 7th – 11th 2018

Federation internationale du beton (fib) Melbourne, Australia, ISBN 978-18-7704-014-6

Particle-matrix proportioning of high strength lightweight aggregate concrete

Elisabeth Leite Skare, Jelena Zivkovic, Stefan Jacobsen, Jan Arve Øverli

Proceedings of SynerCrete'18: Interdisciplinary Approaches for Cement-based Materials and Structural Concrete: Synergizing Expertise and Bridging Scales of Space and Time. Vol. 1&2, Funchal, Madeira Island, Portugal, October 24th – 26th 2018

Rilem publications 2018 ISBN 978-2-35158-211-4

Brittleness of high-strength lightweight aggregate concrete

Jelena Zivkovic, Mladena Lukovic, Jan Arve Øverli, Dick Hordijk

Proceedings of SynerCrete'18: Interdisciplinary Approaches for Cement-based Materials and Structural Concrete: Synergizing Expertise and Bridging Scales of Space and Time. Vol. 1&2, Funchal, Madeira Island, Portugal, October 24th – 26th 2018

Rilem publications 2018 ISBN 978-2-35158-211-4

Failure of lightweight aggregate concrete under compressive strain gradients

Jelena Zivkovic, Jan Arve Øverli

Proceedings of the 15th Nordic mini seminar: Structural lightweight aggregate concrete. Trondheim, Norway, February 20th 2019

Norsk Betongforening 2019 ISBN 978-82-8208-066-8

Effect of loading rate on the fracture energy of lightweight aggregate concrete subjected to three-point bending test

Jelena Zivkovic, Javad Seyed Mohammad, Filippo Berto, Jan Arve Øverli

Proceedings of the 15th Nordic mini seminar: Structural lightweight aggregate concrete. Trondheim, Norway, February 20th 2019

Norsk Betongforening 2019 ISBN 978-82-8208-066-8

Confined lightweight aggregate concrete behavior and influencing factors

Jelena Zivkovic, Jan Arve Øverli

Proceedings of the XXIV Nordic Concrete Research Symposium, Sandeffjord, Norway, August 17th – 20th 2021.

Norsk Betongforening 2021 (accepted for publication and presentation at the Symposium)

Articles in popular scientific magazines :

Gjør lettbetong mer anvendbar

Jelena Zivkovic, Jan Arve Øverli

Byggeindustrien, 2017 (No. 17), p. 33

Other publications:

Structural lightweight aggregate concrete.

Jan Arve Øverli, Jelena Zivkovic

Workshop proceedings No. 15 by the Nordic concrete federation, Oslo, Norway, 45 pp.

Norsk Betongforening 2019 ISBN 978-82-8208-066-8

Declaration of authorship

Jelena Zivkovic planned and conducted the work in most of the experiments, evaluated the results, and wrote most of the above-listed publications and this thesis.

Elisabeth Leite Skare contributed in the laboratory and at the Norbetong AS stationary plant by preparing the various concrete mixes and documenting the results.

Egil Fagerholt (Department of Structural Engineering, NTNU) helped with setting up experiments, carried out the DIC investigations and documented the results for the experiments.

Master students, Christian Lund, Jon Myhre Sakshaug, Simon André Petersen, Henrik Nesje Johannesen, Jonas Andås Belayachi, Khaled Bastami, Aleksander Hammer and Håvard Lauvsland, contributed in the laboratory by preparing specimens for testing, conducting experiments, and documenting the results.

All the above also contributed in discussions of methods and results in addition to reviewing the manuscript.

Abbreviations

NDC	Normal density concrete
NWC	Normal weight concrete
LWA	Lightweight aggregate
LWAC	Lightweight aggregate concrete
DLWAC	Dry lightweight aggregate concrete
WLWAC	Wet lightweight aggregate concrete
FLWAC	Fibre lightweight aggregate concrete
DIC	Digital image correlation
ITZ	Interfacial transition zone
SG	Strain gauge
LVDT	Linear variable differential transformer
EC2	Eurocode 2: NS-EN 1992-1-1:2004+NA2008
PVA	Polyvinyl alcohol fibres
SLC	Structural lightweight concrete
ND	Normal density
NWA	Normal weight aggregate

Part I – Extended Summary

1. Introduction

Concrete, a material generally composed of cement, water, and coarse aggregates, is one of the most widely used building materials in the world. Concrete has the ability to be shaped to the desired dimensions of structures and is known as an inexpensive and durable material. Where a light aggregate is used instead of coarse aggregate or aggregate and sand, the concrete becomes lightweight aggregate concrete (LWAC), with a high strength-to-weight ratio compared to normal weight aggregate concrete (NWC).

Replacing conventional coarse aggregate with lightweight aggregate has a huge influence on mechanical properties of the concrete. The main scepticism of designers about using more LWAC is rooted in its poorer mechanical characteristics compared to conventional NWC. But the standards [EN-1992-1-1, 2004; NS3473, 2003; ACI213R-03, 2003; Fib Bulletin 8, 2000] do not distinguish between different lightweight aggregates and every concrete mix with a different lightweight aggregate (LWA) presents a particular case with its own characteristics.

The main reason for using LWAC is to reduce the dead weight of structures, which is the basic cost driver in the offshore concrete industry and other large infrastructure projects. However, use of LWAC as a mainstream construction material in the construction industry is still limited, which can partly be explained by its brittleness and uncontrolled crack propagation at the material level compared to normal weight concrete (NWC) [Chandra and Berntsson, 2003; Bologna, 1974; Castrodale et al., 2017; EuroLightCon1998–2000, Lo et al., 2007; Helland et al., 2000; Holand et al., 1995]. This means LWAC structures subject to dynamic loading may have problems with energy dissipation and loss of concrete cover. Moreover, due to the redistribution of forces, the inherent safety in structures relies on ductility. Energy dissipation in flexure is mainly related to the yielding (and yielding reversal) of the reinforcement, but the stress-strain characteristics of the concrete in compression play an important role in limiting the amount of yielding possible before break-down of the plastic zones [Cousins et al., 2013; CUR report 173, 1995]. Compared to LWAC, the stress-strain diagrams of normal weight concrete are characterized by a more linear ascending branch and a steeper descending branch [Nedreliid, 2012]. Less certain is the actual break-down of the sections involving splitting failure with loss of concrete cover. Research on how to improve the ductility of LWAC structures to ensure they are safe and reliable is therefore vital to make LWAC a more competitive material.

Typical oven-dry densities of LWAC are between 300–2000 kg/m³ and LWAC is 20–30% lighter than NWC [EN-1992-1-1, 2004; NS3473, 2003; ACI213R-03, 2003]. Concrete with natural lightweight aggregate has been used in construction since ancient Greek and Roman times. LWAs have been manufactured and used more commonly since 1917 [Chandra and Berntsson, 2003; Spitzer, 1995]. In Norway, the most commonly used lightweight aggregates are Norwegian Leca and German Liapor [EuroLightCon, 1998–2000]. This research focused on an American lightweight aggregate from North Carolina, an argillite slate called Stalite [Stalite Structural, 2020; Castrodale et al., 2017]. The results and performance of LWAC containing Stalite is compared with LWACs with aggregates Leca and Liapor [Thorenfeldt and Stemland, 1995; Bjerkeli and Tomaszewicz, 1987–1990; Markeset, 1993]. My research focused on high-strength LWACs and structural lightweight concrete (SLC) with a strength of 60 MPa or higher [EuroLightCon BE96-3942/R36, 2000].

The research work for this thesis ranged from the material level to large-scale experiments, with comparisons and a focus on existing design codes. Part I of the thesis introduces the research framework, focusing on methodology that can register and capture ultimate strains in large structural elements, but also presenting the main outcomes of the work. The detailed research contributions can be found in the journal papers collected in Part II.

1.1. Objectives and scope

My research had two main objectives. The first objective was to increase knowledge and understanding of the ultimate response of LWAC members exposed to compression and bending, but we also wanted to investigate how various confinement factors (stirrup spacing, the amount of longitudinal reinforcement, and the thickness of concrete cover) affect the ductility of members in compression. The ultimate strain in compression at peak load is the governing value for design, and we wanted to create a design base for LWAC with Stalite as the lightweight aggregate based on experimental testing on large samples. It was also essential to consider the post-peak response in these large structural elements since this is important for the evaluation of residual capacity and safety. We also investigated the influence of polyvinyl alcohol (PVA) fibres, type KURALON [<http://kuralon-frc.kuraray.com/whats/characteristics>], on confinement for elements exposed in compression. Finally, we needed to evaluate and describe the softening behaviour and check existing concrete confinement models that might be applicable to LWAC exposed to compression and bending.

The second main objective in this research was related to the brittleness of LWAC. Rapid crack propagation and brittleness are disadvantages of LWAC, and they affect the behaviour of the concrete wherever tensile strength is important, as for instance in shear strength. To analyse this, we carried out shear tests on beams with and without shear reinforcement under four-point bending. We also investigated the moisture condition of the aggregate and its influence on brittleness. Fracture energy is a measurement of brittleness, and we used it to compare Stalite with NWC and with other types of lightweight aggregate.

1.2. Limitations

The limitations of the study can be summarized as follows:

- The research work carried out and presented in this thesis is only valid for lightweight aggregate concrete with Stalite as aggregate. The preparation procedures, considerations and philosophy can be used for other LWACs, but the results presented are only valid for LWAC with Stalite.
- In the experimental programmes, only longitudinal and vertical strains were measured in beams and prisms. To develop a triaxial material model applicable for design and analyses, the confining pressure is necessary, which means that the transversal strains also need to be measured.
- The research tested and considered short-term loading only.

2. Background

2.1. Lightweight aggregate Stalite

The lightweight aggregate Stalite has been proven to be a suitable aggregate in concrete used for structural applications. The foothills region of North Carolina is the only place where slate is extracted as raw material to produce Stalite. The region is called the “Tillery Formation” and contains argillite slate. The argillite slate is a laminated, fine-grained siltstone of clastic rock, see Figure 1a and b. The aggregate can achieve up to 30% less unit weight than a normal density aggregate (NDA). The bulk density ranges from 720–880 kg/m³ for coarse aggregate and 960–1120 kg/m³ for fine aggregate. With a 24h water absorption of approximately 6% and relatively high particle strength, concrete containing Stalite can achieve over 83 MPa of compressive strength. The low absorption of the aggregate allows for easy mixing and pumping of the concrete. The hardness of the material is

equivalent to that of quartz [[Stalite Structural, 2020](#); Castrodale et al., 2017]. When producing Stalite, it is first and foremost important to test-drill and analyse the samples to find the right raw material. The raw material is then crushed to the optimum size, see Figure 1c, and stored in silo.



Figure 1: a) Stone of argillite slate; b) LWA Stalite; and c) Fractions of Stalite material [[Stalite Structural, 2020](#)].

The actual production involves preheating the materials before they are fed into a rotary kiln. The rotary kiln is angled with a slight incline and the materials are heated slowly to a maximum

temperature of 1200 °C. The dimensions of the rotary kiln are 3.4 m in diameter and 49 m in length. When heated to 1200 °C, the slate becomes sufficiently plastic to form expanded gases stored in small incoherent pores. The material is then cooled so that the pores persist; this gives a lower dead weight and relatively low absorbency. The cooling takes place with air, and not water, to prevent possible crystallization. The final crushed material has various fractions: 0–4.75 mm (fines), 9.5 mm (3/8”), 12.5 mm(1/2”), and 18 mm (3/4”) [Stalite Structural, 2020; Castrodale et al., 2017].

2.2. Fundamental behaviour of lightweight concrete at the material level

To understand LWAC behaviour at the structural level, we need knowledge about LWAC behaviour at the material level. It is well known that cracking in LWAC differs from NWC because the cracking path goes through the aggregate since in this matrix the aggregate is the weaker part, whereas in NWC, where the aggregate is the strongest part, cracking goes around it. That results in greater brittleness, increased sensitivity to stress concentrations, and more sudden crack propagation in LWAC, but it also results in a higher strain capacity in the material itself. Equality or smaller differences in strength between aggregate and matrix lead to increased strain capacity. If lightweight aggregate is porous and only partly saturated during mix preparation, an interfacial transition zone (ITZ) is created between aggregates and cement matrix [Yong et al., 2009], see Figure 2.

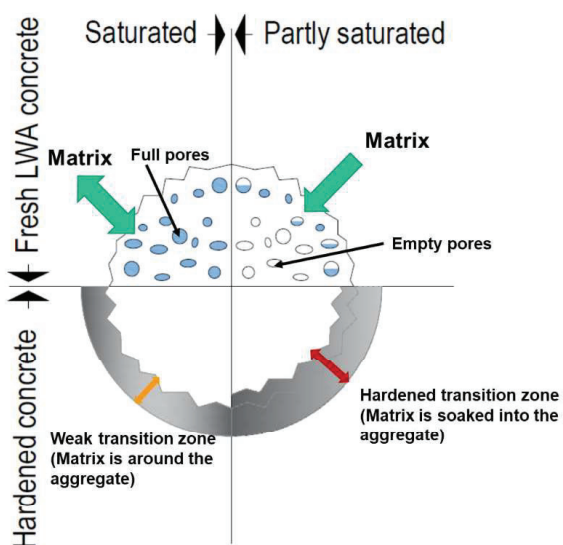


Figure 2: ITZ zone in LWAC concrete

A strengthened ITZ zone can determine the cracking path, so it goes both around and through the aggregate, see Figure 3. This increases the stress and strain capacity of the LWAC.

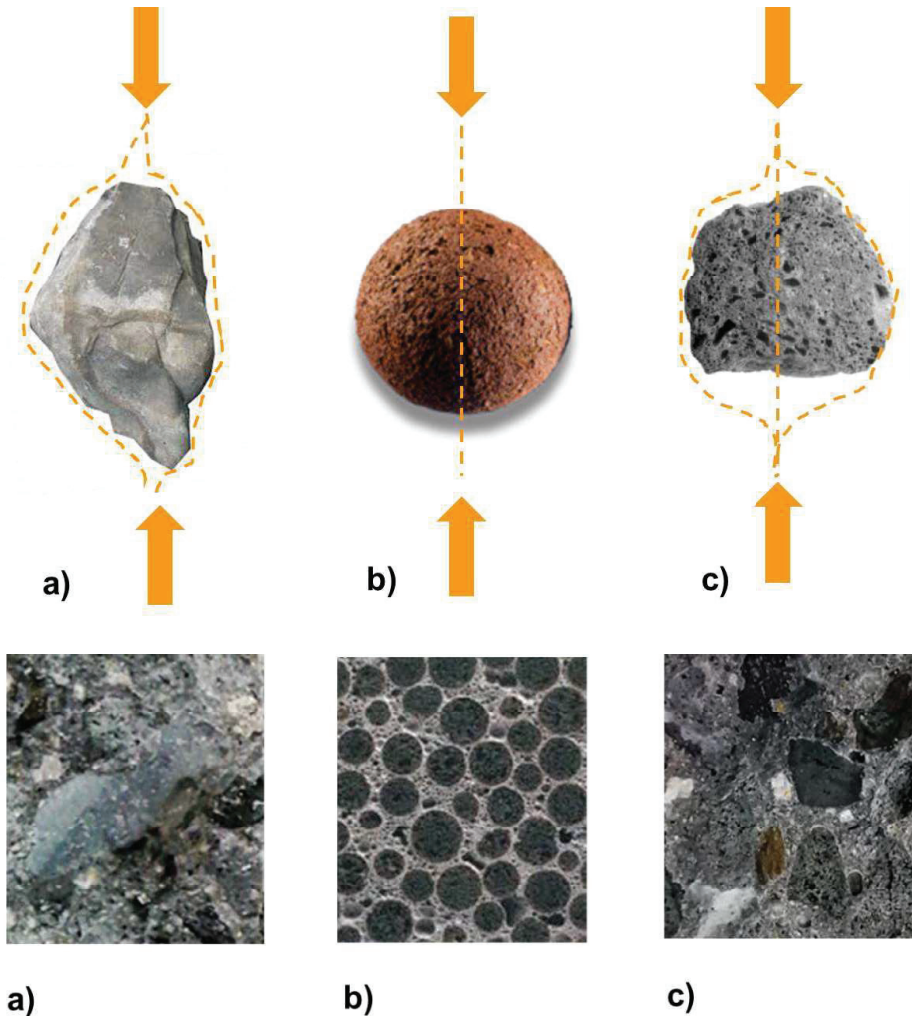


Figure 3: At the top, the cracking paths, and at the bottom, views of cracked concrete under an optical magnifier for a) normal weight aggregate Årdal (private photo; b) lightweight aggregate (e.g. Leca and Liapor [<https://leca.asia/>; <http://www.liapor.com/en/applications/structural-engineering/insulating-concrete/high-density-lightweight-concrete/what-is-high-density-lc-r.html>]); and c) lightweight aggregate produced using rotary kiln methodology (e.g. Stalite [[Stalite Structural, 2020](#)])

The production process for some lightweight aggregates, like Leca and Liapor, creates a nice shell and very little porosity, so no ITZ is achieved in the concrete mix and the cracking path always goes through the lightweight aggregate [EuroLightCon BE96-3942/R8, 2000; Holand et al., 1995].

Lightweight aggregates that are produced using a rotary kiln process have large open pores and, just by using partly dry aggregate, it is easy to achieve a strong ITZ zone in the concrete mix [Castrodale et al., 2017; [Stalite Structural, 2020](#)]. This leads to a more complex cracking mechanism where the cracking goes through and around the aggregate, which increases the fracture energy and strain capacity of the concrete and reduces its brittleness. The various cracking paths are shown in Figure 3.

2.3. Ductility and brittleness

The ductility of a structure is defined as its ability to deform inelastically without significant loss of strength. It is very challenging to measure and quantify ductility. It can be defined at various levels in a structure – at a material, sectional, element, or global level. To increase ductility in LWAC structures, confinement effects can be introduced using various forms of reinforcement detailing. Confinement can also be increased by adding fibre reinforcement to LWAC [Øverli and Jensen, 2014]. The focus in my research was to investigate how confinement affects the ductile behaviour of LWAC in compression. The quantification of confinement must start at the material level, but the goal is increased ductility at the structural level. It is known that confinement effects only appear in large-scale elements [Nedreliid, 2012; Øverli and Jensen, 2014]. So, we would need applicable test methods and the production of some large-scale elements. Furthermore, we would need to model the confinement effects for use in the structural analysis and design of LWAC structures. To accomplish all this would require a combination of experimental work and numerical analysis [Øverli and Jensen, 2014; Filaj et al., 2016; Radic et al., 2013; Shah et al., 1983; Bouafia et al., 2014; Hansen, 1993; Watanabe et al., 2004]. In a structural member or a structure, ductility is normally presented as the ductility ratio, μ , which is defined as the ratio of maximum deformation to the deformation level corresponding to a yield point, see Figure 4 [Anwar and Najam, 2016; Guo, 2014].

Brittleness describes the fracture behaviour of a material when subjected to stresses. Brittle materials are characterized by small deformations, sensitivity to stress concentrations, and sudden failure followed by rapid crack/fracture development. In concrete, differences in fracture behaviour are attributed to the type of aggregate. LWAC is known as a brittle material, since the aggregate is the weakest part in the concrete matrix [Zhang and GjØrv, 1995; Nedreliid, 2012]. Measures of brittleness like the characteristic length and no softening behaviour in compression after peak stress indicate that LWAC is significantly less ductile than normal density concrete [EuroLightCon, BE96-3942/R8, 2000].

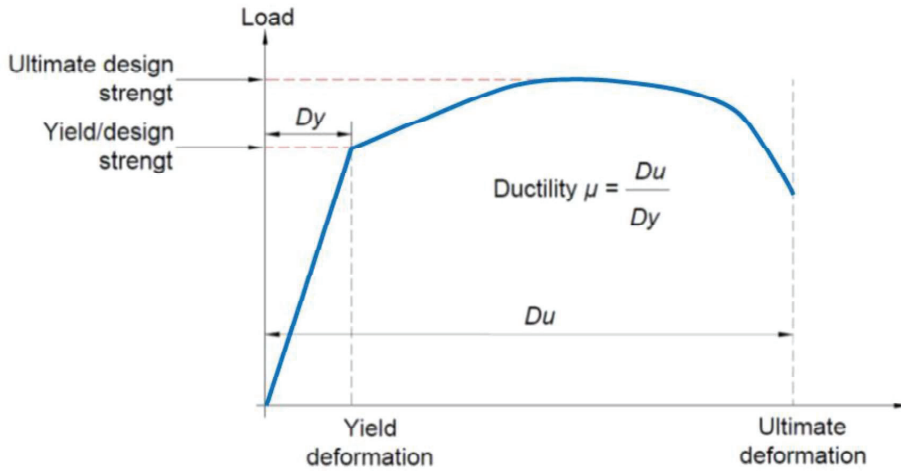


Figure 4: Ductility coefficient [Guo, 2014]

2.4. Ductility and confinement of reinforced concrete cross sections

The mechanical behaviour of confined concrete is characterized by an increase in strength and ductility. The magnitude of the increase is determined by various confinement parameters, such as the compressive strength of the concrete, the diameter, configuration, and strength of the transverse reinforcement (stirrups), the ratio and diameter of longitudinal reinforcement, the section geometry and thickness of concrete cover, etc. To describe and explain the stress-strain relationship of confined concrete in compression, we need the concept of ineffectively and effectively confined areas. In the case of the rectangular cross section, the concrete is longitudinally contracted and laterally expanded with internal micro cracks. Transversal reinforcement generally resists high expansion pressure, and effective confinement by lateral stirrups leads to the enhancement of axial load-carrying capacity. Figure 5 shows the effectively and ineffectively confined areas for a typical reinforced concrete beam.

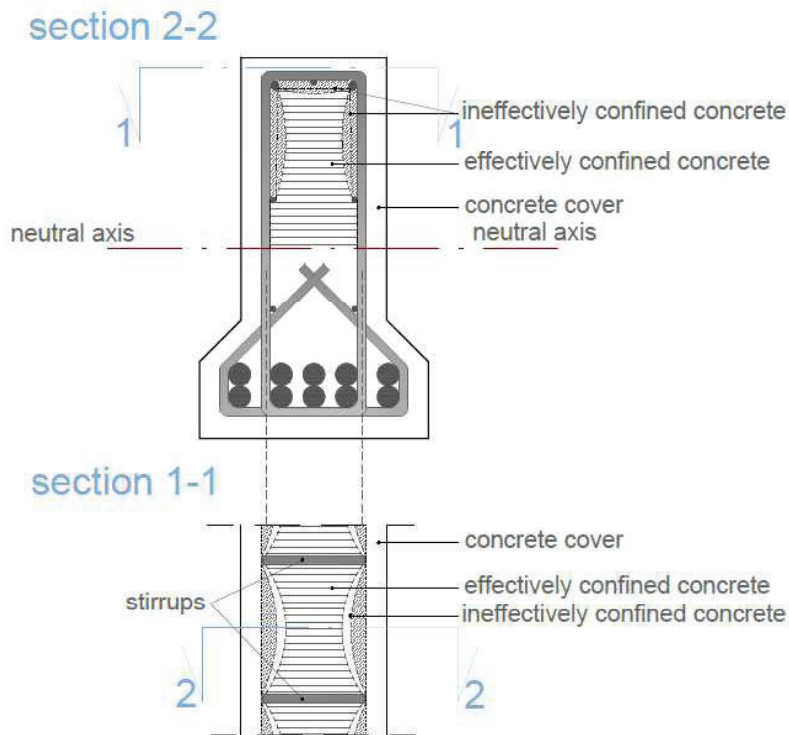


Figure 5: Effectively and ineffectively confined areas in beams. Top: Cross section. Bottom: Longitudinal section.

Figure 5 assumes arching action between the levels of transverse rectangular hoop reinforcement. Arching occurs vertically between layers of transverse hoop bars and horizontally between longitudinal bars. The area of effectively confined concrete is the area of concrete within the centrelines of the perimeter hoop (stirrup) and it is bordered with arches. Midway between the levels of the transverse reinforcement and the arching is the area of ineffectively confined concrete. Longitudinal reinforcement presents the starting and ending points for the arches, which are assumed to arise at failure in the cross-section. Calculation of the effective lateral confining stress and the compressive strength of the confined concrete is based on the effectively confined area.

2.5. Stress-Strain models for confined concrete

Table 1 compares various existing confined concrete models in the literature. These models highlight most of the characteristics of reinforcement, concrete and their geometry which are known to have an influence on the confinement effect and stress-strain behaviour. The table includes the Model Code

2010 and the proposed SINTEF FCB model [fib Model Code 2010, 2013; Hansen et al., 1990; Mander et al., 1988b]. The stress-strain curve for confined concrete in all models was defined with three or four regions: 1) an ascending branch, 2) a constant stress region, 3) a descending branch, and 4) a base limit or horizontal part.

LWAC is only included in the model proposed by Bjerkeli and Tomaszewicz, which is referred to as the SINTEF FCB model [Hansen et al., 1990 and 1993]. The Mander model is the only one that accurately calculates the area of the remaining cross section, taking into account the curvatures that develop in cross sections during loading [Mander et al., 1988a]. Poisson's ratio, which describes the expansion or contraction of a material in directions perpendicular to the direction of loading, is not incorporated in any of the models. The Mander and SINTEF FCB models were selected to validate the results from our experimental study. Both models were adjusted for beam applications and the geometry tested.

Table 1: Overview of stress-strain models for confined concrete in the literature and the parameters included.

Models ▶ Parameters ▼	Mander, Priestley & Park (1988)	Model Code 2010	Kent & Park (1971)	Sheikh & Uzumeri (1982)	Shah et al. (1983)	Elias & Durrani (1988)	Yong et al. (1988)	SINTEF FCB Bjerkeli & Tomaszewicz (1990)
Concrete strength	yes	yes	no ¹	no ¹	yes	no ¹	yes	yes
Steel strength	yes	yes	yes	yes	yes	yes	yes	yes
Amount of lateral reinforcement	yes	yes	yes	yes	yes	yes	yes	yes
Tie spacing	yes	yes	no ²	yes	no ³	yes	yes	yes
Section dimension	yes	yes	yes	yes	yes	yes	yes	yes
Section geometry	circular & square	square	square	square	circular & square	square	square	circular & square
Distribution of longitudinal reinforcement	yes	yes	no	yes	no	no	yes	yes
Poisson's ratio	no	no	no	no	no	no	no	no

1) The compressive strength of plain concrete is included in the model, but the strength increase due to confinement is not a function of the compressive strength.

2) Tie spacing is considered just for the descending branch.

3) The spacing of lateral steel does not affect the concrete behaviour.

Paper 2 presents the validation results. Comparison between the models and the experimental work shows that some adjustments would be needed to fit the experimental results with the theoretical models. However, these adjustments should not change the shape of the stress-strain curve of confined concrete, which has three main parts: 1) a parabolic ascending region between zero and maximum stress, 2) a descending linear part, and 3) a horizontal part until reaching ultimate compressive strain, ϵ_{cu} .

The goal of this work was not to develop a material model for confined lightweight concrete. However, by combining the Mander and the SINTEEF FCB models, this can be done if we make some modifications. Young's modulus must be included and made density dependent. The effective confined area should follow the Mander model and be incorporated in the SINTEF FCB model. Poisson's ratio varies with the type of concrete and increases at high stress levels. It must therefore be included since it dictates the expansion of the concrete cross section and the confinement pressure obtained.

2.6. Design codes

In general, the design codes do not take into account the type of the aggregate used in the concrete [EN-1992-1-1, 2004; NS3473, 2003; Model Code 10,2013], except for some brittle failures, like shear, where they introduce reduction factors depending on the aggregate type. For lightweight aggregate concrete the codes do not distinguish between different types of aggregate. LWAC is classified in standards according to its density. Eurocode 2 (EC2) has special rules for LWAC, including reduction factors based on the density of the concrete [EN-1992-1-1, 2004]. For design, it is essential to determine the stress-strain curve. Equations for E-modulus and strains are multiplied by reduction factors. This results in low values for LWAC's ultimate compressive strain, which eliminates the use of LWAC as a structural material in some cases.

3. Experimental approach

This section gives a summary of an experimental programme carried out to provide a design base for lightweight aggregate concrete with Stalite as the aggregate. It provides an overview of the concrete mixes tested and the mechanical characteristics of each concrete mix. Every step taken in the preparation of the concrete mixes was in accordance with the current standards and

recommendations [ACI 211.2-91, 1991; ACI 213R-03, 2003; ACI 304.5R-91, 1991; EuroLightCon BE96-3942/R4, 1999; [Stalite Structural, 2020](#); Ge et al., 2009; Holand et al., 1995; TEC Services project No. 04-0514, 2015; Yong et al., 2009]. Tests were carried out when the concrete was in a fresh state and later when the concrete had hardened in accordance with the standard procedures [NS-EN 12390-3, 2009; NS-EN 12390-6, 2009; NS-EN 12390-7, 2009; NS 3676, 1987; SINTEF KS14-05-04123, 2007; SINTEF KS14-05-04122, 2007, RILEM TC 148-SSC, 2000]. The methodology and results of the large-scale experimental programme are described in detail in the journal publications. For the detailed recording of the strain fields, we used digital image correlation (DIC) methodology in combination with standard measuring devices: strain gauges (SGs) and linear variable displacement transducers (LVDTs) [Fagerholt, 2012; Fayyada and Leesb, 2014; Lin, 2015]. The first experiment is published in Paper I and provides the base for the other experiments. The second experiment is described in Paper II and Paper IIa, while the third experiment is described in Paper III.

The existing standards do not generally differentiate between the types and characteristics of different lightweight aggregates and that leads to underestimation of the mechanical characteristics and structural behaviour of specific types of lightweight concrete. For all experiments, a detailed capacity calculation was carried out in accordance with standard procedures, see annex B [EN-1992-1-1, 2004; NS3473; NS-EN 1992-1-1:2004+NA:2008, 2008; NS-EN 206:2013+NA:2014, 2014; Sørensen, 2013].

3.1. Overview of the various concrete mixes and technology used in experiments

Table 2 gives an overview of the concrete mixes created and used in this PhD project. The main goal was to produce high-strength LWAC with a cylinder compressive strength of 60 MPa or higher [Smeplass, 1992; Thorenfeldt et al. 1987 and 1995]. The aggregate Stalite, size 1/2", was supplied directly by Axion AS, and distributed directly from North Carolina. Upon arrival, the aggregate was prewetted, but during a storage period in the laboratory, moisture conditions varied, so moisture and absorption measurements were required for all the concrete mixes. To increase ductility and reduce brittleness, one mix included a small amount of polyvinyl alcohol fibres, type KURALON with 8 mm length [Kuraray Co; Savija et al., 2017].

For each experiment, concrete specimens were prepared from the one batch, which was controlled for moisture content in aggregate and sand the day before. Our laboratory mixers have capacities of

250 and 800 litres. For the large-scale experimental programme, the concrete mixture was prepared from one batch at the Norbetong stationary plant. To make it possible to maintain the moisture content and to isolate the aggregate from other aggregates, the exact amount of lightweight aggregate required for whole experiment was loaded in the truck mixer, which had a capacity of about 12 tons. The truck was driven to the stationary mixing plant where it was filled with prepared mortar and driven back to the casting place. The big beam forms were filled using the truck pump and were compacted using a needle vibrator. LWAC with Stalite as aggregate is very suitable for pumping and the slump required is a minimum of 18 cm or more, depending on the estimated casting time.

Table 2: Overview of the concrete mixes used in this PhD project.

Publication	Paper 1	Paper 1	Paper 1	Paper 1	Paper 2	Paper 3
Constituent weight [1000 litres]	DLWAC ₁ ³ [kg/m ³]	WLWAC ₁ ³ [kg/m ³]	FLWAC ₁ ³ [kg/m ³]	WLWAC* ₁ ³ [kg/m ³]	LWAC ₂ ³ [kg/m ³]	LWAC ₃ ³ [kg/m ³]
Cement (Norcem Anlegg FA)	442.3	440.3	397.5	427.5	420.7	399.5
Silica fume (Elkem Microsilica)	23.3	23.2	20.9	22.5	21.9	19.8
Water (free)	146	180.8	163.2	203.7	193.5	167.7
Absorbed water in Stalite+sand (24h)	6.1	38.8	35.9	47.2	49.2	40.1
Water* (added in mixer)	139.9	142	127.3	156.5	144.3	127.6
Sand (Ramlo) 0–2 mm)	230	231	377.3	229.4	232.4	-
Sand (Årdal (NSBR) 0–8 mm)	536.8	539	531	535.5	543	720.3
Aggregate (Stalite ½")	515.4	517.5	493	514	537.1	571.9
Superplasticizer (Mapei Dynamon SR-N)	3.3	3.9	6.2	3.2	5.2	-
Superplasticizer (Sika V. Crete RMC-420)	-	-	-	-	-	2.6
Fibres (Kuralon PVA 8mm)	-	-	6.5	-	-	-
Moisture of the aggregate [%]	0.1	7.9	7.9	12.5	11.43	8.2
Absorption of the aggregate 24h/100h	6.58 / 7.72	6.58 / 7.72	6.58 / 7.72	6.58 / 7.72	6.54 / 8.32	6 / 8.5

* Mix WLWAC* had a strength below 60 MPa and was not further considered in the large-scale experiments
DLWAC₁ (dry lightweight aggregate concrete) means that the aggregate moisture was close to zero, and index 1 means that this concrete mix is described in Paper 1
WLWAC₁ (wet lightweight aggregate concrete) means that the lightweight aggregate was saturated, and index 1 means that this concrete mix is described in Paper 1
FLWAC₁ (fibre lightweight aggregate) concrete means that the lightweight aggregate was made with addition of PVA fibres, and index 1 means that this concrete mix is described in Paper 1

For all concrete mixtures prepared, the fresh concrete characteristics of fresh density, air content and slump were in accordance with the procedures prescribed in Norwegian standards and the prospectus from the company [NS-EN 12390-3, 2009; NS-EN 12390-6, 2009; NS-EN 12390-7, 2009; [Stalite Structural, 2020](#); TEC Services project No: 04-0514, 2015] cf. Table 3.

To achieve good workability in a mix with lightweight aggregate, the particle-matrix method was used for proportioning [Skare et al., 2018]. Stability and slump characteristics of the LWACs were achieved by increasing the matrix volume and content of fines. More details are given in a conference paper that is attached to the thesis, see annex A.

Table 3: Overview of the fresh concrete characteristics for all the concrete mixes used in this PhD project.

Publication	Paper 1	Paper 1	Paper 1	Paper 1	Paper 2	Paper 3
Concrete mix	DLWAC ₁	WLWAC ₁	FLWAC ₁	WLWAC* ₁	LWAC ₂	LWAC ₃
Fresh density [kg/m ³]	1989	2015	2011	1927	2013	1993
Air content [%]	2.5	1.9	2.5	2.4	2.5	2.5
Slump [mm]	170	190	250	250	230	140
Matrix volume [l/m ³]	360	360	360	378	375	326

* Mix WLWAC* had strength below 60 MPa and was not further considered

3.2. Small-scale experimental programme

All the experiments consist of a large-scale part and a small-scale programme, which provided the mechanical characteristics of each concrete mix. Small specimens were tested after 7 and 14 days, and most other specimens after 28 days, to determine the compressive strength, tensile strength and Young's modulus. Small beams were tested later, approx. 60 days after casting, to determine the fracture energy for LWAC. A brief summary of the small-scale test results is given in Table 4.

Table 4: Overview of mechanical properties for the concrete mixes used in this PhD project.

Publication	Paper 1	Paper 1	Paper 1	Paper 2	Paper 3
Concrete mix	DLWAC ₁	WLWAC ₁	FLWAC ₁	LWAC ₂	LWAC ₃
Saturated density ρ_{cs} [kg/m ³]	1997.9	2008.4	2019.2	2006.2	1980
Oven dry density ρ_{cv} [kg/m ³]	1979.9	1864.6	1899.5	1834	1850
Compression cube after 7 days $f_{icm,7}$ [N/mm ²]	51.05	58.14	48.83	56.7	57.3
Compression cube after 28 days $f_{icm,28}$ [N/mm ²]	71.6	77.5	71.0	74.2	73.8
Compression cylinder f_{icm} [N/mm ²]	67	72.92	63.7	65.1	67.5
Tensile strength f_{icm} [N/mm ²]	4.72	4.86	4.54	4.11	4.12
Modulus of elasticity E_{icm} [N/mm ²]	23653	21701	22549	24175	24175
Fracture energy G_f [Nm/mm ²]	79.7	91.6	-	70.5	76.7
Poisson ratio	0.18	0.2	0.19	-	-
Characteristic length l_{ch} [mm]	91.4	84.2	-	100.9	109.2

3.2.1. Fracture energy

Fracture energy is defined as the energy consumed creating a unit of cracked area. Fracture energy is an inverse measure of brittleness. Higher fracture energy means lower brittleness and vice versa. The fracture energy can be determined in small 100×100×1200mm beams in accordance with the SINTEF procedure [SINTEF procedure KS14-05-04123, 2007]. This procedure is quite similar to the Hillerborg-proposed RILEM method [Hillerborg, 2005]. The small beams are just 200 mm longer and the notch is 0.4 instead of 0.5 of the height of the beams. The pre-notched beams are subjected to a three-point bending test. Fracture energy is calculated by dividing the work or energy from the positive part of the load-deformation curve during the test by the fracture area.

For normal density concrete, the fracture energy primarily depends on the water-cement ratio, the maximum aggregate size, and the age of the concrete [Hillerborg, 2005]. Curing conditions also can have a significant influence on the experimentally determined fracture energy (G_F), so the advice is to store the samples in water and take them out some hours before the testing. The aggregate type and content seem to affect the fracture energy of concrete much more than the size of aggregates. This phenomenon is caused by the transition from interfacial fracture to trans-aggregate fracture. The utilization of high-strength aggregates like basalt or fairly heterogenous material like granite leads to an increase in fracture energy values. In both cases, the crack propagation leading to concrete failure is impeded, because breaking tougher aggregates, changes of crack orientation, and multiplication of cracks, all require greater amounts of energy [EuroLightCon, 1998-2000].

The fracture energy (G_F) alone is not enough to characterize the brittleness of concrete. An additional parameter, the characteristic length (l_{ch}), has therefore been introduced. This corresponds to half of the length of a specimen subjected to axial tension, in which just enough plastic strain energy is stored to create one complete fracture surface. The characteristic length decreases as compressive strength increases; the concrete becomes more brittle as its tensile and compressive strength increases [SINTEF procedure KS14-05-04123, 2007].

The equations for determining the fracture energy and characteristic length are given below. In the calculation, only the positive part of the load-displacement curve is used. This is marked as W_0 in Figure 6, p is the weight of the concrete samples, δ is the maximum recorded dilatation, and b , h are the measured width and height of the fracture area.

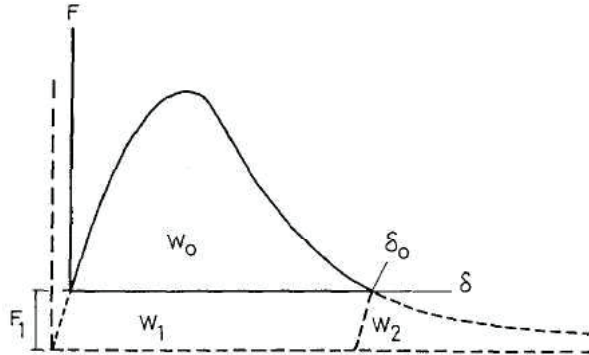


Figure 6: Determination of the fracture energy. The load displacement curve for the three-point bending tests on notched beams [SINTEF procedure KS14-05-04123, 2007].

$$G_F = \frac{W_0 + 2 \cdot 0.4 \cdot p \cdot 9.81 \cdot \delta}{b \cdot h} \text{ [Nm/m}^2\text{]} \quad (3)$$

$$l_{ch} = \frac{E_{ci} \cdot G_F}{f_{ctm}^2} \text{ [mm]} \quad (4)$$

The fracture energy of LWAC with Stalite as aggregate was compared with previous results from many experimental programmes performed at SINTEF [Stemland, 2012]. The main goal was to determine the characteristics of LWAC with Stalite in comparison to normal weight concrete and other lightweight aggregate concretes, see Figure 7. The earlier tests on normal weight aggregate (NWA) concrete indicated a further increase in fracture energy with increasing compressive strength when using stronger aggregates (quartzite and basalt). The aggregate labelled NWA (Granite) was made with coarse aggregate granite. The reference concrete was ND (normal density), made with coarse aggregate called Årdal. The other aggregates used in SINTEF experiments were lightweight aggregates Leca and Liapor, and they are labelled LWA in Figure 7.

Figure 7 shows that the fracture energy depends on the type of used aggregate and using NWA gives concrete with high strength and higher fracture energy than LWAC. There are several types of lightweight concretes and it is obvious from Figure 7 that fracture energy and strength depends on the type of lightweight aggregate. LWAC with Stalite as aggregate has fracture energy lower than NWC but higher than other type of lightweight aggregate. The fracture energy was approximately 20 Nm/m higher than for other LWACs. Thus, the design codes should differ between type of lightweight aggregate since their brittleness is different.

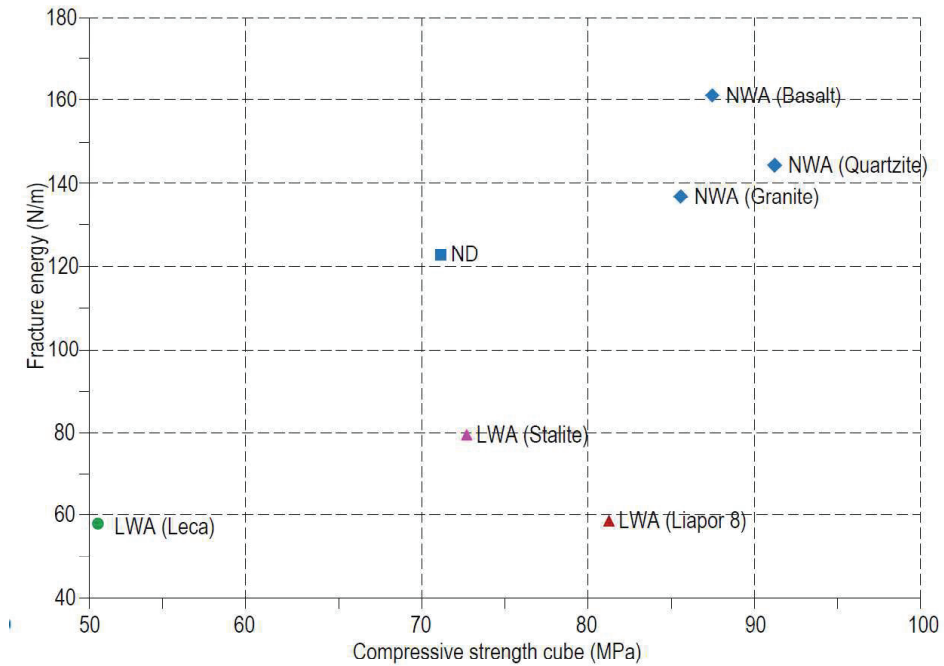


Figure 7: Fracture energy vs. aggregate types.

3.1.1. Effect of loading rate on the fracture energy

A experimental programme using three-point bending tests, see Figure 8, was created to investigate the loading rate dependency of the fracture energy in three different lightweight concretes: DLWAC₁ (dry LWAC with aggregate moisture content 0.1%), WLWAC₁ (wet LWAC with aggregate moisture content 7.9%), and WLWAC*₁ (wet LWAC with aggregate moisture content 12.5 %). It is known from the literature [Ruiz et al., 2010] that the loading-rate for high-strength concrete affects the load-displacement curves used for the calculation of fracture energy. Previous tests have shown that the maximum load increases with an increase in loading rates, yet the corresponding displacement remains almost constant. The fracture energy value increases with the loading rate from 0.01 mm/s. The goal was to investigate whether this phenomenon is even greater for high-strength LWAC.

This type of test was also important for classifying material as brittle, quasi-brittle or ductile.

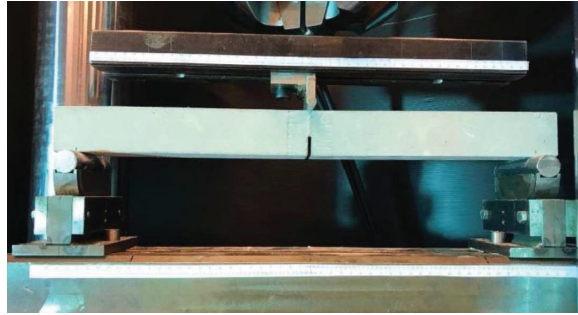


Figure 8: Three-point bending test configuration.

The effect of the aggregate moisture and water/cement ratio on the loading rate sensitivity was also checked. The results showed that increasing the loading rate leads to enhancement of the load-bearing capacity and the fracture energy of the concrete. These results are promising bearing in mind that LWAC in general and high-strength LWAC in particular are brittle in nature, with fast crack and fracture development. Representative load displacement plots of the concrete specimens tested are illustrated in Figure 9.

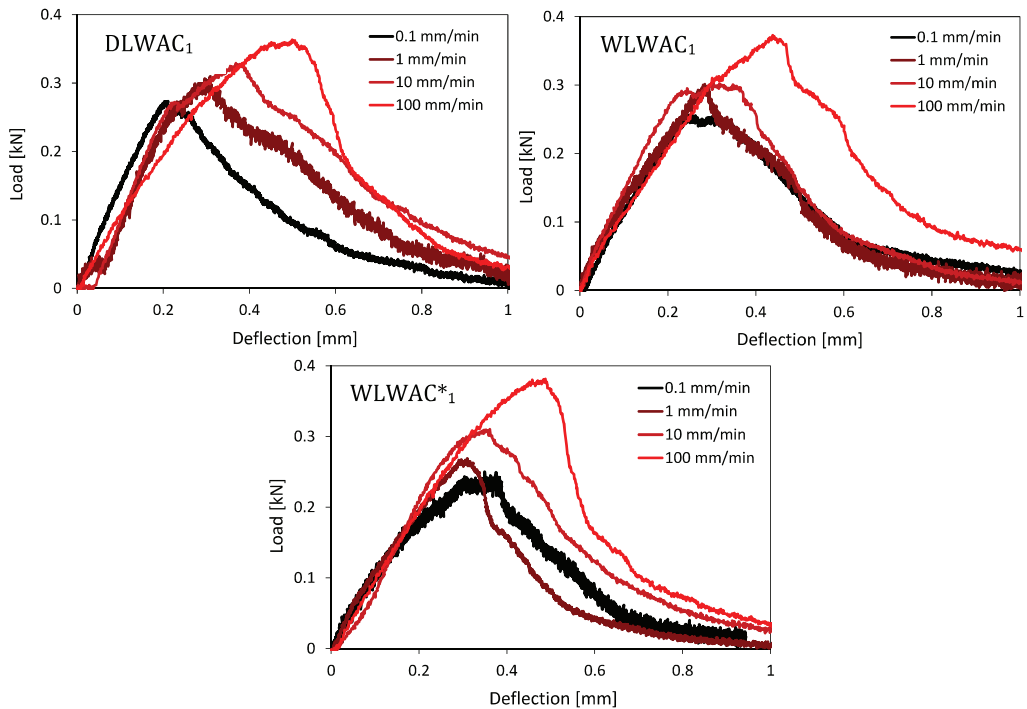


Figure 9: Representative load displacement response of the pre-cracked concrete specimens under three-point bending.

All the prisms showed ductile behaviour; after peak load was reached, the load fell slightly until final failure happened. Through qualitative visual inspection of the fracture, it was observed that the concrete with the saturated aggregate (i.e. WLWAC*₁ with compressive strength above 60 MPa) had the most explosive fractures.

Increasing the loading rate resulted in higher peak load values in all three different concrete specimens, see Figure 10. The concrete with the low water-saturated aggregate (WLWAC₁) had somewhat lower loading rate sensitivity than the concrete with dry aggregate. This can be related to the lower ductility of this concrete compared to DLWAC₁. On the other hand, increasing the moisture of the aggregate to a higher level in WLWAC*₁ results in a higher water-to-cement ratio, leading to lower strength, making it the most loading-rate sensitive concrete in this study. For more results see the paper in annex A.

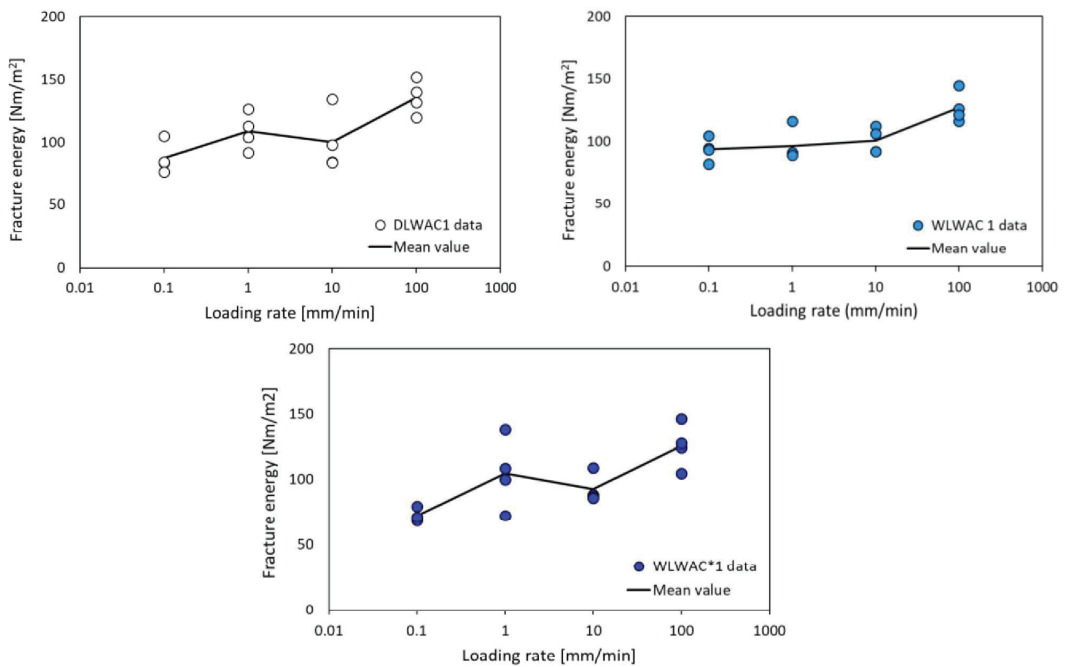


Figure 10: Fracture energy versus loading rate for the pre-cracked concrete specimens under three-point bending.

4. Summary of papers

4.1. The context of work

The methodology, results and main findings for the experimental programme are described in detail in the journal publications. Figure 11 shows how the papers are interrelated to accommodate the main objectives of the thesis. To start with, it was necessary to obtain knowledge about LWAC with Stalite as aggregate (Paper I), and check and understand the performance and measuring techniques that could capture post-peak material behaviour. The requirement was to test high-strength LWAC with a cylinder compressive strength of 60 MPa or greater. Next, we needed to move on to the main objective of this PhD study, to increase knowledge and our understanding of the ultimate response of LWAC members exposed to compression and bending (Paper II and Paper IIa). We also wanted to investigate existing models and compare the results with models in the design codes. Based on the mechanical properties found in Paper I, brittleness and crack propagation were studied in beams experiencing shear failures in Paper III.

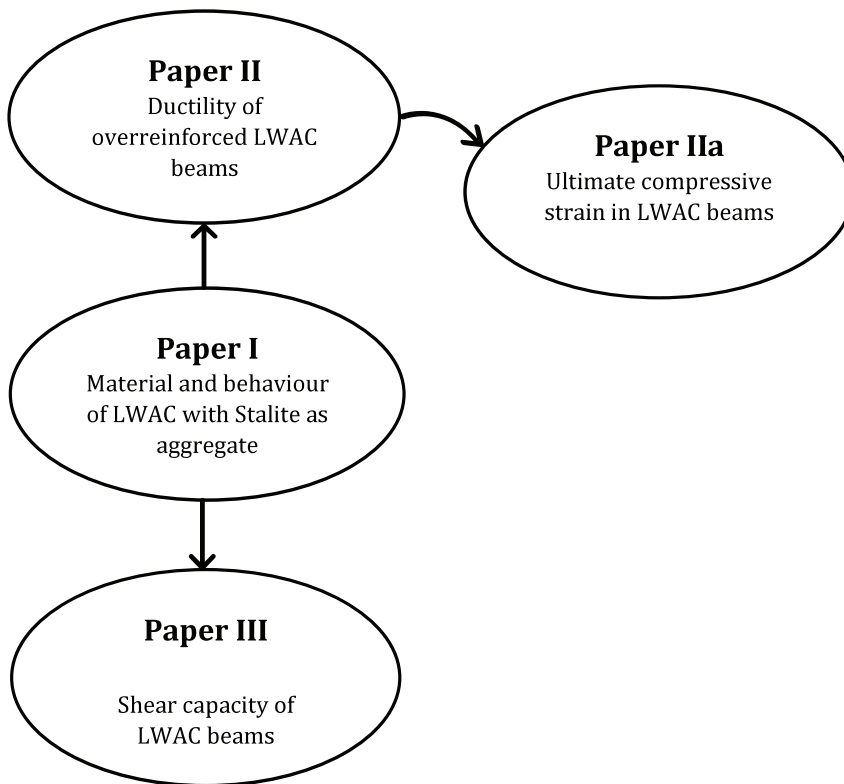


Figure 11: Interrelation of papers.

4.2. Paper I

The main objective in the research for this paper was to provide mechanical properties for LWAC mixes, with dry and saturated lightweight aggregates, and with the addition of fibres. We investigated the behaviour of LWAC under compression and with stress gradients to establish a base and starting point for the large-scale beam experiments. We also tested digital image correlation (DIC) methodology in combination with standard measuring equipment, LVDTs and SGs, to capture as much deformation as possible in the samples tested, see Figure 12. The experimental programme investigated three kinds of LWAC, which were used for the production of 21 prisms. The first two LWACs used dry (0.10% moisture content) or saturated (7.9% moisture content) aggregate.

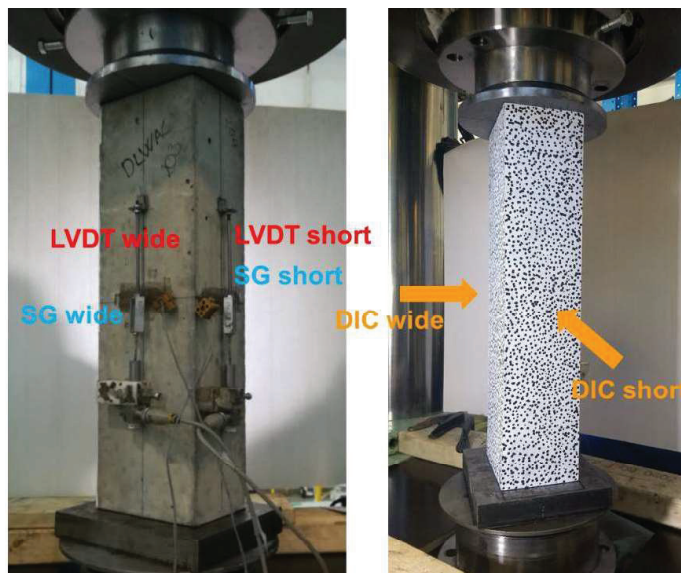


Figure 12: Set-up of measuring devices DIC vs LVDTs and SGs.

The third LWAC used saturated aggregate but also included a small amount (0.5% of volume) of PVA fibres. The prisms were $100 \times 140 \times 480$ mm (width \times length \times height). The samples were loaded centrally and eccentrically in compression. The measuring equipment was able to capture the response of the prisms and the strain level obtained was much higher than expected, especially for the third set of concrete samples with PVA fibres. The strains recorded were in the range from 3.08‰ to 6.82‰. The presence of the PVA fibres contributed significantly to an increased ductility in the third set and brittleness was avoided. Qualitative visual inspection of the LWAC with dry aggregate registered lower brittleness and a combined cracking path, both through and around the aggregate.

All three LWACs with Stalite showed ductile behaviour followed by very high strains. The maximum strain at peak load in compression was approximately 30% greater than predicted by the standards [EN-1992-1-1, 2004; NS3473; NS-EN 1992-1-1:2004+NA:2008, 2008], see Table 5.

Table 5: Comparison of the experimentally determined max strain when prism was centrally loaded with strain obtained from EC2 standard, and comparison of prism and cube compressive strength

Concrete mix	Max strain with centric loading $\mathcal{E}_{cu,exp}$ [mm/m]	Corresponding strain from EC2 $\mathcal{E}_{cu,EC2}$ [mm/m]	% $[\mathcal{E}_{cu,EC2} / \mathcal{E}_{cu,exp}]$	f_{cp} [MPa]	f_c [MPa]	Geometry factor f_c/f_{cp}
DLWAC ₁ [kN]	3.08	2.59	84.1	57.5	77.9	0.73
WLWAC ₁ [kN]	3.4	2.55	75	53.3	80.7	0.66
WLWAC* ₁ [kN]	2.94	2.59	88.1	46.7	77.6	0.60

Mix WLWAC*₁ had strength lower than 60 MPa and was not further considered

f_{cp} : prism compressive strength

f_c : cube compressive strength, average value tested at the same day as prisms

4.3. Paper II

The research for this paper investigated ductility in compression and bending in large-scale beams with reinforcement introducing a confinement effect in LWAC with Stalite as aggregate. Six over-reinforced beams with a compressive strength of 65 MPa and a geometry of 210–330 x 550 x 4500 mm (width x height x length) were subjected to a four-point bending test. The varying parameters in the compressive zone of the beams were the spacing of transverse reinforcement (stirrups), the amount of longitudinal compressive reinforcement, and the thickness of concrete cover. The pre-peak behaviour was similar for all the tested beams, and the ultimate compressive strain at peak load in all the beams was approximately 3.5‰, which is similar to the level expected for NWC. Beams without stirrups or with large stirrup spacing had a very brittle response after peak load. As expected, the beams with more stirrups showed a ductile response and were able to withstand a high level of load, with increasing deflection and spalling of the concrete cover after maximum load, before concrete crushing in the compression zone.

The paper compares existing theoretical material models, the Mander model and the SINTEF FCB model [Mander et al., 1988a; Hansen et al., 1990 and 1993], with the experimental results. The models overestimate the peak stress, and the ascending branch in the models is somewhat steeper than in the experimental results. The SINTEF model gives better predictions of ultimate strains and the E-modulus, while the Mander model mostly overestimates these values. Neither model directly

includes the Poisson ratio, which influences the confinement, and which is slightly lower for LWAC than for NWC.

With reduced stirrup spacing, the ultimate capacity, deflection and ductility all increased. Concrete confined with increased longitudinal compressive reinforcement showed the greatest ultimate capacity, but post-peak behaviour was influenced by stirrup spacing. Stirrup distribution provided greater lateral pressure on the compressive zone and therefore greater ultimate compressive strength and ductility. In summary, it is possible to increase the ductility of LWAC structures by appropriate reinforcement detailing and achieve results close to the response of NWC structures.

4.4. Paper IIa

This paper was motivated by the achievements and conclusions from Paper II. In practice, the major concern about using lightweight aggregate concrete (LWAC) in structural applications is attached to its more brittle post-peak material behaviour and reduced ultimate strain, especially in compression. In beam tests, ultimate compressive strains measured using DIC combined with strain gauges and LVDTs were in the range of 3.4–3.8‰. This indicates that the standards underestimate ultimate compressive strain in LWAC structures.

4.5. Paper III

The main findings in this paper are related to research where failure depends on the tensile strength of this type of LWAC. Rapid crack propagation and brittleness are among the main disadvantages of LWAC and they affect the behaviour of the concrete wherever the tensile strength is important, as for instance in shear strength. To analyse this, we carried out shear tests on beams with and without shear reinforcement under four-point bending. This experimental investigation involved five beams made of lightweight concrete with Stalite as aggregate. The main goals were to investigate the behaviour and capacity of the beams with and without shear reinforcement when subjected to a four-point bending test and then compare those results with previous experimental work, see Figure 14. The main test parameters were the shear span ratio (a/d) and the amount of the shear reinforcement. Where the load was closer to the supports and the percentage of steel in the beam was high, the inclined crack penetrated deeply into the compressive zone at a load level well below that corresponding to yielding of flexural bars. This result, with higher stresses and strength of beams, shows failure happened below the theoretical full flexural capacity. For beams with the larger shear

span ratio (4.0), the calculations predicted by the standards match well with the experimental results, while the standards greatly underestimate the ultimate capacity in beams with the lower shear span ratio (2.3). Comparison with similar tests on other types of lightweight concretes and normal density concretes also showed that the shear stress at inclined cracking of the beams decreased with an increase in shear span ratio (a/d).

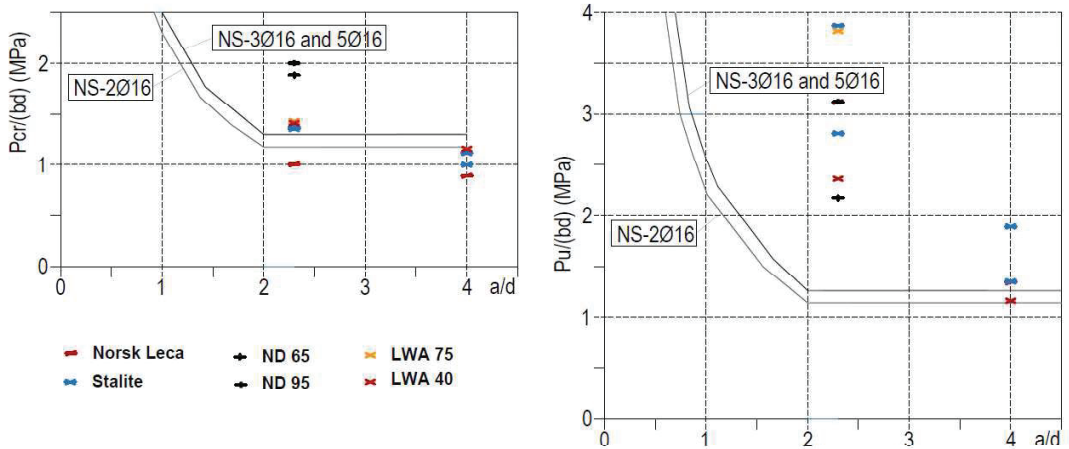


Figure 14: Comparison with previous experimental work.

For concretes tested in this experiment and in previous investigations, the ratio between the load observed at diagonal cracking and the predicted strengths was within the same range. However, the ratio between the observed load at failure and the strengths predicted was significantly higher for the lightweight concrete used in this investigation. Existing standards underestimate shear capacity because they do not differentiate between shear span values (a). The beams tested were more ductile than expected, and cracking was similar to that observed in normal weight concrete beams. This experimental investigation shows that the design strength for shear in beams without shear reinforcement should be based on inclined cracking loads.

5. Conclusions

This project encompassed research experiments necessary to create a design base for lightweight aggregate concrete with Stalite as aggregate.

Work started with small-scale experiments in which the main material characteristics and measuring techniques were tested. The ductility of structural members arises from local triaxial stress

conditions that develop within the compressive zone prior to failure. The higher the triaxial stress at a critical cross section, the greater the corresponding strains, and the greater the resulting ductility of the structure. This stress develops just prior to failure, so only ductility is affected and not the maximum load-carrying capacity of the structural member. The use of LWAC concrete leads to less stress triaxiality in a member as a result of smaller transverse expansion of the concrete prior to failure. This explains why the ductility of LWAC members is somewhat less than with conventional concrete.

Due to its brittle nature, LWAC has a much more explosive crack formation than NWC. The brittle crack propagation process in LWAC influences the spalling of the concrete cover in a compression zone. Once started, the cracks often propagate immediately to failure. This is due to the low strength of the LWA, resulting from cracks often going through the aggregate. In this research, the situation was different due to the moisture conditions of the LWA used. A strong ITZ was created and the resulting aggregate interlock strongly affected brittleness and crack propagation. The cracking line went both through and around the aggregate, resulting in higher strains and ductility in the structural member. The aggregate interlock effect depends a lot on the type of aggregate, but the standards do not differentiate between different types of LWAs, which means that the standards automatically underestimate the characteristics of LWAC structures.

At the material level, it was noticed that the moisture content in aggregate influences the cracking path, making a big difference between DLWAC and WLWAC. WLWAC showed the most brittle and explosive behaviour. With just a small addition of PVA fibres, FLWAC concrete, ductility was significantly increased, brittleness reduced, and without spoiling the concrete after failure. Ductility is calculated by using the D-ductility index, and FLWAC has the highest.

The fracture energy tests, as a measure of brittleness, classified LWAC with aggregate Stalite as a quasi-brittle material, and values for the fracture energy and characteristic length lie between other LWAC concretes (with Leca and Liapor) and normal weight concretes. Increasing the loading rate results in higher peak-load values in all three kinds of concrete. According to the test results, increasing the loading rate from 0.1 mm/min to 1 mm/min resulted in slightly higher fracture energy, while the lowest and the highest fracture energy values were obtained when the specimens were tested at 0.1 mm/min and 100 mm/min respectively. The LWAC in which the aggregate had the highest moisture content was the most loading-rate-sensitive concrete in this study.

The large-scale beams test demonstrates one of the main hypotheses: the large effect small secondary stresses have on compressive strength. The measuring techniques, DIC, SGs and LVDTs, were in a good agreement and able to capture the ultimate behaviour of the LWAC. DIC enabled detailed strain fields to be observed and showed that the max registered strain is slightly higher. The DIC pictures enabled localization of strains, while the LVDTs measured average strains over a given distance. The test results indicate that the beams with reduced stirrup spacing had the most ductile behaviour. Increasing the longitudinal compressive reinforcement caused only a slight increase in ductility but contributed the most to an enhancement in load-carrying capacity. Beams with smaller concrete cover showed somewhat greater ductility as a result of a smaller drop in residual cross section, while beams with more concrete cover had greater load-carrying capacity followed by less ductility. Generally, when the top concrete cover is thicker, less of the cross section will be confined, and a reduction in confinement will generally lead to less ductile behaviour.

The second large-scale beam experimental programme contributed to a better understanding of the lower tensile strength in LWAC and the shear capacity of the beams. The shear stress at inclined cracking of the beams decreased with an increase of the shear span-to-effective-height ratio (a/d). For beams with larger shear span ratio (4.0), the calculations predicted by the standards match well with the experimental results, while the standards greatly underestimate the ultimate capacity in beams with the lower shear span ratio (2.3). The calculation of the shear capacity according to existing standards does not take into account the position of the load or the shear span (a). The standards only differentiate between beams with or without shear reinforcement. This experimental investigation showed that the design strength for shear in beams and slabs without shear reinforcement should be based on inclined cracking loads.

This thesis reviewed existing material models and two of them showed the best potential for presenting the behaviour of LWAC: the Mander model and the SINTEF FCB model [Mander et al., 1988a; Hansen et al., 1990 and 1993]. Measured strains and calculated stresses from high strain distribution in large-scale beam experiments were compared with existing Mander and SINTEF FCB models. Both models overestimate the peak stress, and the ascending branch in the models is somewhat steeper than in the experimental results. The SINTEF model gives better predictions of ultimate strains and the E-modulus, while the Mander model mostly overestimates these values. Neither model directly includes the Poisson ratio, which influences the confinement and is slightly lower for LWAC than for NWC.

EC2 has special rules for LWAC. The standard contains reduction factors and special regulations that are applied to regular design criteria. The results in this study indicate that EC2 underestimates LWAC, because the maximum strains measured in the beams were 1.3–1.5 times greater than EC2 allows for this type of concrete.

In general, LWAC with Stalite aggregate was much more ductile than expected, and the structural performance of beam elements made from LWAC with Stalite is very similar to those one made from NWC.

6. Future research

The research for this thesis investigated the material and structural behaviour in compression and bending of LWAC with aggregate Stalite. The broad experimental programme included all the necessary tests to create a design base for this type of concrete. However, there is still room for improvement and future research in the field of interest.

Improvements in current standard documentation

The characteristics of LWAC mostly depend on the type of LWA used. EC2 does not differentiate between different types of LWAs used in LWAC. The experimental results of this study indicate that EC2 underestimates Stalite as an aggregate. Since LWAC with Stalite showed behaviour similar to NWC in this study, investigation of LWAC as a structural material should be continued.

Measuring devices during experimental programme

The DIC generally showed very good agreement with the standard measuring devices and was the only methodology able to capture load after failure. To provide realistic behaviour of any concrete and to register triaxial stresses, a 3D DIC set-up will be needed, though it may be possible to make do with a 2D set-up. The confining pressure is crucial for the confined concrete, so in order to capture three-dimensional expansion of cross/section there is a need for measuring devices in all three directions.

Long-term loading

Nowadays we are all witnesses of the extended service life of many structures, so it will be nice to

see the structural performance of this type of LWAC exposed to long-term loading. This is a very challenging task because it requires a long-term experimental programme.

Confinement material model

It is possible to develop a confinement material model in compression which depends on the type of lightweight aggregate. This material model should include a density dependent E-modulus and the Poisson's ratio.

7. References

- ACI 211.2-91. (1991). Standard Practice for Selecting Proportions for Structural LWAC.
- ACI213R-03. (2003). Guide for structural lightweight aggregate concrete (ACI Committee 213). Farmington Hills, MI: American Concrete Institute.
- ACI 304.5R-91. (1991). Batching, Mixing and Job Control of Lightweight Concrete.
- ACI-ASCE Committee 426. (1973). The Shear Strength of Reinforced Concrete Members. ASCE, *Journal of the Structural Division* 99(6), 1091–1187.
- Ahmad S.H., Xie Y., Yu T. (1995). Shear Ductility of Reinforced Lightweight Concrete Beams of Normal Strength and High Strength Concrete, *Cement & Concrete Composites* 17(2), 147–159.
- Anwar N. and Najam F.A. (2016). Structural Cross-Sections: Analysis and Design. Chapter 6 – Ductility of cross-sections. Butterworth-Heinemann, 391–481.
- Asgeirsson H. (1994) Hekla Pumice in Lightweight Concrete. The Icelandic Building Research Institute (IBRI) Publication no. 66, 45 pp.
- Bjerkeli L., Tomaszewicz A., & Jensen J.J. (1990). Deformation properties and ductility of high-strength concrete. *High-Strength Concrete: Second International Symposium*, American Concrete Institute, Detroit, MI., 215–238.
- Bjerkeli L. and Tomaszewicz A. (1987). High-strength concrete. SP1 Beams and Columns. Report 1.1: Ductility of spirally reinforced columns. SINTEF Report STF65 F87040.
- Bjerkeli L. and Tomaszewicz A. (1988). High-strength concrete. SP1 Beams and Columns. Report 1.2: Ductility of reinforced small-scale square columns. SINTEF Report STF65 F88051.
- Bjerkeli L. and Tomaszewicz A. (1988). High-strength concrete. SP1 Beams and Columns. Report 1.3: Ductility of reinforced large-scale rectangular columns. SINTEF Report STF65 F88068.
- Bjerkeli L., Tomaszewicz A. (1988). High-strength concrete. SP1 Beams and Columns. Report 1.5: Ductility of eccentrically loaded square columns. SINTEF Report STF65 F88068.
- Bologna G. (1974). Lightweight Aggregate Concrete: Technology and World Applications. Cembureau, Associazione Italiana Technico Economica del Cemeto, pp 312.
- Bouafia Y., Iddir A., Kachi M.S., Dumontet H. (2014). Stress-strain relationship for the confined concrete. *Proceedings of joint WCCM XI, ECCM V and ECFD VI, Barcelona, Spain*.
- Castrodale R.W., Valum R. and Harmon K.S. (2017). High-Performance Lightweight Concrete Bridges and Buildings. *Proceedings of The Eleventh High Performance Concrete (11th HPC) & The Second Concrete Innovation Conference (2nd CIC)*, Tromsø, Norway, Paper no. 40.
- Chandra S. and Berntsson L. (2003). Lightweight Aggregate Concrete. Noyes Publications, New York.

- Chandra S. and Leif B. (2002). *Lightweight Aggregate Concrete*. USA. Noyes publications-William Andrew Publishing.
- Chapman D.D. and Castrodale R.W. (2016). Sand Lightweight Concrete for Prestressed Concrete Girders in Three Washington State Bridges. *Proceedings of the 2016 National Bridge Conference*, Nashville. Precast/Prestressed Concrete Institute, Chicago, Paper 81, 22p.
- Cousins T., Roberts-Wollmann C. and Brown M.C. (2013), High-Performance/High-Strength Lightweight Concrete for Bridge Girders and Decks. National Cooperative Highway Research Program, Report 733. Transportation Research Board, Washington, DC.
- CUR report 173(1995). Structural Behaviour of Concrete with Coarse Lightweight Aggregates. CUR-Centre for Civil Engineering Research and Codes, Gouda, Netherlands.
- den Uijl J.A., Stroband J. and Walraven J.C. (1995). Splitting Behaviour of Lightweight Concrete. *CEB/FIP International Symposium on Structural Lightweight Aggregate*, Sandefjord, Norway, 154–163.
- Elias H.E. and Durrani A.J. (1988). Confinement of Prestressed Concrete Columns. *PCI Journal* 33(3), 123–141.
- EN-1992-1-1 (2004). Eurocode 2, Design of concrete structures – Part 1-1: General rules and rules for buildings. Brussels, Belgium: CEN European Committee for Standardization.
- EuroLightCon. Document BE96-3942/R2 (1998). Lwac Material Properties.
- EuroLightCon. Document BE96-3942/R4 (1999). Methods for Testing Fresh Lightweight Aggregate Concrete.
- EuroLightCon. Document BE96-3942/R8 (2000). Properties of lightweight concretes containing Lytag and Liapor.
- EuroLightCon. Document BE96-3942/R36 (2000). High strength LWAC in construction elements.
- Fagerholt E. (2012). Field measurements in mechanical testing using close-range photogrammetry and digital image analysis (PhD Thesis), Norwegian University of Science and Technology, Department of Structural Engineering, Trondheim, Norway, 167 pp.
- Fayyada T.M. and Leesb J.M. (2014). Application of Digital Image Correlation to Reinforced Concrete Fracture. *Procedia Materials Science* 3, 1585–1590.
- Fib bulletin 8. Lightweight aggregate concrete. (2000). Lusanne (Switzerland): International Federation for Structural Concrete.
- Fib International Federation for Structural Concrete: fib Model Code for concrete Structures 2010. Ernst & Sohn, Berlin (2013).
- Fib/CEB Bulletin Information (1990). High strength concrete. State of the art report, No 197.
- Filaj E., Seranaj A. and Leka E. (2016) Confined Concrete Behavior Influencing Factors. *International Research Journal of Engineering and Technology (IRJET)* 3(7), 36–44.
- Ge Y., Kong L., Zhang B. and Yuan J. (2009). Effect of Lightweight Aggregate Pre-wetting on Microstructure and Permeability of Mixed Aggregate Concrete. *Journal of Wuhan University of Technology-Mater. Sci. Ed.* 24(5), 838–842.
- Guo Z. (2014). Principles of Reinforced Concrete. Elsevier
- Hansen E.A. and Tomaszewicz A. (1990). High-strength concrete. SP1 Beams and Columns. Report 1.8: Confinement models. SINTEF Report STF65 F90071.
- Hansen E.A. (1993). High-strength concrete. SP1 Beams and Columns. Report 1.6: Ductility of overreinforced beams. SINTEF Report STF70 A93079.
- Haug, A.K. and S. Fjeld. (1996). A floating concrete platform hull made of lightweight aggregate concrete. *Engineering Structures* 18(11), 831–836.

- Helland I., Holand I. and Smepllass S. (2000). Proceedings of Second International symposium on structural lightweight aggregate concrete, Kristiansand, Norway. Norwegian Concrete Association.
- Hillerborg A. (2005), The theoretical basis of a method to determine the fracture energy GF of concrete, *RILEM Technical Committees, Materials and Structures*, 18(4),291–296.
- Holand I., Hammer T.A. and Fluge F. (1995). Proceedings of International Symposium on Structural Lightweight Aggregate Concrete, Sandefjord, Norway. Oslo: Norwegian Concrete Association.
- Jensen T.M. and Øverli J.A. (2013). Experimental study on flexural ductility in over-reinforced lightweight aggregate concrete beams: FA 3 Aesthetics and technical performance SP 3.3. Structural Performance, COIN Project report no 47, 2013.
- Kent D.C. and Park R. (1971). Flexural members with confined concrete. *Journal of the Structural Division, Proc. of the American Society of Civil Engineers*, 97(ST7), 1969–1990
- Kotsovos M.D. (1983). Effect of testing techniques on the post-ultimate behaviour of concrete in compression. *Materials and Structures* 16(1), 3–12.
- Kuraray Co: Characteristics of KURALON (PVA fibres), PVA fibres application. Japan, available: <http://kuralon-frc.kuraray.com/whats/characteristics>
- Leca-lightweight aggregate, available: <https://leca.asia/>
- Liapor-lightweight aggregate, available: <http://www.liapor.com/en/applications/structural-engineering/insulating-concrete/high-density-lightweight-concrete/what-is-high-density-lc-r.html>
- Lin S. (2015). Strain Measurement by Digital Image Correlation, DESY Report.
- Lo T.Y., Tang W.C., Cui H.Z. (2007). The effects of aggregate properties on lightweight concrete. *Building and Environment* 42(8),3025–3029.
- Mander J.B. (1983). Seismic design of bridge piers. PhD Thesis, Univ. of Canterbury, New Zealand.
- Mander J.B., Priestley M.J.N., and Park R. (1988a). Observed stress-strain behavior of confined concrete. *Journal of Structural Engineering*, 114(8), 1827–1849.
- Mander J.B., Priestley M.J.N. and Park R. (1988b). Theoretical stress-strain model of confined concrete. *Journal of Structural Engineering*, 114(8), 1804–1826.
- Markeset G. (1993). Failure of concrete under compressive strain gradients. *Bulletin No.110 (PhD Thesis)*, Norwegian Institute of Technology, Department of Structural Engineering, University of Trondheim, Trondheim, Norway, 168 pp.
- McCormick N. and Lord J. (2012). Digital Image Correlation for Structural Measurements. *Proceedings of the Institution of Civil Engineers – Civil Engineering* 165(4),185–190.
- Melby K. (2000). Use of high strength LWAC in Norwegian bridges. Paper presented at the International symposium on structural lightweight aggregate concrete, Norwegian Concrete Association, Kristiansand, Norway, June 18–22.
- Nahhas T.M. (2013). Flexural behavior and ductility of reinforced lightweight concrete beams with polypropylene fiber. *Journal of Construction Engineering and Management* 1(1), 4–11.
- Nedrelid H. (2012). Towards a better understanding of the ultimate behaviour of lightweight aggregate concrete in compression and bending. *Bulletin No.123 (PhD Thesis)*, Norwegian University of Science and Technology, Department of Structural Engineering, Trondheim, Norway, 214 pp.
- Newman J.B. and Owens P. (2003). Advanced Concrete Technology, Chapter 2 – Properties of Structural Lightweight Concrete. Butterworth-Heinemann, Elsevier, Oxford, Great Britain pp25.
- NS-EN 1992-1-1:2004+NA: 2008. (2008). Eurocode 2: Design of concrete structures – General rules and rules for buildings, Standard Norway.

- NS 3473 (2003). Concrete structures – Design and detailing rules, Norges Standardiseringsråd – Norwegian Standard Institution. Norge.
- NS 3576-3:2012. (2012). Armeringsstål – mål og egenskaper – del 3: Kamstål B500NC. Standard Norge.
- NS-EN 12390-3:2009. (2009). Testing hardened concrete – Part 3: Compressive strength of test specimens Lysaker: Standard Norway.
- NS-EN 12390-6:2009. (2009). Testing hardened concrete – Part 6: Tensile strength of test specimens Lysaker: Standard Norway.
- NS-EN 12390-7:2009. (2009). Testing hardened concrete – Part 7: Density of hardened concrete. Lysaker: Standard Norway.
- NS 3676. (1987) Concrete testing – Hardened concrete – Modules of elasticity in compression. Norway: Standard Norway.
- NS-EN 206:2013+NA: 2014. (2014). Betong, Spesifikasjon, egenskaper, framstilling og samsvar, Norges Standardiseringsråd, Norge. (in Norwegian)
- Øverli J.A. (2017). Towards a better understanding of the ultimate behaviour of LWAC in compression and bending. *Engineering Structures* 151,821–838.
- Øverli J.A. and Jensen T.M. (2014). Increasing ductility in heavily reinforced LWAC structures. *Engineering Structures*, 62–63, 11–22.
- Popovic S. (1973). A Numerical Approach to the Complete Stress Strain Curves for Concrete. *Cement and Concrete Research* 3(5), 583–599.
- Radic J., Markic R., Harapin A., Matesan D. (2013). Effect of confined concrete on compressive strength of RC beams. *Advances in concrete Construction* 1(3), 215–225.
- RILEM TC 148-SSC (2000). Strain softening of concrete – Test methods for compressive softening, Test method for measurement of the strain-softening behavior of concrete under uniaxial compression. *Materials and Structures* 33, 347–351.
- Ruiz G., Zhang X.X., Yu R.C., Porrás R., Poveda E., del Viso J. (2010). Loading rate effect on the fracture behaviour of high-strength concrete. *EPJ Web of Conferences* 6, 23007. https://www.epj-conferences.org/articles/epjconf/pdf/2010/05/epjconf_ICEM14_23007.pdf
- Savija B., Lukovic M., Kotteman G., Chaves F.S., de Mendonça Filho F.F. & Schlangen E. (2017). Development of ductile cementitious composites incorporating microencapsulated phase change materials. *International Journal of Advances in Engineering Sciences and Applied Mathematics* 9(3), 169–180.
- Shah S.P., Naaman A.E., Moreno J. (1983). Effect of confinement on the ductility of lightweight concrete. *The International Journal of Cement Composites and Lightweight Concrete* 5(1), 15–25.
- Sheikh S.A. and Uzumeri S.M. (1982). Analytical Model for Concrete Confinement in Tied Columns. *Journal of the Structural Division*, 108, 2703–2722.
- SINTEF procedure KS14-05-04123 (2007). Fracture energy of prisms with notch in three point bending test, SINTEF Byggeforsk, Trondheim, Norge (in Norwegian).
- Skjølsvold O, Bakken N & Johansen E. (2007). Bestemmelse av E-modul iht NS3676 Losenhausen 5000kN trykkpresse. Betong og natursteinslaboratooriene, KS 14-05-04 122, SINTEF Byggeforsk, Trondheim, Norge (in Norwegian).
- Smeplass S. (1992). Mechanical Properties – Lightweight Concrete. High Strength Concrete. SP4 – Materials Design, SINTEF.
- Spitzer J. (1995). A Review of the Development of Lightweight Aggregate – History & Actual Survey. *International Symposium on Structural Lightweight Aggregate Concrete, Sandefjord, Norway*, 13–21.

- Stalite Structural (2020). <https://www.stalite.com/lwa-benefits>
- Stemland H. (2012). Fracture energy and characteristic length values for Hebron concrete. SINTEF report D6/09-Apr-2012.
- Sørensen S.I. (2013). Betongkonstruksjoner, Beregning og dimensjonering etter Eurokode 2, 2. utgave (in Norwegian).
- TEC Services Project No: 04-0514, TEC Services Sample ID: 14-999 (2015). Interim report of ASTM c330 Carolina Stalite 0, 5 inch coarse lightweight aggregate. TEC Services.
- Thorenfeldt E., Tomaszewicz A. and Jensen J.J. (1987). Mechanical properties of high-strength concrete and application in design. *Proceedings of the Symposium on Utilization of High-Strength Concrete, Tapir, Trondheim, Norway*, 149–159.
- Thorenfeldt E. and Stemland H. (1995). Shear capacity of lightweight concrete beams without shear reinforcement, *International Symposium on Structural Lightweight Aggregate Concrete, Sandefjord, Norway*, 244–245.
- Thorenfeldt E. (1995). Design Criteria of Lightweight Aggregate Concrete. *CEB/FIP International Symposium on Structural Lightweight Aggregate Concrete, Sandefjord, Norway*, 720–732.
- Van den Berg F.J. (1962). Shear Strength of Reinforced Concrete Beams Without Web Reinforcement, Part 2, *ACI Journal Proceeding* 59(11), 1587–1600.
- Watanabe K., Niwa J., Yokota H. and Iwanami M. (2004). Experimental Study on Stress Strain Curve of Concrete Considering Localized Failure in Compression, *Journal of Advanced Concrete Technology* 2(3), 395–407.
- William K.J., and Warnke E.P. (1975). Constitutive model for the triaxial behavior of concrete. *Proceedings of International Association for Bridge and Structural Engineering* 19(3), 1–30.
- Yong Y.K, Nour M.G. and Nawy E.G. (1988). Behavior of Laterally Confined High-Strength Concrete under Axial Loads, *Journal of Structural Engineering, ASCE*, 114(2), 332–351.
- Zararis P.D. and Papadakis G.C. (2001). Diagonal Shear Failure and Size Effect in RC Beams without Web Reinforcement. *Journal Structural Engineering* 127(7), 733–742.
- Zhang J.P. (1997). Diagonal cracking and shear strength of reinforced concrete beams, *Magazine of Concrete Research* 49(178), 55–65.
- Zhang M.H. and Gjorv O.E. (1995). Properties of high-strength lightweight concrete, *CEB/FIP International Symposium on Structural Lightweight Aggregate*, Sandefjord, Norway, 683–693.
- Zhenhai G. (2014). Principles of Reinforced Concrete. Chapter 9 – Confined Concrete. Butterworth-Heinemann, pp 221–252.

Part II - Appended papers



Paper I

Failure of Lightweight Aggregate Concrete in Compression under Stress Gradients

Zivkovic, J. and Øverli J.A.

Nordic Concrete Research, 2019, Vol.60, Issue 1, 51–66
DOI: 10.2478/ncr-2019-0011 / accepted June 25, 2019

A large, bold, white number '1' is centered on a solid black rectangular background.

	
© Article authors. This is an open access article distributed under the Creative Commons Attribution-NonCommercial-NoDerivs licens. (http://creativecommons.org/licenses/by-nc-nd/3.0/).	ISSN online 2545-2819 ISSN print 0800-6377
DOI: 10.2478/ncr-2019-0011	Received: April 1, 2019 Revision received: June 21, 2019 Accepted: June 25, 2019

Failure of Lightweight Aggregate Concrete in Compression under Stress Gradients



Jelena Zivkovic
M.Sc. PhD-candidate
Department of Structural Engineering
Faculty of Engineering Science
Norwegian University of Science and Technology
N-7491 Trondheim, Norway
e-mail: jelena.zivkovic@ntnu.no



Jan Arve Øverli
PhD, Professor
Department of Structural Engineering
Faculty of Engineering Science
Norwegian University of Science and Technology
N-7491 Trondheim, Norway
e-mail: jan.overli@ntnu.no

ABSTRACT

The objective of this experiment is to investigate the behaviour of lightweight aggregate concrete (LWAC) under compression and with stress gradients. Experimental program contained three sets of LWAC which were used for production of 21 prisms. Lightweight aggregate argillite slate, called Stalite, from North Carolina had been used. The sets differed in using dry (0.10% moisture content) or saturated (7.9% moisture content) aggregate. The third set included a small amount of polyvinyl alcohol fibres (PVA). The geometry of the prisms were 100 × 140 × 480 mm (width × length × height). Prismatic samples were loaded centrally and eccentrically in compression.

From the achieved experimental results, it is visible that the lateral deformation of the most stressed fibre is counteracted by the less stressed fibres that confine compressive stress and increase strains. The obtained strain level was much higher than expected, especially for the third set of concrete samples with PVA fibres. Recorded strains in prisms test was in range from 3.08‰ to 6.82‰). In general, LWAC with Stalite showed ductile behaviour followed with very high strains. The third set of samples included a small amount of polyvinyl alcohol fibres (0.5% of volume fractions) was even more ductile and non-brittle.

Key words: Lightweight Aggregate Concrete, Testing in Compression, Strain level, Centric and Eccentric Loading, Stress Gradients

1. INTRODUCTION

1.1 General

This investigation is part of the ongoing research program “Durable advanced concrete structures (DaCS)”. The part of this program is to investigate structural behaviour of lightweight aggregate concretes (LWAC), concretes with an oven dry density below 2000 kg/m³. The use of lightweight aggregate concrete (LWAC) is limited as a mainstream construction material in structural applications. A reason for that is related to the steepness of the descending branch of the stress-strain curve in compression [1-3]. Material models for compressive failure of concrete are normally based on a uniaxial compressive stress-strain curve obtained from tests, where the main assumption is uniform deformation of the concrete specimens. This assumption is reasonable for the ascending branch of the stress-strain curve, while for the descending branch it is not realistic as it is always accompanied by significant lateral deformations. The lateral deformations are mainly caused by splitting cracks, which are formed and expand during the test. LWAC is characterized by more brittle post-peak material behaviour and uncontrolled crack propagation compared to normal weight concrete (NWC).

In order to describe more in detail, the compressive behaviour and to measure compressive strains, the effect of a stress gradient was introduced and varied in an experimental program. Stress gradients influence both the strength and the ductility [4]. Beam experiments tested in the DACS-project had shown that high strength LWAC with Stalite as aggregate obtained much higher compressive strain levels than expected [1]. The raw material mined by STALITE is an argillite slate located in a geological area known as the Tillery Formation in North Carolina. It is a thinly laminated, grey, fine-grained siltstone, composed of clastic (transported) rock fragments. The Tillery Formation is a complex system that must be selectively mined in order to separate the desirable product from the non-desirable to manufacture a high quality expanded slate aggregate. Raw material is later expanded in a rotary kiln to produce porous structural lightweight aggregate. The cooled, expanded slate is later conveyed to the classification area, where it is crushed and screened into different size fractions. After crushing, the different size fractions are stored in separate silos until they are blended into standard or custom gradation blends. Due to the higher material strength of STALITE slate aggregate, higher strength concretes can be achieved with lower cement contents allowing for more economical concrete mixes [5].

Three sets of test specimens were produced using lightweight aggregate Stalite fraction size ½ inch (12.7 mm), from the same batch, where the water content in aggregate varied between 0.1%

and 7.9%. The present experimental program included three LWACs for the production of 21 prisms. From each concrete, a total of 2x9 + 1x3 prisms and small samples (i.e. cubes and cylinders) were produced. The third set of samples included a small amount of polyvinyl alcohol fibres (0.5% of volume fractions). The geometry of the prisms were 100x140x480 mm (width x length x height). All samples were loaded both, centrally and eccentrically in compression.

The experimental setup of the prisms and the eccentricities were the same as in an earlier experiment and are therefore comparable [4]. The earlier studies looked at the lightweight concrete Liapor 8 and different types of normal weight concrete.

2. EXPERIMENTAL PROGRAMME

2.1 Test specimens

The experimental program consisted of 21 prisms, dimensions 100 × 140 × 480 mm (width × length × height), of plain LWAC which were loaded both centrally and eccentrically in compression. This study looks at the differences of using dry-DLWAC (0.10 % moisture content) or saturated – WLWAC (7.9 % moisture content) aggregate and the influence of adding 0.5% at volume fractions of polyvinyl alcohol fibres – FLWAC. In FLWAC the fibres were combined with the saturated aggregate concrete. The main test variables were the moisture of aggregate and the eccentricity of the loading. For each investigated combination, there were tested 3 samples. The complete test programme is shown in the Table 1.

Table 1-Test program for centrally and eccentrically loaded specimens

Prism No.	Type of concrete	Aggregate moisture [%]	Eccentricity / Number of the specimens		
			$e=0$	$e=h/18$ (140/18 =7.8 mm)	$e=h/6$ (140/6 =23.3 mm)
D1-3 D4-6 D7-9	DLWAC	0.1	3	3	3
W1-3 W4-6 W7-9	WLWAC	7.9	3	3	3
F1 F2 F3	FLWAC	7.9	1	1	1

All prisms had the same geometry that was limited due to capacity of the actuator. The geometry and forms for the prisms are shown in Figure 1. All the specimens were cast vertically in three layers. Each layer was compacted first by stamping by hand and, when the form was filled, by additional compaction using an internal vibrator. The prisms were unmoulded 24 hours after casting and immediately stored in water with the intention of preserving their natural content of moisture to the largest possible extent. The specimens were afterwards stored in the laboratory in water, at the temperature of approximately 20 °C. The bottom of the specimens were prepared for testing by grinding and top of the specimens by sawing (see Figure 1.) and grinding at an age of 28 days.



Figure 1 – Geometry of the prisms (left), Forms for the prisms (centre), Preparation of the prisms (right).

Two days before the testing prisms were taken out from water and prepared for instrumentation. Two sides of the prisms were painted white and highlighted with a black marker for digital correlation method. The strain gauges and Linear Variable Differential Transformers were attached at the two other sides. The test age of the prisms varied from 32 to 60 days.

To establish the mechanical properties of each LWAC, cubes (with dimensions 100×100×100 mm), cylinders (Ø100×200mm) and small beams (100×100×1200mm) were cast to find the stress-strain diagram, the compressive strength for cube and cylinder [6] the tensile strength [7], Young's module of elasticity [8,9], and the fracture energy [10]. All these small specimens were demoulded after 24 hours and kept in water until the testing day. In order to follow material characteristics compression tests on cubes and cylinders were carried out simultaneously with the prisms testing. All the prisms and small samples, cubes and cylinders, were cast from the same concrete batch.

2.2 Material and mix properties

The concrete mixture for each mix DLWAC, WLWAC and FLWAC was prepared from one batch of the aggregate with varying moisture of the aggregate from 0.1% (DLWAC) to 7.9% (WLWAC and FLWAC). The lightweight aggregate was ½" (12.7mm) fraction from Stalite [11]. The moisture content and the absorbed water in the Stalite were measured to be able to design the concrete mix [12]. The moisture content varied from 0.1% to 7.9%, while the absorption for this batch was stable and after 24 hours and 100 hours was 6.58% and 7.72%, respectively. Table 2 gives the concrete mixtures. The mixing was done using two laboratory mixers with capacity of 250 liters and 50 liters. Two different mixing procedures were used. First procedure, called dry, was used for dry-DLWAC mixture, where all dry particles (cement, silica fume and sand) were placed in mixer and mixed for approximately 1 minute. Mixing was constant and aggregate Stalite was added to the rest of dry particles and mixed for 1 min more. Water and superplasticizer were continuously added and adjusted during mixing, until the desired workability of the concrete was achieved. Second procedure, called wet, was used for the wet-WLWAC and fibers-FLWAC mixtures. In the mixer first dry particles cement, silica fume and sand were added and mixed for approximately 30 seconds. Later approximately 70% of water and superplasticizer were added and after 1.5 minute, nice mortar was made. With continuously mixing presaturated aggregate Stalite were added and at the end rest of water and superplasticizer. After 2 minutes, resting and observation of the mixture and workability, additional water were added and superplasticizer until the desired workability of the concrete was achieved.

Table 2 – Concrete mixtures for DLWAC, WLWAC and FLWAC

Constituent weight (1000 liters)	DLWAC Weight [kg/m ³]	WLWAC Weight [kg/m ³]	FLWAC Weight [kg/m ³]
Moisture of the aggregate [%]	0.1	7.9	7.9
Cement (Norcem Anlegg FA)	442.2	440.3	397.5
Silica fume (Elkem Microsilica)	23.3	23.2	20.9
Water (free)	146	180.8	163.2
Absorbed water in Stalite+sand (24 hours)	6.1	38.8	35.9
Water* (added in mixer)	139.9	142	127.3
Sand (Ramlo 0-2 mm)	230	231	377.3
Sand (Årdal (NSBR) 0-8 mm)	536.8	539	531
Aggregate (Stalite 1/2"(12.7mm))	515.4	517.5	493
Superplasticiser (Mapei Dynamon SR-N)	3.3	3.9	6.2
Fibers (Kuralon PVA 8mm)	-	-	6.5
Water*/cement ratio [w/c]	0.32	0.32	0.32

For fiber-FLWAC it was used the same wet mixing procedure with just one additional step. Polyvinyl alcohol fibers (PVA) were added first in nice mortar in order to provide good distribution of the fibers in the concrete. Later procedure was the same.

Polyvinyl alcohol fibres is mostly use to improve the inherent brittleness of cementitious materials and to control cracking. They have very little effect on the flexural strength and deflection capacity. The compressive capacity is slightly reduced while concrete surface of the elements become extremely ductile [13]. In this test the main concern was to deal with brittleness, explosive failure and to improve ductility of LWAC. Because of that PVA fibres were introduced in range 0.5 % at volume fractions. PVA was type “Kuralon RSC15”, 8 mm long with E-modul of 36 MPa [14].

For all prepared concrete mixtures, the fresh concrete characteristics like fresh density [15], air content [16] and slump [16] were followed. Results are given in Table 3.

Table 3 – Fresh concrete characteristics for DLWAC, WLWAC and FLWAC

	DLWAC	WLWAC	FLWAC
Fresh density [kg/m ³]	1989	2015	2011
Air content [%]	2.5	1.9	2.5
Slump [mm]	170	190	250
Matrix volume [l/m ³]	360	360	360

2.3 Test Setup and the procedure

All the prisms were loaded in an electro-hydraulic, servo-controlled actuator with a maximum compressive load capacity of 1000 kN. Prisms were first preloaded with 100 kN and later the load was constantly applied with a loading rate of 0.3 mm/minute until failure. This is displacement control test and load was applied centrally and eccentrically, which was provided by varying

stress gradients. Test set and the stress diagrams for the applied eccentricities, based on the assumption of linear stress-strain relationship, are shown in Figure 2.

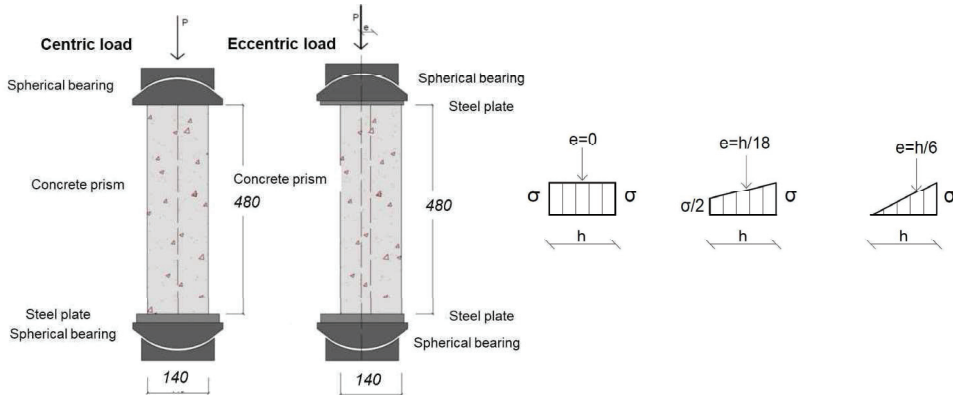


Figure 2 – Test setup for centrally and eccentrically loading. Stress distribution based upon linear theory for the different eccentricities (h is the height of the cross section).

The loading system was equipped with spherical ball bearings in direct connection to the top and the bottom surface of the prisms to ensure free rotation. The ball bearings were arranged in such a way that their rotation center lay on the surface of the specimens. Control lines were drawn on the contact plates of the bearings to ensure correct placement of the prisms. The contact surface between the ball and the concave ring of the bearings was lubricated prior to each test so as to reduce the friction at the sliding surface as much as possible [4]. Photos of the prism in the testing machine is shown in Figure 3.

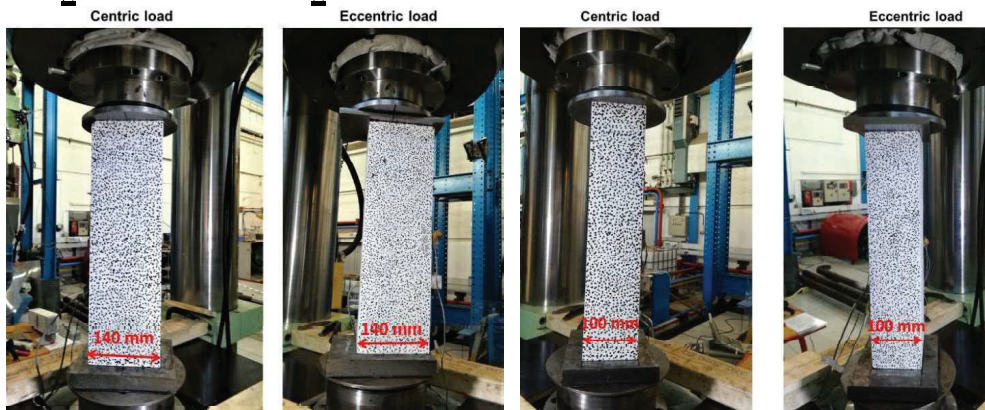


Figure 3 – Prism in the 1000 kN testing machine. Wide side-140mm (left) and short side-100 mm (right).

2.4 Instrumentation

All the tested prisms were instrumented with the same measuring devices. Strain levels at the concrete area were recorded with strain gauges (SG) and Linear Variable Differential Transformers (LVDT) at two sides of the prism, called LVDT short and LVDT wide. On the other

two sides, called DIC short and DIC wide, Digital Image Correlation (DIC) was used [17]. The location of the measuring devices is shown in Figure 4.

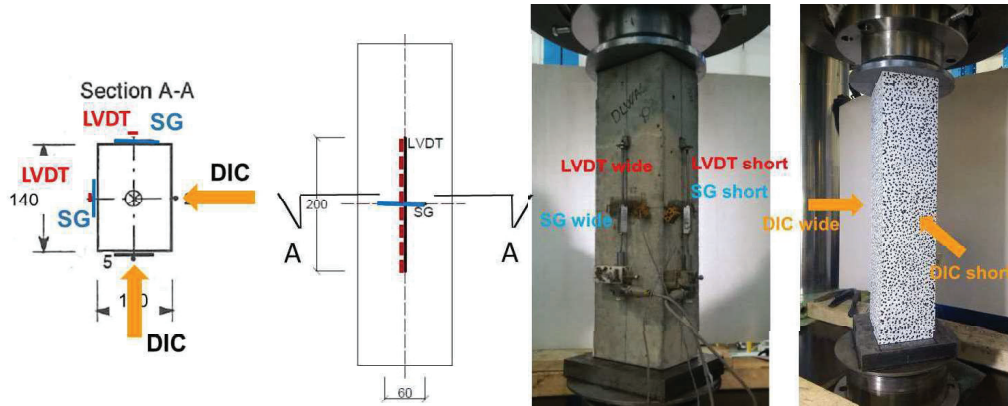


Figure 4 – Position of measuring devices for centric and eccentric loading.

The measuring length of the LVDT for observation of longitudinal direction of middle section was 200 mm. In addition, strain gauges with length 60 mm (type FLA-6-11-5L with gauge resistance of $119.5 \pm 0.5 \Omega$) were inserted in the middle section for observation of transversal direction. DIC was used on other two sides of the prism where the complete strain field was registered. In the eccentric load situation the DIC side was chosen as the one with the maximum stress and where the highest strains were expected. For DIC was used set of two cameras and each were placed orthogonally in relation to the area of observation. That represent 2D DIC, see Figure 5.

All measuring devices (LVDTs and SGs) together with the load cell were connected to HBM eight channel spider to record the data. From here, data were sent to the computer using a specific software program, where the data were processed and stored in a text file. The deflection and load measurements were carried out as a control during the whole test. The output data were recorded by the data acquisition system. Pictures were taken at failure.

Since this was a compressive test and it is known that lightweight aggregate concrete can have very explosive failure special safety precautions were required during testing. Consequently, a plexiglass chamber around the concrete sample was used. It ensured that all parts of the concrete would stay inside of chamber when failure happened.

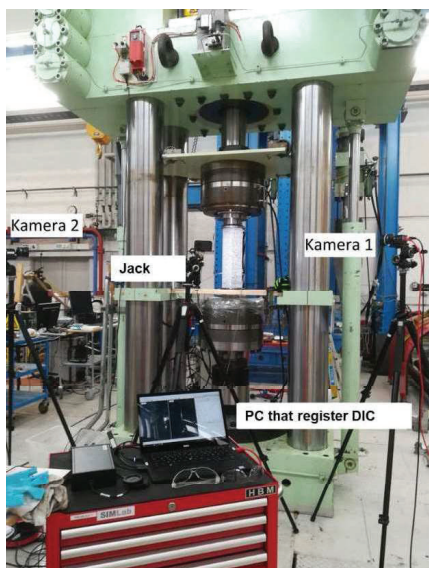


Figure 5 – Setup of the registration equipment.

3. EXPERIMENTAL RESULTS

3.1 Results for small specimens

Small specimens were tested after 28 days for determination of compressive strength, tensile strength and Young's modulus. Small beams for fracture energy for DLWAC were tested after 60 days and for WLWAC after 36 days. The fracture energy is determined on small $100 \times 100 \times 1200$ mm beams according to SINTEF procedure [18]. This procedure is quite similar to the Hillerborg [10] proposed RILEM method. Small beams are just for 200 mm longer and notch is 0.4 instead of the 0.5 of the beam heights. Beams were first prenotched with notch depth 40 mm and tested in three-point bending test. Fracture energy is calculated when work or energy from the positive part of load-deformation curve observed during test is divided with fracture area. The aggregate type and content affect the result of fracture energy of concrete much stronger than the size of aggregates due to transition from the interfacial fracture to the trans-aggregate fracture. A brief summary of the small-scale test results is given in Table 4.

Table 4 – Mechanical properties for DLWAC, WLWAC and FLWAC

	DLWAC	WLWAC	FLWAC
Saturated density ρ_{cs} [kg/m ³]	1997.9	2008.4	2019.2
Oven dry density ρ_{cv} [kg/m ³]	1979.9	1864.6	1899.5
Compression strength for cube after 7 days $f_{cm,7}$ [N/mm ²]	51.1	58.1	48.8
Compression strength for cube after 28 days $f_{cm,28}$ [N/mm ²]	71.6	77.5	71.
Compression strength for cylinder after 28 days $f_{cm,28}$ [N/mm ²]	67	72.9	63.7
Tensile strength after 28 days $f_{ctm,28}$ [N/mm ²]	4.7	4.9	4.5
Modulus of elasticity after 28 days $E_{1cm,28}$ [N/mm ²]	23653	21701	22549
Fracture energy after 32 days G_F [Nm/m ²]	79.7	82	74.9

Concrete class measured from all small samples was LC65 and higher which represents a high strength lightweight concrete. The compressive failures of cubes and cylinders were very explosive which is typical for high strength and lightweight concrete [1].

3.2 Results for prisms

Figures 6 and 7 show the experimental results registered with LVDTs and SGs for the centrically and eccentrically loaded prisms.

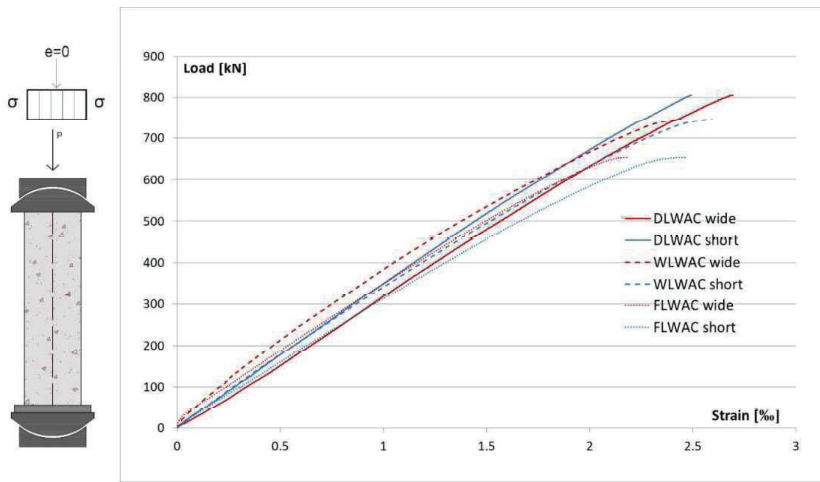


Figure 6 – Load-strain relationship for centric loading.

The load-strain relationship at centricity and eccentricity $h/18$ and $h/6$ are shown in Figure 6 and 7. The strains recorded with LVDTs represent lower strains that were registered during testing. For each loading case 3 prisms were tested. The curves are mean values from three tests, except FLWAC.

Table 5 - Test results

Prism Nr.	Type of concrete	Aggreg. moist. [%]	$f_{ic,cube}$ [MPa]	$f_{ic,prism}$ [MPa]	Eccentricity [mm]	P_{max} [kN]	P_{calc} [kN]	$\epsilon_{c,LVDT}$ [%]	$\epsilon_{c,DIC}$ [%]
1-3	DLWAC	0.1	77.9	57.5	e=0	804	763	2.69	3.12
4-6					e=7.77	668	513	2.51	3.47
7-9					e=23.33	495	382	2.70	3.81
1-3	WLWAC	7.9	80.7	53.5	e=0	746	791	2.59	3.40
4-6					e=7.77	648	531	2.19	3.69
7-9					e=23.33	541	395	2.96	4.53
1	FLWAC	7.9	77.6	46.7	e=0	653	760	2.46	2.94
2					e=7.77	669.9	511	2.18	4.54
3					e=23.33	577.8	380	3.38	6.82

Where $f_{ic,cube}$ is compressive cube strength; $f_{ic,prism}$ is compressive prism strength (P_{max} divided with prism cross section $100 \times 140 \text{ mm}$); P_{max} – load level of maximum load; P_{calc} – hand calculation of maximum load; $\epsilon_{c,LVDT}$ – maximum concrete compressive strain recorded with LVDT; $\epsilon_{c,DIC}$ – maximum concrete compressive strain recorded with DIC.

In addition to this results Table 5 shows summary of all registered results. In the case of eccentrically loaded prisms, the compressive strain registered with LVDT presents the side that was less stressed, see Figure 7, while strains registered by DIC were at the most stressed side. In the case of centrally loaded prisms we can notice very good agreement between LVDTs (see Figure 6) and DIC measuring method. Average compressive strain levels recorded in all the prisms were between 3.08‰ and 6.82‰.

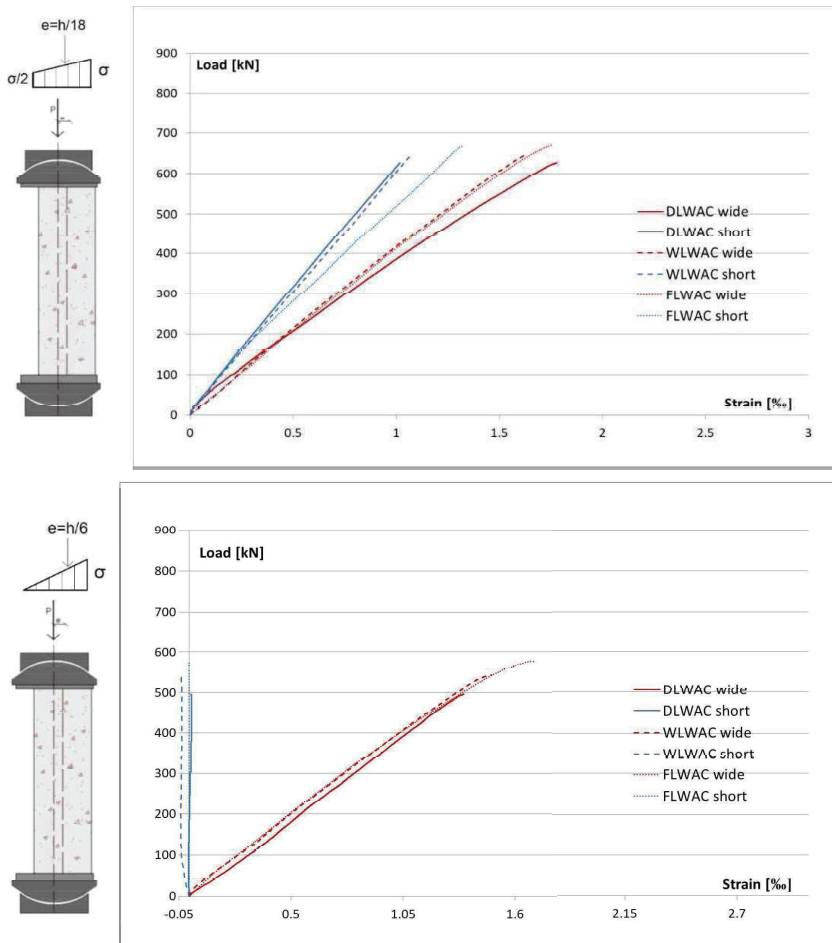


Figure 7 – Load-strain relationship at eccentricities $e=h/18$ (top) and $e=h/6$ (bottom).

3.3 Failure mode and crack patterns of the prisms

For a concrete specimen loaded in compression the fundamental failure mode is a combination of both axial splitting and sliding. However, the influence of each failure mode depends on concrete material factors such as concrete composition, type of aggregate and maximum aggregate size.

For LWAC it is well known that the weakest part in matrix is aggregate itself and cracking line goes usually through the aggregate [4].

For centrally loaded prisms two types of failure happened: shear, sliding mode of failure (when micro-cracks coalesce to inclined localized shear bands) and longitudinal failure (axial splitting happened when a critical lateral deformation is exceeded), see Figure 8.

At eccentrically loaded prisms longitudinal failure occurred, opening of longitudinal tensile cracks led to the final failure, cracks proceeded within the damage zone. The typical mode of failure for the eccentrically loaded prisms is illustrated in Figure 8. For all samples, the breaking length l_b and breaking depth d_b of the fracture were recorded. Table 6 shows the fracture size. In final fase the centrally loaded prisms had longitudinal breaks that went in center of the sample and therefore it was not possible to measure the breaking length l_b and breaking depth d_b of the fracture.

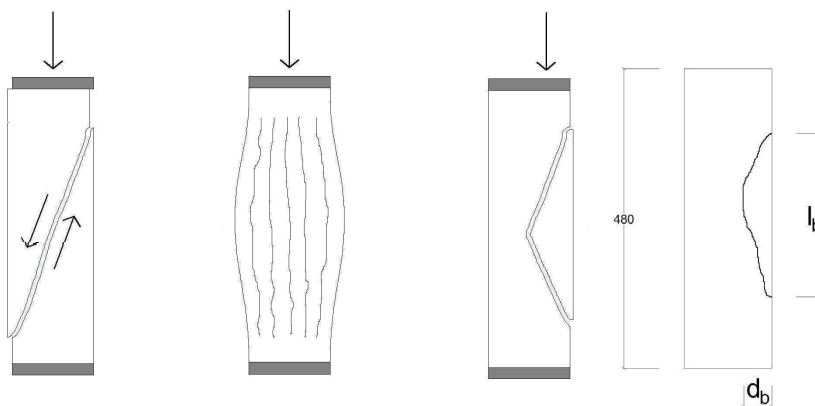


Figure 8 – Sketch of oblique shear fracture (left), longitudinal break (centre) and longitudinal tensile break at eccentric load (right). Typical mode of failure for the eccentrically loaded prisms (right).

Table 6 – Fracture size for eccentrically loaded prisms for DLWAC, WLWAC and FLWAC

e=7.77 mm	DLWAC	WLWAC	FLWAC
l_b [mm]	440	470	340
d_b [mm]	110	110	60
l_b / d_b	4	4.3	5.6
e=23.33 mm	DLWAC	WLWAC	FLWAC
l_b [mm]	370	410	290
d_b [mm]	40	280	50
l_b / d_b	9.2	5.1	5.8

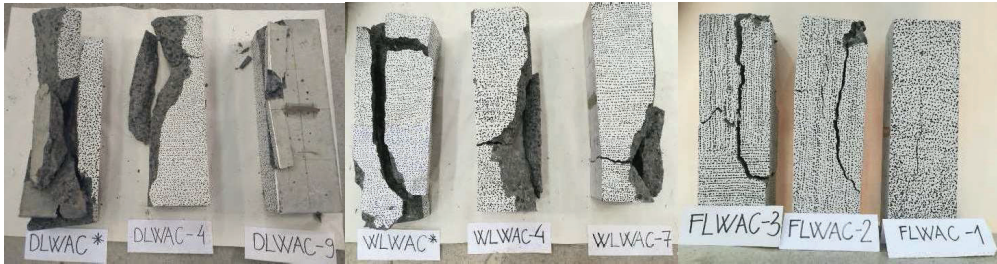


Figure 9 – Cracking pattern for centrally and eccentrically $h/18$ and $h/6$ loaded samples.

Crack propagation depended on the loading conditions. Prisms subjected to centrally loading cracked from the centre of the sample and experienced large cracks and the lowest ultimate compressive strain was registered. Prisms that were loaded eccentrically only cracked at the most stressed part with higher strains. Prisms that were loaded under larger eccentricity experienced just small cracking, see Figure 9.

Through qualitative visual inspection of the fracture, it was discovered that in the concrete with dry Stalite, the fractures both penetrated and travelled around the aggregate particles (approximately 60% aggregate cracked), while in the concrete with saturated Stalite, the fracture to a much larger degree only penetrated the particles (almost 95% aggregate cracked). The concrete with the saturated Stalite had the most explosive fractures. By introducing a small amount of fibers (0,5% of the cement mass) the concrete became significantly more ductile and did not have brittle behaviour. The fracture was not explosive, and the prisms kept together afterwards. In general measured breaking length and depth were significantly smaller for FLAC than for DLWAC and WLWAC.

4. DISCUSSION AND CONCLUSION

A stress gradient test has been used to investigate strains and ductility. The test was done by loading prisms centrally or with two different eccentricities. The proportions of the prisms and eccentricities were the same as in an earlier experiment and are therefore comparable. This study investigates differences using dry (0.10 % moisture content) or saturated (7.9 % moisture content) aggregate Stalite, and the effect of polyvinyl alcohol fibres on the compressive behaviour of LWAC. Crack propagation depended on the loading conditions. Prisms subjected to centrally loading experienced large cracks and the lowest ultimate compressive strain, while prisms loaded eccentrically only cracked at the most stressed part with higher strains. By using DIC, detailed strain fields of the observed compressive zones have been recorded, see Figure 10.

From the achieved experimental results, it is visible that the lateral deformation of the most stressed fibre is counteracted by the less stressed fibres that confine compressive stress. Close to the peak load the lateral deformations near the free surface become pronounced. Finally, in the post-peak region two different fractures developed and ultimate strains increased. In general, larger eccentricity lead to increased strains (recorded strains in prisms test was in range from 3.08‰ to 6.82‰).

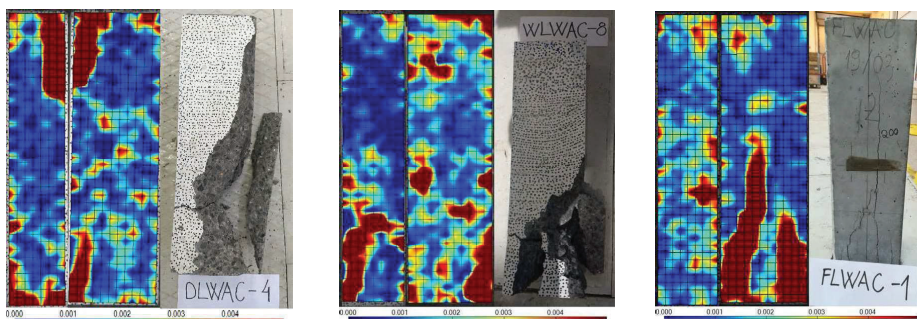


Figure 10 – Strain field for DLWAC (left), WLWAC (centre) and FLWAC (right) just before the final failure. Strain range from 0‰ till 5‰.

In general, measuring devices were in a good agreement, but close to failure, larger strains and localization were measured using DIC, compared to the strain values measured with the SGs and LVDTs. The concrete with the water saturated aggregate had somewhat higher strains and ductility than the concrete with dry aggregate. Through qualitative visual inspection of the fracture, it was observed that the concrete with the saturated aggregate had the most explosive fractures. By introducing a small amount of fibers (0.5% of volume fractions) the concrete became significantly more ductile, with a maximum compressive strain of 6.82 ‰, and the fracture was not explosive. FLWAC samples in final faze kept together afterwards. Eurocode 2 [19] does not differ between lightweight concrete with different types of aggregates and underestimated the largest strains in this experiment by 75-88 %.

4.1 Comparison with previous experimental work

The experimental setup of the prisms and the eccentricities were the same as in an earlier experiment and are therefore comparable [4]. The earlier studies looked at the lightweight concrete Liapor 8 and different types of normal weight concrete. Table 7 compares new and old experiments. A ductility index D is calculated as:

$$D = \frac{\varepsilon_{cu} - \varepsilon_{el}}{\varepsilon_{el}} \cdot 100\% \quad (1)$$

where ε_{cu} is maximum compressive strain and ε_{el} is strain corresponding to elastic state. In elastic state strains are reversible which recovers while applied stresses are being removed. Plastic strains yield in the specimen before reaching peak point (maximum compressive strains before failure). Elastic and plastic zone of specimen depends on the stiffness, brittleness and ductility of specimen. Concrete is more ductile if difference between elastic and maximum strain is larger. In that case ductility index D is larger as well. Specimen having higher strength will lead to smaller strains and elastic portion in this case will be more. Concrete is a brittle material and it shows smaller value of strains before failure.

Table 7 - Comparison with experimental work from 1993 [2]

Type of concrete	Eccentricity [mm]	$f_{c,prism}$ [MPa]	$f_{c,cube}$ [MPa]	\mathcal{E}_{cu} [%]	D_{LVDT} [%]	D_{DIC} [%]
DLWAC	e=0			3.12		
	e=7.77	57.5	77.9	3.47	11.2	13.3
	e=23.33			3.81		
WLWAC	e=0			3.40		
	e=7.77	53.5	80.7	3.69	15.1	14.9
	e=23.33			4.53		
FLWAC	e=0			2.94		
	e=7.77	46.7	77.6	4.54	37.2	37.6
	e=23.33			6.82		
Liapor 8	e=0			3.12		
	e=7.77	86.8	93.8	3.41	9.6	
	e=23.33			3.55		
Gneiss/ Granite	e=0			2.61		
	e=7.77	81.4	104.1	2.97	14.5	
	e=23.33			3.16		
Basalt	e=0			2.72		
	e=7.77	89.0	105.1	3.31	31.7	
	e=23.33			3.45		
Quartzite	e=0			2.47		
	e=7.77	86.5	106.7	2.81	14.8	
	e=23.33			2.84		

Where $f_{c,prism}$ is compressive prism strength; $f_{c,cube}$ is compressive cube strength; \mathcal{E}_{cu} – maximum concrete compressive strain; D_{LVDT} – ductility index calculated from maximum concrete compressive strain recorded with LVDT; D_{DIC} – ductility index calculated from maximum concrete compressive strain recorded with DIC.

It is clear that LWAC with Stalite showed more ductile behaviour than LWAC with Liapor 8. Compared to normal density concretes the ductility is similar while registered strains are much higher. When adding just small amount of polyvinyl alcohol fibers, the ductility increase, ductility index is doubled.

The results from this experiment are promising for increased use of high strength lightweight aggregate concrete with Stalite as aggregate for concrete structures. High strains and ductility show that concrete with Stalite can be considered as a product in between lightweight aggregate concrete and normal weight concrete. It combines the ductility from normal weight concrete with the low density from lightweight aggregate concrete. In general, based on this experimental results the use of high strength concrete with Stalite as aggregate should be increased because of the favourable combination of high strength with low density.

5. ACKNOWLEDGEMENT

The work presented in this paper is part of ongoing PhD study in scope of the DACS project (Durable Advanced Concrete Solutions). The DACS partners are Kværner AS (project owner), Norwegian Research Council, Axion AS (Stalite), AF Gruppen Norge AS, Concrete Structures AS, Mapei AS, Multiconsult AS, NorBetong AS, Norcem AS, NPRA (Statens vegvesen), Norwegian University of Science and Technology (NTNU), SINTEF Byggforsk, Skanska Norge

AS, Unicon AS and Veidekke Entreprenør AS. Jelena Zivkovic would like to express her utmost gratitude to the supervisors and all the project partners for contributions and making this PhD study possible. J. Zivkovic would like to thank to Master students Aleksander Hammer and Håvard Lauvsland for the help during experimental work.

REFERENCES

1. Zivkovic J & Øverli J A: “Ultimate compressive strain in lightweight aggregate concrete beams”. *Proceedings*, 12th fib International PhD Symposium in Civil Engineering, Prague, Czech Republic, August 2018, pp. 829–836.
2. Nedrelid H: “Towards a better understanding of the ultimate behavior of lightweight aggregate concrete in compression and bending”. *Bulletin* No.123 (PhD Thesis), Norwegian University of Science and Technology, Department of Structural Engineering, Trondheim, Norway, 2012, 214 pp.
3. Øverli J A: “Towards a better understanding of the ultimate behavior of LWAC in compression and bending”. *Engineering Structures*, No. 151, 2018, pp. 821–838.
4. Markeset G: “Failure of concrete under compressive strain gradients”. *Bulletin* No.110 (PhD Thesis), Norwegian Institute of Technology, Department of Structural Engineering, University of Trondheim, Trondheim, Norway, 1993, 168 pp.
5. Carolina Stalite Company: “Production of Stalite”. Salisbury, North Carolina, USA available: <https://www.stalite.com/production>.
6. Standard Norge: “Testing hardened concrete - Compressive strength of test specimens”. Part 3, NS-EN 12390-3:2009, Lysaker, Norway, 2009, 24 pp.
7. Standard Norge: “Testing hardened concrete – Tensile strength of test specimens”. Part 6, NS-EN 12390-6:2009, Lysaker, Norway, 2009, 16 pp.
8. Skjølsvold O, Bakken N & Johansen E : “Bestemmelse av E-modul iht NS3676 Losenhausen 5000kN trykkpresse”. Betong og natursteinslaboratoriene, KS 14-05-04 122, SINTEF Byggforsk, Trondheim, Norge, 2007. (in Norwegian)
9. Standard Norge: “Concrete testing - Hardened concrete - Modules of elasticity in compression”. NS 3676, Norway, 1987, 20 pp.
10. Hillerborg A: “The theoretical basis of a method to determine the fracture energy G_F of concrete”. RILEM Technical Committees, *Materials and Structures*, Vol. 18, Issue 4 2005, pp. 291-296.
11. Carolina Stalite Company: “Benefits of using Stalite”. North Carolina, USA , accessed October 21. 2009. <http://www.stalite.com/why-use-stalite.php?cat=138.html>.
12. American Concrete Institute: “Guide for structural lightweight aggregate concrete”. ACI213R–03, Farmington Hills, MI, United States, 2003, 38 pp.
13. Savija B, Lukovic M, Kotteman G, Chaves F S, de Mendoca Filho F F & Schlangen E: “Development of ductile cementitious composites incorporating microencapsulated phase change materials”. *International Journal of Advances in Engineering Sciences and Applied Mathematics*, Vol. 9, Issue 3, 2017, pp. 169-180.
14. Kuraray Co: “Characteristics of KURALON (PVA fibres), PVA fibres-application”. Japan, available: <http://kuralon-frc.kuraray.com/product-application>
15. Standard Norge: “Testing hardened concrete - Density of hardened concrete”. Part 7,

- NS-EN 12390-7:2009, Lysaker, Norway, 2009, 16 pp.
16. European Union – Brite EuRam III: “Methods for Testing Fresh Lightweight Aggregate Concrete”. BE96-3942/R4, December 1999, 51 pp.
 17. McCormick N & Lord J: “Digital Image Correlation for Structural Measurements”. ICE institution, *Civil Engineering*, 165 (CE4), 2012, pp. 185–190.
 18. SINTEF procedure: “Fracture energy of prisms with notch in three point bending test”. KS14-05-04123, September 2007, 3pp.
 19. European committee for standardization: “Eurocode 2: Design of concrete structures – General rules and rules for buildings”. Part 1-1, EN 1992-1-1 (2004), 2004, 225 pp.

Paper II

Confinement in Bending of High-Strength Lightweight Aggregate Concrete Beams
Zivkovic, J. and Øverli J.A.

Manuscript submitted to Engineering Structures (October 2020)

2

This paper is awaiting publication and is not included in NTNU Open

Paper IIa

Ultimate compressive strain in lightweight aggregate concrete beams

Zivkovic, J. and Øverli J.A.

Proceedings of the 12th fib International PhD Symposium in Civil Engineering Materials
(July 2018), Prague, Czech Republic, 2018, ISBN 978-80-01-06401-6. pp. 829–836

2a

Ultimate compressive strain in lightweight aggregate concrete beams

Jelena Zivkovic and Jan Arve Øverli

*Department of Structural Engineering,
Norwegian University of Science and Technology (NTNU),
Trondheim, Norway*

Abstract

The major concern when using lightweight aggregate concrete (LWAC) in structural applications compared to normal weight concrete (NWC) is the more brittle post-peak behaviour and reduced ultimate strain, especially in compression. To investigate this six LWAC over-reinforced beams, with geometry 210-330x550x4500 mm, were subjected to four point bending with a constant moment zone of 1m between loading points. In this zone were varied main test parameters: the spacing of transverse reinforcement, amount of longitudinal compressive reinforcement and size of concrete cover. Strains were measured combining DIC, strain gauges and LVDTs. Five the tested beams showed ductile behaviour and ultimate compressive strain registered in the beams was in range 3.4-3.8%. This indicate that standards underestimate ultimate compressive strain in LWAC structures from 30-50%.

1 Introduction

Lightweight aggregate concrete (LWAC) has been used as a construction material from ancient times [1], with the main aim to reduce the dead weight of structures. Reduction of weight allows reduction of the structures dimensions, especially in seismic regions and areas with low bearing capacity. Handling and transport of precast elements from LWAC is easier and more economical. Until now, LWAC concrete is applied with great success in many advanced structures like bridges, offshore structures and skyscrapers [2]-[5]. Several different standards define LWAC as concrete with an oven dry density below 2000 kg/m³ and with maximum strength about 80 MPa [6], [7]. Even with the major advantage of reduced weight and high strength-to-weight ratio compared to conventional concrete, the use of LWAC is still limited as a mainstream construction material. The main reason is the more brittle post-peak material behaviour that result with reduced ultimate compressive strain compared to normal density concrete (NWC). The brittleness of concrete is characterized by sensitivity to stress concentrations and a rapid crack/fracture development. For structural analysis, it is essential to know the complete stress-strain curve under uniaxial compression including the descending branch [8], [9]. The main emphasis in this work is on the post-peak strain-softening response, which is for LWAC steep and short since concrete behave in a brittle manner. An experimental program is conducted to investigate the post-peak behaviour of LWAC and ultimate strain in compression and bending. The program consist of six LWAC over-reinforced beams, subjected to four point bending. The geometry of the beams were 210-330 x 550 x 4500 mm (width x height x length). In addition, small samples cubes and cylinders were casted to decide the material quality. The test setup was designed to produce a constant moment zone of one meter between loading points. The main test parameters, varying in the constant compression zone, were the spacing of transverse reinforcement, amount of longitudinal compressive reinforcement and size of concrete cover. The ultimate capacity was evaluated by following the rules in Eurocode and the Norwegian code [6], [7] for design of concrete structures. All the tested beams failed in compression between the two loading points. Reinforcement detailing influenced the cracking of the compression zone in the beams. The beam without transversal reinforcement showed very explosive and brittle behaviour while all other beams showed ductile behaviour. The strain level in the concrete and reinforcement were measured with strain gauges (SG) and Linear Variable Differential Transformers (LVDT) at one side of the beam. On the other side, Digital Image Correlation (DIC) method was used [11], [12]. To produce the concrete, a lightweight aggregate argillite slate from North Carolina, called Stalite [13], was used to achieve an oven-dry density of about 1850 kg/m³ and a compressive cylinder strength of about 65 MPa.

2 Experimental program and methodology

2.1 Test parameters

The experimental program include six over-reinforced LWAC beams which were subjected to a four point bending test, with a constant moment zone of one meter between the loading points. This type of experimental program was proposed in order to eliminate the effect of frictional restraint on post-ultimate deformation, what is typical for uniaxial compression tests [14]. This testing technique allow lateral expansion of the central zone in all directions and provide testing of the LWAC under multiaxial states of stress. Size of the compressive testing zone was approximately 300x1000 mm. The parameters varied in the beams were the stirrup spacing, amount of compressive reinforcement and size of concrete cover. All the beams were overreinforced to provide a compressive bending failure. Outside of the testing zone, all the beams had the same stirrups distribution designed to avoid shear failure. The moment and shear capacity of the beams has been calculated in accordance with Eurocode 2 and Norwegian code [6], [7]. The maximum compressive strain used in the calculation was $\epsilon_{cu2}=2.52\%$. Table 1 describe the test program.

Table 1 Test parameters.

Beam No.	Beam Identification	Stirrup spacing -s [mm]	Concrete cover-c [mm]	Compressive reinforcement A_c	Capacity P_{calc} [kN]
1	LWAC65_20_0	-	20	2 ϕ 12	729
2	LWAC65_20_200	200	20	2 ϕ 12	729
3	LWAC65_20_60	60	20	2 ϕ 12	729
4	LWAC65_20_100	100	20	2 ϕ 12	729
5	LWAC65_40_100	100	40	2 ϕ 12	726
6	LWAC65_40_200*	200	40	2 ϕ 25	800

2.1.1 Test specimens

The beams measured (width x height x length) 210-330 x 550 x 4500 mm. All the beams were over-reinforced with ten ϕ 20 mm bars in tension zone in order to provide compressive failure. Outside the constant bending zone stirrups ϕ 10 mm were distributed along the shear spans on 70mm distance to avoid shear failure. In compressive zone, all beams 1-5 had two longitudinal bars ϕ 16 mm and beam 6 two bars ϕ 25 mm. Short longitudinal bar ϕ 8 mm were set in testing compressive zone in all the tested beams as the carrier of the strain gauges. This bar was able to move together with concrete since it was not fixed at the edges. Stiff anchorage of tension reinforcement at the support was provided with a welding steel plate. Fig. 1 gives the beam geometry and cross section details between the loading points.

All the beams and small samples, cubes and cylinders, were cast from the same concrete batch. The beams were demoulded 24 hours after casting, and stored in the laboratory at approximately 20° C under wet burlaps covered with a plastic sheet. They were uncovered two days before the test. Finally, the beams were painted white for easier detection of cracks and prepared for instrumentation. The test age of the beams varied from 37 to 59 days.

To establish the mechanical properties of the LWAC, cubes (with dimensions 100x100x100 mm), cylinders (ϕ 100x200mm) and small beams (100x100x1200mm) were casted to find the stress-strain diagram, the compressive strength for cube and cylinder, the tensile strength, Young's module of elasticity, and the fracture energy. All these small specimens were demoulded after 24 hours and kept in water until testing day. In order to follow material characteristics compression tests on cubes and cylinders were carried out continuously with the beam testing.

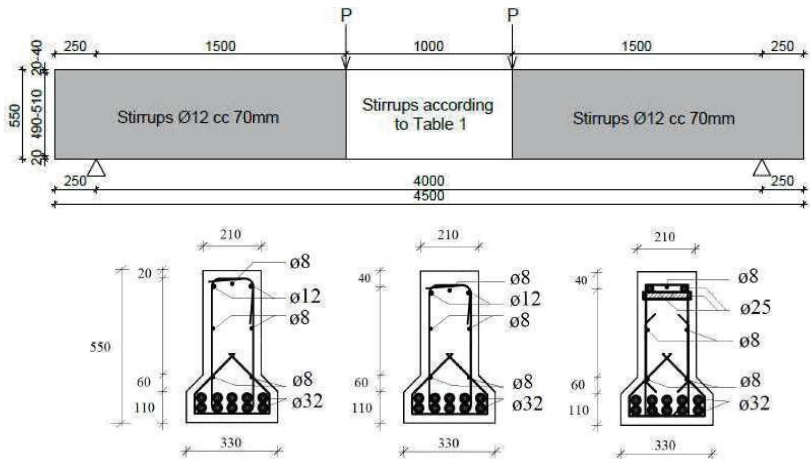


Fig. 1 Beam geometry and reinforcement layouts between the loading points. Dimensions are in [mm].

2.2 Material and mix properties

The concrete mixture was prepared from one batch at a concrete stationary plant and in a concrete truck mixer. Lightweight aggregate was first placed in a concrete truck and later mortar was added. Mixing and transport was done in a concrete truck mixer. The lightweight aggregate was $\frac{1}{2}$ " fraction from Stalite [13]. The moisture content and the absorbed water in the Stalite were measured to be able to design the concrete mix [2]. The moisture content was 11.43%, and the absorption after 24 hours and 100 hours was 6.54% and 8.32%, respectively. Table 2 gives the concrete mixture. The mixing was done using combination of concrete stationary plant capacity 4 m³ and concrete truck mixer 6 m³ laboratory mixer. Mixing was done continuously in a truck mixer during a transport of 15 minutes. Characteristics of the fresh concrete were: density 2013 kg/m³, air content 2.4% and slump 230 mm. The reinforcement was of the type B500NC [15]. Assumed yielding stress of the reinforcement was 530 MPa.

Table 2 Concrete mix for LWAC 65.

Constituent	Weight [kg/m ³]
Cement (Norcem Anlegg FA)	430.75
Silica fume (Elkem Microsilica)	22.38
Water (free+absorbed 24 hour)	123.33+55.17=178.5
Sand (Ramlo 0-8 mm)	595.31
Sand (Ramlo 0-2 mm)	249.65
Aggregate (Stalite $\frac{1}{2}$ ")	550
Superplasticizer (Mapei Dynamon SR-N)	5.4

2.3 Test Setup and procedure

Fig. 2 shows the experimental setup. The load was applied by mechanical screw jack and transferred to the test beam through a steel spreader beam. Two steel rollers supported the beam and covered the entire width of the beam. The loading point has free rotation transversal to the beam. Between jacks and the beam surface, it was used a 100 mm wide steel plates and a 15 mm thick fibreboard with the same width. The supports were both free for rotation and displacement in the longitudinal direction. At the supports, only steel plates were between the support and the beam. The supports were placed 250 mm from the beam-ends. To avoid anchorage problems, tension reinforcement bars were welded to the steel plate dimensions 30x60x330mm in this region. The load was measured by an electrical load cell under the screw jack with a maximum capacity 2000 kN. Three linear variable displacement transducers (LVDT), one at the mid-span and two above each loading point measured the deflections of the beam. Additional five LVDTs measured strain at the concrete surface. Three of them measured strains in the compressive zone and two strains in the tensile zone. The LVDTs were placed in the middle cross section and they measured deflection over a distance of 200 mm. In addition, six strain gauges (SG, type FLA-6-11-5L with gauge resistance of $119.5 \pm 0.5 \Omega$) were inserted on the compressive bar $\phi 8$ and tensile reinforcement, inside of the middle cross section. All measuring devices (LVDTs and SGs) together with the load cell were connected to HBM 8 channel spider to record the data. From here, data were forwarded to computer using a specific software program, where they are processed and stored in a text file.

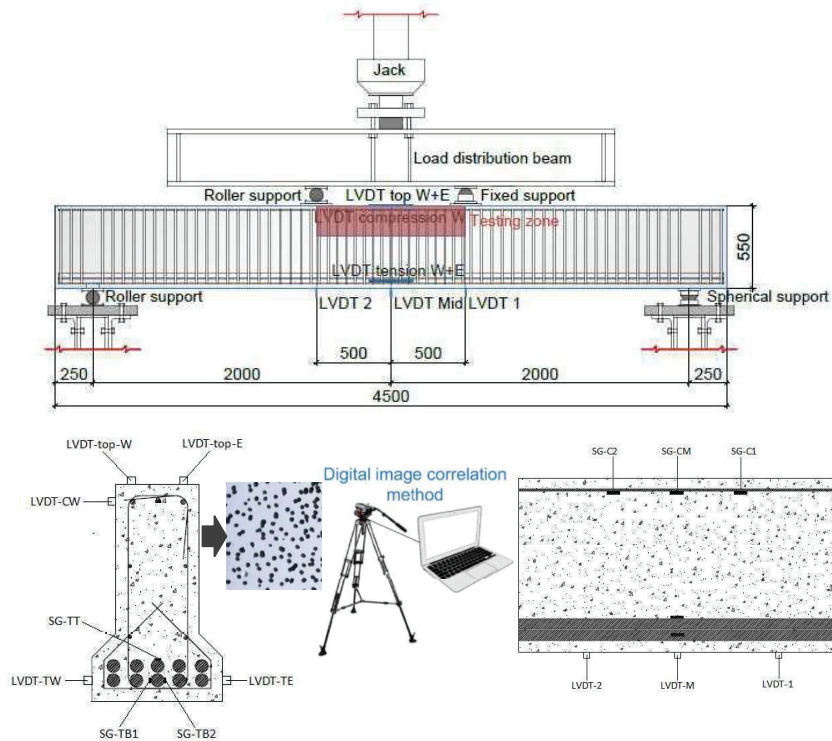


Fig. 2 Top of the figure show experimental set-up of the beam test. At the bottom of the figure, there is sketch of cross section at the middle of testing area with location of each measuring devices. Dimensions are in [mm].

The load was applied step-wise, with load increments of 100 kN up to 70% of calculated capacity. The load increments were then reduced to 50 kN until failure. The rest periods at each load level were three minutes and mainly used to draw the crack progression with dark pen and taking of photos. The tests were displacement controlled with a loading rate 1-1.2 mm/minute, thus, the deflection measurements were carried out as a control during all tests.

3 Experimental results

3.1 Results for small specimens

Small specimens were tested after 28 days for determination of compressive strength, tensile strength and Young's modulus. Small beams for fracture energy were tested after 71 days. A brief summary of the small-scale test results is given in Table 3. Concrete class measured from small samples was LC65 and which represents a high strength lightweight concrete. The compressive failures of cubes and cylinders were very explosive which is typical for high strength and lightweight concrete.

Table 3 Mechanical properties LWAC 65.

Saturated density	$\rho_{cs} = 2013 \text{ kg/m}^3$
Oven dry density	$\rho_{cv} = 1834 \text{ kg/m}^3$
Compression cube after 7 days	$f_{cm,7} = 56.7 \text{ N/mm}^2$
Compression cube after 28 days	$f_{cm,28} = 74.2 \text{ N/mm}^2$
Compression cylinder	$f_{cm} = 65,1 \text{ N/mm}^2$
Tensile strength	$f_{ctm} = 4.03 \text{ N/mm}^2$
Modulus of elasticity	$E_{cm} = 24175 \text{ N/mm}^2$
Fracture energy	$G_F = 70.5 \text{ Nm/m}^2$
Characteristic length	$l_{ch} = 104 \text{ mm}$

3.2 Capacity of the beams

Table 4 shows the results of the tested beams. The beams were tested 37 days (beam 1), 50 days (beam 2 and 3), 55 days (beam 4), 57 days (beam 5) and 59 days (beam 6) after casting. Each beam experienced spalling of the concrete cover in compression between the loading points. Spalling defines the first load peak in the load-deflection curves. The load decreased at this stage for some minutes, before the applied load again increased. The load, then, continued to increase until the concrete cover in the web started to spoil. This defines as a second load peak and is a more smooth peak. The second spalling resulted in a larger drop in the load bearing capacity and deformations increased fast. Any attempt to increase load after second peak was not possible and residual capacity of the beam decreased until the final failure.

Table 4 presents the obtained results: the force when the first bending crack occurred (P_{icr}), force of first shear crack (P_{cr}), force corresponding to first peak load (P_1), force corresponding to second peak load (P_2) and force corresponding to the failure load (P_u). The table also gives average strains (ϵ_c) recorded by two LVDTs placed in the compression zone. Value of recorded maximum strains correspond to first peak load level. The average tension strain (ϵ_t) represents the two LVDTs placed on both bottom beam sides in the tensile zone. The bending capacity (P_{calc}) for all the tested beams was calculated according to Eurocode 2 and Norwegian standard [6], [7]. When calculating the capacity of the beams compressive strength, tensile strength, E-modulus and strains in a concrete were multiplied by a reduction factors η_1 , η_2 and those values are respectively 0.746 and 0.918.

Table 4 Results from beam testing.

Beam Identification	$f_{c,cube}$ [MPa]	P_{calc} [kN]	P_{fer} [kN]	P_{cr} [kN]	P_1 [kN]	P_2 [kN]	P_u/P_{calc} [kN]	ϵ_c [%]	ϵ_t [%]
LWAC65_20_0	75.4	729	53	318	724	-	0.99	3.70	-
LWAC65_20_200	78.3	729	54	350	645	629.4	0.88	3.77	2.04
LWAC65_20_60	78.3	729	78	319	707	686.5	0.97	3.74	2.41
LWAC65_20_100	79.4	729	69	324	700	-	0.96	3.75	2.08
LWAC65_40_100	79.4	726	64	339	663	588.9	0.91	3.61	2.17
LWAC65_40_200*	79.4	800	64	250	750	652.9	0.94	3.40	2.35

4 Discussion

For all the tested beams failure occurred when the compression zone between the loading points started to crack. This type of failure defines a compressive failure in the bending moment zone. Cracking of the compression zone was different for each beam depending on the test parameters: stirrup spacing, size of concrete cover and amount of the compressive reinforcement.

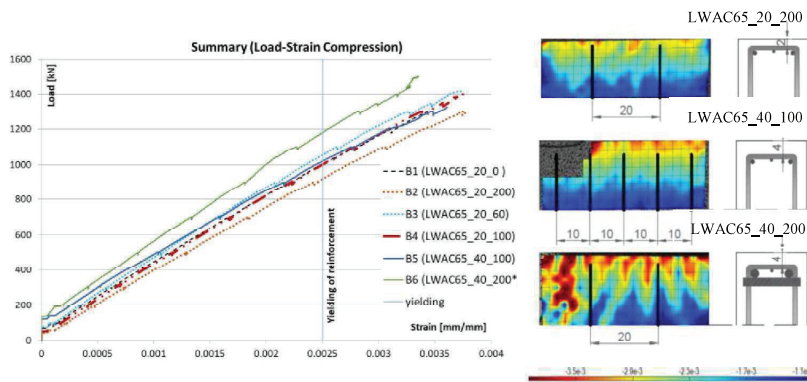


Fig. 3 Left side of the figure shows graph where is plotted average strain in compression at the mid-span versus total applied load. At the right side are plotted strain fields recorded by digital image correlation method for the first peak load level.

The first bending cracks observed in the constant moment region on the tension side, was at load levels from 25 til 53 kN. First cracking depends on the stirrups density in testing area. Since beam without any stirrups in testing area did not have any confinement this beam cracked for lowest load level. As the load increased, new bending cracks propagated symmetrically until they reached the top of the beam flange. Development of bending cracks slowed down when shear cracks appeared. The first shear cracks appeared in the middle of the shear zone, between the neutral axis and the beam flange. Additional loading lead to further crack propagation of both bending and shear area. Crack propagation for certain load steps are very similar for all the tested beams. From Table 4 it is obvious that beams which contain the stiff compressive reinforcement and most stirrups in testing area was able to sustain the largest load before spalling of the concrete cover. From Fig. 3 it can be seen that the compressive longitudinal reinforcement yielded for the largest load level. Beams with large stirrup spacing and small concrete cover showed the fastest spoiling and increase in crack propagation. When the applied load reached first peak, the cross section for all the beams was reduced due to the spalling

of the top concrete cover with load automatically decreasing. It is obvious that beams with large concrete cover has higher drop in capacity and the second peak load level was lower. In final face, spoiling of the web occurred and load drop very fast, while deformations increased, see Fig. 3. Beams with more dense stirrups can sustain more loading after first peak and they showed behaviour that is more ductile. In beam without stirrups in testing area and with low concrete cover second peak load was not registered. The beam failed immediately after first peak load level. Since all the beams were over-reinforced, tensile reinforcement did not yield.

From Fig. 3 it can be concluded that strains recorded by measuring devices LVDTs and DIC was the same. Ultimate compressive strain registered in the beams was in range 3.4-3.8%. By using DIC, detailed strain fields of the observed compressive zones have been recorded, and DIC was able to measure strain after spoiling of the top concrete cover together with LVDTs. From the detailed strain field it can be seen localisation of the largest strains in areas prior to failure. It is also visible that strains distribution followed reinforcement detailing. In a beam with the largest compressive reinforcement, strains were deeper. The same holds for concrete cover, with larger cover, large strains are deeper and spalling of concrete follows reinforcement layout. In addition, it is visible that reinforcement layout influence the most crack development. Cracks were formed between stirrups. Having in mind that EC2 [6] has special rules for LWAC, which are reduction factors applied to regular design criteria, the results in this study indicate that EC2 underestimates LWAC. Recorded maximum strains in the tested beams were for 30-50 % larger than the standard allowed maximum strain ($\epsilon_{cu2}=2.52\%$), for this type of concrete.

In general, observed cracking in all the tested beams were very similar as could be expected in normal weight concrete beams, see Fig. 4.



Fig. 4 Figure of the failure for beam 4 (LWAC65_20_100).

5 Conclusions

For all tested beams in this research cracking were similar. All the beams showed ductile behaviour since they were able to increase loading after formation of shear cracks. Cracking of the testing area depend on the test parameters varied in the experiment. Beams with dense stirrup spacing showed small, shallow cracks and spoiling were smallest. In beams where cover was deeper spoiling and cracking were larger. The beam containing the largest compressive reinforcement resisted the largest load. Beam without stirrups in testing area failed at first peak load level. Measuring devices were able to capture the ultimate compressive strain in LWAC beams.

In general, the characteristics of LWAC depend on the type of lightweight aggregate. EC2 does not differentiate between types of aggregate used in LWAC. From the experimental results, it can be seen that EC2 underestimates ultimate strain level with 30-50%. This study with LWAC indicates bending behaviour similar to NDC. From the experimental program, it can be concluded that by proper reinforcement detailing it is possible to achieve ductile response of lightweight concrete structures. The response in the tested beams were only a small reduction in load capacity after reaching a peak load, followed by an increased deformation. By being able to document a larger ultimate compressive strain in LWAC beams, an increased use of LWAC in structural applications are possible. Further investigations of LWAC as a structural material should therefore continued.

Acknowledgements

The work presented in this paper is part of an ongoing PhD study in the DACS project (Durable Advanced Concrete Solutions). The DACS partners are Kværner AS (project owner), Norwegian Research Council, Axion AS (Stalite), AF Gruppen Norge AS, Concrete Structures AS, Mapei AS, Multiconsult AS, NorBetong AS, Norcem AS, NPRA (Statens vegvesen), Norwegian University of Science and Technology (NTNU), SINTEF Byggeforsk, Skanska Norge AS, Unicon AS and Veidekke Entreprenør AS. The first author would like to express her outmost gratitude to the supervisors and all the project partners for contributions and making this PhD study possible. In addition, special gratitude goes to master students Simon André Petersen, Henrik Nesje Johannesen, Jonas Andås Belayachi and Khaled Bastami for help during production and testing in this study.

References

- [1] Satish, C., and B. Leif. 2002. *Lightweight Aggregate Concrete*. USA. Noyes publications-William Andrew Publishing.
- [2] ACI Committee 213. (ACI213R-03). *Guide for structural lightweight aggregate concrete*. 2003. Farmington Hills (MI, United States): American Concrete Institute.
- [3] Melby, K. 2000. "Use of high strength LWAC in Norwegian bridges." Paper presented at the International symposium on structural lightweight aggregate concrete, Norwegian Concrete Association, Kristiansand, Norway, June 18-22.
- [4] Castrodale, R. W., J. Zivkovic, and R. Valum. 2017. "Material Properties of High Performance Structural Lightweight Concrete." Paper presented at the Eleventh High Performance Concrete (11th HPC) & the Second Concrete Innovation Conference (2nd CIC) Tromsø, Norway, March 6-8.
- [5] Haug, A. K., and S. Fjeld. 1996. "A floating concrete platform hull made of lightweight aggregate concrete." *Engineering Structures* 18(11):831-836.
- [6] EN-1992-1-1. 2004. "Eurocode 2, Design of concrete structures – Part 1-1: General rules and rules for buildings". Brussels, Belgium: CEN European Committee for Standardization.
- [7] NS-EN 1992-1-1:2004+NA: 2008. 2008. "Eurocode 2: Design of concrete structures – General rules and rules for buildings", Standard Norway.
- [8] RILEM TC 148-SSC: Strain softening of concrete - Test methods for compressive softening, Test method for measurement of the strain-softening behavior of concrete under uniaxial compression. 2000. *Materials and Structures* 33:347-351.
- [9] Nedreliid, H. 2012. "Towards a better understanding of the ultimate behaviour of lightweight aggregate concrete in compression and bending." PhD diss., Norwegian University of Science and Technology.
- [10] Overli, J. A. 2017. "Towards a better understanding of the ultimate behaviour of LWAC in compression and bending." *Engineering Structures* 151:821-838.
- [11] Fayyada, T. M., and J. M. Leesb. 2014. "Application of Digital Image Correlation to Reinforced Concrete Fracture." *Procedia Materials Science* 31:585-1590. 20th European Conference on Fracture (ECF20).
- [12] McCormick, N., and J. Lord. 2012. "Digital Image Correlation for Structural Measurements." *Proceedings of the Institution of Civil Engineers - Civil Engineering* 165(4):185-190.
- [13] Carolina Stalite Company. 2009. "Benefits of using Stalite." Accessed October 21. <http://www.stalite.com/why-use-stalite.php?cat=138.html>.
- [14] Kotsovos, M. D. 1983. "Effect of testing techniques on the post-ultimate behaviour of concrete in compression." *Materials and Structures* 16(1):3-12.
- [15] NS 3576-3:2012. 2012. "Armeringsstål - mål og egenskaper - del 3: Kamstål B500NC." Standard Norge.

Paper III

Behaviour and Capacity of Lightweight Aggregate Concrete Beams with and without Shear Reinforcement

Zivkovic, J. and Øverli J.A.

Nordic Concrete Research, 2017, Vol.57, Issue 2, 59-72

ISBN: 978-82-8208-058-3

3

Behaviour and Capacity of Lightweight Aggregate Concrete Beams with and without Shear Reinforcement



Jelena Zivkovic, Ph.D Student
 Department of Structural Engineering
 Faculty of Engineering Science
 Norwegian University of Science and Technology
 7491 Trondheim, Norway
 E-mail: jelena.zivkovic@ntnu.no



Jan Arve Øverli
 Professor, Ph.D
 Department of Structural Engineering
 Faculty of Engineering Science
 Norwegian University of Science and Technology
 7491 Trondheim, Norway
 E-mail: jan.overli@ntnu.no

ABSTRACT

The main disadvantages of lightweight aggregate compared with normal weight concrete are its brittleness at the material level in compression and uncontrolled crack propagation. This experimental investigation consists of five beams with lightweight concrete with Stalite as aggregate. Main goals were to investigate behaviour and capacity of the beams with and without shear reinforcement subjected to four-point bending test and compare those results with previous experimental work. The main test parameters were the shear span ratio (a/d) and amount of the shear reinforcement. Existing standards underestimate shear capacity because they do not differ between shear span (a). Tested beams were more ductile than expected, and cracking was similar as for normal weight concrete beams. According to this experimental investigation, the shear capacity in beams without shear reinforcement should be based on inclined cracking loads.

Keywords: Lightweight aggregate concrete, testing, shear reinforcement, bending, ductility.

1. INTRODUCTION

This investigation is part of the ongoing research programme, “Durable advanced concrete structures (DACs)”. One part of this programme is to investigate the structural behaviour of lightweight aggregate concretes (LWAC), i.e. concretes with an oven-dry density below 2000 kg/m³. A general characteristic of LWAC is its very high degree of brittleness at the material level and especially in compression, which results in sensitivity to stress concentrations and rapid crack/fracture development. This influences the behaviour of concrete where its tensile strength is important, as for instance with its shear and bond strength. To investigate the behaviour of LWAC, beams with and without shear reinforcement were subjected to a four-point bending test. The main test parameters were the shear span length to effective height ratio (a/d) and amount of shear reinforcement. For all beams, the shear loads at diagonal cracking and at failure were plotted as a function of the a/d ratio and compared with previous experimental work. For comparison, tested beams were of the same size and with the same area of compression and tension reinforcement as in earlier shear tests on other normal density (ND) and lightweight aggregate (LWA) concrete beams [1,2]. In addition small specimens were used

to find the compressive strength [3, 4], splitting tensile strength [5], Young's modulus [6, 7], and fracture energy [8].

To produce the concrete, a lightweight aggregate Stalite was used to achieve an oven-dry density of about 1850 kg/m³ and a compressive strength of about 65 MPa. Agreggate Stalite is the argillite slate, laminated, fine-grained siltstone of clastic rock. The foothills region of North Carolina is the only place where slate is exhausted as raw material to produce Stalite. The bulk density ranges from 720-1120 kg/m³ for both coarse and fine aggregate and the hardness of the material is equivalent to that of the quartz [9, 10].

2. EXPERIMENTAL TEST PROGRAM AND RESULTS

2.1 Test specimens

Five reinforced LWA concrete beams with and without shear reinforcement were tested in a four point bending test. The loading system was designed to produce a constant moment in the middle part of the beam. The cross section ($b \times h$) of the beams was 150x250 mm and the length 2900 mm. The main test parameters that were warried in this test were the shear span length to effective height ratio (a/d) and amount of shear reinforcement. In the ratio a/d , a is the shear span (the length between loading point and support) and d the effective height of the cross section (the distance from the top surface to the centre of the tensile reinforcement), which in this case is 219 mm. Two pairs of beams without shear reinforcement each with shear span ratio $a/d=2.3$ and $a/d=4.0$ were tested. In addition one beam, which contained shear reinforcement distributed between the support and loading point and with shear ratio $a/d=3.43$ was tested. An overview of the test programme is shown in Table 1.

Table 1-The main test parameters

Beam	a [mm]	d [mm]	a/d [-]	A_c [cm ²]	A_t [cm ²]	s [mm]	$f_{c,cyl}$ [MPa]	$A_t / (b \times d)$ [%]
1	504	219	2.3	1.57	6.03	-	67.5	1.83
2	504	219	2.3	1.57	6.03	-	67.5	1.83
3	876	219	4	1.57	6.03	-	67.5	1.83
4	876	219	4	1.57	6.03	-	67.5	1.83
5	750	219	3.43	1.57	6.28	100	67.5	1.91

Where a is shear span; d is effective hight; a/d is shear span ratio; A_c — area of compressive reinforcement; A_t — area of tensile reinforcement; s is stirrup spacing; $f_{c,cyl}$ —compressive cylinder strength.

All the beams had three $\varnothing 8$ mm stirrups in each anchorage zone (behind the supports). Beams without shear reinforcement had just two stirrups in the constant moment region below applied forces, while there were no stirrups in the shear spans. One of the tested beams contained shear reinforcement distributed along the shear span. Reinforcement on the tension side consisted of three $\varnothing 16$ mm bars in beams with shear span ratio $a/d=2.3$ and 4.0 and beam with $a/d=3.43$ had two $\varnothing 20$ mm bars. As compressive reinforcement, two $\varnothing 10$ mm bars were used in all the beams. Longitudinal and cross section details of the beam specimens are shown in Figure 1.

All the beams and small samples, cubes and cylinders, were cast from the same concrete batch. The beams were demoulded 24 hours after casting and further cured in the laboratory under wet burlaps covered with a plastic sheet. Two days before the testing beams were taken out and prepared for instrumentation. Finally, the beams were painted white for easier detection of cracks.

Small samples, which were cast in order to identify the mechanical properties of the LWAC, included 12 cubes (with dimensions 100x100x100 mm), 15 cylinders (ϕ 100x200mm) and 3 small beams (100x100x1200mm). From mentioned samples, the authors derived the stress-strain diagram, compressive strength for cube and cylinder, tensile strength, Young's modulus of elasticity and fracture energy. All small specimens were demolded after 24 hours and kept in water until testing day. Compression test on cubes and cylinders were carried out in the start, middle and last day of beam testing.

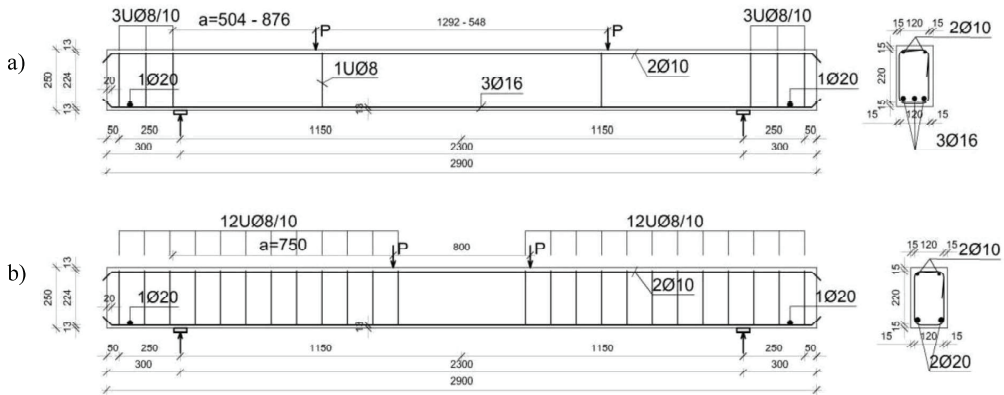


Figure 1 – Reinforcement and cross section details for the beams a) without and b) with shear reinforcement

2.2 Material and mix properties

The concrete mixture was prepared from one batch. The lightweight aggregate was the ½” fraction from Stalite [11]. The moisture content and the absorbed water in the Stalite were measured, which was necessary input when designing the concrete mix [12, 13]. The moisture content was 8.2%, and the absorption after 24 hour and 100 hours was 6 % and 8.5%, respectively. Table 2 gives the concrete mixture.

Table 2 – Concrete mixture for LWAC 65

Constituent	Weight [kg/m ³]
Cement (Norcem Anlegg)	398.21
Silica fume (Elkem Microsilica)	19.62
Water (free+absorbed 24 hour)	93.87+40.12=134
Sand (Årdal (NSBR) 0/8 mm)	745.56
Aggregate (Stalite 1/2")	618.79
Superplasticiser (Sika ViscoCrete RMC-420)	3.20

The mixing was done using a 0.8 m³ laboratory mixer. First cement, silica fume, Stalite and sand were mixed for approximately 2 min. Water and superplasticiser were continuously added and adjusted during mixing, until the desired workability of the concrete was achieved.

Characteristics of the fresh concrete were: density 1990 kg/m³, air content 2.6 % [14] and slump 140 mm [15]. The reinforcement was of the type B500NC [16]. The yielding stress of the reinforcement assumed in calculation is approximately 560 MPa.

2.3 Test Setup and procedure

The load was applied with a mechanical screw jack and was transferred to the test beam through a steel spreader beam, which was supported, on two steel rollers covering the entire width of the beam. The loading point has free rotation transversal to the beam. Between jacks and the beam surface, it was used 50 mm wide steel plates and a 15 mm thick fibreboard with the same width. The supports were both free for rotation and displacement in the longitudinal direction. At the supports, only steel plate was between the support and the beam. The supports were placed 300 mm from the beam-ends. To avoid anchorage problems, short $\phi 20$ mm reinforcement bars were welded to the tensile reinforcement in this region. The load was measured using electrical load cell under the screw jack of maximum capacity 1000 kN. Instrumentation set-up differs between beams with and without shear reinforcement. Figure 2 shows the layout of the test set-up for the beams with and without shear reinforcement and view from the laboratory.

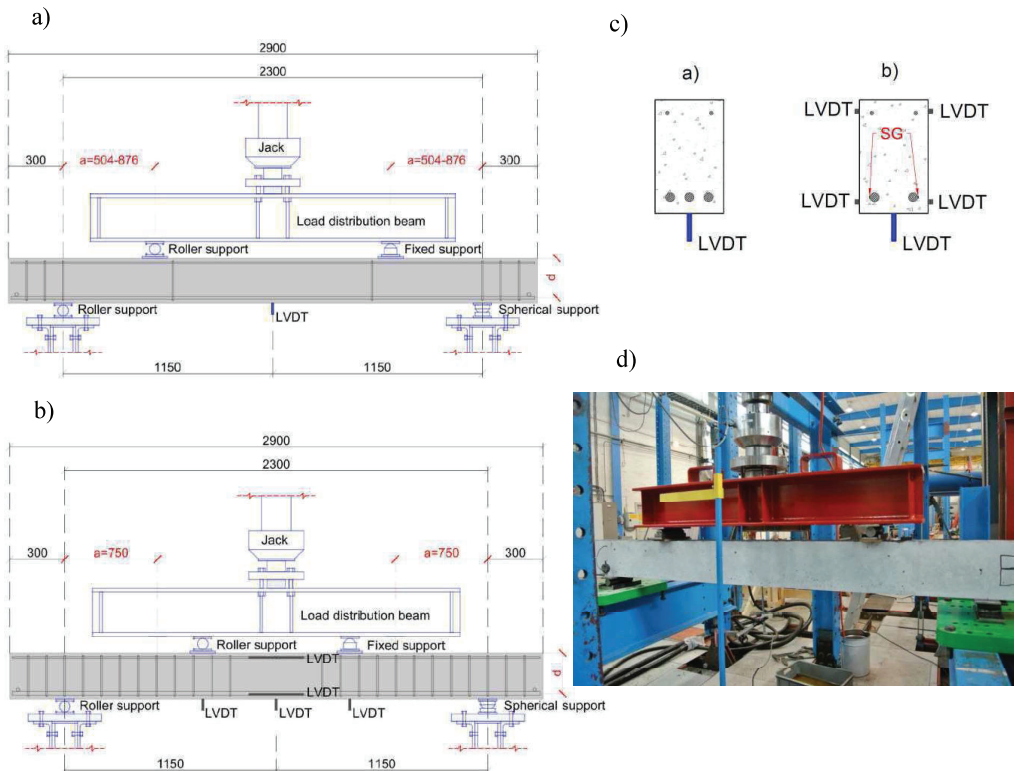


Figure 2 – Test set-up off beams a) without shear reinforcement; b) with shear reinforcement; c) detail middle cross section for beam without and with shear reinforcement; d) view from the laboratory.

For observation of beam with shear reinforcement, more instrumentation was used. Linear Variable Displacement Transducers (LVDT) measured the deflections in the middle of the beam span in all the beams. In beam with shear reinforcement additional LVDT were used for measuring deformations under the loading points and over the middle cross section. Length of LVDT for observation of middle section was 200 mm. In addition, in this beam strain gauges

(SG, type FLA-6-11-5L with gauge resistance of $119,5 \pm 0,5 \Omega$) were inserted on the tensile reinforcement inside of the middle cross section. All measuring devices (LVDTs and SGs) together with the load cell were connected to HBM eight channel spider to record the data. From here, data were sent to computer using a specific software program, where they are processed and stored in a text file.

The load was applied stepwise in increment of 20 kN for the beams without shear reinforcement until failure. For the beam 5, with shear reinforcement, an increment of 40 kN was used since calculated capacity was doubled. The first tested beam was beam 1, one of two beams with shear span ratio 2.3. This beam was tested with loading steps of 10 kN. Since there was too many steps and testing takes, more than 2 hours loading steps were increased on 20 kN for the next beam with 2.3 ratio and for the two beams with 4.0 ratio. This is displacement control test with loading rate 0.5 mm/minute for the beams without shear reinforcement and 1 mm/minute for beam with shear reinforcement. The deflection measurements were carried out as a control. At each step, deflections in the middle section and under the loading points were measured. The loading time for each step takes about 10 minutes, from what 5 minutes was break and mainly used to draw the crack progression with dark pen. The output data were recorded by the data acquisition system. Pictures were taken after each step and failure.

3. EXPERIMENTAL RESULTS

3.1 Results for small specimens

Concrete class measured from small samples was LC65 and that actually represents high strength lightweight concrete. The compressive failures of cubes and cylinders were very explosive which is typical for high strength and lightweight concrete.

Small specimens were tested after 28 days for determination of compressive strength, 29 days for tensile strength and Young's modulus. Small beams for fracture energy were tested after 36 days. A brief summary of the small scale test results is given in Table 3.

Table 3 – Mechanical properties for LWAC

Saturated density	$\rho_{cs} = 1980 \text{ kg/m}^3$
Oven dry density	$\rho_{cv} = 1850 \text{ kg/m}^3$
Compression cube after 7 days	$f_{cm,7} = 57,3 \text{ N/mm}^2$
Compression cube after 28 days	$f_{cm,28} = 73,8 \text{ N/mm}^2$
Compression cylinder	$f_{cm} = 67,5 \text{ N/mm}^2$
Tensile strength	$f_{ctm} = 4,05 \text{ N/mm}^2$
Modulus of elasticity	$E_{cm} = 24175 \text{ N/mm}^2$
Fracture energy	$G_F = 76,7 \text{ Nm/m}^2$

3.2 Capacity of the beams

Table 4 shows the results of the tested beams. In the table, the following forces are plotted: the forces when the first bending crack occurred (P_{fcr}), force of diagonal cracking (P_{cr}) and failure force (P_u). The shear capacity ($P_{calc} = V_{Rd,c}$) for both pairs of the beams without shear reinforcement was calculated according to Eurocode 2 [17, 18, 19] and Norwegian standard NS 3473 [20, 21] and those values were 42.8 kN and 44.6 kN, respectively. Calculation of shear capacity according to both standards was influenced by external load but position of the load

was not taken into account, which resulted with the same capacity for the beams with shear span ratio 2.3 and 4. Calculated shear capacity for all the tested beams plotted in the table 4 was according to Eurocode 2 [17, 18, 19]. Shear capacity according to Eurocode 2 for the beam 5 which contain shear reinforcement was almost doubled and that value is 92.85 kN. Shear capacity for beam with ratio 2.3 and 4 was also calculated according to Norwegian standard NS 3473 and that value was plotted in table 5. Reason for this is that all previous results for comparison were calculated by using the same standard NS 3473. Tensile strength used in this calculation is obtained from small scale testing [5] and later interpolated according to NS 3473. For lightweight concrete the values are multiplied by a reduction factor $(0,30+0,70\rho/\rho_1)$, where ρ is the dry density of the lightweight concrete and $\rho_1=2400 \text{ kg/m}^3$. Hence, with a dry density of 1850 kg/m^3 the reduction factor was 0,839.

The beams were tested 30 days (beam 1_ with shear ratio 2.3), 31 days (2_2.3), 34 days (3_4.0 and 4_4.0) and 35 days (5_3.43) after casting.

Table 4-Test parameters and results of first cracking, diagonal cracking, failure loads and calculated shear capacity in accordance with EC2[17,18]

Beam	<i>a</i> [mm]	<i>d</i> [mm]	<i>a/d</i>	P_{fcr} [kN]	P_{cr} [kN]	P_u [kN]	P_{calc} [kN]	P_{cr}/P_{calc}	P_u/P_{calc}
1	504	219	2.3	25	45	92.3	42.8	1.05	2.15
2	504	219	2.3	22.5	44.5	127.2	42.8	1.04	2.97
3	876	219	4	21	36.8	44.4	42.8	0.86	1.04
4	876	219	4	21	33	62	42.8	0.77	1.44
5	750	219	3.43	25	40	91.4	92.85	0.43	0.98

In all the beams first cracking started for approximately, same load level of 21-25 kN. Formation of the first shear diagonal cracks depend and differs from the shear span ratio. So in the beams with higher shear span ratio shear cracks formed for lower load level, while by reducing shear span (*a*), distance between loading point and support, shear capacity increased.

3.3 Load-deformation relationship

The load–deformation relationship was followed during the entire test. Figure 3 shows the load–deformation relationship for the centre point of the cross section at middle span for all the five beams. As expected, beams that do not contain shear reinforcement along the shear span and with low shear span ratio 2.3, had higher capacity. Beam 2, with shear span ratio 2.3 had even higher capacity than the beam 5 that contain shear reinforcement. The resemblance between two identical beams is quite good before failure. As expected, the response depends on the shear span ratio. With a low ratio a concrete strut forms making a direct load transfer of the point load to the support. The load and deformation can increase several times the shear cracking load. However, the ultimate load is more unpredictable in this case. For a high shear span ratio, pure shear governs the failure mode. The failure loads for these two beams can be defined to be the same. Beam 4 with shear span ratio 4.0 was able to sustain a higher load after significant deformations, but it is not possible to rely on such deformations in a design situation. As expected the beam with shear reinforcement showed significant ductility, deflections are doubled for the same load level and before failure this beam were able to sustain even increase of loading. In addition, one of the beam with shear span ratio 2.3 showed very ductile behaviour. In general, all the tested beams are in the very good agreement considering the main test parameter shear span ratio.

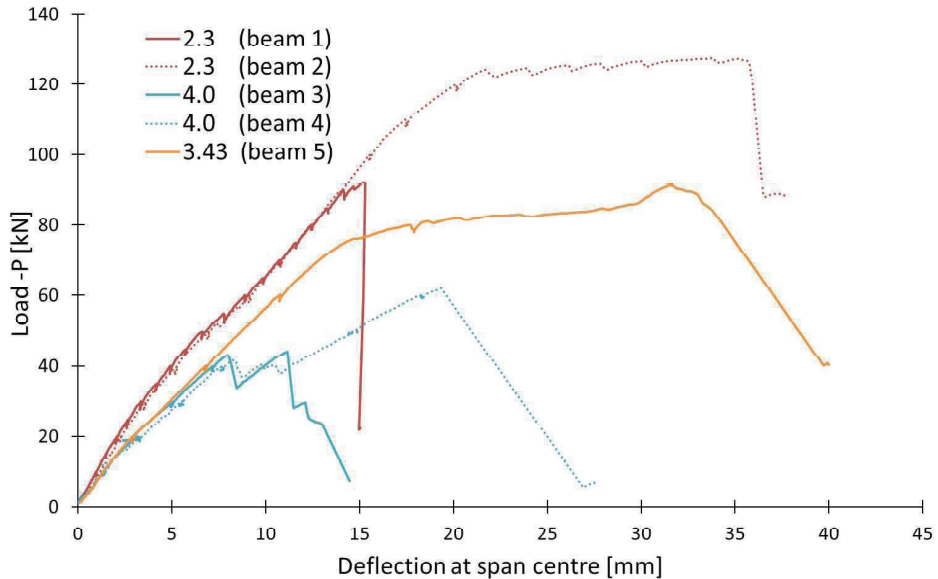


Figure 3 – Load deflection curves for all the tested beams

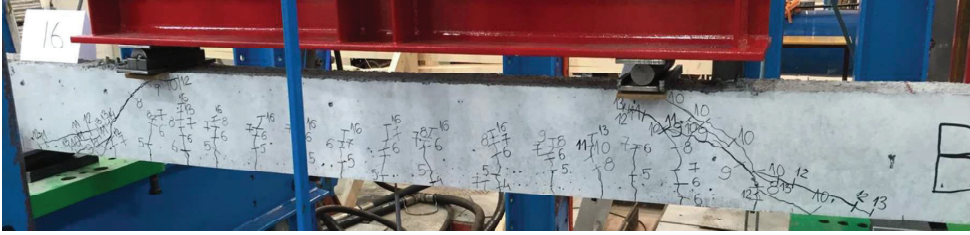
Results of strain distribution were observed and recorded over the middle cross section just in beam 5 with shear ratio 3.43. Since those results cannot be compared with first four tested beams 1-4. they are not plotted here.

4. DISCUSSION

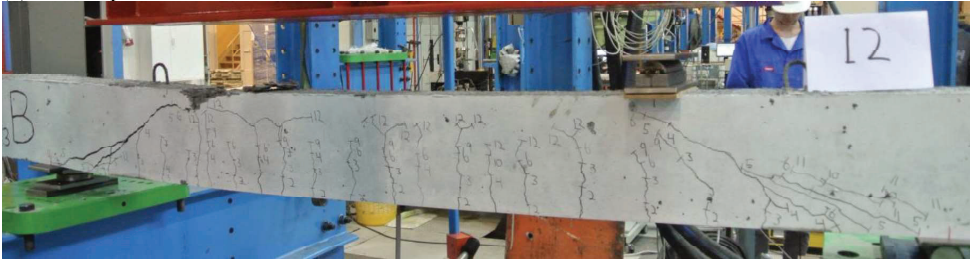
4.1 Failure modes, cracking patterns and capacity of the beams

The first cracks in all beams started to develop in the constant moment region, between the loading points, on the tension side for load levels between 20 and 40 kN, depending on the a/d ratio. As load increased cracks formed along the entire length of the constant moment region and wider. When flexural bending cracks stopped to develop, suddenly, the diagonal shear cracks occurred, but the beams did not fail immediately. The beams with a/d ratio of 2.3 formed directly the diagonal inclined shear crack. These cracks appeared suddenly developing from the tension side of the beam towards the compression side near the point loads. For beams with ratio 2.3 diagonal cracks formed at higher load levels than for beams with ratio 4.0. For beams with ratio 4.0 the diagonal shear cracks propagated from one of the flexural bending cracks at the tension side. For beams with shear reinforcement and shear span ratio 3.43 cracking started from the tension side. Location of cracks depends from reinforcement layout. Flexural bending cracks start to form between stirrups. Later diagonal shear cracks propagated from flexural bending cracks. For a certain load level propagation of diagonal cracks was stopped due to shear reinforcement while propagation of bending cracks were continued. At the end, bending cracks led to failure in beam with shear reinforcement, while in beams without shear reinforcement diagonal shear cracks lead to failure. Figure 4 showed the final failure state of all the tested beams.

(a) Shear span ratio 2.3 - beam 1



(b) Shear span ratio 2.3 - beam 2



(c) Shear span ratio 4.0 - beam 3



(d) Shear span ratio 4.0 - beam 4



(d) Shear span ratio 3.43 - beam 5



Figure 4 – Final failure state for beams (a) 2.3-1; (b) 2.3-2; (c) 4.0-3; (d) 4.0-4 and (e) 3.43-5

In general, beams with lowest shear span ratio had higher capacity, see Table 4. Formation of cracks for beams with ratios 4.0 and 3.43 was equal in both shear spans. For beams with ratio 4.0 failure happened suddenly in one of the shear span, while beam with ratio 3.43 failed in compression between the loading points. In the beams with ratio 2.3 shear cracking was more non-symmetrical, with more and larger cracks at one end of the beam, and beams failed at the shear span.

Failure that happened between support and the loading point, shear zone, is defined as shear tension failure or shear compression failure depending which zone cracked [22, 23]. Here we can notice that beams with ratio 2.3 in the final failure phase cracked always under the loading points so they had shear compression failure. In beams with ratio 4.0 development of cracks on a tension shear zone were wide, cracks followed tensile reinforcement, and they even continued in anchorage area, so they had shear tension failure.

Behavior of beam with ratio 3.43 in beginning matches well with beams with ratio 4.0. However, due to shear reinforcement this beam had approximately double jump in capacity and at the end cracking of compression zone between loading point happened. This type of failure can be defined as bending compression failure [22, 23].

In general, cracking and failure mechanism for beams without web shear reinforcement, which is typical for NWC, is that crack will appear in the shear span by increasing the load. Owing to the presence of the shear stresses, they bend towards the axis of the beam. Other secondary cracks due to stress redistribution may also appear. The development of the diagonal cracks stops at a certain load level, while the crack propagating into the compression zone. The beam either collapses simultaneously with the appearance of this diagonal crack or continue to sustain higher load until crushing the concrete in the compression zone. The term diagonal crack load is in this work defined as the load when the formation of the specific shear crack happened, which later develops into shear failure. The load for which the testing beam collapses is the ultimate load or load carrying capacity [24, 25, 26].

Due to the brittle nature for LWAC it is typical that diagonal cracking load is equal to ultimate load. However, after formation of diagonal cracks in this experiment beams were able to carry an increase the loading [26, 27]. The cracks propagated almost horizontally along the tensile reinforcement and diagonally into the compression zone. In some cases the cracks even passed the loading point and into the constant moment region. In the final stage, the shear cracks opened widely together with sliding along of the diagonal cracks and resulted in crushing of the concrete close to the loading point, see Figure 4. In the beam that contained shear reinforcement formation of cracks have determined by reinforcement layout and for the certain load level development of shear cracks is limited and stopped with shear reinforcement. This resulted in significant increase in capacity and contribute to ductile behavior of the beam. Even this as all the tested beams are from lightweight aggregate concrete, this beam was able to withstand increase of loading in final failure phase.

4.2 Comparison with previous experimental work

Similar tests have earlier been carried out for higher strength concrete classes of normal density and lightweight aggregate concretes. Table 5 shows a comparison of these tests with the present investigation tests with $a/d = 2.3$ and with $a/d = 4.0$ for the beams without shear reinforcement. Beam with shear span ratio 3.43 is out of the comparison since this beam contained shear reinforcement. In all previous investigation the tests conditions were the same, including the rig,

the cross section and the amount and distribution of reinforcement [1,2]. Shear capacity for all the previously tested beams were calculated according to Norwegian standard NS 3473 [20, 21]. Because of the comparison shear capacity for the beams with shear span ratio 2.3 and 4 was also calculated according to the same standard and that value was 44.6 kN. Again all the beams without shear reinforcement have the same capacity since standard in calculation of the shear capacity do not include the load position.

The concrete types compared with previous investigations are ND65, ND95, LWA75, LWA40 and LWAC_Leca. The ND65 and ND95 concretes had normal density aggregates from Årdal with maximum aggregate size 16 mm. The mean cylinder strengths of these concretes were 54 and 78 MPa and the dry density was between 2300 and 2350 kg/m³.

The LWA75 concrete had natural sand (0-4 mm) and Liapor 8 (lightweight aggregate [28, 29]) in the coarse fraction from 4 to 16 mm. The mean cylinder strength of this concrete was 58 MPa and the dry density about 1900 kg/m³. The LWA40 had natural sand (0-4 mm) and Leca 700 aggregate (4-16 mm), while LWAC_Leca also had Leca but several fractions (Leca sand (0-4 mm, crushed), Leca sand (2-4 mm, round), Leca 7 (4-8 mm) and Leca 7 (8-12 mm)). The mean cylinder strengths of these concretes were 37 and 42,7 MPa, and the dry densities about 1600 and 1320 kg/m³, respectively [1]. For all of these concretes capacity was calculated according to NS3473 (P_{calc}).

The results of main interest for this comparison is the ratio between the observed shear diagonal cracking load and calculated capacity and also ratio between obtained failure load and capacity.

Table 5 - Comparison of the shear strengths for beams with $a/d = 2.3$ and 4.0 , shear capacity is calculated in accordance with NS3473[20]

Beam/Aggregate	a/d	$f_{lc,cyl}$ [MPa]	P_{cr} [kN]	P_u [kN]	P_{calc} [kN]	P_{cr} / P_{calc}	P_u / P_{calc}
1/Stalite	2.3	67.5	45	92.3	44.6	1.01	2.07
2/Stalite	2.3	67.5	44.5	127.2	44.6	1.00	2.85
ND65/Årdal	2.3	54	62.2	71.6	55.1	1.13	1.30
ND95/Årdal	2.3	78	66.7	103.5	57.3	1.16	1.81
LWA75/Liapor 8	2.3	58	47.1	126.1	52.0	0.91	2.43
LWA40/Leca	2.3	37	46.6	77.9	39.3	1.19	1.98
LWA_Leca_mix	2.3	42.7	34.3	102.9	42.1	0.81	2.44
3/Stalite	4	67.5	36.8	44.4	44.6	0.82	0.99
4/Stalite	4	67.5	35	62	44.6	0.78	1.39
LWA40/Leca	4	37	38.2	38.2	39.30	0.97	0.97
LWA_Leca_mix	4	42.7	29.4	44.1	42.10	0.70	1.05

where a/d is shear span ratio; $f_{lc,cyl}$ -compressive cylinder strength; P_{cr} - load level for first shear crack; P_u - load level of maximum load; P_{calc} - calculated shear capacity according to Norwegian standard NS3473 [20].

For beams with $a/d = 2.3$, the ratio between shear diagonal cracking load and calculated load was larger or equal to 1.0 for all concretes except LWA75 and LWA_Leca_mix. This indicates that they are on the conservative side. For LWA75 and LWAC_Leca_mix, this ratio was less than 1.0, indicating a higher drop in shear strength than predicted by NS 3473. The ratio between ultimate load and calculated one for all LWA concretes was almost 2 or higher, which shows that LWA concretes in general can withstand more loading than predicted by standards.

For normal density concretes, this ratio was lower. In general, it is obvious that shear capacity calculated by standards is significantly underestimated compared with experimental results.

It can be observed that the ultimate load capacity for the beams 1 and 2 with shear span ratio 2.3 was slightly higher than for the beams with normal weight concretes ND65 and ND95. This result was expected because LWAC concrete with Stalite as aggregate have the same behaviour as normal weight concrete. Slightly higher ultimate load than for normal weight concrete might be result of stronger transition zone between the aggregate and the matrix, which result in cracking development around and trough lightweight aggregate.

The ND65, ND95 and LWA75 concretes were not tested with ratio $a/d = 4.0$. For beams with $a/d = 4.0$, the ratio between shear diagonal cracking load and calculated load for both concretes tested was below 1.0 – indicating that beams with $a/d = 4.0$ had a certain drop in capacity [1,12]. The ratio between ultimate load and calculated one for all the beams is around or higher than 1.0 – indicating that standards are applicable for larger shear span ratios. In general, calculation by standards matches well with experimental results for the beams with ratio 4.0. The same can be noted from the Table 4 for the beam 5 with ratio $a/d = 3.43$, where the ultimate capacity predicted by standard matches well with experimental one.

For tested LWA concrete with Stalite as aggregate, the diagonal cracking load was close to other lightweight aggregate concretes, while the failure load was higher, especially in the case of $a/d = 4.0$.

In comparison with normal density concretes ND65 and ND95, the diagonal cracking load for normal concretes was approximately 30% higher, while failure load for LWAC with Stalite was significantly higher.

Actually, from this experimental investigation from high importance is the fact that after shear diagonal crack were formed beams can withstand increase of load from 30 to 50 %, which is of great importance having in mind that here is tested lightweight aggregate concrete. In addition, by introducing the shear reinforcement in beams with very similar shear span ratio, 4.0 and 3.43, ultimate capacity will increase and nature of failure differ from shear failure to bending failure.

5. CONCLUSIONS

For all tested beams in this experiment, the shear stress at inclined cracking of the beams decreased with an increase in the shear span to effective height ratio (a/d). Cracking propagation in the tested beams showed that they were more ductile than expected, which should promote increased investigation and structural use of this type of LWAC. Beam with shear reinforcement showed significant ductility compared to other tested beams.

For beams with larger shear span ratio (3.43 and 4.0) calculations predicted by standards, match well with experimental results, while standards underestimate a lot ultimate capacity in beams with lower sheer span ratio (2.3). Calculation of the shear capacity according to existing standards do not take into account position of the load, shear span a . Standards just differ between the beams congaing or not shear reinforcement. According to this experimental investigation, the design strength for shear in beams and slabs without shear reinforcement should be based on inclined cracking loads.

Comparison with similar tests on other types of lightweight concretes and normal density concretes showed the same that the shear stress at inclined cracking of the beams decreased with an increase in shear span ratio (a/d). For concretes tested in this experiment and in previous investigation ratio between the load observed at diagonal cracking and the predicted strengths was in the same range. However, the ratio between observed load at failure and the strengths predicted was significantly higher for the lightweight concrete used in this investigation.

6. FURTHER RESEARCH

During this experimental work was observed that the load-carrying capacity of LWAC members is very similar to that of corresponding ND concrete members. The high strength-to-weight ratio of LWAC compared to ND concrete means that increased use of the material in structural applications would be both economical and environmentally friendly. In the continuation of this project, a better understanding of the ultimate behaviour of LWAC in compression and bending by varying different reinforcement detailing will be of main interest.

7. ACKNOWLEDGMENT

The work presented in this paper is part of ongoing PhD study in scope of the DACS project (Durable Advanced Concrete Solutions). The DACS partners are Kværner AS (project owner), Norwegian Research Council, Axion AS (Stalite), AF Gruppen Norge AS, Concrete Structures AS, Mapei AS, Multiconsult AS, NorBetong AS, Norcem AS, NPRA (Statens vegvesen), Norwegian University of Science and Technology (NTNU), SINTEF Byggforsk, Skanska Norge AS, Unicon AS and Veidekke Entreprenør AS. The first author would like to express her outmost gratitude to the supervisors and all the project partners for contributions and making this PhD study possible. In addition, special gratitude goes to master students Christian Lund and Jon Myhre Sakshaug who helped during production and testing of the samples for this experiment.

8. REFERENCES

1. E. Thorenfeldt , H. Stemland, “Shear capacity of lightweight concrete beams without shear reinforcement”, International Symposium on Structural Lightweight Aggregate Concrete, Sandefjord, Norway, 20-24 June 1995 , pp. 244-245.
2. J. Zivkovic, J.A. Øverli, “Shear capacity of lightweight concrete beams without shear reinforcement”. Proceedings of The Eleventh High Performance Concrete (11th HPC) & The Second Concrete Innovation Conference (2nd CIC) Tromsø, Norway 2017.
3. Standard Norge. NS-EN 12390-3:2009. Testing hardened concrete - Part 3: Compressive strength of test specimens Lysaker: Standard Norge; 2009.
4. K. Watanabe, J. Niwa, H. Yokota and M. Iwanami, “Experimental Study on Stress Strain Curve of Concrete Considering Localized Failure in Compression“, Journal of Advanced Concrete Technology Vol. 2, No.3; 2004: 395-407.
5. Standard Norge. NS-EN 12390-6:2009. Testing hardened concrete - Part 6: Tensile strength of test specimens Lysaker: Standard Norge; 2009.

6. Skjølsvold O, Bakken N, Johansen E. KS 14-05-04-122: Bestemmelse av E-modul iht NS3676 Losenhausen 5000kN trykkpresse. SINTEF Byggforsk: Betong og natursteinslaboratooriene; 2007.
7. Standard Norge. NS 3676. Concrete testing - Hardened concrete - Modules of elasticity in compression. Norway: Standard Norge; 1987.
8. A. Hillerborg, "The theoretical basis of a method to determine the fracture energy G_f of concrete", RILEM Technical Committees, Materials and Structures, July 1985, Volume 18, Issue 4 :291-296.
9. R.W. Castrodale, J. Zivkovic, and R. Valum. Material Properties of High Performance Structural Lightweight Concrete. Proceedings of the Eleventh High Performance Concrete (11th HPC) & the Second Concrete Innovation Conference (2nd CIC) Tromsø, Norway 2017.
10. EuroLightCon. Lwac Material Properties. Document BE96-3942/R2, December 1998.
11. TEC Services. Interim report of astm c330 Carolina Stalite 0, 5 inch coarse lightweight aggregate. TEC Services Project No: 04-0514, TEC Services Sample ID: 14-999, 2015.
12. ACI Committee 213. Guide for Structural Lightweight Aggregate Concrete (ACI 213R-03). American Concrete Institute. Farmington Hills, MI, United States: American Concrete Institute; 2003.
13. Yong G.E., Kong L., Zhang B., Jie Y., Effect of Lightweight Aggregate Pre-wetting on Microstructure and Permeability of Mixed Aggregate Concrete, Journal of Wuhan University of Technology-Mater. Sci. Ed. October 2009, Vol 24; Issue 5: 838-842.
14. Standard Norge. NS-EN 12390-7:2009. Testing hardened concrete - Part 7: Density of hardened concrete. Lysaker: Standard Norge; 2009.
15. Methods for Testing Fresh Lightweight Aggregate Concrete (Document BE96-3942/R4, December 1999)
16. Standard Norge. Armeringsstål - mål og egenskaper - del 3: Kamstål B500NC. NS 3576-3:2012, 2012.
17. EN 1992-1-1 (2004), "Eurocode 2: Design of concrete structures – Part 1 -1: General rules and rules for buildings".
18. NS-EN 1992-1-1:2004+NA: 2008. Eurocode 2: Design of concrete structures - General rules and rules for buildings. Standard Norway. Norway; 2008.
19. Svein Ivar Sørensen. Betongkonstruksjoner, Beregning og dimensjonering etter Eurokode 2, 2.utgave, 2013
20. NS 3473 Norges Standardiseringsråd, "NS3473 Concrete structures – Design and detailing rules", Norges Standardiseringsråd. Norge; 2003.

21. NS-EN 206:2013+NA: 2014 (2014): "Betong, Spesifikasjon, egenskaper, framstilling og samsvar", Norges Standardiseringsråd. Norge; 2014.
22. ACI-ASCE Committee 426, "The Shear Strength of Reinforced Concrete Members" ACI Structural Division, Proceeding of ASCE, Vol.99, No.ST6, June 1973, pp.1091-1187.
23. Van Den Berg F. J., "Shear Strength of Reinforced Concrete Beams Without Web Reinforcement, Part 2" ACI Journal Proceeding, Vol. 59, No. 11, 1962, pp.1587-1600.
24. J.P Zhang, Diagonal cracking and shear strength of reinforced concrete beams, Magazine of Concrete Research, 1997, 49, No. 178, Mar. 55-65.
25. Zararis P., Papadakis G., "Diagonal Shear Failure and Size Effect in RC Beams without Web Reinforcement." J. Struct. Eng., 10.1061/ (ASCE) 0733-9445(2001)127:7(733), 733-742.P.
26. T.M. Jensen, J. A. Øverli, "Experimental study on flexural ductility in over-reinforced lightweight aggregate concrete beams" , COIN Project report no 47-2013, (2013).
27. S. H. Ahmad, Y. Xie , T. Yu, "Shear Ductility of Reinforced Lightweight Concrete Beams of Normal Strength and High Strength Concrete", Cement & Concrete Composites 17 (1995) 147- 159.
28. Properties of lightweight concretes containing Lytag and Liapor (Document BE96-3942/R8, March 2000)
29. Lo T.Y., Tang W.C., Cui H.Z., The effects of aggregate properties on lightweight concrete. Building and Environment 2007; 42:3025-3029.

Annex A – Conference papers

Paper 1

Shear capacity of lightweight concrete beams without shear reinforcement

Jelena Zivkovic, Jan Arve Øverli

*Proceedings of the Eleventh High Performance Concrete (11th HPC) & The Second Concrete Innovation Conference (2nd CIC), Tromsø, Norway, March 6th – 8th 2017
Norwegian Concrete Association / Tekna 2017 ISBN 978-82-8208-054-5*

A large, white, serif numeral '1' is centered on a dark blue rectangular background that occupies the right side of the page.

SHEAR CAPACITY OF LIGHTWEIGHT AGGREGATE CONCRETE BEAMS WITHOUT SHEAR REINFORCEMENT



Jelena Zivkovic
PhD, Researcher
Department of Structural Engineering
Faculty of Engineering Science and Technology
Norwegian University of Science and Technology
N-7491 Trondheim
E-mail: jelena.zivkovic@ntnu.no



Jan Arve Overli
PhD, Professor
Department of Structural Engineering
Faculty of Engineering Science and Technology
Norwegian University of Science and Technology
N-7491 Trondheim
E-mail: jan.overli@ntnu.no

ABSTRACT

The main disadvantages of lightweight aggregate concrete (LWAC) compared with normal weight concrete are its brittleness at the material level in compression and the risk of uncontrolled crack propagation. The brittleness of concrete is characterized by its sensitivity to stress concentrations and rapid crack/fracture development. This paper presents results from an experimental investigation with Stalite as the lightweight aggregate. The main goals were to investigate beams subjected to shear and to compare these results with previous experimental work. Four lightweight concrete beams without shear reinforcement were tested in four-point bending. The main test parameter was the shear span length to effective height ratio (a/d). The shear loads of all beams at diagonal cracking and at failure were plotted as a function of the a/d ratio and compared with previous results. Small specimens were also tested to find the compressive strength, splitting tensile strength, Young's modulus, and fracture energy. The beams tested did not show brittle behaviour. After the formation of shear diagonal cracks, the beams were able to resist increased loading. In general, the beams were more ductile than expected. The results obtained during this testing show that this type of LWAC has almost the same behaviour as normal weight concrete.

Keywords: lightweight aggregate concrete, shear capacity, ductility, bending test.

1. INTRODUCTION

1.1 General

This investigation was part of the ongoing research programme, “Durable advanced concrete structures (DACS)”. One part of this programme is to investigate the structural behaviour of lightweight aggregate concretes (LWAC), i.e. concretes with an oven-dry density below 2000 kg/m³. One general characteristic of LWAC is its very high degree of brittleness at the material level in compression. Brittleness in concrete is characterized by sensitivity to stress concentrations and rapid crack/fracture development. This influences the behaviour of concrete where its tensile strength is important, as for instance with its shear and bond strength.

To investigate the brittleness of LWAC, it was decided to subject beams without shear reinforcement to shear in a four-point bending test. The main test parameter was the shear span length to effective height ratio (a/d). The shear loads of all beams at diagonal cracking and at failure were plotted as a function of the a/d ratio. For comparison, the tests were carried out on beams with the same size and reinforcement as used in earlier shear tests on other normal density (ND) and lightweight aggregate (LWA) concretes [1]. In addition, small specimens were used to find the compressive strength [3, 10], splitting tensile strength [11], Young’s modulus [14], and fracture energy [15].

The project aimed for an oven-dry density of about 1800 kg/m³ and a compressive strength of about 60 MPa.

2. EXPERIMENTAL TEST PROGRAMME

2.1 Test specimens

Four reinforced LWA concrete beams without shear reinforcement were subjected to a four point bending test. The loading system was designed to produce a constant moment in the middle of the beam. The beams measured (width x height x length) 150 x 250 x 2900 mm. Four beams were tested, two with $a/d = 2.3$ and two with $a/d = 4.0$. In the ratio a/d , a is the length of the shear span and d is the effective height of the cross section (the distance from the top surface to the centre of the tensile reinforcement), which in this case was 219 mm. An overview of the test programme is shown in Table 1.

Table 1 – The main test parameters

Beam	Tensile reinforcement		Shear span a (mm)	Effective height d (mm)	a/d
	Bars	$A_s / (bxd)$ (%)			
2.3-1	3Ø16	1.82	876	219	2.3
2.3-2	3Ø16	1.82	876	219	2.3
4.0-1	3Ø16	1.82	504	219	4.0
4.0-2	3Ø16	1.82	504	219	4.0

The beams had three Ø8 mm stirrups in each anchorage zone (behind the supports) and two in the constant moment region below applied forces. There were no stirrups in the shear spans. This layout of transverse reinforcement was used to provide shear failure. Reinforcement on the tension side consisted of three bars Ø16 mm. As compressive reinforcement, two Ø10 mm bars were used. Longitudinal and cross section details of the beam specimens are shown in Figure 1.

The beams were demoulded 24 hours after casting and further cured in the laboratory under wet burlaps covered with a plastic sheet. Two days before the testing, the beams were taken out and prepared for instrumentation. Finally, the beams were painted white for easier detection of cracks

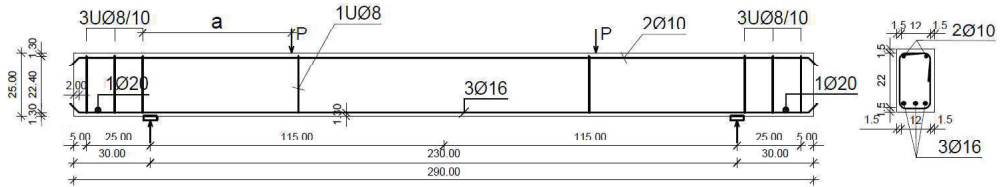


Figure 1 – Reinforcement and cross section details for the beams

To establish the mechanical properties of the LWAC, 12 cubes (with dimensions 100x100x100 mm), 15 cylinders (Ø100x200mm) and three small beams (100x100x1200mm) were cast to find the stress-strain diagram, the compressive strength for cube and cylinder, the tensile strength, Young's module of elasticity, and the fracture energy. All these small specimens were demoulded after 24 hours and kept in water until testing day. The compression tests on cubes and cylinders were carried out at the start, in the middle, and on the last day of beam testing.

2.2 Material and mix properties

The concrete mixture was prepared from one batch. The lightweight aggregate was the ½" fraction from Stalite [16]. The moisture content and the absorbed water in the Stalite were measured – necessary input for designing the concrete mix [2, 20]. The moisture content was 8.2%, and the absorption after 24 hours and 100 hours was 6% and 8.5%, respectively. Table 2 gives the concrete mixture.

Table 2 – Concrete mixture for the LWAC

Constituent	Weight [kg/m ³]
Cement (Anlegg)	398.21
Silica fume (Elkem Microsilica)	19.62
Water (free)	93.87
Absorbed water (24 hours)	40.12
Sand (Årdal (NSBR) 0.8 mm)	745.56
Aggregate (Stalite 1/2")	618.79
Superplasticizer (Sika ViscoCrete RMC-420)	3.20

The mixing was done using a 0.8 m³ laboratory mixer. First cement, silica fume, Stalite and sand were mixed for approximately 2 min. Water and superplasticizer were then continuously added and adjusted during mixing, until the desired workability of the concrete was achieved.

Characteristics of the fresh concrete were: density 1990 kg/m³, air content 2.6% [12] and slump 140 mm [17]. The reinforcement was of the type B500NC [9]. The yielding stress of the reinforcement was assumed to be approximately 530 MPa.

2.3 Test setup and procedure

The load was applied through a mechanical screw jack and was transferred to the test beam through a steel spreader beam, which was supported on two steel rollers extending the entire width of the beam. The loading point had free rotation transversal to the beam. Steel plates and a 15 mm thick fibreboard with the same width were used between the jack and the beam surface. The supports were both free for rotation and displacement in the longitudinal direction. Only steel plates were used between the supports and the beam. The supports were located 300 mm from the beam ends. To avoid anchorage problems, a 20 mm bar was welded to the tensile reinforcement in this region. The load was measured using

electrical load cell under the screw jack with a maximum capacity of 1000 kN. The deflections were measured using a Linear Variable Displacement Transducer (LVDT). The LVDT was located under the middle of the beam span. The load cell and the LVDT were connected to a data acquisition system to record the data. Figure 2 shows the test setup for the beams.

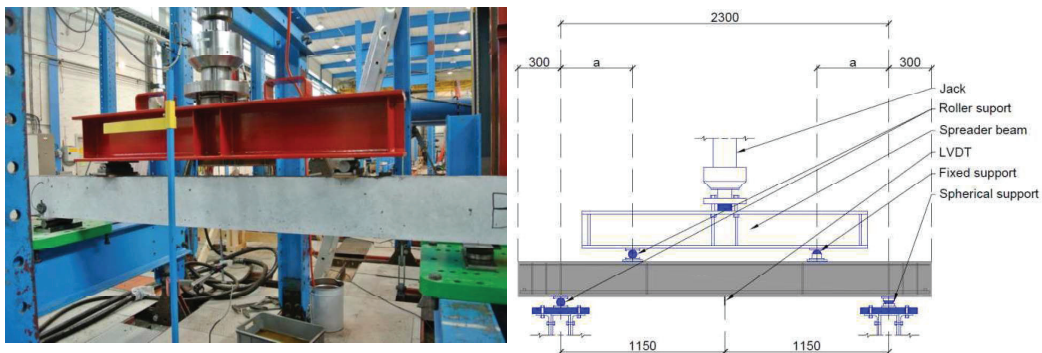


Figure 2 – Test setup of beams

The load was applied to the specimens in steps of 20 kN until failure. The first beam tested (2.3-1) had loading steps of 10 kN. At each step, the deflection was measured in the middle section and at the supports for control. The loading time at each step was generally less than 10 minutes. Half of this time was used to draw the crack progression with a dark pen. The output data were recorded by the data acquisition system. Pictures were taken after each step and failure. The deflection measurements were only carried out as a control.

3. EXPERIMENTAL RESULTS

3.1 Results for small specimens

A brief summary of the small-scale test results is given in Table 3. The compressive failures of cubes and cylinders were very explosive, as for high-strength concrete. Since the concrete class was LC65, this represents high-strength lightweight concrete [13].

Small specimens were tested after 28 days to determine compressive strength, and after 29 days to determine tensile strength and Young's modulus of elasticity. Small beams were tested after 36 days to determine their fracture energy.

Table 3 – Mechanical properties for LWAC

Saturated density	$\rho_{es} = 1980 \text{ kg/m}^3$
Dry density	$\rho_{ev} = 1850 \text{ kg/m}^3$
Cube compression after 7 days	$f_{1cm,7} = 57.3 \text{ N/mm}^2$
Cube compression after 28 days	$f_{1cm,28} = 73.8 \text{ N/mm}^2$
Cylinder compression	$f_{1cm} = 67.5 \text{ N/mm}^2$
Tensile strength	$f_{1ctm} = 4.05 \text{ N/mm}^2$
Modulus of elasticity	$E_{1cm} = 24175 \text{ N/mm}^2$
Fracture energy	$G_F = 76.7 \text{ Nm/m}^2$

3.2 Capacity of the beams

Table 4 shows the results of the beam tests. The table includes the forces when the first bending crack occurred (P_{fcr}), the force of the diagonal cracking (P_{cr}) and the failure shear force (P_u). The shear capacity of the beam has been calculated in accordance with Eurocode 2 [4, 7, 8] and NS 3473 [5, 6], and these values are 42.8 kN and 44.6 kN, respectively. The tensile strength used in the calculation was obtained from the small-scale testing [11] and later interpolated in accordance with NS 3473. For lightweight concrete, the values are multiplied by a reduction factor $(0.30+0.70\rho/\rho_1)$, where ρ is the dry density of the lightweight concrete and $\rho_1 = 2400 \text{ kg/m}^3$. This means that with a dry density of 1850 kg/m^3 the reduction factor was 0.839.

The beams were tested 30 days (2.3-1), 31 days (2.3-2) and 34 days (4.0-1 and 4.0-2) after casting.

Table 4 – First cracking, diagonal cracking and failure loads, and comparison with calculated shear strengths in accordance with NS3473

Beam	a/d	P_{fcr} [kN]	P_{cr} [kN]	P_u [kN]	P_{calc} [kN]	P_{cr} / P_{calc}	P_u / P_{calc}	$P_{cr}/b*d$ [MPa]	$P_u/b*d$ [MPa]
(2.3-1)	2.3	25	45	92.25	44.6	1.01	2.07	1.37	2.81
(2.3-2)	2.3	22.5	44.5	127.15	44.6	1.00	2.85	1.35	3.87
(4.0-1)	4	21	36.75	44.35	44.6	0.82	0.99	1.12	1.35
(4.0-2)	4	21	33	62	44.6	0.78	1.39	1.00	1.89

3.3 Load-deflection relationship

The load-deflection curves for the centre point are given in Figure 3 for the four beams. The resemblance between two identical beams is quite good before failure. As expected, the response depends on the shear ratio and beams with a low shear ratio have higher capacity. With a low ratio, a concrete strut forms making a direct load transfer of the point load to the support.

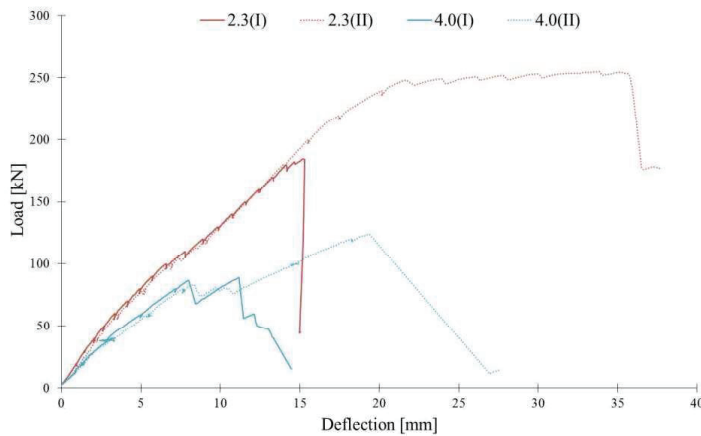


Figure 3 – Load-deflection curves for the four beams

The load and deflection can increase to several times the shear cracking load. However, the ultimate load is more unpredictable in this case. With a high shear ratio, pure shear governs the failure mode. The failure loads for these two beams can be defined to be the same. Beam 4.0-2 was able to sustain a higher load after significant deflection, but it is not possible to rely on such deflection in a design situation.

3.4 Cracking pattern and failure modes

The first flexural cracks in all beams started to develop in the constant moment region on the tension side at load levels between 20 and 40 kN, depending on the a/d ratio. As the load increased, cracks formed along the entire length of the constant moment region. Finally, diagonal shear cracks occurred, but the beams did not immediately fail. The beams with $a/d = 2.3$ formed diagonally inclined shear cracks. These cracks appeared suddenly, developing from the tension side of the beam towards the compression side near the point loads. The diagonal cracks formed at higher load levels in the beams with $a/d = 2.3$ than in the beams with $a/d = 4.0$. In the latter, the diagonal shear cracks propagated from one of the flexural cracks that had started in the moment region. The beams with the lowest shear ratio had approximately twice the capacity; see Table 4. The formation of cracks in beams with $a/d = 4.0$ was fairly equal in both shear spans, and failure happened suddenly in one shear span. In the beams with $a/d = 2.3$, shear cracking was less symmetrical, with more and larger cracks at one end of the beam.

The cracking and failure mechanism in beams without web shear reinforcement, which is usual in NWC, is that cracks will appear in the shear span with increasing load. Owing to the presence of shear stresses, they bend towards the axis of the beam. Other secondary cracks due to stress redistribution may also appear. The development of the diagonal cracks stops at a certain load level when the cracks propagate into the compression zone. The beam either collapses simultaneously with the appearance of the diagonal crack or continues to sustain higher load until the concrete in the compression zone is crushed. The term diagonal cracking load is defined in this paper as the load when the specific shear crack is formed that goes on to lead to shear failure. The load at which the beam collapses is the ultimate load or the load-carrying capacity [21, 22, 23].

Due to the brittle nature of LWAC, the diagonal cracking load is usually equal to the ultimate load. In this experiment, however, the beams could carry increasing load after the diagonal cracks formed [23, 24]. The cracks propagated almost horizontally along the tensile reinforcement and diagonally into the compression zone. In some cases, the cracks even passed the loading point and entered the constant moment region. In the final stage, the shear cracks opened wide as the diagonal cracks spread along the beam and this resulted in the crushing of the concrete close to the loading point, see Figure 4.

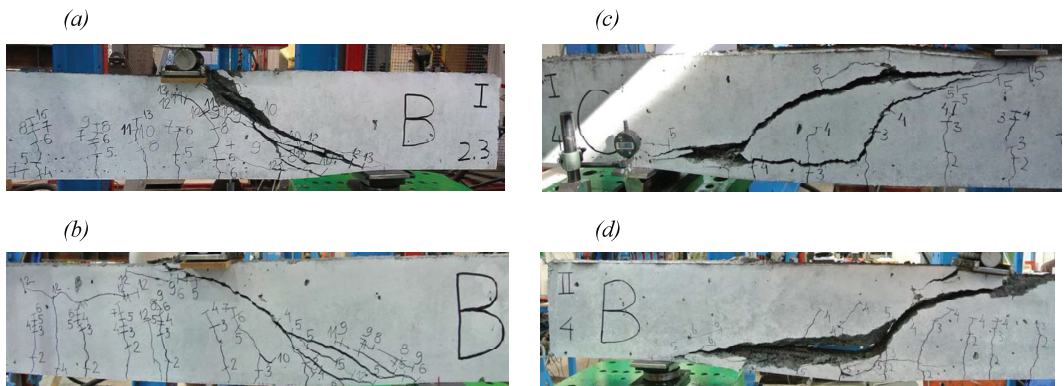


Figure 4 – Final failure state of beams (a) 2.3-1; (b) 2.3-2; (c) 4.0-1 and (d) 4.0-2

4. DISCUSSION

Similar tests have been carried out previously for high-strength concrete classes of normal density and lightweight aggregate concretes. Tables 5 and 6 show these tests compared with the present investigation on beams with $a/d = 2.3$ and $a/d = 4.0$, respectively. The test conditions were the same, including the rig, the cross section, and the amount of reinforcement [1].

The concrete types tested in the previous investigations were ND65, ND95, LWA75, LWA40 and LWAC_Leca. The ND65 and ND95 concretes had normal density aggregates from Årdal with a maximum aggregate size of 16 mm. The mean cylinder strengths of these concretes were 54 and 78 MPa, respectively, and the dry density was between 2300 and 2350 kg/m³.

The LWA75 concrete had natural sand (0-4 mm) and Liapor 8 (lightweight aggregate [18, 19]) in the coarse fraction from 4-16 mm. The mean cylinder strength of this concrete was 58 MPa and the dry density about 1900 kg/m³. The LWA40 had natural sand (0-4 mm) and Leca 700 aggregate (4-16 mm), while the LWAC_Leca also included Leca, but in several fractions: Leca sand (0-4 mm, crushed), Leca sand (2-4 mm, round), Leca 7 (4-8 mm) and Leca 7 (8-12 mm). The mean cylinder strengths of these concretes were 37 and 42.7 MPa, and their dry densities were about 1600 and 1320 kg/m³, respectively [1]. For all of these concretes, capacity was calculated in accordance with NS3473 (P_{calc}).

The results of main interest in this comparison are the ratio between the observed shear diagonal cracking load (P_{cr}) and the calculated capacity (P_{calc}) and the ratio between the observed failure load (P_u) and the calculated capacity (P_{calc}). Table 5 gives the results for beams with $a/d = 2.3$ and Table 6 gives results for beams with $a/d = 4.0$.

Table 5 – Comparison of the shear strengths for beams with $a/d = 2.3$

Beam	a/d	P_{cr} [kN]	P_u [kN]	P_{calc} [kN]	$P_{cr}/$ P_{calc}	$P_u/$ P_{calc}	$P_{cr}/b*d$ [MPa]	$P_u/b*d$ [MPa]
(2.3-1)	2.3	45	92.25	44.6	1.01	2.07	1.37	2.81
(2.3-2)	2.3	44.5	127.15	44.6	1.00	2.85	1.35	3.87
ND65	2.3	62.2	71.6	55.1	1.13	1.30	1.88	2.17
ND95	2.3	66.7	103.5	57.3	1.16	1.81	2.02	3.14
LWA75	2.3	47.1	126.1	52.0	0.91	2.43	1.43	3.82
LWA40	2.3	46.6	77.9	39.3	1.19	1.98	1.41	2.36
LWAC Leca	2.3	34.3	102.9	42.1	0.81	2.44	1.04	3.13

Table 6 – Comparison of the shear strengths for beams with $a/d = 4.0$

Beam	a/d	P_{cr} [kN]	P_u [kN]	P_{calc} [kN]	$P_{cr}/$ P_{calc}	$P_u/$ P_{calc}	$P_{cr}/b*d$ [MPa]	$P_u/b*d$ [MPa]
(4.0-1)	4	36.8	44.4	44.6	0.82	0.99	1.12	1.35
(4.0-2)	4	35	62	44.6	0.78	1.39	1.07	1.89
LWA40	4	38.2	38.2	39.30	0.97	0.97	1.16	1.16
LWAC Leca	4	29.4	44.1	42.10	0.70	1.05	0.89	1.34

For beams with $a/d = 2.3$, the ratio between P_{cr}/P_{calc} was larger or equal to 1.0 for all concretes except LWA75 and LWAC_Leca. This indicates that they are on the safe side. For LWA75 and LWAC_Leca, this ratio was less than 1.0, indicating a higher drop in shear strength than predicted by NS3473. The

ratio between P_u/P_{calc} for all LWA concretes was almost 2 or higher, which shows that LWA concretes in general can stand more loading than predicted. For normal density concretes, this ratio was lower.

The ND65, ND95 and LWA75 concretes were not tested at $a/d = 4.0$. For beams with $a/d = 4.0$, the ratio between P_{cr}/P_{calc} for both concretes tested was below 1.0 – indicating that beams with $a/d = 4.0$ have a certain drop in capacity [1, 5].

In general for the LWA concretes tested, the diagonal cracking load was close to other lightweight aggregate concretes, while the failure load was higher, especially in the case of $a/d = 4.0$. The shear stresses of all beams at diagonal cracking and failure were plotted as a function of the a/d ratio, as shown in Figure 5.

Figure 5 also includes predictions in accordance with NS3473. For beams with $a/d = 2.3$, most of the diagonal cracking values lie below the predicted curves, while for beams with $a/d = 4.0$ all values are above. The shear stresses at failure load for all beams with $a/d = 2.3$ are high above the predicted curves, and are significantly above the predicted curves for beams with $a/d = 4.0$. LWA40 has the highest shear stress at failure, while its shear stress at diagonal cracking is similar to other LWA concretes.

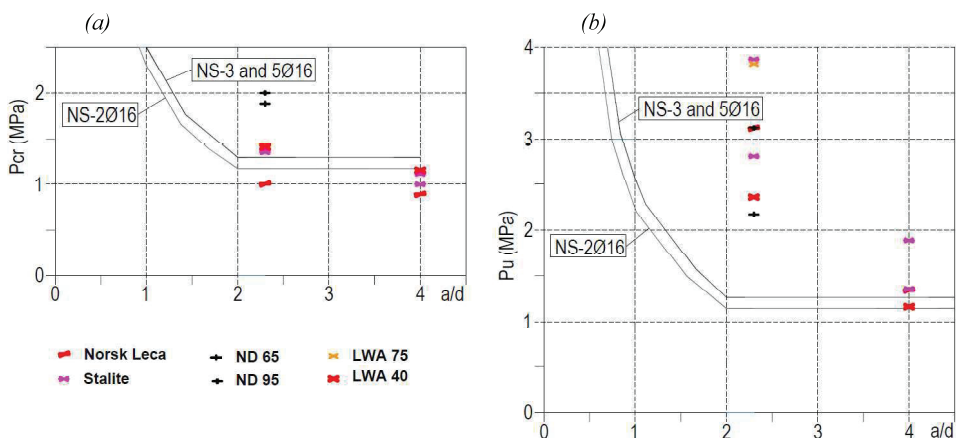


Figure 5 – The shear stress versus a/d ratio at diagonal cracking (a) and failure (b)

5. CONCLUSIONS

For all concretes tested in this research, the shear stress at inclined cracking of the beams decreased with an increase in the shear span to effective height ratio (a/d).

The results from small-scale testing were in good agreement with the results obtained from beam testing. Cracking propagation in the beams showed they were not as brittle as expected and was similar to cracking in normal density concrete. The beams tested were more ductile than expected, which should promote increased investigation and structural use of this type of LWAC. In that case, the design strength for shear in beams and slabs without shear reinforcement should be based on inclined cracking loads.

Comparison with similar tests on other types of lightweight concrete and normal density concretes showed that the ratio between the load observed at diagonal cracking and the predicted strengths was in the same range. However, the ratio between the load at failure observed and the strengths predicted was significantly higher for the lightweight concrete used in this investigation.

Acknowledgment

This research forms part of the DACS project (Durable Advanced Concrete Solutions). The financial contribution of the Norwegian Research Council is gratefully acknowledged. The DACS partners are: Kværner Concrete Solution AS (project owner), Axion AS (Stalite), AF Gruppen Norge AS, Concrete Structures AS, Mapei AS, Multiconsult AS, NorBetong AS, Norcem AS, NPRA (Statens vegvesen), Norges teknisk-naturvitenskapelige universitet (NTNU), SINTEF Byggforsk, Skanska Norge AS, Unicon AS and Veidekke Entreprenør AS.

6. REFERENCES

1. E. Thorenfeldt, H. Stemland, "Shear capacity of lightweight concrete beams without shear reinforcement", International Symposium on Structural Lightweight Aggregate Concrete, Sandefjord, Norway, 20-24 June 1995: 244-245.
2. ACI Committee 213. Guide for Structural Lightweight Aggregate Concrete (ACI 213R-03). American Concrete Institute. Farmington Hills, MI, United States: American Concrete Institute; 2003.
3. K. Watanabe, J. Niwa, H. Yokota and M. Iwanami, "Experimental Study on Stress-Strain Curve of Concrete Considering Localized Failure in Compression", Journal of Advanced Concrete Technology Vol. 2, No. 3; 2004: 395-407.
4. EN 1992-1-1 (2004), "Eurocode 2: Design of concrete structures – Part 1-1: General rules and rules for buildings".
5. NS 3473 Norges Standardiseringsråd (2003): "Concrete structures – Design and detailing rules", Norwegian Standard Institution.
6. NS-EN 206:2013+NA: 2014 (2014): "Betong, Spesifikasjon, egenskaper, framstilling og samsvar", Norwegian Standard Institution.
7. Standard Norge. NS-EN 1992-1-1:2004+NA: 2008. Eurocode 2: Design of concrete structures - General rules and rules for buildings. Norway: Standard Norge; 2008.
8. S.I. Sørensen. Betongkonstruksjoner, Beregning og dimensjonering etter Eurokode 2, 2. utgave, 2013
9. Standard Norge. Armeringsstål - mål og egenskaper - del 3: Kamstål B500NC. NS 3576-3:2012, 2012.
10. Standard Norge. NS-EN 12390-3:2009. Testing hardened concrete - Part 3: Compressive strength of test specimens, Lysaker: Standard Norge; 2009.
11. Standard Norge. NS-EN 12390-6:2009. Testing hardened concrete - Part 6: Tensile strength of test specimens, Lysaker: Standard Norge; 2009.
12. Standard Norge. NS-EN 12390-7:2009. Testing hardened concrete - Part 7: Density of hardened concrete. Lysaker: Standard Norge; 2009.
13. EuroLightCon. High strength LWAC in construction elements (Document BE96-3942/R36, June 2000).

14. Standard Norge. NS 3676. Concrete testing - Hardened concrete - Modulus of elasticity in compression. Norway: Standard Norge; 1987.
15. A. Hillerborg, "The theoretical basis of a method to determine the fracture energy G_f of concrete", RILEM Technical Committees, Materials and Structures, Volume 18, Issue 4, 1985: 291-296.
16. TEC Services. Interim report of ASTM C330 Carolina Stalite $\frac{1}{2}$ inch coarse lightweight aggregate. TEC Services Project No: 04-0514, TEC Services Sample ID: 14-999, 2015.
17. EuroLightCon. Methods for Testing Fresh Lightweight Aggregate Concrete (Document BE96-3942/R4, December 1999).
18. EuroLightCon. Properties of lightweight concretes containing Lytag and Liapor (Document BE96-3942/R8, March 2000).
19. T.Y. Lo, W.C. Tang, H.Z. Cui, "The effects of aggregate properties on lightweight concrete". Building and Environment Vol. 42; 2007: 3025-3029.
20. Y. Ge, L. Kong, B. Zhang, J. Yuan., "Effect of Lightweight Aggregate Pre-wetting on Microstructure and Permeability of Mixed Aggregate Concrete", Journal of Wuhan University of Technology-Mater. Sci. Ed., Vol. 24; Issue 5; 2009: 838-842.
21. J.P Zhang, "Diagonal cracking and shear strength of reinforced concrete beams", Magazine of Concrete Research, Vol. 49, No. 178; 1997; 55-65.
22. P.D. Zararis, G.C Papadakis, "Diagonal Shear Failure and Size Effect in RC Beams without Web Reinforcement". J. Struct. Eng., Vol. 127: Issue 7; 2001: 733-742.
23. T.M. Jensen, J.A. Øverli, Experimental study on flexural ductility in over-reinforced lightweight aggregate concrete beams, COIN Project report no 47 (2013).
24. S.H. Ahmad, Y. Xie, T. Yu, "Shear Ductility of Reinforced Lightweight Concrete Beams of Normal Strength and High Strength Concrete", Cement & Concrete Composites Vol. 17; 1995: 147-159.

Paper 2

Material properties of high performance structural lightweight concrete

Reid W. Castrodale, Jelena Zivkovic, Rolf Valum

*Proceedings of the Eleventh High Performance Concrete (11th HPC) & The Second Concrete Innovation Conference (2nd CIC), Tromsø, Norway, March 6th – 8th 2017
Norwegian Concrete Association / Tekna 2017 ISBN 978-82-8208-054-5*



2

MATERIAL PROPERTIES OF HIGH PERFORMANCE STRUCTURAL LIGHTWEIGHT CONCRETE

Reid W. Castrodale
President, Castrodale Engineering Consultants, PC, USA

Jelena Zivkovic
NTNU, Norway

Rolf Valum
AXION, Norway

ABSTRACT

Structural lightweight concrete incorporating manufactured lightweight aggregate has been used in bridges and buildings in the USA and elsewhere in the world for nearly 100 years. Applications include its use in the central portions of the main span of several of the longest concrete box girder bridges in the world, including the current world record main span of 301 m for the Stolma Bridge in Norway. However, some owners, design engineers and contractors are reluctant to use structural lightweight concrete because they are not familiar with it or they think that it is a new, untested material. This reluctance should be dispelled by recent data on the material properties of structural lightweight concrete that demonstrate the great potential for its use for structures exposed to extreme environmental conditions.

This paper discusses properties of structural lightweight concrete that provide potential benefits for bridge and off-shore structures. The paper focuses on structural lightweight concrete made with lightweight aggregates manufactured in the US, especially an expanded slate called STALITE. The paper presents test results for lightweight concrete with compressive strengths up to at least 70 MPa; tensile strengths and fracture energy comparable to normal weight concrete; creep and shrinkage in the range of normal weight concrete which confirms use of conventional design expressions for estimating creep, shrinkage and prestress losses; ductility under seismic loading that meets energy dissipation requirements; long-term durability resulting from reduced cracking tendency and permeability; a reduced coefficient of thermal expansion that with other properties would be beneficial for long-span structures exposed to variation in temperature and also mass concrete.

A better understanding of these properties of modern structural lightweight concrete will encourage bridge designers to use lightweight concrete to improve structural efficiency and economy, and to obtain longer lasting structures.

Keywords: Lightweight concrete, bridges, off-shore structures, compressive strength, tensile strength, modulus of elasticity, creep, shrinkage, durability, ductility, thermal properties, fracture energy

INTRODUCTION

Structural lightweight concrete incorporating manufactured lightweight aggregate has been used in bridges and off-shore structures in the USA and elsewhere in the world for nearly 100 years. It has been used successfully in a wide variety of bridges, including major structures such as the central portion of the 301 m-long main span of the Stolma bridge in Norway, which holds the current world record for the longest main span. However, some owners, design engineers and contractors are reluctant to use structural

lightweight aggregate concrete because they are not familiar with it or they think that it is a new, untested material even though information has been available for many years on the use of lightweight concrete for bridges [1,2].

Recent test results and production experience for modern lightweight concrete presented in this paper reveal that the material, which in most cases has properties equal to or superior to conventional concrete, offers significant opportunities for improved efficiency, economy and durability for bridges and other structures, even those exposed to extreme environmental conditions. A better understanding of these properties of modern structural lightweight concrete will encourage bridge designers to use lightweight concrete to improve structural efficiency and economy, and to obtain longer lasting structures.

After a brief introduction to lightweight aggregate and lightweight concrete, several properties of structural lightweight concrete are discussed that provide potential benefits for bridge and off-shore structures. The paper focuses on structural lightweight concrete made with lightweight aggregates manufactured in the US, especially an expanded slate called STALITE. The paper presents test results for lightweight concrete with compressive strengths up to at least 70 MPa; tensile strengths, fracture energy and characteristic lengths comparable to normal weight concrete; creep and shrinkage in the range of normal weight concrete which confirms use of conventional design expressions for estimating creep, shrinkage and prestress losses; ductility under seismic loading that meets energy dissipation requirements; long-term durability resulting from reduced cracking tendency and permeability; reduced coefficient of thermal expansion that with other properties would be beneficial for long-span structures exposed to variation in temperature and also mass concrete.

Most of the data reported in this paper are from studies conducted in the USA. Concrete compressive strengths reported are for cylinders unless noted otherwise.

LIGHTWEIGHT AGGREGATE

Structural lightweight aggregate in the USA is produced using shale, clay and slate. The materials are expanded at high temperatures in a rotary kiln to produce a porous aggregate in which the vitrified material has a hardness similar to quartz. Properties of lightweight aggregate vary between sources, but structural light-weight concrete can be produced using aggregate from all sources.

The bulk density of coarse lightweight aggregate ranges from about 720 to 880 kg/m³, and from about 960 to 1120 kg/m³ for fine aggregate. The largest lightweight aggregate grading used in the USA is 22 mm.

Water absorption of lightweight aggregate (LWA) is greater than the absorption of normal weight aggregate (NWA), ranging from 6% to more than 25% by mass depending on the source. Most pores in the aggregate are not connected which results in the relatively low absorption for such a porous material. To obtain more consistent workability and hardened properties, lightweight aggregate is generally prewetted prior to batching to satisfy its higher absorption before it is added to a concrete mixture.

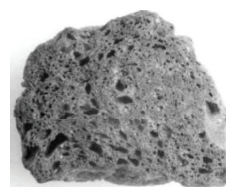


Figure 1. Lightweight aggregate particle

Internal curing

The water absorbed in prewetted lightweight aggregate is released into the paste as the cementitious materials hydrate and react. This provides an internal curing effect that improves the properties of the

concrete and its tolerance to conditions that may cause early cracking. Any lightweight concrete mixture with prewetted lightweight aggregate provides internal curing, but replacement of a portion of the fine aggregate in a conventional concrete mixture with prewetted fine lightweight aggregate can be used to provide internal curing in concrete mixes where reduced density is not required. An introduction to the concept of internal curing with lightweight fines appears in an article by Weiss, et al. [3].

LIGHTWEIGHT CONCRETE

To make lightweight concrete, lightweight aggregate is used for some or all of the aggregate in a mixture. Since lightweight aggregate is simply a lighter rock, the same admixtures can be used and batching, placing and finishing can be accomplished using the same procedures and equipment. Prewetting lightweight aggregate before batching allows lightweight concrete to be pumped long distances or to high elevations. With proper mix proportioning, lightweight concrete can have a high flow or even be self-consolidating.

The most common type of lightweight concrete in the USA, “sand lightweight concrete,” uses lightweight coarse aggregate rather than normal weight coarse aggregate. If all of the aggregate in a concrete mixture, i.e., both coarse and fine aggregates, is lightweight aggregate, the lowest density is achieved and the mixture is “all lightweight concrete.” By blending lightweight and normal weight aggregates, a mixture can be developed with any density in the range between all lightweight and normal weight concrete.

Material Properties

Structural properties of lightweight concrete have been obtained from both research studies and field production of lightweight concrete for structures. Previous test results for lightweight concrete often showed a reduction in tensile and shear strengths and an increase in creep and shrinkage. However, recent test results for these properties of lightweight concrete are much closer to, or even exceed, results for conventional normal weight concrete. Tests also show that lightweight concrete has essentially the same or even improved durability compared to normal weight concrete with the same quality and compressive strength. The modulus of elasticity and coefficient of thermal expansion for lightweight concrete are less than normal weight concrete, but these reduced properties can be beneficial in some design situations.

The length of this paper is limited, so it is not possible to present much data. Additional information can be obtained from the references or by contacting the authors.

Density

Normal weight concrete typically has a density of around 2300 kg/m³; sand lightweight concrete generally has a density in the range of 1750 to 2000 kg/m³; and all lightweight concrete can have a density as low as 1400 kg/m³.

Because lightweight aggregate has a higher absorption, lightweight concrete typically loses mass with time as excess absorbed water migrates out of the concrete. The mass loss is greater when higher absorption aggregates are used. Because this mass loss is greater than for normal weight concrete, the term “equilibrium density” has been defined as the density achieved after moisture loss has occurred [4]. Designers often specify the equilibrium density for lightweight concrete and use it for the dead load of concrete (plus an allowance for the weight of reinforcement). However, the fresh density of the concrete must also be known or specified for use as the criterion for material acceptance at placement. For high strength lightweight concrete using low absorption aggregate, the reduction in density with drying is expected to be minor and can be neglected.

Compressive Strength

Conventional concrete compressive strengths specified for design are easily achieved with lightweight concrete. Several projects in the USA have used lightweight concrete in pretensioned bridge girders with design compressive strengths from 60 to 70 MPa [5,6]. Lightweight concrete mixtures are designed for a specified compressive strength using the same approach that is used for normal weight concrete. Lightweight concrete generally requires more cementitious material or a lower w/cm to reach the same compressive strength as a normal weight mix. Experience with field production of lightweight concrete has shown strength gain with time is comparable to normal weight concrete.

Tensile Strength

It has long been assumed that the tensile strength of lightweight concrete is less than the tensile strength of normal weight concrete with the same compressive strength. As a result, design properties of lightweight concrete related to tensile strength have been reduced in design specifications for quantities such as shear and development length. However, recent tests reveal tensile strengths for normal and high strength lightweight concrete that exceed the tensile strength assumed for normal weight concrete with the same compressive strength.

Recent test data on lightweight concrete bridge deck mixes [7] illustrate this point. Researchers used three sources of lightweight aggregate for the test mixes. Test results demonstrated that the splitting tensile strength of the lightweight concrete bridge deck mixes for all of the lightweight aggregate sources and types of mixture exceeded the splitting tensile strength for the normal weight concrete control mix as well as the expected splitting tensile strength of normal weight concrete computed using the equation in the *AASHTO LRFD Bridge Design Specifications* [8]. It is interesting to note that the splitting tensile strength of the normal weight concrete control mixture was 88% of the expected value for normal weight concrete where the lightweight concrete mixtures were equal to or up to 8% greater than the expected tensile strength. These results refute the general assumption that the tensile strength of lightweight concrete is less than normal weight concrete.

The bridge design code in the USA [8] gives designers the option to compute the design modification factor for lightweight concrete based on a specified splitting tensile strength. If the splitting tensile strength specified is equal to the expected tensile strength for normal weight concrete, a lightweight concrete member can be designed with a reduction factor equal to one for shear and other quantities related to concrete tensile strength. If this is the case, no reduction is made and the design is the same as if the concrete were normal weight concrete. Based on the data from these tests, this approach could be taken by specifying a splitting tensile strength of 2,92 MPa which would eliminate the reduction factor for lightweight concrete by setting it equal to unity.

Modulus of Elasticity

The porous nature of lightweight aggregate reduces its stiffness. Therefore, when lightweight aggregate is used in concrete, the modulus of elasticity is also reduced. A concrete density term has been included in the equation for modulus of elasticity in US design codes since the 1960s. A new equation for the modulus of elasticity has recently been adopted in the US bridge design code [8]. The equation still includes the density of concrete, but the effect of density is greater because the exponent on the density has been changed from 1,5 to 2. The new equation for the modulus of elasticity, E_c , gives a better estimate for both lightweight concrete and high strength concrete [9].

$$E_c = 0,0017K_1 (w_c)^{2,0} (f'_c)^{0,33}$$

where: K_1 = correction factor for source of aggregate; w_c = concrete unit weight (kg/m^3); and f'_c = concrete compressive strength (MPa) [units conversion by author]

For sand lightweight concrete with a density of 1840 kg/m^3 , the predicted modulus is 63% of the value for normal weight concrete (2320 kg/m^3) and for all lightweight concrete with a density of 1600 kg/m^3 , the predicted modulus is 48% of the value for normal weight concrete. As with normal weight concrete, the actual modulus of elasticity for concrete may vary significantly from the value computed using the equation.

Creep and Shrinkage

It has generally been assumed that creep and shrinkage of lightweight concrete are greater than for normal weight concrete with the same compressive strength. Some early data showed this relationship. However, recent tests [10,11,12] show creep and shrinkage of higher strength lightweight concrete in the range of normal weight concrete. Figures 2 and 3 present creep and shrinkage data for 70 MPa compressive strength concrete mixes for prestressed girders.

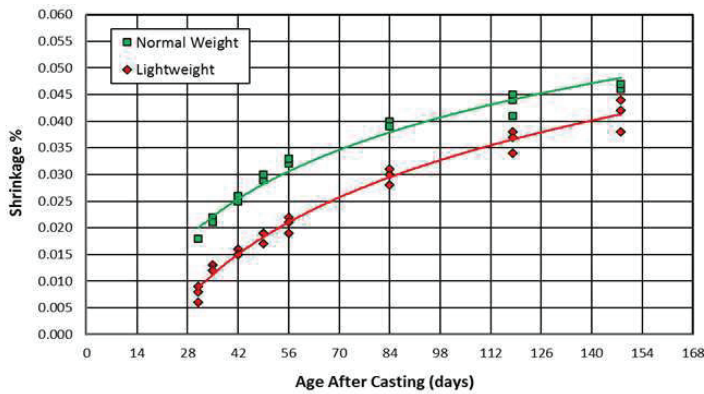


Figure 2: Creep of high strength lightweight and normal weight concretes [12]

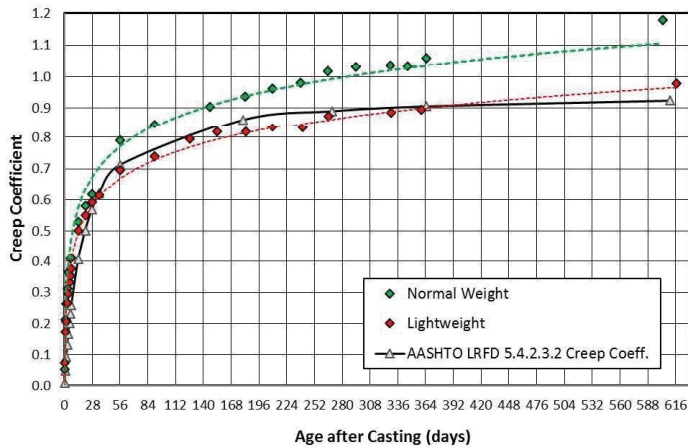


Figure 3: Shrinkage of high strength lightweight and normal weight concretes [12]

It is important to recognize that the lightweight concrete mix discussed above had a total cementitious content of 363 kg/m^3 cement plus 61 kg/m^3 of Class F fly ash for a total cementitious content of 424 kg/m^3 , while the normal weight concrete mixture had 341 kg/m^3 of cement [12]. It is surprising that even though the lightweight concrete mixture had a significantly greater cementitious content than the normal weight concrete (nearly 25%), it still had less shrinkage than the normal weight concrete mix.

Tests also show prestress losses for lightweight concrete girders are within the expected range for normal weight concrete [10,11]. This allows current code expressions for estimating creep, shrinkage and prestress losses to be used for lightweight concrete without modification.

Durability

For bridges and off-shore structures, long-term durability is always a concern because of the extreme conditions to which these structures are exposed. While durability of concrete depends on a wide range of factors, two primary factors are permeability and cracking. Compared to normal weight concrete with the same quality and compressive strength, lightweight concrete has been shown to have reduced cracking tendency and reduced permeability as discussed below.

The properties of lightweight concrete that contribute to enhanced durability include its reduced modulus of elasticity and reduced coefficient of thermal expansion (which is discussed below). The internal curing effect when prewetted lightweight aggregate is used provides improved hydration of cement and more complete reaction of supplementary cementitious materials for more effective use of cementitious materials and reduced permeability. The improved bond between lightweight aggregate particles and the paste, along with the more complete hydration, improve the quality of the interfacial transition zone (ITZ), significantly reducing the porosity of the ITZ that contributes to increased permeability in conventional concrete. The reduced stiffness of lightweight aggregate provides a more homogeneous stiffness of the concrete composite, reducing micro-cracking around the perimeter of aggregate particles, a major source of higher permeability. An extended discussion of the durability of lightweight concrete is available [13].

Ductility and Seismic Applications

Lightweight concrete has obvious benefits for bridges designed for seismic loadings because its lower density reduces the mass of a structure and therefore the seismic demand on the structure. Material tests often show lightweight concrete to have more brittle behaviour than normal weight concrete with the same compressive strength, especially for lower compressive strength mixes. Therefore, some designers expect lightweight concrete to have limited use for structures where ductility is required during a seismic or other extreme loading event.

Tests of seismically loaded lightweight concrete bridge piers demonstrated “that lightweight concrete, when properly detailed, will perform as well as normal weight concrete ...” [14] A later series of tests reported showed that “the strength of the lightweight concrete shear-resisting mechanism appears to be lower than the normal-strength mechanism when subjected to reversed cyclic loads” and strength reduction factors were proposed for use in design [15]. While the recommended concrete strength reductions were significant, the reduced mass of a lightweight concrete structure would significantly reduce the seismic lateral forces to which a structure would be subjected during a seismic event. Therefore, it was concluded that the “reduction in shear demand will more than compensate for the reduced strength of the concrete shear-resisting mechanism.”

Thermal Properties

The coefficient of thermal expansion for structural lightweight concrete is less than for normal weight concrete with the same strength. The reduced thermal expansion can be beneficial for mass concrete elements, highly restrained structures, and long-span structures exposed to variations in temperature.

Thermal properties have been measured for sand lightweight and all lightweight concrete mixtures representing typical bridge deck mixes. Behavior of these mixes were compared to a normal weight concrete mixture [7]. The lightweight concrete mixtures used lightweight aggregate from three sources, one manufactured from each of the following raw materials: shale, clay and slate. Results indicated that the coefficients of thermal expansion for sand lightweight concrete and all lightweight concrete mixtures were about 80% and 65%, respectively, of the coefficient for the normal weight concrete control mixture. Results were very similar between the three types of lightweight aggregate.

Because of its insulating properties, lightweight concrete responds to changes in ambient temperature more slowly than normal weight concrete. The combination of a reduced response to temperature change and a reduced strain associated with a change in temperature (coefficient of thermal expansion) should decrease daily thermal movements of long bridges constructed with lightweight concrete.

Furthermore, the combined effect of the reduced coefficient of thermal expansion with a reduced modulus of elasticity for lightweight concrete may provide benefits for mass concrete placements and structures that have a high degree of internal restraint, such as off-shore structures or pontoons for floating bridges. With this combination of properties, the stress caused by a change in temperature will be reduced because the stress is proportional to the product of the coefficient of thermal expansion and the modulus of elasticity, both of which are reduced for lightweight concrete. The result may be that larger temperature differentials within mass concrete elements could be allowed before cracking is expected to occur if lightweight concrete were used. In highly restrained sections, the equal or possibly reduced shrinkage for lightweight concrete mixtures further increases the reduced cracking tendency of lightweight concrete.

Fracture Energy and Characteristic Length

Term of fracture energy, G_f , is used as a materials characteristic to describe the resistance of concrete subjected to tensile stresses, or, more accurately, the energy required to propagate a tensile crack of unit area. This characteristic is mostly influenced by aggregate type, kind of matrix, age of concrete, and curing conditions. In fib model code [16] indicates that for lightweight concrete the maximum crack opening depends on the type of aggregate and the kind of matrix. The effect of aggregate type is caused by the transition from the interfacial fracture to the trans-aggregate fracture. The utilization of high strength and homogeneous aggregate, even if they are light, leads to an increase of the G_f values. Thus, tests to determine fracture energy [17] are mandatory if related information on lightweight concrete is used for analysis and design. In software for nonlinear calculations and design, especially when lightweight aggregate is used, fracture energy is one of required input data.

The effect of aggregate replacement and how it influenced fracture energy is more evident from Figure 4 which shows test results for normal weight and lightweight concrete mixtures. In those tests, reference concrete was the normal density concrete (ND). In subsequent test, the aggregate in the ND concrete was replaced with stronger aggregates (granite, quartzite and basalt). MIX indicates a combination of STALITE lightweight aggregate and sand in a proportion of 50% of each. LWA symbol indicates lightweight concrete with either Liapor or STALITE aggregates [18,19,20].

An additional parameter, the characteristic length l_{ch} , is used to better characterize the brittleness of concrete. It corresponds to the half of the length of a specimen subjected to axial tension, in which just

enough elastic strain energy is stored to create one complete fracture surface. An increase of the concrete brittleness is indicated by the decrease of the characteristic length. An increase in fracture energy also results in an increase in the characteristic length. The brittleness number (B) of a structure is defined as the ratio of the "L-length" of a part of the structure to the characteristic length of the material ($B = L/l_{ch}$). Characteristic lengths calculated for the concrete mixtures described above are shown in Figure 5.

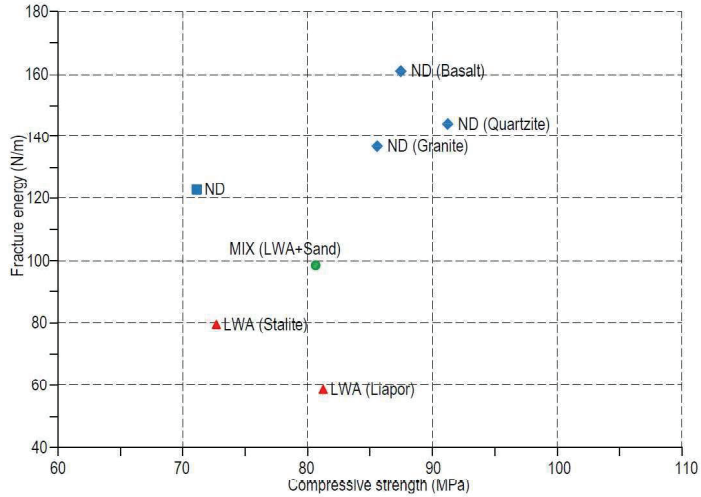


Figure 4: Fracture energy versus compressive strength for lightweight and normal weight concretes

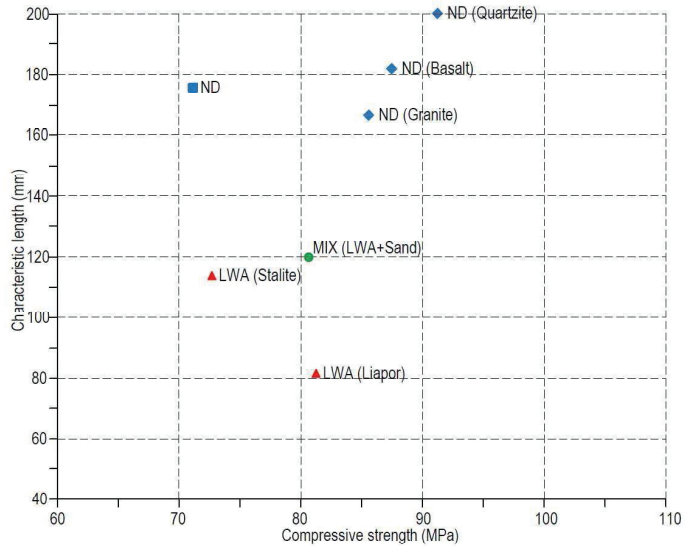


Figure 5: Characteristic length versus compressive strength for lightweight and normal weight concretes

CONCLUSIONS

The information presented in this paper provides insight into the properties of modern lightweight concrete. The properties discussed provide justification for using lightweight concrete in bridges for obvious reasons related to reduction of weight, but also for improved durability from reduced cracking and permeability. The successful completion of many bridges, as reported in a paper submitted to the Concrete Innovation Conference by some of the same authors, gives further support for the increased use of the material. With a better understanding of the properties of modern structural lightweight concrete, designers can use this material to achieve greater economy, longer spans, and increased service lives for bridges.

REFERENCES

- [1] FIP Commission on Prestressed Lightweight Concrete. Report of the FIP Commission on Prestressed Lightweight Concrete. *PCI J.* 1966; 12(3): 68-93.
- [2] TY Lin International. *Criteria for designing lightweight concrete bridges*. FHWA-RD-85-045. Federal Highway Administration, U.S. Department of Transportation, Washington, DC. 1985.
- [3] Weiss J, Bentz D, Schindler A, et al. Internal curing. *Structure*. 2012; 19(1): 10-14.
- [4] ASTM International. *Standard test method for determining density of structural lightweight concrete*. ASTM C567-05. ASTM International, West Conshohocken, Pa. 2005. 3 p.
- [5] Liles P, Holland RB. High strength lightweight concrete for use in precast, prestressed concrete bridge girders in Georgia. *HPC Bridge Views*. 2010; 61: 1-3.
- [6] Holland RB, Kahn LF. High strength light-weight concrete properties of the I-85 ramp over State Route 34,” *HPC Bridge Views*. 2010; 61: 4-8.
- [7] Byard BE, Schindler AK. *Cracking tendency of lightweight concrete*. Highway Research Center, Auburn, Ala. 2010.
- [8] American Association of State Highway and Transportation Officials. *AASHTO LRFD Bridge Design Specifications*. 7th Ed. AASHTO, Washington, DC. 2014.
- [9] Greene GG, Graybeal BA. *Lightweight concrete: Mechanical properties*. FHWA- HRT-13-062. Federal Highway Administration, U.S. Department of Transportation, Washington, DC. 2013.
- [10] Cousins T, Roberts-Wollmann C, Brown MC. *High-performance/high-strength lightweight concrete for bridge girders and decks*. National Cooperative Highway Research Program Report 733. Transportation Research Board, Washington, DC. 2013
- [11] Lopez M, Kahn LF, Kurtis KE. Creep and shrinkage of high-performance lightweight concrete. *ACI Mater J*. 2004;101(5):391-399.

- [12] Chapman DD, Castrodale RW. Sand light-weight concrete for prestressed concrete girders in three Washington State bridges. Paper 81 Proceedings of the 2016 National Bridge Conference, 2016 Mar 3-6; Nashville. Precast/Prestressed Concrete Institute, Chicago, Ill. 2016. 22 p.
- [13] Castrodale RW, Harmon KS. Durability of lightweight concrete bridges. Paper 48. Proceedings of the 2008 National Bridge Conference, 2008 Oct 4-7; Orlando. Precast/Prestressed Concrete Institute, Chicago, Ill. 2008. 35 p.
- [14] Kowalsky MJ, Priestley MJN, Seible F. Dynamic behavior of lightweight concrete bridges. *ACI Struct J*. 2000; 97(4): 602-618.
- [15] Hendrix SE, Kowalsky MJ. Seismic shear behavior of lightweight aggregate concrete square columns. *ACI Struct J*. 2010; 107(6): 680-688.
- [16] CEB-FIP, Code-type models for concrete behavior – Background of fib Model Code for Concrete Structures 2010 , International Federation of Structural Concrete (fib) , 2013.
- [17] Hillerborg, A. The theoretical basis of a method to determine the fracture energy GF of concrete. RILEM Technical Committees, Materials and Structures, July 1985, 18(4): 291-296.
- [18] Thorenfeldt E, Stemland H. Shear capacity of lightweight concrete beams without shear reinforcement. International Symposium on Structural Lightweight Aggregate Concrete, Sandefjord, Norway, 20-24 June 1995: 244-245.
- [19] Thorenfeldt E, Drangsholt G. Shear capacity of small scale beams, High Strength Concrete, SP2-Plates and Shells, Report 2.1, October 1987.
- [20] EuroLightCon, *Tensile strength as design parameter*. Document BE96-3942/R32. June 2000.

Paper 3

Shear capacity of lightweight aggregate concrete beams without shear reinforcement

Jelena Zivkovic, Jan Arve Øverli

*Proceedings of the XXIII Nordic Concrete Research Symposium, Aalborg, Denmark,
August 21st – 23rd 2017.*

Norsk Betongforening 2017 ISBN 978-82-8208-056-9

3

Shear Capacity of lightweight aggregate concrete beams without shear reinforcement



Jelena Zivkovic, Ph.D
Department of Structural Engineering
Faculty of Engineering Science
Norwegian University of Science and Technology
7491 Trondheim, Norway
E-mail: jelena.zivkovic@ntnu.no



Jan Arve Øverli
Professor, Ph.D
Department of Structural Engineering
Faculty of Engineering Science
Norwegian University of Science and Technology
7491 Trondheim, Norway
E-mail: jan.overli@ntnu.no

ABSTRACT

The main disadvantages of lightweight aggregate concrete (LWAC) compared with normal weight concrete are its brittleness at the material level in compression and uncontrolled crack propagation. This experimental investigation consists of beams with lightweight concrete with Stalite as aggregate. Main goal were to investigate beams without shear reinforcement subjected to shear in four-point bending test and compare those results with previous experimental work. The main test parameter was the shear span length to effective height ratio (a/d). Tested beams did not show brittle behaviour. Beams were more ductile than expected, and cracking was similar as for normal weight concrete beams.

Keywords: Lightweight Aggregate Concrete, Testing, Shear Reinforcement, Shear capacity, Ductility.

1. INTRODUCTION

This investigation was part of the ongoing research programme, “Durable advanced concrete structures (DACs)”. One part of this programme is to investigate the structural behaviour of lightweight aggregate concretes (LWAC), i.e. concretes with an oven-dry density below 2000 kg/m³. A general characteristics of LWAC is its very high degree of brittleness at the material level in compression, which result in sensitivity to stress concentrations and rapid crack/fracture development. This influences the behaviour of concrete where its tensile strength is important, as for instance with its shear and bond strength. To investigate the brittleness of LWAC, beams without shear reinforcement were subjected to shear in a four-point bending test. The main test parameter was the shear span length to effective height ratio (a/d). For all beams, the shear loads at diagonal cracking and at failure were plotted as a function of the a/d ratio and compared with previous results. For comparison, tested beams were the same size and with the same reinforcement as in earlier shear tests on other normal density (ND) and lightweight aggregate (LWA) concretes [1]. To produce the concrete, a lightweight aggregate Stalite was used to achieve an oven-dry density of about 1800 kg/m³ and a compressive strength of about 60 MPa.

2. EXPERIMENTAL TEST PROGRAM AND RESULTS

The experimental program consist of four reinforced LWAC beams without shear reinforcement, which were subjected to a four point bending test, to produce a constant moment in the middle of the beam. The program and results are given in Table 1. The beams measured (width x height x length) 150 x 250 x 2900 mm. Longitudinal and cross section details of the beam specimens are shown in Figure 1.

Table 1-Test parameters and results for diagonal cracking, failure loads and calculated shear strengths in accordance with NS3473[2]

Beam	a [mm]	d [mm]	a/d	P_{cr} [kN]	P_u [kN]	P_{calc} [kN]	P_{cr} / P_{calc}	P_u / P_{calc}
1	876	219	2.3	45	92.3	44.6	1.01	2.07
2	876	219	2.3	44.5	127.2	44.6	1.00	2.85
3	504	219	4	36.8	44.4	44.6	0.82	0.99
4	504	219	4	33	62	44.6	0.78	1.39

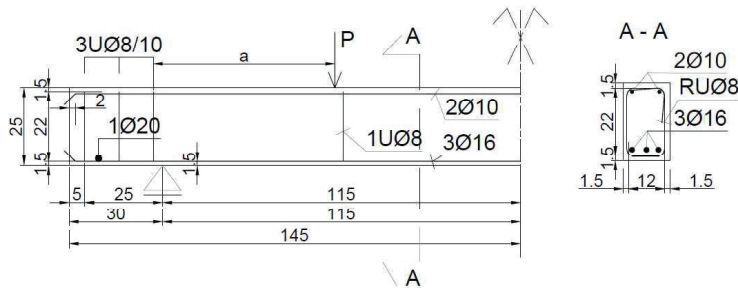


Figure 1 – Reinforcement and cross section details for the beams

The shear capacity of the beam has been calculated in accordance with NS 3473 [2] and Eurocode 2 [3], and these values are 42.8 kN and 44.6 kN, respectively.

3. DISCUSSION

The cracking and failure mechanism in beams without web shear reinforcement, which is usual in NWC, is that cracks will appear in the shear span with increasing load. The term diagonal cracking load is defined in this paper as the load when the specific shear crack is formed that goes on to lead to shear failure. The load at which the beam collapses is the ultimate load or the load-carrying capacity. Due to the brittle nature of LWAC, the diagonal cracking load is usually equal to the ultimate load. In this experiment, however, the beams could carry increasing load after the diagonal cracks formed. The cracks propagated almost horizontally along the tensile reinforcement and diagonally into the compression zone. In the final stage, the shear cracks opened wide as the diagonal cracks spread along the beam and this resulted in the crushing of the concrete close to the loading point.

Similar tests have been carried out previously for high-strength concrete classes of normal density concretes ND65 and ND95 and lightweight aggregate concretes LWA75, LWA40 and LWA_Leca_mix. Table 2 shows these tests compared with the present investigation on beams with $a/d = 2.3$ and $a/d = 4.0$, respectively. The test conditions were the same, including the rig,

the cross section, and the amount of reinforcement [1]. For all of these concretes, capacity was calculated in accordance with NS3473 (P_{calc}).

Table 2 - Comparison of the shear strengths for beams with $a/d = 2.3$ and 4.0

Beam/Aggregate	a/d	Cylindar Strength [MPa]	P_{cr} [kN]	P_u [kN]	P_{calc} [kN]	P_{cr} / P_{calc}	P_u / P_{calc}
1/Stalite	2.3	67.5	45	92.3	44.6	1.01	2.07
2/Stalite	2.3	67.5	44.5	127.2	44.6	1.00	2.85
ND65/Årdal	2.3	54	62.2	71.6	55.1	1.13	1.30
ND95/Årdal	2.3	78	66.7	103.5	57.3	1.16	1.81
LWA75/Liapor 8	2.3	58	47.1	126.1	52.0	0.91	2.43
LWA40/Leca	2.3	37	46.6	77.9	39.3	1.19	1.98
LWA_Leca_mix	2.3	42.7	34.3	102.9	42.1	0.81	2.44
3/Stalite	4	67.5	36.8	44.4	44.6	0.82	0.99
4/Stalite	4	67.5	35	62	44.6	0.78	1.39
LWA40/Leca	4	37	38.2	38.2	39.30	0.97	0.97
LWA_Leca_mix	4	42.7	29.4	44.1	42.10	0.70	1.05

The results of main interest in this comparison are the ratio between the observed shear diagonal cracking load (P_{cr}) and the calculated capacity (P_{calc}), and the ratio between the observed failure load (P_u) and the calculated capacity (P_{calc}).

For beams with $a/d = 2.3$, the ratio between P_{cr}/P_{calc} was larger or equal to 1.0 for all concretes except LWA75 and LWA_Leca_mix. This indicates that they are on the safe side. For LWA75 and LWAC_Leca_mix, this ratio was less than 1.0, indicating a higher drop in shear strength than predicted by NS3473. The ratio between P_u/P_{calc} for all LWA concretes was almost 2 or higher, which shows that LWA concretes in general can stand more loading than predicted. For normal density concretes, this ratio was lower.

The ND65, ND95 and LWA75 concretes were not tested with ratio $a/d = 4.0$. For beams with $a/d = 4.0$, the ratio between P_{cr}/P_{calc} for both concretes tested was below 1.0 – indicating that beams with $a/d = 4.0$ have a certain drop in capacity [1,2].

For tested LWA concrete with Stalite as aggregate, the diagonal cracking load was close to other lightweight aggregate concretes, while the failure load was higher, especially in the case of $a/d = 4.0$.

In comparison with normal density concretes ND65 and ND95, the diagonal cracking load for normal concretes were approximately 30% higher, while failure load for LWAC with Stalite was significantly higher. In general, here is actually from high importance the fact that after shear diagonal crack were formed beams can stand increase of load from 30 to 50 %.

4. CONCLUSIONS

For all concretes tested in this research, the shear stress at inclined cracking of the beams decreased with an increase in the shear span to effective height ratio (a/d). Cracking propagation in the tested beams showed they were more ductile than expected, which should promote increased investigation and structural use of this type of LWAC. According to this experimental

investigation, the design strength for shear in beams and slabs without shear reinforcement should be based on inclined cracking loads. Comparison with similar tests on other types of lightweight concrete and normal density concretes showed that the ratio between the load observed at diagonal cracking and the predicted strengths was in the same range. However, the ratio between the load at failure observed and the strengths predicted was significantly higher for the lightweight concrete used in this investigation.

Acknowledgment

This research forms part of the DACS project (Durable Advanced Concrete Solutions). The DACS partners are Kværner AS (project owner), Axion AS (Stalite), AF Gruppen Norge AS, Concrete Structures AS, Mapei AS, Multiconsult AS, NorBetong AS, Norcem AS, NPRA (Statens vegvesen), Norwegian University of Science and Technology (NTNU), SINTEF Byggforsk, Skanska Norge AS, Unicon AS and Veidekke Entreprenør AS. The project gratefully acknowledges the Norwegian Research Council for financial contribution.

5. REFERENCES

- [1] E. Thorenfeldt, H. Stemland, "Shear capacity of lightweight concrete beams without shear reinforcement", International Symposium on Structural Lightweight Aggregate Concrete, Sandefjord, Norway, 20-24 June 1995: 244-245.
- [2] NS 3473 Norges Standardiseringsråd (2003): "Concrete structures – Design and detailing rules", Norwegian Standard Institution.
- [3] Standards Norway. NS-EN 1992-1-1:2004+NA: 2008. Eurocode 2: Design of concrete structures - General rules and rules for buildings. Norway Standard Norge; 2008.

Paper 4

Strain level and cracking of the lightweight aggregate concrete beams

Jelena Zivkovic, Jan Arve Øverli

*Proceedings of the 12th Nordic mini seminar: Crack width calculation methods
for large concrete structures. Oslo, Norway, August 29th – 30th 2018.*

Norsk Betongforening 2017 ISBN 978-82-8208-057-6

4

Strain level and cracking of the lightweight aggregate concrete beams

	<p>Jelena Zivkovic M.Sc. PhD-candidate Department of Structural Engineering Faculty of Engineering Science Norwegian University of Science and Technology N-7491 Trondheim, Norway e-mail: jelena.zivkovic@ntnu.no</p>
	<p>Jan Arve Overli PhD, Professor Department of Structural Engineering Faculty of Engineering Science Norwegian University of Science and Technology N-7491 Trondheim, Norway e-mail: jan.overli@ntnu.no</p>

ABSTRACT

The main disadvantages of lightweight aggregate concrete (LWAC) compared with normal weight concrete (NDC) are its brittleness at the material level in compression and uncontrolled crack propagation. This experimental investigation consists of six beams with lightweight concrete with Stalite as aggregate. Main goal were to investigate cracking and strain level in compression of the beams subjected in four-point bending test. Compressive strain level was much higher than expected, and cracking was similar as for normal weight concrete beams.

Key words: Lightweight Aggregate Concrete, Testing, Bending, Strain level, Shear Reinforcement.

1. INTRODUCTION

1.1 General

This investigation is part of the ongoing research program “Durable advanced concrete structures (DaCS)”. One part of this program is to investigate structural behaviour of lightweight aggregate concretes (LWAC), concretes with an oven dry density below 2000 kg/m³. General characteristic of LWAC is the very high degree of brittleness at the material level and especially in compression. The brittleness of concrete is characterized by sensitivity to stress concentrations and a rapid crack/fracture development. This influences the behaviour of concrete where the tensile strength is important, as for instance the shear and bond strength [1,2].

To investigate the cracking and strain level of LWAC in compression, six beams with different reinforcement layout were subjected in a four-point bending test. The test setup was designed to produce a constant moment zone of 1 m between the loading points. The size of the beams were (width x height x length) 210-330 x 550 x 4500 mm. The main test parameters were the stirrup spacing, amount of compressive reinforcement and size of concrete cover. All the beams failed in compression between the two loading points. Cracking of the compression area in the beams depending the most of the reinforcement detailing. Cracking of the beam without shear

reinforcement in compression area was the largest, while beam that contain shear reinforcement at the dense spacing had the smallest cracking. Strain level in the concrete and reinforcement were recorded with strain gauges (SG) and Linear Variable Differential Transformers (LVDT) at one side of the beam. On the other side Digital Image Correlation (DIC) method was used [3,4]. Average compressive strain level recorded in all the beams was in scope 3,4‰ and 3,8‰. In addition, for control of the material characteristics small specimens were tested. To produce the concrete, a lightweight aggregate Stalite was used to achieve an oven-dry density of about 1850 kg/m³ and a compressive cylinder strength of about 65 MPa.

2. EXPERIMENTAL TEST PROGRAM AND RESULTS

The experimental program consist of six reinforced LWAC beams which were subjected to a four point bending test, with a constant moment zone of 1m between the loading points. Main test parameters that were varied in the testing zone were the stirrup spacing, amount of compressive reinforcement and size of concrete cover. All the beams were overreinforced in order to provide the bending failure. Outside of the testing zone, all the beams had the same stirrups distribution designed to avoid shear failure. The program and results are given in Table 1. The beams measured (width x height x length) 210-330 x 550 x 4500 mm. Detailed test setup of the beams and reinforcement layout of cross section are shown in Figure 1.

Table 1-Test parameters and results

Beam	s [mm]	c [mm]	A_c	$f_{lc,cube}$ [MPa]	P_{fcr} [kN]	P_{cr} [kN]	P_u [kN]	P_{calc} [kN]	P_u/P_{calc}	ϵ_c [‰]	ϵ_t [‰]
1	-	20	2 ϕ 12	74.2	53	318	724	729	0.99	3.70	-
2	200	20	2 ϕ 12	74.2	54	350	645	729	0.88	3.77	2.04
3	60	20	2 ϕ 12	74.2	78	319	707	729	0.97	3.74	2.41
4	100	20	2 ϕ 12	74.2	69	324	700	729	0.96	3.75	2.08
5	100	40	2 ϕ 12	74.2	64	339	663.4	726	0.91	3.61	2.17
6	200	40	2 ϕ 25	74.2	64	250	750	800	0.94	3.4	2.35

where s is stirrup spacing; c -size of concrete cover; A_c -compressive reinforcement; $f_{lc,cube}$ -compressive cube strength; P_{fcr} - load level for first bending crack; P_{cr} - load level for first shear crack; P_u - load level of maximum load; P_{calc} - calculated load according EC2[5]; ϵ_c - average concrete compressive strain; ϵ_t - average concrete tension strain;

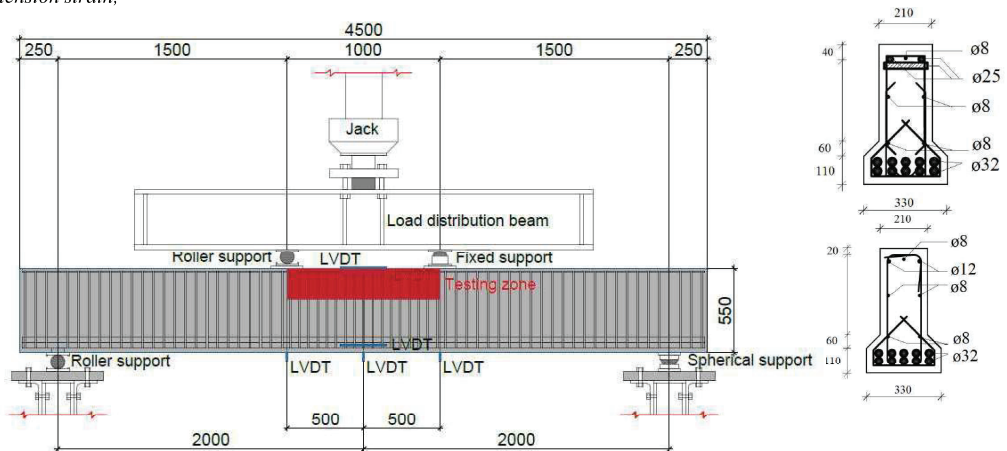


Figure 1 – Detailed test setup of beams and cross sections with the reinforcement layout

The moment and shear capacity of the beams has been calculated in accordance with Eurocode 2 [5], and these values are 729 kN, 726 kN and 800 kN respectively. The strain level which is used in calculation was 2,52‰.

3. DISCUSSION

The first bending crack was observed in the constant moment region on the tension side between the loading points. As the load was increased, new bending cracks propagated symmetrically until they reached the top of the beam flange. Development of bending cracks slowed down when shear cracks appeared. The first shear cracks appeared in the middle of the shear zone, between the neutral axis and the beam flange. Additional loading lead to further crack propagation of both bending and shear side. In beam 6, shear cracks appeared from bending cracks, which was different from the other beams. Crack propagation for certain load steps are very similar for all the tested beams. Only difference was in cracking of the compression zone and that depend from tests parameters. Failure happened when compression zone between loading points cracks. This type of failure is defined as compressive failure in the bending moment zone, see Figure 2. In general, observed cracking in all the beams were very similar like for normal weight concrete beams, because all beams were able to stand almost doubled load after formation of diagonal shear cracks. Beams with reduced stirrup spacing and lower concrete cover showed the lowest spoiling and decrease in crack propagation. The beam containing the largest compressive reinforcement resisted the largest load but crack propagation and spoiling were the similar like for the beam with same stirrup spacing and concrete cover. The beam 1, which do not contain stirrups in testing area showed the largest brittle spoiling and uncontrolled crack propagation, typical for LWAC [1,2].



Figure 2— Final failure state of beam 4

By using DIC, detailed strain fields of the observed compressive zones have been recorded, see Figure 3. In general, measuring devices were in a good agreement but in a failure faze larger strains and localization were measured using DIC, compared to the strain values measured with the SGs and LVDTs. Localization of strains actually present nice picture of formed cracks and strains development between them. In addition, it is visible that reinforcement layout will influence the most the crack development and that cracks which will actually lead till failure were formed between stirrups. Average compressive strain level recorded in all the beams was in scope 3,4‰ and 3,8‰. Having in mind that EC2 [5] has special rules for LWAC, which are reduction factors applied to regular design criterion, the results in this study indicate that EC2 underestimates LWAC. Recorded maximum strains in the tested beams were for 30-50 % larger than the allowed maximum strain for this type of concrete.

4. CONCLUSIONS

For all tested beams in this research, cracking of the beams were the similar except for the testing area. All beams showed the ductile behaviour since they were able to stand more loading after formation of shear cracks.

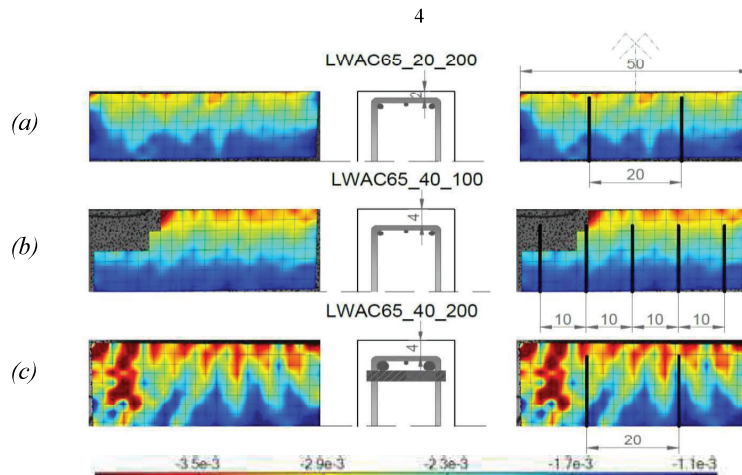


Figure 3– Detailed strain field from 3D-DIC (element size 23mm, colorbar scaling from 1‰-4‰); (a) beam 2; (b) beam 5; (c) beam 6;

Cracking of the testing area depend from the test parameters varied in this experiment. Beams with the dense stirrup spacing showed small, shallow cracks and spoiling were the smallest. In beams where cover was deeper spoiling and cracking were larger. The beam containing the largest compressive reinforcement resisted the largest load.

In general, characteristics of LWAC mostly depend on the type of used lightweight aggregate (LWA). EC2 do not differentiate between types of LWAs used in LWAC. From the experimental results in this experiment, it is indicated that EC2 underestimates strain level 30-50% from one proposed for designing. Since in this study LWAC showed behaviour similar to NDC, further investigation of LWAC as a structural material should be continued. In addition, the way how EC2 treats different types of LWAC should especially be investigated.

Acknowledgment

The work presented in this paper is part of ongoing PhD study in scope of the DACS project (Durable Advanced Concrete Solutions). The DACS partners are Kværner AS (project owner), Norwegian Research Council, Axion AS (Stalite), AF Gruppen Norge AS, Concrete Structures AS, Mapei AS, Multiconsult AS, NorBetong AS, Norcem AS, NPRA (Statens vegvesen), Norwegian University of Science and Technology (NTNU), SINTEF Byggforsk, Skanska Norge AS, Unicon AS and Veidekke Entreprenør AS. Jelena Zivkovic would like to express hers outmost gratitude to the supervisors and all the project partners for contributions and making this PhD study possible.

REFERENCES

- [1] EuroLightCon. Lwac Material Properties. Document BE96-3942/R2, December 1998.
- [2] ACI Committee 213. Guide for Structural Lightweight Aggregate Concrete (ACI 213R-03). American Concrete Institute. Farmington Hills, MI, United States: American Concrete Institute; 2003.
- [3] T.M. Fayyada and J.M Leesb. Application of Digital Image Correlation to Reinforced Concrete Fracture. Procedia Materials Science 3 (2014) 1585 1590, 20th European Conference on Fracture (ECF20), 2014.
- [4] N. McCormick and J. Lord. Digital Image Correlation for Structural Measurements. ICE institution. Civil Engineering, 165 (CE4), pages 185–190, 2012.
- [5] EN 1992-1-1 (2004), “Eurocode 2: Design of concrete structures – Part 1-1: General rules and rules for buildings”.

Paper 5

Confinement in Bending of Lightweight Aggregate Concrete Beams

Jelena Zivkovic, Jan Arve Øverli

Proceedings of the 5th International fib Congress – Melbourne, Australia, October 7th – 11th 2018
Federation internationale du beton (fib) Melbourne, Australia, ISBN 978-18-7704-014-6



5

Confinement in Bending of Lightweight Aggregate Concrete Beams

Jelena Zivkovic¹ and Jan Arve Øverli²

¹ Department of Structural Engineering, Norwegian University of Science and Technology, NTNU, Trondheim, Norway

Abstract

The use of lightweight aggregate concrete (LWAC) is limited as a mainstream construction material in structural applications. One reason is the more brittle post-peak material behaviour and uncontrolled crack propagation compared to normal density concrete (NWC). In general, concrete itself is not a ductile material. Without reinforcement, the concrete is not able to offer significant resistance in the inelastic domain of the response. To improve the ductility of reinforced concrete structures the confinement effect from reinforcement must be taken into account. This paper presents the influence of different factors on the effectiveness of confinement in compression. To test confinement of LWAC, six over-reinforced beams were subjected to four point bending test. The geometry of the beams were 210-330 x 550 x 4500 mm (width x height x length). The experiment setup was designed to produce a constant moment zone of one meter between loading points, where all the beams should collapse. The main parameters varied in the testing zone were: spacing of transversal reinforcement, amount of longitudinal compressive reinforcement and size of concrete cover. From the achieved experimental results, spacing of transverse reinforcement had the largest influence on the ductility. In general, it is possible to increase the ductility of LWAC structures by appropriate reinforcement detailing and lead them close to the response of NWC structures. Having in mind the major advantage of LWAC, which is reduced weight and high strength-to-weight ratio compared to conventional concrete, structural applications using LWAC should be increased significantly.

Keywords: Confined lightweight concrete, ductility, transversal reinforcement, longitudinal reinforcement, concrete cover.

1 Introduction

Lightweight aggregate concrete (LWAC) is defined as concrete with an oven dry density below 2000 kg/m³ and with maximum strength about 80 MPa [1-4]. The major advantage of LWAC is reduced weight. Regardless, the use of LWAC is limited as a mainstream construction material in structural applications due to more brittle post-peak material behaviour, uncontrolled cracking and reduced ductility [5]. Ability of the material to sustain significant inelastic deformations after the peak load without a significant variation in the resisting capacity prior to collapse is known as ductility. To be able to evaluate the ductility of concrete structures a knowledge of the complete stress-strain curve in compression including the descending portion is necessary [5-7]. It is available very little information about complete curve of lightweight aggregate concrete. Main reason is the difficulty to capture post-peak behaviour with the conventional testing techniques and machines. When testing small samples in compression from even conventional concrete failure is often brittle. When reinforced concrete sections are subjected to large deformations, their ability to carry load depends primarily on the behaviour of confined concrete [8]. Confinement in any concrete is achieved by the suitable placement of reinforcement. Effectiveness of confined reinforced concrete member depends on: cross-sectional properties of the structural member, stress-strain behaviour of concrete and steel and type and loading rate and strain gradient [7-9]. This paper presents results from experimental testing of ductility of high strength LWAC concrete beams to investigate confinement in the compression zone. Six over-reinforced LWAC beams were subjected to four point bending test in order to create constant compression zone between loading points. The test set-up is created in order to capture post peak behaviour in compression. The testing zone were analyzed to study the effect of different stirrup spacing, size of concrete cover and amount of longitudinal compressive reinforcement, on beam carrying capacity and ductility.

The geometry of the beams were 210-330 x 550 x 4500 mm (width x height x length). In addition, small samples cubes, cylinders and small beams were casted to follow the material properties [10]. The ultimate capacity was evaluated by following the rules in Eurocode and the Norwegian code [3], [4] for design of concrete structures. All the tested beams failed in compression between the two loading points. Reinforcement detailing influenced the cracking of the compression zone in the beams. The beam without transversal reinforcement showed very explosive and brittle behaviour while all other beams showed ductile behaviour. The strain level in the concrete and reinforcement were measured with strain gauges (SG) and Linear Variable Differential Transformers (LVDT) at one side of the beam. On the other side, Digital Image Correlation (DIC) method was used [11], [12]. To produce the concrete, a lightweight aggregate argillite slate from North Carolina, called Stalite [10], was used to achieve an oven-dry density of about 1850 kg/m³ and a compressive cylinder strength of about 65 MPa.

2 Experimental program and methodology

2.1 Test parameters

The experimental program consist of six reinforced LWAC beams with a constant moment zone of 1m between the loading points. This type of experimental program was proposed in order to eliminate the effect of frictional restraint on post-ultimate deformation, what is typical for uniaxial compression tests [7]. This testing technique allow lateral expansion of the central zone in all directions and provide testing of the LWAC under multiaxial states of stress. Size of the compressive testing zone was approximately 300x1000 mm. Parameters varied in the testing zone were the stirrup spacing, amount of compressive reinforcement and size of concrete cover. The program are given in Table 1.

Table 1. Test parameters

Beam Identification	Concrete cover c (mm)	Tension reinforcement A_t	Compression reinforcement A_s	Stirrup spacing s (mm)	$P_{capacity}$ [kN]
1	20	10 ϕ 32	2 ϕ 12	-	729
2	20	10 ϕ 32	2 ϕ 12	200	729
3	20	10 ϕ 32	2 ϕ 12	60	729
4	20	10 ϕ 32	2 ϕ 12	100	729
5	40	10 ϕ 32	2 ϕ 12	100	726
6	40	10 ϕ 32	2 ϕ 25	200	800

The moment and shear capacity of the beams has been calculated in accordance with Eurocode 2 [2] and Norwegian code [3]. The beams measured (width x height x length) 210-330 x 550 x 4500 mm. All the beams were over-reinforced, using 10 ϕ 32, in order to provide the bending failure by concrete crushing in compression zone. Outside of the testing zone, all the beams had the same stirrups ϕ 12/70mm, designed to avoid shear failure. In compressive zone, all beams 1-5 had two longitudinal bars ϕ 12 mm and beam 6 two bars ϕ 25 mm. Short longitudinal bar ϕ 8 mm were set in testing compressive zone in all the tested beams as the carrier of the strain gauges. This bar was able to move together with concrete since it was not fixed at the edges. Stiff anchorage of tension reinforcement at the support was provided with a welding steel plate. Fig. 1 gives the beam geometry. Fig. 2 illustrate the testing area where have been wearied tests parameters. On the same figure is also shown the middle beam cross section.

To record the strain in the mid span cross section combination of digital image correlation method (DIC), linear variable displacement transducers (LVDT) and strain gauges (SG) have been used. The results of interest from the testing are load level at the peak 1 (P_1) when spoiling of the concrete cover on top of cross

section occurred and load level at the peak 2 (P_2), when sides of cross section spoiled and final failure was reached.

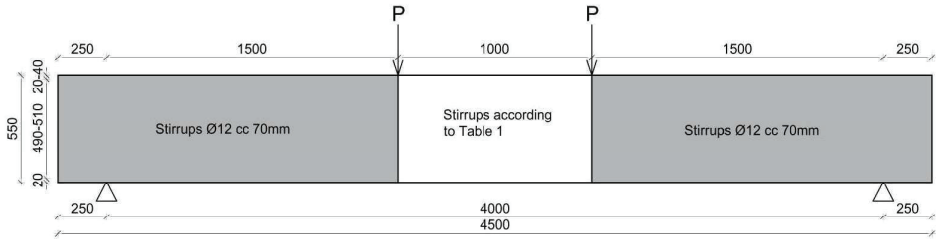


Fig. 1 Beam geometry. Dimensions are in [mm].

All the beams and small samples, cubes and cylinders, were cast from the same concrete batch. The beams were demolded 24 hours after casting, and stored in the laboratory at approximately 20°C under wet burlaps covered with a plastic sheet. They were uncovered two days before the testing. Finally, the beams were painted white for easier detection of cracks and prepared for instrumentation. The test age of the beams varied from 37 to 59 days.

To establish the mechanical properties of the LWAC, cubes (with dimensions 100x100x100 mm), cylinders (Ø100x200mm) and small beams (100x100x1200mm) were casted to find the stress-strain diagram, the compressive strength for cube and cylinder, the tensile strength, Young's module of elasticity, and the fracture energy. All these small specimens were demolded after 24 hours and kept in water until testing day. In order to follow material characteristics compression tests on cubes and cylinders were carried out continuously with the beam testing.

2.2 Concrete mix and reinforcement

The concrete mix was prepared from one batch at a concrete stationary plant and in a concrete truck mixer. Lightweight aggregate was first placed in a concrete truck and later mortar was added. Mixing and transport was done in a concrete truck mixer. The lightweight aggregate was ½" fraction from Stalite , argillite slate from North Carolina. In order to design concrete mix the moisture content and the absorbed water in the Stalite were measured. The moisture was 11.43%, and the absorption after 24 hours and 100 hours was 6.54% and 8.32%, respectively. Table 2 gives the concrete mix recipe. The mixing was done using combination of concrete stationary plant capacity 4 m³ and concrete truck mixer 6 m³. Characteristics of the fresh concrete were: density 2013 kg/m³, air content 2.4% and slump 230 mm. The reinforcement was of the type B500NC [1]. Assumed yielding stress of the reinforcement was 530 MPa.

Table 2. Concrete mix for LWAC 65

Constituent	Weight [kg/m ³]
Cement (Norcem Anlegg FA)	430.75
Silica fume (Elkem Microsilica)	22.38
Water (free+absorbed 24 hour)	123.33+55.17=178.5
Sand (Ramlo 0-8 mm)	595.31
Sand (Ramlo 0-2 mm)	249.65
Aggregate (Stalite ½")	550
Superplasticizer (Mapei Dynamon SR-N)	5.4

2.3 Test set-up of measuring devices

The load was applied by mechanical screw jack and transferred to the test beam through a steel spreader beam.

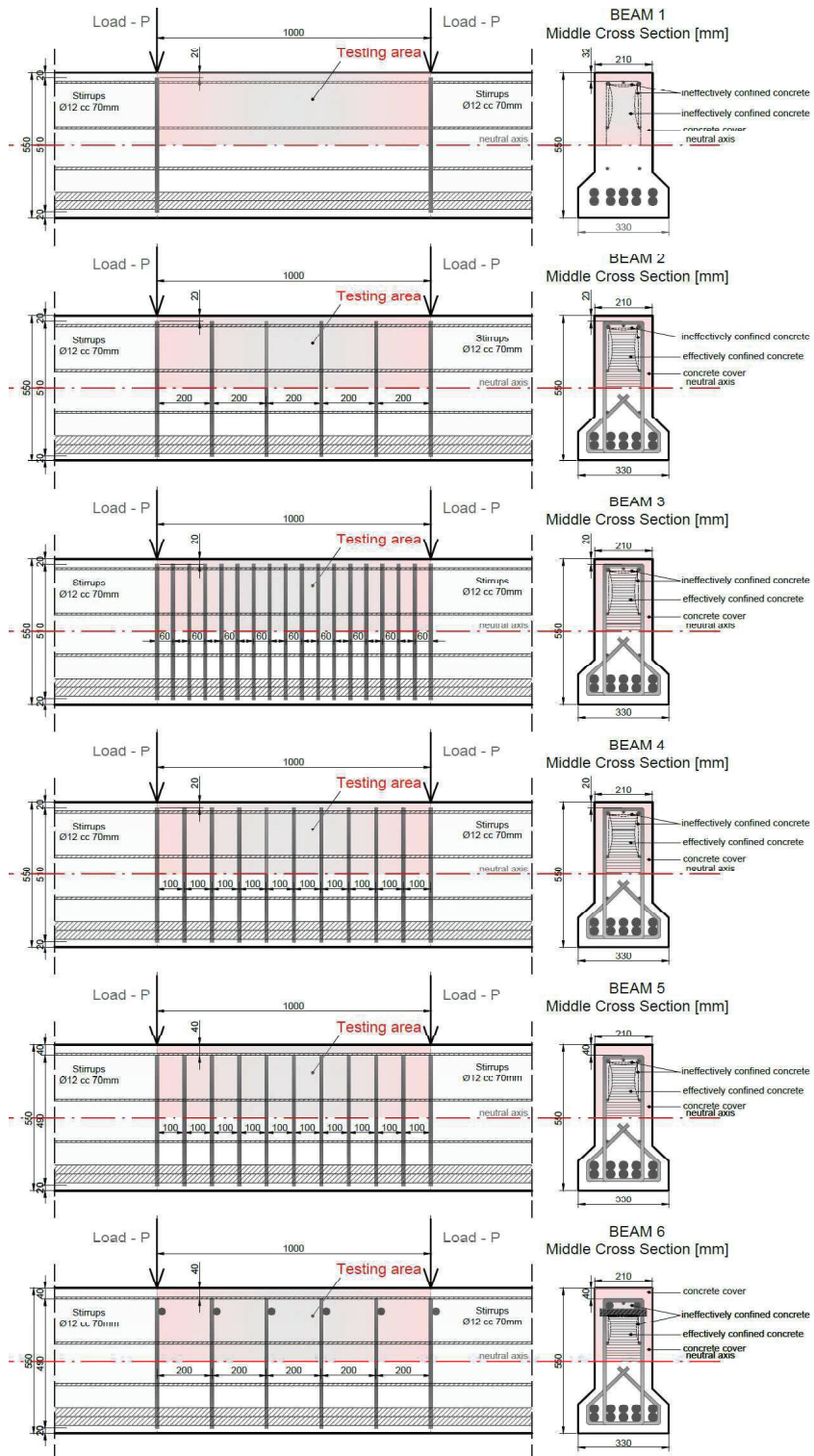


Fig. 2 Testing area with corresponding beam middle cross section. Dimensions are in [mm].

Two steel rollers supported the beam and covered the entire width of the beam. The loading point has free rotation transversal to the beam. Between jacks and the beam surface, it was used a 100 mm wide steel plates and a 15 mm thick fibreboard with the same width. The supports were both free for rotation and displacement in the longitudinal direction. At the supports, only steel plates were between the support and the beam. The supports were placed 250 mm from the beam-ends. To avoid anchorage problems, tension reinforcement bars were welded to the steel plate dimensions 30x60x330mm in this region. The load was measured by an electrical load cell under the screw jack with a maximum capacity 2000 kN. Three linear variable displacement transducers (LVDT), one at the mid-span and two above each loading point measured the deflections of the beam. Additional five LVDTs measured strain at the concrete surface. Three of them measured strains in the compressive zone and two strains in the tensile zone. The LVDTs were placed in the middle cross section and they measured deflection over a distance of 200 mm. In addition, six strain gauges (SG, type FLA-6-11-5L with gauge resistance of $119.5 \pm 0.5 \Omega$) were inserted on the compressive bar $\varnothing 8$ and tensile reinforcement, inside of the middle cross section. All measuring devices (LVDTs and SGs) together with the load cell were connected to HBM 8 channel spider to record the data. From here, data were forwarded to computer using a specific software program, where they are processed and stored in a text file. The load was applied step-wise, with load increments of 100 kN up to 70% of calculated capacity. The load increments were then reduced to 50 kN until failure. The rest periods at each load level were three minutes and mainly used to draw the crack progression with dark pen and taking of photos. The tests were displacement con-trolled with a loading rate 1-1.2 mm/minute, thus, the deflection measurements were carried out as a control during all tests. Fig. 3 shows the experimental setup and fig. 4 middle beam cross section with all measuring devices.

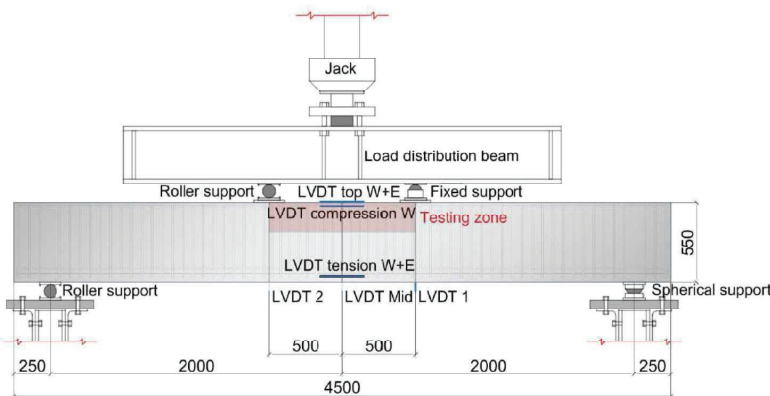


Fig. 3 Experimental set-up of the beam test. Dimensions are in [mm].

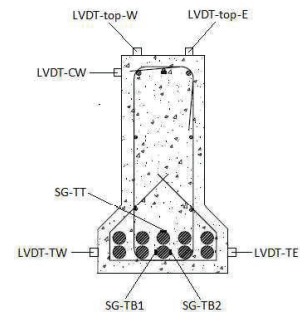


Fig. 4 Middle beam cross section with measuring devices

3. Experimental results

3.1 Results for small specimens

Small specimens were tested after 28 days for determination of compressive strength, tensile strength and Young's modulus. Small beams for fracture energy were tested after 71 days. A brief summary of the small-scale test results is given in Table 3. Concrete class measured from small samples was LC65 and which represents a high strength lightweight concrete. The compressive failures of cubes and cylinders were very explosive which is typical for high strength and lightweight concrete.

Table 3. Material properties for LWAC 65

Saturated density	$\rho_{cs} = 2013 \text{ kg/m}^3$
Oven dry density	$\rho_{cv} = 1834 \text{ kg/m}^3$
Compression cube after 7 days	$f_{cm,7} = 56.7 \text{ N/mm}^2$
Compression cube after 28 days	$f_{cm,28} = 74.2 \text{ N/mm}^2$
Compression cylinder	$f_{cm} = 65,1 \text{ N/mm}^2$
Tensile strength	$f_{ctm} = 4.03 \text{ N/mm}^2$
Modulus of elasticity	$E_{ctm} = 24175 \text{ N/mm}^2$
Fracture energy	$G_F = 70,5 \text{ Nm/m}^2$
Characteristic length	$l_{ch} = 104 \text{ mm}$

3.2 Results for the beams

The beams were tested 37 days (beam 1), 50 days (beam 2 and 3), 55 days (beam 4), 57 days (beam 5) and 59 days (beam 6) after casting. Each beam experienced spalling of the concrete cover in compression between the loading points. Spalling defines the first load peak in the load-deflection curves. The load decreased at this stage for some minutes, before the applied load again increased. The load, then, continued to increase until the concrete cover in the web started to spoil. This defines as a second load peak and is a smoother peak. The second spalling resulted in a larger drop in the load bearing capacity and deformations increased fast. Any attempt to increase load after second peak was not possible and residual capacity of the beam decreased until the final failure. Table 4 shows the results of the tested beams, where $P_{s,cr}$ correspond the force when the first shear crack occurred, P_1 is force of first peak load level and P_2 force of the second peak load level. The table also gives average strains (ϵ_c) recorded by two LVDTs placed in the compression zone. Value of recorded maximum strains correspond to first peak load level. The average tension strain (ϵ_t) represents the two LVDTs placed on both bottom beam sides in the tensile zone. The bending capacity ($P_{capacity}$) for all the tested beams was calculated according to Eurocode 2 and Norwegian standard [3], [4]. When calculating the capacity of the beams compressive strength, tensile strength, E-modulus and strains in a concrete were multiplied by a reduction factors η_I, η_E .

Table 4. Test parameters and results

Beam	Cover c (mm)	$f_{c,cube}$ (MPa)	Stirrup spacing (s)		$P_{capacity}$ [kN]	$P_{s,cr}$ [kN]	P_1 [kN]	P_2 [kN]	ϵ_c [‰]	ϵ_t [‰]
			Compress.reinf.(A_s)							
			A_s	s (mm)						
1	20	75.4	2 \emptyset 12	-	729	318	724	-	3.70	-
2	20	78.3	2 \emptyset 12	200	729	350	645	629	3.77	2.04
3	20	78.3	2 \emptyset 12	60	729	319	707	687	3.74	2.41
4	20	79.4	2 \emptyset 12	100	729	324	700	-	3.75	2.08
5	40	79.4	2 \emptyset 12	100	726	339	663	589	3.61	2.17
6	40	79.4	2 \emptyset 25	200	800	250	750	653	3.40	2.35

4 Discussion

Fig. 5 showed the cracking of the testing area. The first bending cracks observed in the constant moment region on the tension side, was at load levels from 25 til 53 kN. First cracking depends on the stirrups density in testing area. Since beam without any stirrups in testing area did not have any confinement this beam

cracked for lowest load level. As the load increased, new bending cracks propagated symmetrically until they reached the top of the beam flange.

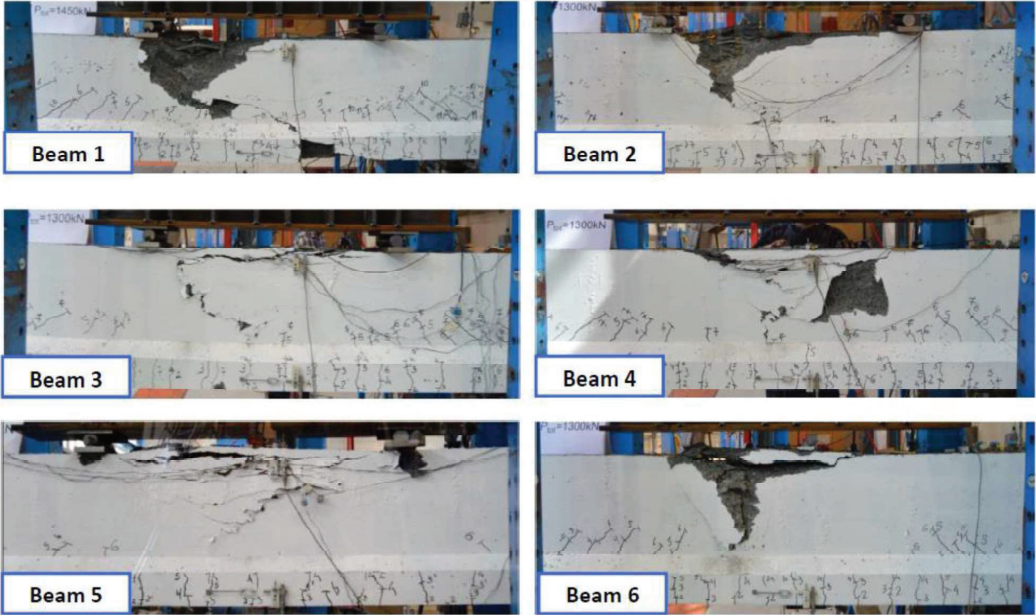


Fig. 5 Cracking of the testing area between loading points.

Development of bending cracks slowed down when shear cracks appeared. The first shear cracks appeared in the middle of the shear zone, between the neutral axis and the beam flange. Additional loading lead to further crack propagation of both bending and shear area. Crack propagation for certain load steps are very similar for all the tested beams. From Table 4 it is obvious that beams which contain the stiff compressive reinforcement and most stirrups in testing area was able to sustain the largest load before spalling of the concrete cover. The compressive longitudinal reinforcement yielded in all the tested beams before first peak spoiling happened. The phase when spilling of the concrete cover on the top of cross section happened is defined as a spoiling at the first peak load (P_1). See fig. 6 where are shown all the cracking phases and remaining cross section after final failure.

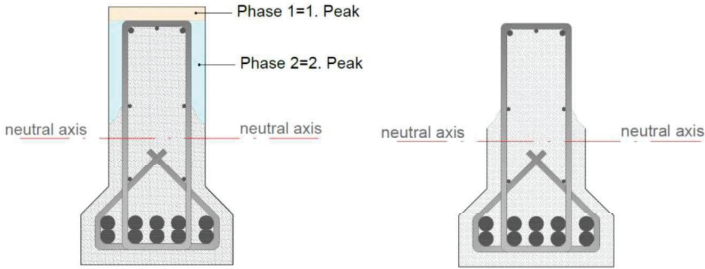


Fig. 6 Cracking phases and remaining cross section after final failure.

Spoiling of the concrete cover at the sides of the cross section happened for the second load level (P_2). This was at the same final failure of the beam. Beams with large stirrup spacing and small concrete cover showed the fastest spoiling and increase in crack propagation. When the applied load reached first peak load, the cross section for all the beams was reduced due to the spalling of the top concrete cover with load

automatically decreasing. It is obvious that beams with large concrete cover has higher drop in capacity and the second peak load level was lower. In finale face, spoiling of the web occurred and load drop very fast, while deformations increased, see Fig. 6 and. Beams with more dense stirrups can sustain more loading after first peak and they showed behaviour that is more ductile. In beam without stirrups in testing area and with low concrete cover second peak load was not registered. The beam failed immediately after first peak load level. Since all the beams were over-reinforced, tensile reinforcement did not yield.

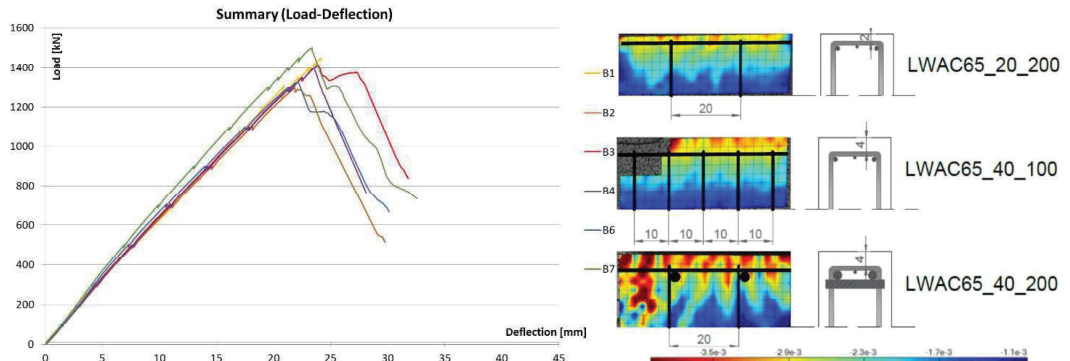


Fig. 7 Left side of the figure shows graph where is plotted total applied load versus deflection at the mid-span. At the right side are plotted strain fields recorded by digital image correlation method for the first peak load level.

From Fig. 7 and Table 4 it can be concluded that strains recorded by measuring devices LVDTs and DIC was the same. Ultimate compressive strain registered in the beams was in range 3.4-3.8%. By using DIC, detailed strain fields of the observed compressive zones have been recorded, and DIC was able to measure strain after spoiling of the top concrete cover together with LVDTs. From the detailed strain field it can be seen localisation of the largest strains in areas prior to failure. It is also visible that strains distribution followed reinforcement detailing. In a beam with the largest compressive reinforcement, strains were deeper. The same holds for concrete cover, with larger cover, large strains are deeper and spalling of concrete follows reinforcement layout. In addition, it is visible that reinforcement layout influence the most crack development.

In general, observed cracking in all the tested beams were very similar as could be expected in normal weight concrete beams, see fig. 5.

5 Conclusion

All the tested beams showed ductile behaviour since they were able to withstand increase of loading after formation of shear cracks (load level for first shear crack $P_{s,cr}$). Cracking was similar in all the tested beams. By decreasing stirrup spacing, the ultimate capacity, deflection and ductility increased. Beams with larger concrete cover withstand larger load. However, due to a reduced concrete core, capacity and ductility decreased. Concrete confined with increased longitudinal compressive reinforcement showed the largest ultimate capacity, but post-peak behaviour was influenced by stirrups spacing. Stirrups distribution provide greater lateral pressure on compressive zone and thus, greater ultimate compressive strength and ductility.

Test set-up together with measuring devices were able to capture the ultimate compressive strain in LWAC beams. The obtained ultimate compressive strain, ϵ_c , was much higher than typically given in design codes for LWAC. In general, the characteristics of LWAC depend on the type of lightweight aggregate. EC2 does not differentiate between types of aggregate used in LWAC. From the experimental results, it can be seen that EC2 underestimates ultimate strain level.

This study showed that it was possible to increase the ductility of LWAC structures by appropriate reinforcement detailing. For all the tested beams failure occurred when the compression zone between the loading points started to crack. This type of failure defines a compressive failure in the bending moment zone. Cracking of the compression zone was different for each beam depending on the test parameters: stirrup spacing, size of concrete cover and amount of the compressive reinforcement. Cracking of the testing area depend on the test parameters varied in the experiment. Bending behaviour observed in this experimental work is similar to NDC. Further investigations of LWAC as a structural material should therefore continued.

Acknowledgement

The work presented in this paper is part of an ongoing PhD study in the DACS project (Durable Advanced Concrete Solutions). The DACS partners are Kværner AS (project owner), Norwegian Research Council, Axion AS (Stalite), AF Gruppen Norge AS, Concrete Structures AS, Mapei AS, Multiconsult AS, NorBetong AS, Norcem AS, NPRA (Statens vegvesen), Norwegian University of Science and Technology (NTNU), SINTEF Byggforsk, Skanska Norge AS, Unicon AS and Veidekke Entreprenør AS. The first author would like to express her outmost gratitude to the supervisors and all the project partners for contributions and making this PhD study possible. In addition, special gratitude goes to master students Simon André Petersen, Henrik Nesje Johannesen, Jonas Andås Belayachi and Khaled Bastami for help during production and testing in this study.

References

1. Satish, C., and Leif B. 2002. *Lightweight Aggregate Concrete*. USA. Noyes publications-Wiliam Andrew Publishing.
2. American Concrete Institute, "Guide for Structural Lightweight Aggregate Concrete (ACI 213R-03)", ACI Committee 213, 2003, Farmington Hills, MI, United States.
3. EN-1992-1-1. 2004. "Eurocode 2, Design of concrete structures – Part 1-1: General rules and rules for buildings". Brussels, Belgium: CEN European Committee for Standardization.
4. NS-EN 1992-1-1:2004+NA: 2008. 2008. "Eurocode 2: Design of concrete structures – General rules and rules for buildings", Standard Norway.
5. Nedreliid, H., "Towards a better understanding of the ultimate behaviour of lightweight aggregate concrete in compression and bending." PhD diss., Norwegian University of Science and Technology, 2012, Trondheim, Norway.
6. Øverli, J. A., "Towards a better understanding of the ultimate behaviour of LWAC in compression and bending." *Engineering Structures*, Vol. 151, 2017, pp 821–838.
7. S.P. Shah and A.E.Naaman, et al., "Effect of confinement on the ductility of lightweight concrete.", *The international Journal of Cement Composites and Lightweight Concrete*, Vol. 5, Number 1, February 1983, pp 15-25.
8. Radic, J., Markic, R., et al., "Effect of confined concrete on compressive strength of RC beams», *Advances in concrete Construction*, vol.1, no.3, 2013, pp 215-225.
9. T.M. Jensen and J.A. Øverli. "Experimental study on flexural ductility in over reinforced lightweight aggregate concrete beams. ", COIN Project report, 47, 2013.

Paper 6

Particle-matrix proportioning of high strength lightweight aggregate concrete

Elisabeth Leite Skare, Jelena Zivkovic, Stefan Jacobsen, Jan Arve Øverli

Proceedings of SynerCrete'18: Interdisciplinary Approaches for Cement-based Materials and Structural Concrete: Synergizing Expertise and Bridging Scales of Space and Time.

Vol. 1&2, Funchal, Madeira Island, Portugal, October 24th – 26th 2018

Rilem publications 2018 ISBN 978-2-35158-211-4

6

PARTICLE-MATRIX PROPORTIONING OF HIGH STRENGTH LIGHTWEIGHT AGGREGATE CONCRETE

Elisabeth Leite Skare ^{(1),(2),(3)}, **Jelena Zivkovic** ⁽¹⁾, **Stefan Jacobsen** ⁽¹⁾, **Jan Arve Øverli** ⁽¹⁾

(1) Department of Structural Engineering, Norwegian University of Science and Technology (NTNU), NO-7491 Trondheim, Norway

(2) NorBetong AS (HeidelbergCementGroup), Heggstadmyra 6, NO-7080 Heimdal, Norway

(3) Department of Mechanical Engineering, Technical University of Denmark, 2800 Lyngby, Denmark

Abstract

Production of lightweight aggregate concretes (LWAC) requires specific knowledge and processes in order to achieve good workability of paste and concrete. A particularly demanding case is high strength lightweight aggregate concrete, i.e. having 28-day characteristic compressive strength in the range 60-80 N/mm² with oven dry density equal or less than 2000 kg/m³. Coarse manufactured lightweight aggregates themselves often lack particles smaller than 2 mm, which together with open aggregate porosity causes a certain loss of workability during the first minutes after mixing. An efficient way of improving this is by particle-matrix proportioning. The desired concrete workability can be obtained by combining the filler modified paste with a suitable amount of coarse aggregate particles. In order to investigate this, several different LWAC mixes have been tested with the lightweight aggregate Stalite, an argillite slate from the US. We found that the particle-matrix proportioning approach can give desired workability of the LWAC mixes. This methodology is economical since no increase in cement and admixtures dosage is needed.

Keywords: Lightweight aggregate concrete, Crushed fines, Proportioning, Workability of paste, Concrete

1. Introduction

The material properties of lightweight aggregate concrete (LWAC) are mainly depending on the properties of the used lightweight aggregate (LWA). LWA has different water absorption properties, geometry, surface, shape, rigidity, porosity and density compared to normal density aggregate, which all together have impact on LWAC [1]. One of the main challenges in preparation of LWAC is to achieve good workability and stability of the mix. Two main challenges encountered when making the LWAC are different density of the LWA and the paste that may cause LWA segregation by floating, and estimation of mix water absorption of LWA that can cause very unstable concrete and lack of control of effective mass ratio. Most of the

lightweight aggregates are split to several fractions. Coarser fractions of the lightweight aggregates are often very precisely fractioned and do not contain fines. One more challenge is to provide good packing of aggregate and paste, which might be difficult when using just one specific fraction of prefabricated LWA. Porosity of the LWA is in the range from 2 till 30% of volume, which in a mix, if not presaturated, absorbs a large amount of mix water from the fresh paste [2,3]. The most demanding case is preparation of high strength lightweight aggregate concrete. In order to achieve desired strength of LWAC, larger sizes of LWA, $\geq 8\text{mm}$, are required, which often are in lack of particles smaller than 2 mm. Together with open porosity and high absorption, this causes a certain loss of workability during the first minutes after mixing. A previous investigation has found that when pre-wetted LWA is used, the workability is influenced little by the LWA type [5]. The aggregate used in this investigation was Stalite, fraction 1/2". The dry aggregate density is 805 kg/m^3 and the saturated surface dry density is 833 kg/m^3 . This paper investigates how the desired concrete workability can be obtained by combining lightweight coarse aggregate particles with a suitable amount of crushed fines, by using the method of particle-matrix proportioning. Several different mixes have been prepared where the amount of the fines were varied, and the workability has been measured according to the well-known slump procedure [4]. In addition, the total amount of water in the mixes have been controlled by measuring the moisture of the aggregate itself.

2. Methodology and results

The workability of the fresh concrete was measured, as well as visual inspection of the stability, in a series of LWAC mixes. The main idea when designing the LWAC mixes was using the particle-matrix proportioning method to obtain necessary workability (slump and stability against LWA floating) in high-strength LWAC mixes, by using a suitable paste. The 1/2 " fraction Stalite, an argillite slate-based LWA, was used in all the mixes, see sieve curves in Fig. 2. The experimental program was made up of four different batches of LWA. For determination of workability the slump test method was used [4], see Fig.1. The stability has been controlled by visual inspection.



Figure 1: Slump method

2.1 Grading

Structural-grade Stalite LWA is made from various raw materials, including suitable slates, fly ashes, or blast furnace slags. The Stalite used in this investigation is first mined from naturally

deposits of argillite slate and later pyroprocessed in a rotary kiln process. After manufacturing the material is divided into proper sizes (3/4", 1/2" and 3/8" with respectively maximum aggregate sizes 18, 12.5 and 9.5 mm, and then their moisture contents is adjusted to a predetermined level. The fraction 1/2" is used in this investigation. Figure 2 shows particle size distributions from 4 different batches used in this study showing good agreement with each other, even though the batches were purchased and transported from different localizations and at different times. Fig 2 also shows that the Stalite has a low content of fines.

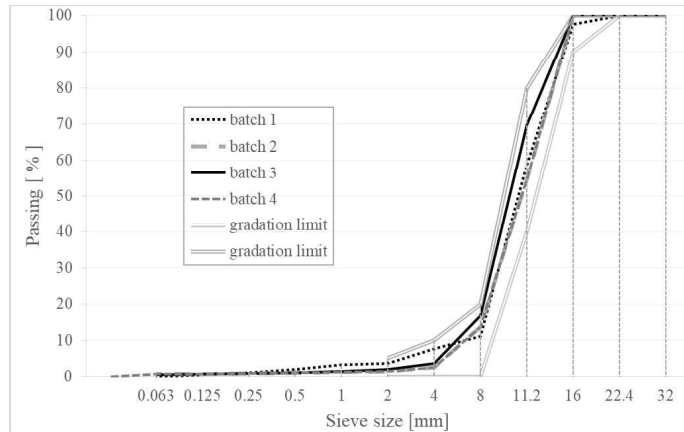


Figure 2: Sieve curves for aggregate Stalite fraction 1/2", batches 1-4,

2.2 Particle-matrix proportioning

Particle-matrix proportioning is a model that is dividing concrete into two phases: a matrix phase and a particle phase. The matrix phase consists of all solid particles less than 125 microns, as well as water and additives. The particle phase consists of all solid particles larger than 125 microns. In the particle-matrix model, the matrix phase fills all voids between the aggregate particles. Workability and consistency of the LWAC follow from the ratio between the phases [4]. This tool, particle-matrix proportioning, is making concrete production more sustainable and economical, optimizing concrete properties by controlling the composition of the particles and the matrix. By adjusting the amount and grading of the fines in the paste and varying volume fraction of the paste, the concrete workability can be controlled and improved substantially [6]. In addition, when using particle-matrix proportioning the stability of LWAC mixes can be improved. When increasing the amount of fines, the internal cohesion increases and that prevents bleeding, paste separation and segregation of LWAC [4]. In this investigation, LWA Stalite is used in all the mixes. Due to the splitting process, the Stalite is in lack of fine particles. A 0-2 mm sand was added to some of the mixes, in order to avoiding gap-graded aggregate and hence reduce the volume fraction of paste needed to obtain workable concrete.

2.3 Experimental program and results

The experimental program consists of eleven different LWAC mixes, see Tab. 1 and Tab. 2. Tab. 1 shows nominal, uncorrected proportions. In Tab. 2 are given properties of fresh concrete.

Table 1: Proportioned concrete mix compositions (kg/m³)

Mix No.	Cement Norcem Anlegg FA [kg]	Microsilica Elkem [kg]	Free Water [kg]	Batch No.	Aggregate Stalite 1/2" [kg]	Sand Årdal 0-8 mm [kg]	Sand Ramlo 0-2 mm [kg]	Absorbed water Stalite +sand	Superplas. Mapei Dyn. SR-N [m.% of cem.]
M1	399.5	19.8	167.7	1	571.9	720.3		40.1	0.64
M2	420.7	21.9	193.5	2	537.1	543.0	232.4	49.2	1.23
M3	420.8	22.2	195.7	2	521.8	543.6	232.9	48.0	1.21
M4	431.8	20.4	176.4	2	566.9	730.1		51.0	1.33
M5	424.4	22.3	174.2	2	575.6	507.6	190.4	41.3	1.06
M6	423.8	22.3	174.0	2	585.1	516.0	193.5	52.5	1.19
M7	427.7	22.5	200.4	2	564.6	560.1	124.5	50.6	1.13
M8	431.8	20.3	176.5	2	581.4	705.0		52.1	1.25
M9	427.5	22.5	203.7	4	514.0	535.5	229.4	47.2	0.73
M10	442.2	23.3	146.0	4	515.4	536.8	230.0	6.1	0.75
M11	440.3	23.2	180.8	3	517.5	539.0	231.0	38.8	0.89

Table 2: Fresh concrete mix parameters

Mix No.	Matrix volume [l/m ³]	w/b	w/p	$\rho_{\text{theoretical}}/\rho_{\text{measured}}$	Slump test [mm]	Stalite Moisture [% of dry aggregate]	Stability: Floating of LWA*	Stability: Bleeding/Halo*
M1	350	0.40	0.33	1920 / 1993	140	8.2	Yes	Yes
M2	375	0.44	0.39	1967 / 2013	230	11.43	No	No
M3	375	0.44	0.39	1967 / -	240	11.43	No	No
M4	365	0.39	0.33	1968 / -	210	8.5	Yes	Yes
M5	360	0.39	0.33	1943 / -	200	6.2	No	Yes
M6	360	0.39	0.33	1921 / -	250	8.5	No	Yes
M7	376	0.44	0.40	1930 / -	230	11.43	No	No
M8	365	0.39	0.33	1922 / -	210	8.5	Yes	Yes
M9	378	0.45	0.41	1967 / 1927	250	12.5	No	No
M10	326	0.31	0.28	1929 / 1989	170	0.1	Yes	No
M11	360	0.39	0.35	1967 / 2015	190	6.3	No	No

* Visual qualitative assessment

The main parameters varied in the mixes were the amount of fines, incorporated in the sand Ramlo 0-2mm, SP-dosage, as well as the moisture content of the LWA Stalite. Pre-wetted LWA Stalite was used in all the mixes, except in mix M10, where Stalite was very dry with a moisture content of 0.1%, see Tab. 2. Aggregate absorbed water was not considered as free water. Measured workability was in the range from 140 mm to 250 mm. This workability experiment has been done in combination with a casting experiment, and mixers with different capacities have been used, depending on the necessary concrete amount. Mix M1 has been mixed in an 800 litres capacity mixer, while mixes M9-M11 has been produced in a 250 litres capacity mixer, both with vertical pedals. The mortar in mix M3 has been produced at a concrete plant, and mixed together with the Stalite in the concrete truck mixer. The remaining mixes are trial mixes, performed in a mixer with a capacity of 10 litres with vertical pedals.

In addition, stability of LWAC was controlled, by visual qualitative assessment. In the mixes M1, M4, M8 and M10 it was noted coarse aggregate separation, when LWA particles float on the paste [4]. In the mixes M1, M4, M5, M6 and M8 it was observed slight bleeding as a sheen on the concrete mass and presence of the Mortar Halo [7], see Tab. 2.

3. Discussion

The particle-matrix proportioning method resulted in good workability in terms of stability and slump of the LWACs, by increased matrix volume and content of fines. From Tab.1 and Tab. 2 we see that matrix volumes and admixture dosages seem to explain the observed slump values, since the proportioned w/b- and w/p- ratios not are varying to a large extent among the mixes, as respectively from 0.31-0.45 and 0.28-0.41. The low slump of M1 relates to its low matrix volume and SP dosage. The higher slump of M4 and M8 correspond to high matrix volume and SP dosages. Finally, for M2, M3, M7 and M9 a higher slump is measured due to higher matrix volumes. For M5, M6 and M11 the matrix volumes are all the same but for the mix with lower slump, M11, the SP dosage were lower than for M5 and M6. Mix M10 has the lowest matrix volume due to lower water content in the LWA, i.e absorption of mix water.

For the mixes without fine sand from 0-2 mm, mixes M1, M4 and M8 floating of the LWA and slight bleeding as a water sheen at the edges of the concrete mass and poor paste viscosity were observed. Floating of the LWA was also observed for mix M10 where the Stalite was dry. Floating of the LWA on the paste might be caused by the density differences between the paste and the aggregate. From tab. 2 it is obvious the difference between the theoretical and measured density and they are often offset by 40-50 kg/m³. This huge difference is due to the releasing of water from aggregate during the drying process.

From all mentioned above it is obvious that by using the particle-matrix method, workability and stability may be improved significantly. When controlling the amount of fine sand in the mix it is possible to achieve desired workability, without increasing amount of cement and silica, and particle-matrix proportioning is hence more economical and practice.

4. Conclusions

Desired workability and stability was achieved in almost all LWAC mixes, except for the mixes without any fine sand. The mix with the dry aggregate obtained desired workability as a result of additional fines. By adding fines, it is possible to reduce the amount of water in the mix significantly, and still maintain good workability. Mixes without fine sand from 0-2 mm did not achieve enough stability, it is observed floating of the LWA and slight bleeding as a water sheen at the edges of the concrete mass. In general, particle-matrix proportioning by increasing the matrix volume by addition of sand is an economical and practical method, since sand is a more widespread and cheaper ingredient than cement and silica. In addition, methodology is not fully developed and future research have to be carried out.

Acknowledgement

The work presented in this paper is part of an ongoing PhD studies in the DACS project (Durable Advanced Concrete Solutions) and in the MiKS project (Microproportioning with Crushed Sand). The DACS partners are Kværner AS (project owner), Norwegian Research Council, Axion AS (Stalite), AF Gruppen Norge AS, Concrete Structures AS, Mapei AS, Multiconsult AS, NorBetong AS, Norcem AS, NPRA (Statens Vegvesen), Norwegian University of Science and Technology (NTNU), SINTEF Byggforsk, Skanska Norge AS, Unicon AS and Veidekke Entreprenør AS. The MiKS partners are Norcem AS, Norstone AS, Norbetong AS, Feiring Bruk AS, Skanska, SINTEF, National Institute of Standards and Technology (NIST), Norwegian University of Science and Technology (NTNU) and Technical University of Denmark (DTU).

References

- [1] ACI Committee 213, 2003, "Guide for Structural Lightweight-Aggregate Concrete (ACI 213R-03)", American Concrete Institute, Farmington Hills, MI, United States.
- [2] Punkki J. and Gjørsv O.E., Effect of water absorption by aggregate on properties of high-strength lightweight concrete, Proceedings from the International Symposium on Structural Lightweight Aggregate Concrete, Sandefjord, Norway (1995), 604-616.
- [3] ACI 211.2-98, 1998, (Reapproved 2004) "Standard Practice for Selecting Proportions for Structural Lightweight", ACI Manual of concrete practice, Part1, PP. 211.2-1-17.
- [4] S. Jacobsen et al, Concrete Technology 1. TKT 4215. Kompendium. Norwegian University of Science and Technology (2016), Chap. 3, 3-6 and 13-14; and Chap. 4, 12-22.
- [5] Hammer T.A. and Smeplass S., The influence of the lightweight aggregate properties on material properties of the concrete, Proceedings from the International Symposium on Structural Lightweight Aggregate Concrete, Sandefjord, Norway (1995), 517-532.
- [6] R.Cepuritis, Development of crushed sand for concrete production with microproportioning, PhD thesis, Norwegian University of Science and Technology (2016)
- [7] A. El hassan et al, The Impacts of Visual Stability Index on Flowability and Segregation I Properties of Self-Consolidating Concrete, Proceedings from the Transportation Research Board 94th Annual Meeting , Washington DC, United States (2015).

Paper 7

Brittleness of high-strength lightweight aggregate concrete
Jelena Zivkovic, Mladena Lukovic, Jan Arve Øverli, Dick Hordijk

Proceedings of SynerCrete'18: Interdisciplinary Approaches for Cement-based Materials and Structural Concrete: Synergizing Expertise and Bridging Scales of Space and Time.
Vol. 1&2, Funchal, Madeira Island, Portugal, October 24th – 26th 2018
Rilem publications 2018 ISBN 978-2-35158-211-4



BRITTLINESS OF HIGH-STRENGTH LIGHTWEIGHT AGGREGATE CONCRETE

Jelena Zivkovic ⁽¹⁾, **Mladena Lukovic** ⁽²⁾, **Jan Arve Øverli** ⁽¹⁾, **Dick Hordijk** ⁽²⁾

(1) Department of Structural Engineering, Norwegian University of Science and Technology (NTNU), NO-7491 Trondheim, Norway

(2) Department of Engineering Structures, Delft University of Technology (TU Delft), 2628 CN Delft, The Netherlands

Abstract

Modern society and infrastructure are facing an increased demand for fast construction. A number of viaducts are aged and will need to be replaced in near future. When considering this replacement task, lightweight, slender bridge is the solution. Dead load reduction and high-strength to weight ratio are the main advantages when using the lightweight aggregate concrete (LWAC). Still, structural applications of LWAC are lacking. The main disadvantage of LWAC compared to regular concrete, which refrains its wider structural application, is its brittleness and uncontrolled crack propagation, especially when LWAC is exposed to compression. One of the ways to improve brittleness and increase the ductility of concrete is by addition of fibers. In this research, preliminary study is performed where fiber reinforced LWAC mixture was designed and tested. The mix consisted of lightweight aggregate Stalite, leading to high-strength LWAC and polyvinyl alcohol fibers (PVA) providing reduced brittleness and explosive failure. Results on fracture behavior and compressive strength with the increased amount of fibers were investigated and showed promising behavior. In future, structural tests (e.g. compression tests on prisms and beams) will be performed to further verify the benefits of combining aggregate Stalite with PVA fibers for structural applications of high-strength LWAC.

Keywords: Lightweight aggregate concrete, Fibres, Brittleness, Ductility, Slender bridges, Innovative bridge design

1. Introduction

Nowadays, the demand for fast construction increases. A special task is that a majority of the bridges and viaducts are aged and will need to be replaced in the near future. Many countries worldwide face a similar problem and a solution for dealing with it is urgently needed. In this context, new materials and techniques can provide cost-effective solutions thereby minimizing the construction time and reducing the traffic hinder. When considering replacement task high-strength lightweight, slender bridge can be an optimal solution [1].

Lightweight aggregate concrete (LWAC) has been used successfully for structural purposes for many years. The preferable structures are floating offshore platforms, marine structures and bridges [2,3]. The main advantage that classified lightweight concretes as a desired material for use is reduced dead weight of a structure, and in long-span bridges and high-rise buildings, dead load is a significant portion of the design load. By reducing the weight of the structure, lightweight concrete also reduces bearing, substructure and foundation design loads that may contribute to cost savings in the structure. For the projects where seismic events must be considered in design, reduction of weight is especially significant since it lead to reduction in seismic design load [4,5]. Another important application for the reduced density of lightweight concrete is its use for concrete elements that are prefabricated (precast) to facilitate easier handling and faster construction [2]. High strength lightweight aggregate concrete, i.e. having 28-day characteristic compressive strength in the range 60-80 N/mm² with oven dry density equal or less than 2000 kg/m³.

Apart from many foreseen benefits and advantages when using LWAC, structural applications is still lacking. The main reason for that compared to normal weight concrete (NWC) is its brittleness and uncontrolled crack propagation, especially faced when LWAC is exposed to compression. The brittleness of concrete is characterized by sensitivity to stress concentrations and a rapid crack/fracture development. This is attributed to the difference in fracture behaviour of two types of concretes: in regular concrete, cracks are formed around the aggregates, following aggregate-paste interface zone whereas in LWAC cracks propagate through the aggregate. As a result, more tortuous cracking route is made in regular concrete leading to more stable crack propagation and higher fracture energy. For structural analysis, it is essential to know the complete stress-strain curve under uniaxial compression including the descending branch. The main concern for designers when using LWAC is steep and short descending branch, since concrete behave in a brittle manner. Therefore, additional brittleness introduced by LWAC should be certainly avoided. In order to improve this disadvantage of the LWAC concrete, a case study on several LWAC mixes was performed, whereby lightweight aggregate Stalite was combined with polyvinyl alcohol fibers (PVA) [6].

2. Future replacement task

In the past, many cast in-situ reinforced concrete plate bridges were built. The main advantage of this bridges were higher slenderness because of multiple intermediate supports over a single span bridge. At the time when cast in-situ plate bridges were built, the construction time and traffic hindrance was not a serious issue as today. Keeping in mind that many of these bridges and viaducts are constructed for a design service life of 50 years, the replacement is needed. Nowadays, with expansion of the road network and serious implications due to traffic hindrance, the main replacement requirements become more demanding. Rebuilding of cast in-situ plate bridges is due to its impact on traffic, undesirable solution and should be avoided. In this context, new materials and techniques can provide cost-effective solutions thereby minimizing the construction time and reducing the traffic hinder. The main requirements for the replacement of the existing structures are: to keep the same traffic profile without additional ground work, to minimize the work on existing foundations and to ease transportation during the construction process and provide joining of separate elements of the bridge. Having in mind all aspects mentioned above, high-strength lightweight, slender bridge can be an optimal solution. With this type of bridge it is possible to keep or reduce bridge height, where traffic profile stays the same or increase. Using of the

prefabricated LWAC box girders reduce the weight of concrete elements, making the use of precast elements more feasible by reducing requirements for shipping, handling and erection. In addition traffic impact is reduced to a minimum during construction time.

3. Case study - LWAC with fibres

3.1 Lightweight aggregate concrete (LWAC)

Structural lightweight aggregate concrete is made when normal weight aggregate (NWA) is replaced with lightweight aggregate (LWA). That is simply lighter a rock, produced using shale, clay or slate, so the same batching and admixtures are used for preparation of lightweight aggregate concrete like the same procedures and equipment as a for conventional concrete. Typical LWAC mixtures that use coarse LWA and conventional sand have a oven-dry density of 1750 to 2000 kg/m³, followed by compressive strength up to 70 MPa (based on cylinder strength). Water absorption of LWA is higher than the absorption of NWA, in the range from 6 % to 25 %. Because LWA has a higher absorption, lightweight concrete typically loses mass with time as excess absorbed water migrates out of the concrete. The oven-dry density as the density achieved after moisture loss has occurred is used for design criteria. As a result of lower density of aggregate, density of LWAC is reduced in range from 25-30% compared with NWA. That is significant in areas where dead load is one of the largest determinative factor, especially in seismic areas. This feature allows the reduction of cross sections, improve structural efficiency and economy.

Density of the LWA is lower than density of the cementitious paste, which require extra care during the production of LWAC. Control of absorption and moisture during production is necessary to produce concrete with consistent properties. LWAC generally requires more cementitious material and lower water-cement (w/c) ratio to achieve higher compressive strength. The porous nature of lightweight aggregate reduces its stiffness. In hardened LWAC, strength and rigidity of the aggregate is lower than that of the paste, leading to crack distribution through aggregate, lower strength development and lower ductility. As a result of that phenomena, fracture energy, tensile strength and E-modulus are lower for LWAC [2-5]. In addition, LWAC have brittle nature, uncontrolled crack/fracture development followed by an explosive failure. Together with the main stress-strain curve under uniaxial compression, where the descending branch is steep and short, this is main concern for the designers when using LWAC as preferable material. One of advantages when using lightweight concrete is improved fire resistance. This feature is significant for building construction where structural elements are often required to provide a certain resistance to fire exposure. The insulating properties of lightweight concrete allow a smaller (and also lighter) thickness of concrete to provide the same resistance as for NWA [2,5]. The significant benefit with respect to durability when using the lightweight concrete is reduced shrinkage. This is provided due to internal curing from the water that is absorbed and stored in aggregate itself [5].

3.2 Tensile strength and shear capacity of LWAC with Stalite as aggregate

Previous experimental investigation dealt with the tension behaviour of LWAC with Stalite as aggregate. Behaviour and ductility of beams with and without shear reinforcement were observed in 4-point bending test. The main test parameters that were varied in those tests were the shear span length to effective height ratio (a/d) and amount of shear reinforcement. All the tested beams showed ductile behaviour because they were able to withstand significant

increase of load after formation of shear splitting cracks. Crack formation in the tested beams were similar as for normal weight concrete. By qualitative visual inspection for all the tested beams without shear reinforcement it was observed explosive, loud and brittle failure [7]. When observing the cracked area, propagation of cracks goes through and around LWA, leading to higher tensile strength and fracture energy [5,7]. High-strength LWAC with Stalite as aggregate showed promising behaviour.

3.3 Polyvinyl alcohol fibres (PVA)

Polyvinyl alcohol fibers (PVA) is mostly use to improve the inherent brittleness of cementitious materials and to control cracking. They have very little effect on the flexural strength and deflection capacity. The compressive capacity is slightly reduced while concrete surface of the elements become extremely ductile [8].

3.4 Experimental program, results and discussion

Small experimental program have been created in order to create non brittle and ductile high-strength LWAC. The main concern was to deal with brittleness, explosive failure and to improve ductility of LWAC. Because of that PVA fibres was introduced in range 0.5 to 1 % at volume fractions. PVA was type “Kuralon RSC15”, 8 mm long with E-modul of 36 MPa. All the concrete mixes have been prepared from the same batch of LWA Stalite, argillite slate from North Carolina.

Table 1: Concrete mix compositions (kg/m³) and fresh concrete properties.

Constituent	LWAC65	FLWAC65 with 0.5 % fibres	FLWAC65* with 0.5 % fibres	FLWAC65 with 1% fibres
Cement (Norcem Anlegg FA)	431.1	414.4	397.5	435.5
Silica fume (Elkem Microsilica)	22.7	21.8	20.9	22.9
Water (free)	177	170.1	163.2	206.3
Absorbed water *sand+aggregate	53.6	49.3	46.7	45.6
Sand (Ramlo 0-8 mm)	552.6	559.1	531	517.5
Sand (Ramlo 0-2 mm)	236.8	239.6	377.3	221.8
Aggregate (Stalite ½")	530.5	536.72	493	496.8
Superplasticizer (Mapei Dynamon SR-N)	5.4	5.1	6.2	6
Synthetic fibres (% of volume)	-	6.5	6.5	13
Fresh concrete properties				
Matrix volume [l/m ³]	360	360	360	400
Slump [mm]	240	35	40	10
Fresh density [kg/m ³]	2013	1900	2011	1663

Stalite was completely saturated to avoid water exhaustion from the paste and in addition have been controlled moisture and absorption of the aggregate just before the mix preparation. One concrete mix (LWAC 65) was prepared as a reference one without addition of the fibres, while three mixes contain fibres. Tab. 1 shows all the concrete mixes and fresh concrete characteristics. All the mixes have been prepared in laboratory controlled conditions, in a mixer with vertical pedals and capacity 25 liters. In order to provide good distribution of the fibres in FLWAC, first was prepared paste where were added fibres and later was introduced aggregate with continuous mixing. From the LWAC and FLWAC mixes have been casted several cubes and cylinders for the testing and following of compressive strength at 7, 14, 28, 38 and 46 days. At age of 28 days cylinders from all the prepared concretes were tested under compression to get E modulus [9]. From that test it was plotted stress-strain diagram, see Fig. 1. It can be noticed that LWAC65 showed brittle behaviour, when failure happened load immediately failed down, while all other mixes with fibres showed ductile behaviour with very smooth peak load where load goes slowly down and samples can sustain additional loading .

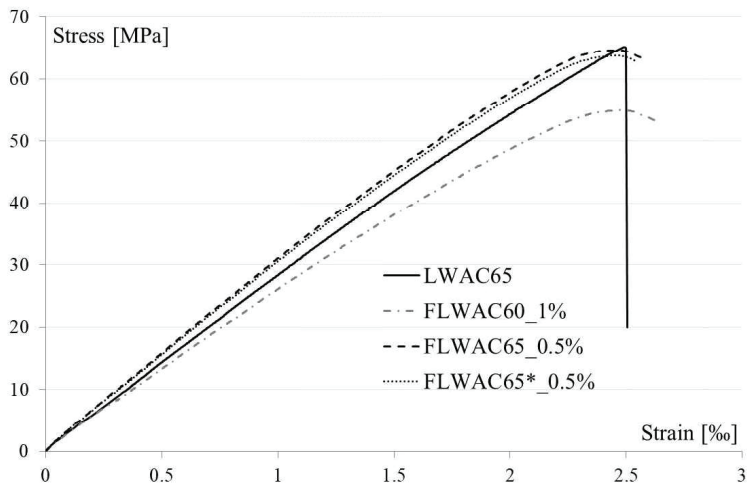


Figure 1: Stress-strain diagram for all the tested mixes at age 28 days

When testing lightweight aggregate concretes it was noticed that by adding the fibres, even in small amounts, workability of the concrete mix was significantly reduced. Concrete like this is very tough to cast, especially in sections that contain a lot of reinforcement is tough to embed this concrete. Mix FLWAC 65* contain more fine sand, fraction 0-2mm, in order to provide more stable paste and concrete, but still workability was very low. That happens because fibres arrest water which is wrapped around them. From the other side through qualitative visual inspection of the fracture, all three FLWAC concretes did not show any brittleness and explosive failure compared to LWAC 65. It was surprising that all the FLWAC cubes and cylinders kept together afterwards and can sustain additional loading. By adding the fibres in amount of 0.5% compressive strength is very slightly reduced while effect on the brittleness is the same like for mix with 1% of the fibres. For the FLWAC mix that contain 1% of the fibres compressive strength is significantly reduced, almost 18%.

4. Conclusions

When using the LWAC the weight of the structure can be reduced for the 25-30 %. Having this in mind, like all the other mentioned advantages, LAWAC seems to be a promising material for any structural applications, especially for the replacement bridge task. By introducing a small amount of PVA fibres, just 0.5%, the lightweight concrete became non brittle and without an explosive behaviour. In addition small amount of fibres did not influenced the compressive strength of concrete. In the future, structural tests (e.g. compression tests on prisms and beams) will be performed to further verify the benefits of combining aggregate Stalite with PVA fibers for structural applications of high-strength LWAC.

Acknowledgement

The work presented in this paper is part of an ongoing PhD studies in the DACS project (Durable Advanced Concrete Solutions). The DACS partners are Kværner AS (project owner), Norwegian Research Council, Axion AS (Stalite), AF Gruppen Norge AS, Concrete Structures AS, Mapei AS, Multiconsult AS, NorBetong AS, Norcem AS, NPRA (Statens Vegvesen), Norwegian University of Science and Technology (NTNU), SINTEF Byggforsk, Skanska Norge AS, Unicon AS and Veidekke Entreprenør AS.

References

- [1] A. Reitsema, M. Lukovic, D. Hordijk, Towards slender, innovative concrete structures for replacement of existing viaducts, fib Symposium 2016 Performance-based Approaches for Concrete Structures Cape Town (2016).
- [2] Castrodale, R. W. et al, High-performance lightweight concrete bridges and buildings, Eleventh High Performance Concrete (11th HPC) & the Second Concrete Innovation Conference (2nd CIC), Tromsø, Norway (2017).
- [3] Sandvik, M. and Hammer, T. A., The development and use of high performance lightweight concrete in Norway, International Symposium on Structural Lightweight Aggregate Concrete, Sandefjord, Norway (1995), 617-627
- [4] ACI 213R-03, Guide for Structural Lightweight Aggregate Concrete, American Concrete Institute, ACI Committee 213, Farmington Hills, MI, USA (2003).
- [5] Castrodale, R. W., Zivkovic, J. et al., Material properties of high performance structural lightweight concrete, Eleventh High Performance Concrete (11th HPC) & the Second Concrete Innovation Conference (2nd CIC), Tromsø, Norway (2017)
- [6] Kuraray Co, Characteristics of KURALON (PVA fibres), PVA fibres-application, available: <http://kuralon-frc.kuraray.com/product-application>
- [7] Zivkovic, J. and Øverli, J. A., Behavior and capacity of lightweight aggregate concrete beams with and without shear reinforcement. Nordic Concrete Research. Volume 57(2) (2017), 59-72
- [8] Savija, B. et al., Development of ductile cementitious composites incorporating microencapsulated phase change materials, International Journal of Advances in Engineering Sciences and Applied Mathematics, Volume 9, Issue 3, (2017), 169-180
- [9] NS 3676, Norwegian standard, Concrete testing-Hardened concrete-Modules of elasticity in compression. NSF, Oslo, Norway (1987)

Paper 8

Failure of lightweight aggregate concrete under compressive strain gradients

Jelena Zivkovic, Jan Arve Øverli

Proceedings of the 15th Nordic mini seminar: Structural lightweight aggregate concrete.

Trondheim, Norway, February 20th 2019

Norsk Betongforening 2019 ISBN 978-82-8208-066-8



Failure of lightweight aggregate concrete under compressive strain gradients

	<p>Jelena Zivkovic M.Sc. PhD-candidate Department of Structural Engineering Faculty of Engineering Science Norwegian University of Science and Technology N-7491 Trondheim, Norway e-mail: jelena.zivkovic@ntnu.no</p>
	<p>Jan Arve Overli PhD, Professor Department of Structural Engineering Faculty of Engineering Science Norwegian University of Science and Technology N-7491 Trondheim, Norway e-mail: jan.overli@ntnu.no</p>

ABSTRACT

The use of lightweight aggregate concrete (LWAC) is limited as a mainstream construction material in structural applications. Partly this is related to the brittleness in compression compared to normal density concrete. Research done in the DACS-project has shown that high strength LWAC with Stalite as aggregate has much higher compressive strain levels than expected [1]. A strain gradient test, by loading prisms centrally and eccentrically, has been used to investigate strains and ductility in compression. The obtained strain level was much higher than expected.

Key words: Lightweight Aggregate Concrete, Testing in Compression, Strain level, Centric and Eccentric Loading, Strain Gradients

1. INTRODUCTION

This investigation is part of the ongoing research program “Durable advanced concrete structures (DaCS)”. The part of this program is to investigate structural behaviour of lightweight aggregate concretes (LWAC), concretes with an oven dry density below 2000 kg/m³. The use of lightweight aggregate concrete (LWAC) is limited as a mainstream construction material in structural applications. A reason for that is related to the steepness of the descending branch of the stress-strain curve in compression [2]. Material models for compressive failure of concrete are normally based on a uniaxial compressive stress-strain curve obtained from tests, where the main assumption is uniform deformation of the concrete specimens. This assumption is reasonable for the ascending branch of the stress-strain curve, while for the descending branch is not realistic as it is always accompanied by significant lateral deformations. The lateral deformations are mainly caused by splitting cracks, which are formed and expand during the test. LWAC is characterized by more brittle post-peak material behaviour and uncontrolled crack propagation compared to normal density concrete (NWC).

In order to describe more in detail the compressive behaviour and to measure compressive strains, the effect of a strain gradient was introduced and varied in an experimental program. Strain gradients influences both the strength and the ductility [3]. Beam experiments tested in the

DACS-project has shown that high strength LWAC with Stalite as aggregate obtained much higher compressive strain levels than expected [1]. The present experimental program included three batches of LWAC for the production of 21 prisms. The batches differed in using dry (0,10 % moisture content) or saturated (7,9 % moisture content) aggregate. The third batch included a small amount of polyvinyl alcohol fibres. Lightweight aggregate argillite slate, called Stalite, fraction size ½ inch, from North Carolina have been used. The geometry of the prisms were 100 x 140 x 480 mm (width x length x height). All samples were loaded centrally and eccentrically in compression. From the achieved experimental results it is visible that the lateral deformation of the most stressed fibre is counteracted by the less stressed fibres and that confine compressive stress. Close to the peak load the lateral deformations near the free surface become pronounced. Finally, in the post-peak region two different fractures developed and ultimate strains increased. In general larger eccentricity lead to increased strains (recorded strains in prisms test was in range from 3,08‰ and 6.82‰).

2. EXPERIMENTAL TEST PROGRAM AND RESULTS

The experimental program consist of 21 prisms, dimensions 100 x 140 x 480 mm (width x length x height), of plain LWAC which were loaded centrally and eccentrically in compression. This study looks at the differences of using dry-DLWAC (0,10 % moisture content) or saturated – WLWAC (7,9 % moisture content) aggregate, and the influence of adding 0.5% per cement mass of polyvinyl alcohol fibres – FLWAC, influence the compressive behaviour. Strain level at the concrete area were recorded with strain gauges (SG) and Linear Variable Differential Transformers (LVDT) at two sides of the prism. On the other two sides Digital Image Correlation (DIC) was used [4]. All the prisms were loaded in an electro-hydraulic, servo-controlled displacement machine with a capacity of 1000kN. Prisms were first preloaded with 100kN and later load was constantly applied with a loading rate of 0.3 mm/minute until failure. Average compressive strain levels recorded in all the prisms was between 3,08‰ and 6.82‰. In addition, for control of the material characteristics, compressive strength, tensile strength, E-modulus and fracture energy specimens were tested. To produce the concrete, a lightweight aggregate Stalite was used from the same batch to achieve an oven-dry density of about 1850 kg/m³ and a compressive cylinder strength of approximately 65 MPa. Test program and results are given in Table 1. Detailed test setup of the prisms is shown in Figure 1.

Table 1-Test program and results

Prism Nr.	Type of concrete	Aggreg. Moist. [%]	$f_{c,cube}$ [MPa]	$f_{c,prism}$ [MPa]	Eccentricity [mm]	P_{max} [kN]	P_{calc} [kN]	$\epsilon_{c,LVDT}$ [‰]	$\epsilon_{c,DIC}$ [‰]
1-3					e=0	804	763	2.69	3.12
4-6	DLWAC	0.1	77.9	57.5	e=7.77	668	513	2.51	3.47
7-9					e=23.33	495	382	2.70	3.81
1-3					e=0	746	791	2.59	3.40
4-6	WLWAC	7.9	80.7	53.5	e=7.77	648	531	2.19	3.69
7-9					e=23.33	541	395	2.96	4.53
1					e=0	653	760	2.46	2.94
2	FLWAC	7.9	77.6	46.7	e=7.77	669.9	511	2.18	4.54
3					e=23.33	577.8	380	3.38	6.82

Where $f_{c,cube}$ is compressive cube strength; $f_{c,prism}$ is compressive prism strength (P_{max} divided with prism cross cestion 100x140mm) ; P_{max} – load level of maximum load; P_{calc} – hand calculation of maximum load; $\epsilon_{c,LVDT}$ – maximum concrete compressive strain recorded with LVDT; $\epsilon_{c,DIC}$ – maximum concrete compressive strain recorded with DIC;

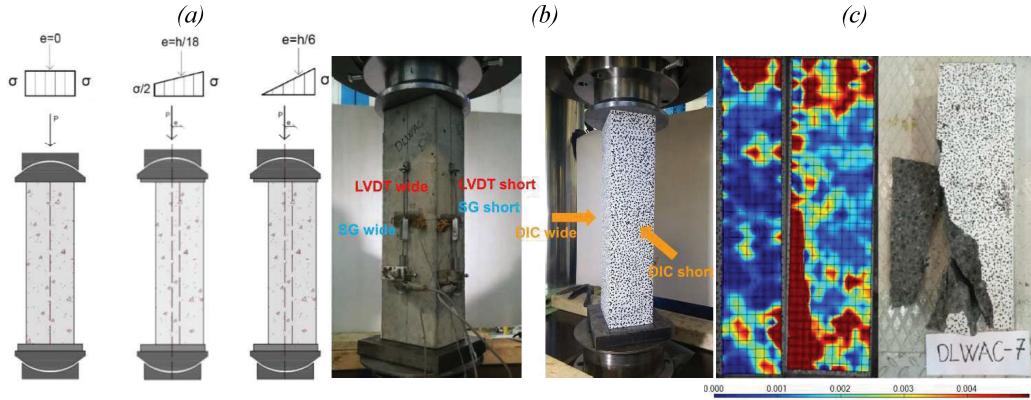


Figure 1 – (a) Detailed test setup of prisms with loading conditions; (b) setup of measuring devices at all four sides; (c) detailed strain field recorded with DIC just before failure and failure of prism

3. DISCUSSION AND CONCLUSIONS

This study investigates at the differences using dry or saturated aggregate, and the effect of polyvinyl alcohol fibres on the compressive behaviour of LWAC. Crack propagation depended on the loading conditions. Prisms subjected to centrally loading experienced large cracks and the lowest ultimate compressive strain., while prisms loaded eccentrically only cracked at the most stressed part with higher strains. By using DIC, detailed strain fields of the observed compressive zones have been recorded, see Figure 1(c). In general, measuring devices were in a good agreement, but close to failure larger strains and localization were measured using DIC, compared to the strain values measured with the SGs and LVDTs. The concrete with the water saturated aggregate had somewhat higher strains and ductility than the concrete with dry aggregate. Through qualitative visual inspection of the fracture, it was observed that the concrete with the saturated aggregate had the most explosive fractures. By introducing a small amount of fibres (0,5% of the cement mass) the concrete became significantly more ductile, with a maximum compressive strain of 6,82 ‰, and the fracture was not explosive. Eurocode 2 [5] does not differ between lightweight concrete with different types of aggregates, and underestimated the largest strains in this experiment by 75-88 %.

The experimental setup of the prisms and the eccentricities were the same as in an earlier experiment and are therefore comparable [3]. The earlier studies looked at the lightweight concrete Liapor 8 and different types of normal weight concrete. Table 2 compare new and old experiments. A ductility index D is calculated as:

$$D = \frac{\epsilon_{cu} - \epsilon_{el}}{\epsilon_{el}} \cdot 100\% \quad (1)$$

where ϵ_{cu} is maximum compressive strain and ϵ_{el} is strain corresponding to elastic state. It is clear that LWAC with Stalite showed more ductile behaviour compared with LWAC with Liapor 8. Compared to normal density concretes the ductility is very similar while registered strains are much higher. When adding just small amount of polyvinyl alcohol fibres the ductility is doubled.

Table 2 - Comparison with experimental work from 1993 [2]

Type of concrete	Eccentricity [mm]	$f_{ic,prism}$ [MPa]	$f_{ic,cube}$ [MPa]	ϵ_{cu} [%]	D_{LVDT} [%]	D_{DIC} [%]
DLWAC	e=0			3.12		
	e=7.77	57.5	77.9	3.47	11.2	13.3
	e=23.33			3.81		
WLWAC	e=0			3.40		
	e=7.77	53.5	80.7	3.69	15.1	14.9
	e=23.33			4.53		
FLWAC	e=0			2.94		
	e=7.77	46.7	77.6	4.54	37.2	37.6
	e=23.33			6.82		
Liapor 8	e=0			3.12		
	e=7.77	86.8	93.8	3.41	9.6	
	e=23.33			3.55		
Gneis/ Granitt	e=0			2.61		
	e=7.77	81.4	104.1	2.97	14.5	
	e=23.33			3.16		
Basalt	e=0			2.72		
	e=7.77	89.0	105.1	3.31	31.7	
	e=23.33			3.45		
Kvartsitt	e=0			2.47		
	e=7.77	86.5	106.7	2.81	14.8	
	e=23.33			2.84		

Where $f_{ic,prism}$ is compressive prism strength; $f_{ic,cube}$ is compressive cube strength; ϵ_{cu} – maximum concrete compressive strain ; D_{LVDT} – ductility index calculated from maximum concrete compressive strain recorded with LVDT; D_{DIC} – ductility index calculated from maximum concrete compressive strain recorded with DIC;

Acknowledgment

The work presented in this paper is part of ongoing PhD study in scope of the DACS project (Durable Advanced Concrete Solutions). The DACS partners are Kværner AS (project owner), Norwegian Research Council, Axion AS (Stalite), AF Gruppen Norge AS, Concrete Structures AS, Mapei AS, Multiconsult AS, NorBetong AS, Norcem AS, NPRA (Statens vegvesen), Norwegian University of Science and Technology (NTNU), SINTEF Byggforsk, Skanska Norge AS, Unicon AS and Veidekke Entreprenør AS. Jelena Zivkovic would like to express her utmost gratitude to the supervisors and all the project partners for contributions and making this PhD study possible. J. Zivkovic would like to thank to Master students Aleksander Hammer and Håvard Lauvland for the help during experimental work.

REFERENCES

- [1] Zivkovic, J. and Øverli, J.A.: “Ultimate compressive strain in lightweight aggregate concrete beams”, *fib PhD Symposium in Prague*, pp. 829–836, (2018).
- [2] EuroLightCon. “Lwac Material Properties”. Document BE96-3942/R2, December 1998.
- [3] G. Markestet.: “Failure of concrete under compressive strain gradients”. PhD diss., Norwegian Institute of Technology, University of Trondheim, Norway. (1993)
- [4] N. McCormick and J. Lord.: “Digital Image Correlation for Structural Measurements”. ICE institution. Civil Engineering, 165 (CE4), pp. 185–190 (2012).
- [5] EN 1992-1-1 (2004), “Eurocode 2: Design of concrete structures – Part 1-1: General rules and rules for buildings”.

Paper 9

Effect of loading rate on the fracture energy of lightweight aggregate concrete subjected to three-point bending test

Jelena Zivkovic, Javad Seyed Mohammad, Filippo Berto, Jan Arve Øverli


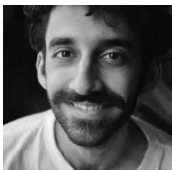


Proceedings of the 15th Nordic mini seminar: Structural lightweight aggregate concrete.

Trondheim, Norway, February 20th 2019

Norsk Betongforening 2019 ISBN 978-82-8208-066-8

9

Effect of loading rate on the fracture energy of lightweight aggregate concrete subjected to three-point bending test

	<p>Jelena Zivkovic M.Sc. PhD-candidate Department of Structural Engineering Faculty of Engineering Science Norwegian University of Science and Technology N-7491 Trondheim, Norway e-mail: jelena.zivkovic@ntnu.no</p>
	<p>Seyed Mohammad Javad Razavi M.Sc. PhD-candidate Department of Mechanical and Industrial Engineering Faculty of Engineering Science Norwegian University of Science and Technology N-7491 Trondheim, Norway e-mail: javad.razavi@ntnu.no</p>
	<p>Filippo Berto PhD, Professor Department of Mechanical and Industrial Engineering Faculty of Engineering Science Norwegian University of Science and Technology N-7491 Trondheim, Norway e-mail: filippo.berito@ntnu.no</p>
	<p>Jan Arve Øverli PhD, Professor Department of Structural Engineering Faculty of Engineering Science Norwegian University of Science and Technology N-7491 Trondheim, Norway e-mail: jan.overli@ntnu.no</p>

ABSTRACT

This study investigates the effect of loading rate on the fracture energy of lightweight aggregate concrete (LWAC) in the laboratory using three-point bending test. In addition, the effect of aggregate moisture and water/cement ratio on loading rate sensitivity was followed. Results show that increasing the loading rate leads to enhancement of the load-bearing capacity and fracture energy of the concrete. These results are promising having in mind that LWAC and especially high strength LWAC have brittle nature and fast crack/fracture development.

Keywords: Lightweight Aggregate Concrete, Three-point bending, Fracture energy, Loading rate

1. INTRODUCTION

This investigation is part of the ongoing research program “Durable advanced concrete structures (DaCS)”. The part of this program is to investigate structural behaviour of lightweight aggregate

concretes (LWAC), concretes with an oven dry density below 2000 kg/m³ [1]. One of the main problem considering the use of LWAC is brittleness followed with fast crack/fracture development. In order to test behaviour of LWAC under different loading rates special experimental program was created. Three sets of test specimens were produced using lightweight aggregate argillite slate from North Carolina, called Stalite, fraction size ½ inch, from the same batch, where the water content in aggregate varied by 0.1%, 7,9% and 12.5%. From each concrete, 16 small beams and small samples (i.e. cubes and cylinders) were produced. The geometry of the beams was 50 × 50 × 550 mm (width × height × length). All samples were pre-notched and loaded under three-point bending. The loading rate was varied from 0.1 mm/min to 100 mm/min.

2. EXPERIMENTAL TEST PROGRAM AND RESULTS

The experimental program consist of 48 small beams, dimensions 50 × 50 × 550 mm (width × height × length). Beams were produced from three different lightweight aggregate concretes marked as dry-DLWAC (contain lightweight aggregate (LWA) with 0.10% moisture content) and saturated one marked as WLWAC-1 (LWA with 7.9% moisture content) and WLWAC-2 (LWA with 12.5% moisture content). Concrete recipes are given in Table 1.

Table 1 – Concrete mixture for DLWAC, WLWAC-1 and WLWAC-2

Constituent	DLWAC Weight [kg/m ³]	WLWAC-1 Weight [kg/m ³]	WLWAC-2 Weight [kg/m ³]
Moisture of the aggregate [%]	0.1	7.9	12.5
Water/cement ratio [w/c]	0.32	0.33	0.37
Cement (Norcem Anlegg FA)	442.2	440.3	427.5
Silica fume (Elkem Microsilica)	23.3	23.2	22.5
Water (free)	146	180.8	203.7
Absorbet water Stalite+sand (24 hours)	6.1	38.8	47.2
Sand (Ramlo) 0-2 mm)	230	231	229.4
Sand (Årdal (NSBR) 0-8 mm)	536.8	539	535.5
Aggregate (Stalite 1/2")	515.4	517.5	514
Superplasticiser (Mapei Dynamon SR-N)	3.3	3.9	3.1

Prior to the fracture tests, a set of cylindrical specimens were tested for each type of concrete using compressive and tensile tests to obtain the compressive and tensile strengths of the studied concretes. According to the test results, the compressive strengths were 82 MPa (DLWAC), and 84.8MPa (WLWAC-1) and 74.6MPa (WLWAC-2) and tensile strengths were 4.72 MPa (DLWAC), 4.86MPa (WLWAC-1) and 4.09MPa (WLWAC-2).

All the prisms were loaded under three point bending with an electro-hydraulic, servo-controlled displacement machine with a capacity of 100kN (see Figure 1). Testing span was 500 mm and beams were pre-notched in middle span, with notch length of 20 mm. Load was constantly applied with four different loading rates of 0.1, 1, 10 and 100 mm/min until failure. The applied load and the corresponding displacement in the middle span were recorded with the load cell during the whole test.

3. DISCUSSION AND CONCLUSIONS

The loading rate dependency of the fracture energy in three different lightweight concretes namely DLWAC, WLWAC-1 and WLWAC-2 with different moisture levels of lightweight aggregates has been investigated in this research. The representative load-displacement plots of the tested concrete specimens are illustrated in Figure 2.



Figure 1 – Three-point bending test configuration.

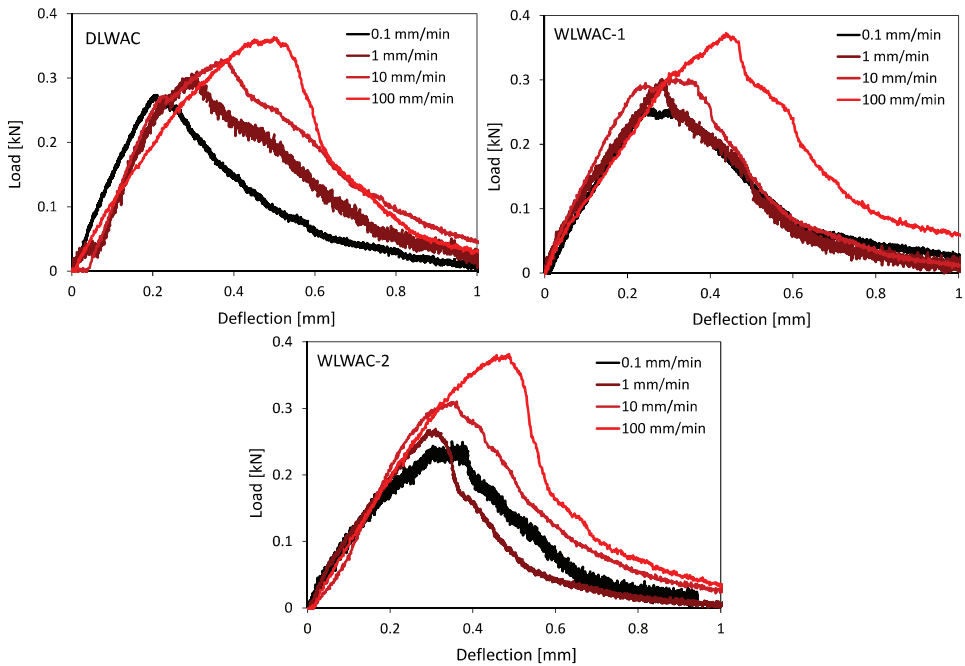


Fig. 2. Representative load-displacement response of the tested pre-cracked concrete specimens under three-point bending.

All the prisms showed ductile behaviour, after peak load was reached load slightly fail down until final failure happened. Through qualitative visual inspection of the fracture, it was observed that the concrete with the saturated aggregate (i.e. WLWAC-2) had the most explosive fractures. These results are of special interest having in mind that here was tested high strength LWAC, compressive strength above 60 MPa [1].

The fracture energies of the tested concretes were then calculated using the standard procedure proposed by SINTEF [2] and the results are given in Fig. 3. According to the SINTEF standard for fracture testing, the fracture energy G_f was calculated as:

$$G_f = \frac{W_o + 2 \cdot 0,4 \cdot p \cdot 9,81 \cdot \delta}{b \cdot h} \left[\frac{Nm}{m^2} \right] \quad (1)$$

where W_o is positive area under load-displacement graph, and p is weight of the concrete samples, δ is maximum recorded dilatation and b, h are measured width and height of fracture area.

According to Figure 2, increasing the loading rate results in higher peak load values in all three different concrete specimens, having 28%, 21% and 41% higher peak load values under 100 mm/min loading rates compared to 0.1 mm/min loading rate for DLWAC, WLWAC-1 and WLWAC-2, respectively. The same trend of improvement was observed dealing with the fracture energies of the tested specimens (see Figure 3).

Although fracture energy of the tested DLWAC, WLWAC-1 and WLWAC-2 specimens under standard static loading rate of 0.1 mm/min [2] was 87.6, 93.8 and 72.1 Nm/m², however, increasing the loading rate up to 100 mm/min increased these values to 136, 128.2 and 125.8 Nm/m² having and enhancement of 55%, 36% and 74%, respectively. According to the test results, increasing the loading rate from 0.1 mm/min to 1 mm/min resulted in enhancement of the fracture energies, however, only limited changes were observed when the loading rate was increased from 1 mm/min to 10 mm/min. In general, the lowest and the highest fracture energy values were obtained for the case that the specimens were tested under 0.1 mm/min and 100 mm/min.

The concrete with the low water saturated aggregate (i.e. WLWAC-1) had somewhat lower loading rate sensitivity than the concrete with dry aggregate. This can be related to the lower ductility of the mentioned concrete compared to DLWAC. On the other hand, increasing the moisture of the aggregate to a higher level in WLWAC-2 results in higher water to cement ratio leading to lower strength of the concrete making it the most loading rate sensitive concrete in this study.

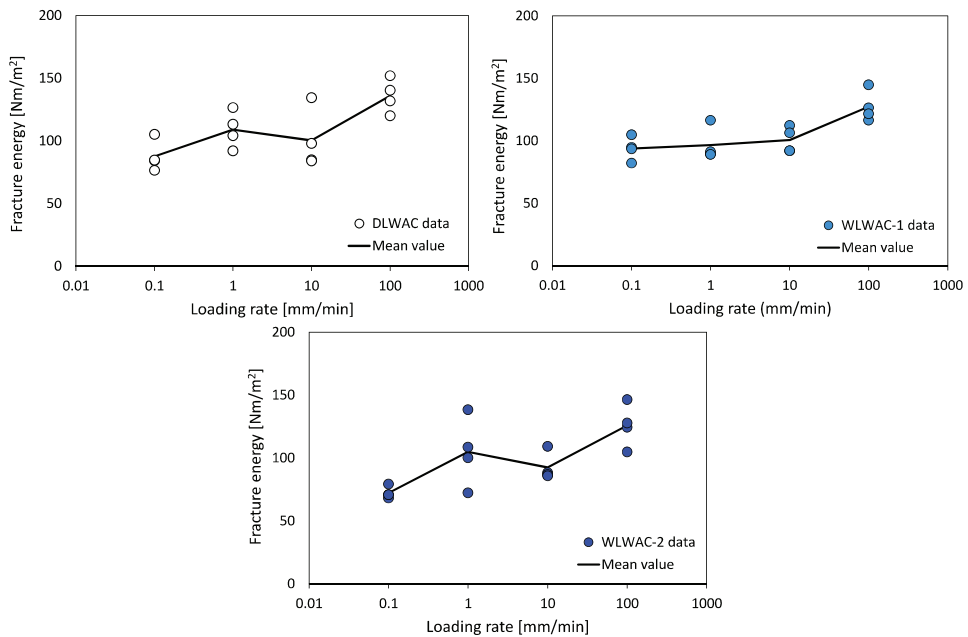


Fig. 3. Fracture energy versus loading rate for the tested pre-cracked concrete specimens under three-point bending.

Acknowledgment

The work presented in this paper is part of ongoing PhD study in scope of the DACS project (Durable Advanced Concrete Solutions). The DACS partners are Kværner AS (project owner), Norwegian Research Council, Axion AS (Stalite), AF Gruppen Norge AS, Concrete Structures AS, Mapei AS, Multiconsult AS, NorBetong AS, Norcem AS, NPRA (Statens vegvesen), Norwegian University of Science and Technology (NTNU), SINTEF Byggforsk, Skanska Norge AS, Unicon AS and Veidekke Entreprenør AS.

REFERENCES

- [1] EuroLightCon. "Lwac Material Properties". Document BE96-3942/R2, December 1998.
- [2] SINTEF procedure KS14-05-04123.

Paper 10

Confined lightweight aggregate concrete behavior and influencing factors

Jelena Zivkovic, Jan Arve Øverli

*Proceedings of the XXIV Nordic Concrete Research Symposium,
Sandefjord, Norway, August 17th – 20th 2021.*

Norsk Betongforening 2021 (accepted for publication and presentation at the Symposium)



10

Confined lightweight aggregate concrete behavior and influencing factors



Jelena Zivkovic, Ph.D
Department of Structural Engineering
Faculty of Engineering Science
Norwegian University of Science and Technology
7491 Trondheim, Norway
E-mail: jelena.zivkovic@ntnu.no



Jan Arve Øverli
Professor, Ph.D
Department of Structural Engineering
Faculty of Engineering Science
Norwegian University of Science and Technology
7491 Trondheim, Norway
E-mail: jan.overli@ntnu.no

ABSTRACT

The use of lightweight aggregate concrete (LWAC) is limited as a mainstream construction material in structural applications due to more brittle post-peak material behavior and uncontrolled crack propagation compared to normal density concrete (NWC). To improve the ductility of LWAC structures the confinement effect from reinforcement was considered. Confinement in lightweight aggregate concrete was achieved by suitable placement of the transverse reinforcement in conjunction with longitudinal reinforcement. In addition, influence of concrete cover is checked. By interpreting in qualitative and quantitative terms the results achieved, it is possible to increase the ductility of LWAC structures by appropriate reinforcement detailing.

Keywords: Confined lightweight concrete, ductility, transversal reinforcement, longitudinal reinforcement, concrete cover.

1. INTRODUCTION

The ability of the structure or its components, or the used material itself, to offer the resistance in the inelastic domain of response is called by the general term “ductility”. Generally, concrete itself is not a ductile material and to improve that the confinement effect from reinforcement must be introduced [1]. Lightweight aggregate concretes (LWAC), i.e. concretes with an oven-dry density below 2000 kg/m³, are generally characterized with very high degree of brittleness at the material level, and with decreased ductility, especially in compression [2]. This paper presents the influence of different factors on the effectiveness of confinement in compression in bending for LWAC concrete beams. To test confinement of LWAC, six over-reinforced beams were subjected to four-point bending test. The experiment setup was designed to produce a constant moment zone of one meter between loading points, where all the beams should collapse. The testing zone were analysed to study the effect of different stirrup spacing, amount of longitudinal compressive reinforcement and size of concrete cover, on beam ductility and carrying capacity. To produce the concrete, a lightweight aggregate Stalite was used to achieve

an oven-dry density of about 1850 kg/m^3 and a compressive strength of about 65 MPa. The reinforcement was of the type B500NC and the yielding stress of the reinforcement was assumed to be approximately 530 MPa. The aim of this paper is to study, the influence of different factors in the confined concrete behavior.

2. EXPERIMENTAL TEST PROGRAM AND RESULTS

The experimental program consists of six reinforced LWAC beams with a constant moment zone of 1m between the loading points. The geometry of the beams were 210-330 x 550 x 4500 mm (width x height x length). Parameters varied in the testing zone were the stirrup spacing (s), amount of compressive reinforcement (A_s) and size of concrete cover (c). All the beams were over-reinforced, using 10 ϕ 32, in order to provide the bending failure by concrete crushing in compression zone. Outside of the testing zone, all the beams had the same stirrups spacing, designed to avoid shear failure. The experimental program with test parameters and results are given in Table 1. Experimental set-up with detail cross sections of the testing zone are given at Figure 1. To record the strain in the mid span cross section combination of digital image correlation method (DIC), linear variable displacement transducers (LVDT) and strain gauges (SG) have been used.

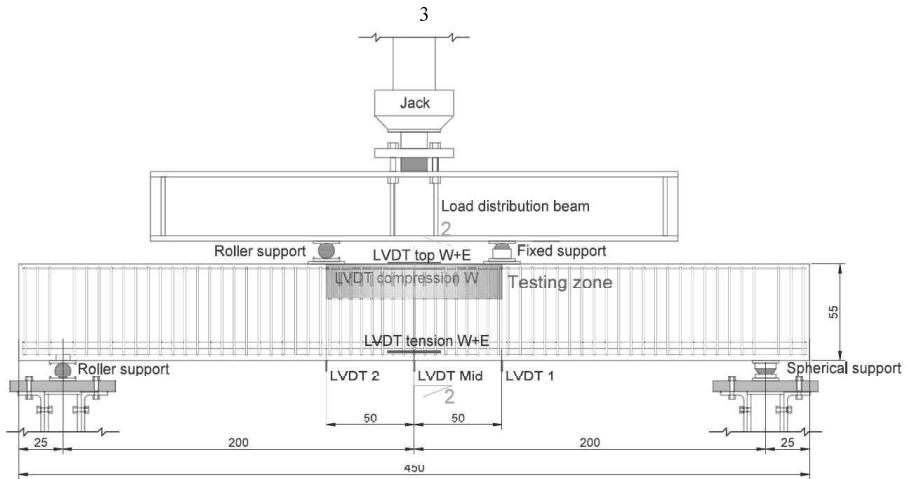
Table 1-Test parameters and results

B.	c (mm)	$f_{lc,cube}$ (MPa)	Stirrup spacing (s) Compres.reinf(A_s)		$P_{calc.}$ [kN]	$f'_{cc,exp}$ [MPa]	$f'_{cc,calc.}$ [MPa]	P_1 [kN]	P_2 [kN]	ϵ_{cu} [‰]	ϵ_t [‰]
			A_s	s (mm)							
1	20	75.4	2 ϕ 12	-	729	80.3	65	724	-	3.70	-
2	20	78.3	2 ϕ 12	200	729	73	66.6	645	629	3.77	2.04
3	20	78.3	2 ϕ 12	60	729	87.4	87.6	707	687	3.74	2.41
4	20	79.4	2 ϕ 12	100	729	70.2	75.4	700	-	3.75	2.08
5	40	79.4	2 ϕ 12	100	726	83.4	75.8	663	589	3.61	2.17
6	40	79.4	2 ϕ 25	200	800	83.4	65.9	750	653	3.40	2.35

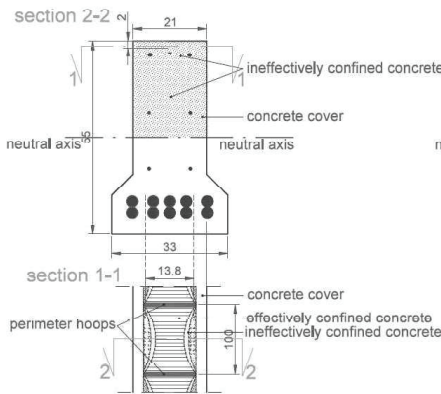
The results of interest from the testing are load level at the peak 1 (P_1) when spoiling of the concrete cover on top of cross section occurred and load level at the peak 2 (P_2), when sides of cross section spoiled, and final failure was reached. The technical elements that served as a judgement foundation were: confined concrete compressive strength (f'_{cc}), ultimate compressive strain (ϵ_{cu}) and load level at peak 1 and 2. Experimental confined concrete compressive strength ($f'_{cc,exp}$) is calculated during test from the results that were recorded by LVDT and SG in compression zone. Confined concrete compressive strength ($f'_{cc,calc}$) was calculated with adjusted theoretical stress-strain model proposed by Mander [3]. Referring to Figure 1, the arching action occurs horizontally between longitudinal reinforcement and vertically between layers of transverse hoop bars. The effectively confined area of concrete at hoop level is found by subtracting the area of the parabolas containing the ineffectively confined concrete.

3. DISCUSSION AND CONCLUSIONS

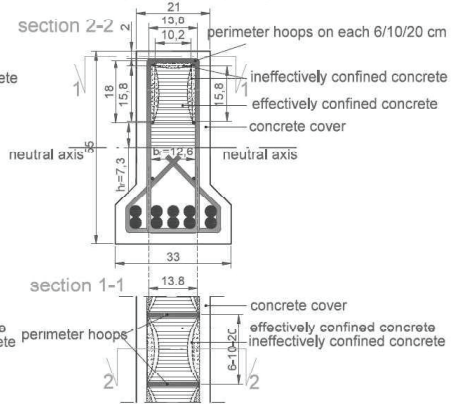
The confinement mechanism is quite complex and should be understood in detail, considering every possible influencing factor, based on stress-strain model. Tests have shown that the confinement of concrete by suitable arrangement of transverse and longitudinal reinforcement results in a significant increase in both the strength and ductility of compressed concrete.



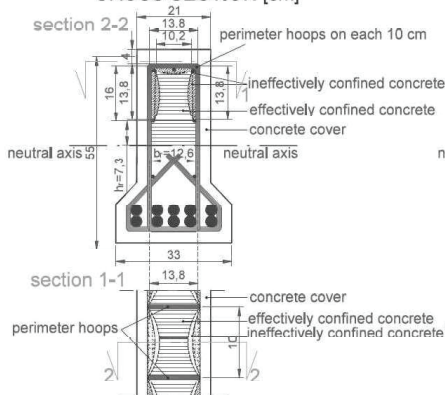
**BEAM 1
CROSS SECTION [cm]**



**BEAM 2, 3 and 4
CROSS SECTION [cm]**



**BEAM 5
CROSS SECTION [cm]**



**BEAM 6
CROSS SECTION [cm]**

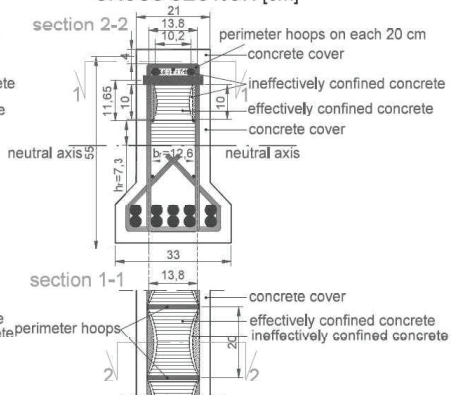


Figure 1 – Experimental set-up of the beam test. Cross section details with reinforcement for the beams. Dimensions are in [cm].

All the tested beams showed ductile behaviour since they were able to withstand increase of loading after formation of shear cracks. Strength and ductility in structural members are the function of the qualities of the constituent material. Test results showed that the transvers reinforcement is the most important confining factor and the “beating heart” of the confinement mechanism. By decreasing stirrup spacing, confined concrete compressive strength, ultimate compressive strain, deflection and ductility increased. The concrete cover is unconfined and will eventually become ineffective after the compressive strength is attained, but the core concrete continues to carry stress at high strain. Beams with larger concrete cover withstand larger load and confined concrete compressive strength was higher while ultimate compressive strain was lower, because remaining section was smaller. However, due to a reduced concrete core, capacity and ductility decreased. Concrete confined with increased longitudinal compressive reinforcement showed the largest ultimate capacity, but post-peak behaviour was influenced by stirrups spacing. The presence of several longitudinal bars well distributed around the perimeter of the section, tied across the section will also contribute the confinement of the concrete. Stirrups distribution provide greater lateral pressure on compressive zone and thus, greater ultimate compressive strength and ductility. Generally, the obtained ultimate compressive strain, ϵ_{cu} , was much higher than typically given in design codes for LWAC [4]. The main conclusion from the testing program given above is that it is possible to increase significantly the ductility and strength of LWAC structures by appropriate reinforcement detailing.

Acknowledgment

The work presented in this paper is part of an ongoing PhD study in the DACS project (Durable Advanced Concrete Solutions). The DACS partners are Kværner AS (project owner), Norwegian Research Council, Axion AS (Stalite), AF Gruppen Norge AS, Concrete Structures AS, Mapei AS, Multiconsult AS, NorBetong AS, Norcem AS, NPRA (Statens vegvesen), Norwegian University of Science and Technology (NTNU), SINTEF Byggforsk, Skanska Norge AS, Unicon AS and Veidekke Entreprenør AS. The first author would like to express her special gratitude to master students Simon André Petersen, Henrik Nesje Johannesen, Jonas Andås Belayachi and Khaled Bastami for help during production and testing in this study.

4. REFERENCES

- [1] EuroLightCon. “Lwac Material Properties”. Document BE96-3942/R2, December 1998.
- [2] E. Filaj, A. Seranaj and E. Leka, “Confined concrete behavior influencing factors”, International Research Journal of Engineering and Technology, Volume 3, Issue 7 July 2016: 36-43.
- [3] J.B. Mander, M.J.N. Priestley and R. Park, “Theoretical stress-strain model for confined concrete”, J.Struct. Eng. ASCE 1988, 114(8):1804-1826.
- [4] EN 1992-1-1 (2004), “Eurocode 2: Design of concrete structures – Part 1-1: General rules and rules for buildings”.

Articles in popular scientific magazines **11**

Gjør lettbetong mer anvendbar
Jelena Zivkovic, Jan Arve Øverli

Byggeindustrien, 2017 (No. 17), p. 33

A large, stylized white number '11' is centered within a dark blue square. The number is composed of two identical '1' characters placed side-by-side. The '1's have a slightly irregular, hand-drawn appearance with a small gap between them.



Jonas Andås Belayachi, Khaled al Bastami, Jelena Zivkovic, Simon Andre Petersen og Henrik Nesje Johannesen (NTNU) studerer bruddtøyning i trykk og duktilitet av lettbetongbjelker ved 4-punkts lastsituasjonstest. Foto: S. Seehuus (NTNU)

Gjør lettbetong mer anvendbar

Den største ulempen med lettbetong (LWAC) sammenlignet med normal betong (NDC) er sprøhet og ukontrollert sprekkutbredelse. Det gir lave trykktøyninger og redusert duktilitet. Gjennom størskala bjelkeprøving har vi vist at ulempen kan utlignes med smartere armeringsbruk.

Jelena Zivkovic og Jan Arve Øverli
Inst. for konstruksjonsteknikk

Lettbetong
Lettbetong inneholder lett, grovt tilslag, sand eller noen ganger til og med lett sand. Tilslaget gir en lav ovenstørr betongdensitet på 300-2000 kg/m³. Sammenlignet med normal betong kan lettbetong oppnå 20% lavere vekt, noe som gir en rekke fordeler. Blant annet kan betongen bli mer økonomisk å anvende.

Det finnes flere typer lettilslag. I vårt eksperimentet er Stalite benyttet. Stalite blir produsert i North Carolina fra ekspandert skifer. Prosessen gir tilslaget porer, som er en fordel under blanding og pumpling av betongen.

Prøveprogram

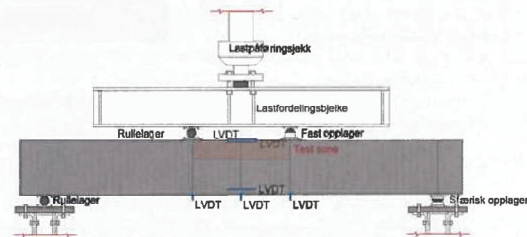
For å kvantifisere og forklare duktilitet (plastisk deformasjon) i konstruksjoner av lettbetong er begrepet omhyllingseffekt innført. For å oppnå forskjellige omhyllingseffekter har vi variert bøyelavstand, mengde trykkarmering og størrelsen på overdekning. Vi begynte først å kvantifisere duktilitet på materialnivå, men konkluderte fort med at effekten kun viser seg på

store elementer. Derfor gikk vi over til å teste bjelker. Siden det kreves store og mange testbjelker, var flere masterstudenter involverte.

Det eksperimentelle programmet bestod av syv overarmerte lettbetongbjelker med dimensjoner 4500x550x210 mm³ (lengde x høyde x bredde). Disse ble påført last gjennom en firepunkts bøyetest. Betongens oppførsel i trykksone mellom punktlastene ble observert. Trykksone lengden var en meter. Ph.d.-kandidat Jelena Zivkovic produserte, og undersøkte oppførselen til, alle bjelkene sammen med masterstudentene Simon Andre Petersen, Henrik Nesje Johannesen, Khaled al Bastami og Jonas Andås Belayachi.

Resultater

Prøvingen viste at det er mulig å gjøre lettbetong mer anvendbar i retning av normal betong ved å variere avstanden mellom skjærbøyler, mengde trykkarmering og størrelse på overdekning. Maksimale trykktøyninger i alle bjelkene var omtrent 40% høyere enn tillatt tøyning beregnet etter Eurokode 2 for denne typen betong. Alle bjelkene med skjærarmering i testsonen viste duktil oppførsel. De klarte å motvirke en gitt last for økte tøyninger før de gikk til brudd.



4,5 m lang lettbetongbjelke ved 4-punkts lastsituasjonsprøving. Illustrasjon: J. Zivkovic.

Generelt vil type tilslag avgjøre hvilke egenskaper betongen får. Siden Eurokode 2 ikke tar hensyn til ulike tilslag, vil Eurokoden undervurdere noen typer lettbetong.

DaCS-prosjektet

Undersøkelsen av duktilitet i lettbetong er en del av forskningsprosjektet: Durable advanced Concrete Solutions (DaCS). Målet for prosjektet er å utvikle kunnskap, metoder og verktøy som muliggjør bærekraftige og konkurransedyktige betongkonstruksjoner som tåler strenge miljøpåskjenninger i et arktisk marint miljø. Den omtalte prøvingen inngår i arbeidspakken «Ductile Lightweight Aggregate Concrete (LWAC)». Her deltar Kværner, NTNU, Statens

vegvesen, SINTEF, Multiconsult, Axion AS, Norcem, AF Gruppen, Skanska, Veidekke, Unicon, Mapei, NorBetong og Concrete Structures. Disse er også finansielle partnere sammen med Norges forskningsråd.

Hovedmål

Det endelige målet med vår forskningsaktivitet er å kunne modellere omhyllingseffekten for dimensjonering av lettbetongkonstruksjoner. Dette krever en kombinasjon av eksperimentelle resultater og numerisk analyse. Hovedmålet er å skaffe et godt nok grunnlag for å kunne benytte lettbetong på en effektiv måte. Prosjektet skal være ferdig i 2019.

Annex B - Database and supplementary information

Most of this PhD thesis is based on experimental work. To enable further research and potential use of the results, they were stored in the Zenodo database approved by NTNU. The link to the data base is:

<http://doi.org/10.5281/zenodo.4117937>

Database structure:

1. Experiment 1 – Stress strain gradients test

Concrete mix

Small-scale results

Large-scale results

Manuals

Photos

Video

2. Experiment 2 – Large-scale beam test

Concrete mix

Small-scale results

Large-scale results

Manuals

Photos

Video

3. Experiment 3 – Shear capacity

Concrete mix

Small-scale results

Large-scale results

Manuals

Photos

Video

4. Experiment 4 – Influence of loading rate on fracture and ductility

Concrete mix
Small-scale results
Large-scale results
Manuals
Photos
Video

5. Experiment 5 – Small-scale test LWAC with PVA fibres

Concrete mix
Small-scale results
Manuals
Photos
Video

**Doctoral thesis at the Department of Structural Engineering
of the Norwegian University of Science and Technology**

**DEPARTMENT OF STRUCTURAL ENGINEERING
NORWEGIAN UNIVERSITY OF SCIENCE AND TECHNOLOGY**

N-7491 TRONDHEIM, NORWAY
Telephone: +47 73 59 47 00

"Reliability Analysis of Structural Systems using Nonlinear Finite Element Methods",
C. A. Holm, 1990:23, ISBN 82-7119-178-0.

"Uniform Stratified Flow Interaction with a Submerged Horizontal Cylinder",
Ø. Arntsen, 1990:32, ISBN 82-7119-188-8.

"Large Displacement Analysis of Flexible and Rigid Systems Considering
Displacement-Dependent Loads and Nonlinear Constraints",
K. M. Mathisen, 1990:33, ISBN 82-7119-189-6.

"Solid Mechanics and Material Models including Large Deformations",
E. Levold, 1990:56, ISBN 82-7119-214-0, ISSN 0802-3271.

"Inelastic Deformation Capacity of Flexurally-Loaded Aluminium Alloy Structures",
T. Welø, 1990:62, ISBN 82-7119-220-5, ISSN 0802-3271.

"Visualization of Results from Mechanical Engineering Analysis",
K. Aamnes, 1990:63, ISBN 82-7119-221-3, ISSN 0802-3271.

"Object-Oriented Product Modeling for Structural Design",
S. I. Dale, 1991:6, ISBN 82-7119-258-2, ISSN 0802-3271.

"Parallel Techniques for Solving Finite Element Problems on Transputer Networks",
T. H. Hansen, 1991:19, ISBN 82-7119-273-6, ISSN 0802-3271.

"Statistical Description and Estimation of Ocean Drift Ice Environments",
R. Korsnes, 1991:24, ISBN 82-7119-278-7, ISSN 0802-3271.

"Properties of concrete related to fatigue damage: with emphasis on high strength
concrete",
G. Petkovic, 1991:35, ISBN 82-7119-290-6, ISSN 0802-3271.

"Turbidity Current Modelling",
B. Brørs, 1991:38, ISBN 82-7119-293-0, ISSN 0802-3271.

"Zero-Slump Concrete: Rheology, Degree of Compaction and Strength. Effects of
Fillers as Part Cement-Replacement",
C. Sørensen, 1992:8, ISBN 82-7119-357-0, ISSN 0802-3271.

"Nonlinear Analysis of Reinforced Concrete Structures Exposed to Transient Loading",
K. V. Høiseith, 1992:15, ISBN 82-7119-364-3, ISSN 0802-3271.

"Finite Element Formulations and Solution Algorithms for Buckling and Collapse
Analysis of Thin Shells",
R. O. Bjerum, 1992:30, ISBN 82-7119-380-5, ISSN 0802-3271.

"Response Statistics of Nonlinear Dynamic Systems",
J. M. Johnsen, 1992:42, ISBN 82-7119-393-7, ISSN 0802-3271.

"Digital Models in Engineering. A Study on why and how engineers build and operate
digital models for decision support",
J. Høyte, 1992:75, ISBN 82-7119-429-1, ISSN 0802-3271.

"Sparse Solution of Finite Element Equations",
A. C. Damhaug, 1992:76, ISBN 82-7119-430-5, ISSN 0802-3271.

"Some Aspects of Floating Ice Related to Sea Surface Operations in the Barents Sea",
S. Løset, 1992:95, ISBN 82-7119-452-6, ISSN 0802-3271.

"Modelling of Cyclic Plasticity with Application to Steel and Aluminium Structures",
O. S. Hopperstad, 1993:7, ISBN 82-7119-461-5, ISSN 0802-3271.

"The Free Formulation: Linear Theory and Extensions with Applications to Tetrahedral
Elements
with Rotational Freedoms",
G. Skeie, 1993:17, ISBN 82-7119-472-0, ISSN 0802-3271.

"Høyfast betongs motstand mot piggedekkslitasje. Analyse av resultater fra prøving i
Veisliter'n",
T. Tveter, 1993:62, ISBN 82-7119-522-0, ISSN 0802-3271.

"A Nonlinear Finite Element Based on Free Formulation Theory for Analysis of
Sandwich Structures",
O. Aamlid, 1993:72, ISBN 82-7119-534-4, ISSN 0802-3271.

"The Effect of Curing Temperature and Silica Fume on Chloride Migration and Pore
Structure of High Strength Concrete",
C. J. Hauck, 1993:90, ISBN 82-7119-553-0, ISSN 0802-3271.

"Failure of Concrete under Compressive Strain Gradients",
G. Markeset, 1993:110, ISBN 82-7119-575-1, ISSN 0802-3271.

"An experimental study of internal tidal amphidromes in Vestfjorden",
J. H. Nilsen, 1994:39, ISBN 82-7119-640-5, ISSN 0802-3271.

- "Structural analysis of oil wells with emphasis on conductor design",
H. Larsen, 1994:46, ISBN 82-7119-648-0, ISSN 0802-3271.
- "Adaptive methods for non-linear finite element analysis of shell structures",
K. M. Okstad, 1994:66, ISBN 82-7119-670-7, ISSN 0802-3271.
- "On constitutive modelling in nonlinear analysis of concrete structures",
O. Fyrilev, 1994:115, ISBN 82-7119-725-8, ISSN 0802-3271.
- "Fluctuating wind load and response of a line-like engineering structure with emphasis
on motion-induced wind forces",
J. Bogunovic Jakobsen, 1995:62, ISBN 82-7119-809-2, ISSN 0802-3271.
- "An experimental study of beam-columns subjected to combined torsion, bending and
axial actions",
A. Aalberg, 1995:66, ISBN 82-7119-813-0, ISSN 0802-3271.
- "Scaling and cracking in unsealed freeze/thaw testing of Portland cement and silica
fume concretes",
S. Jacobsen, 1995:101, ISBN 82-7119-851-3, ISSN 0802-3271.
- "Damping of water waves by submerged vegetation. A case study of laminaria
hyperborea",
A. M. Dubi, 1995:108, ISBN 82-7119-859-9, ISSN 0802-3271.
- "The dynamics of a slope current in the Barents Sea",
Sheng Li, 1995:109, ISBN 82-7119-860-2, ISSN 0802-3271.
- "Modellering av delmaterialenes betydning for betongens konsistens",
Ernst Mørtzell, 1996:12, ISBN 82-7119-894-7, ISSN 0802-3271.
- "Bending of thin-walled aluminium extrusions",
Birgit Søvik Opheim, 1996:60, ISBN 82-7119-947-1, ISSN 0802-3271.
- "Material modelling of aluminium for crashworthiness analysis",
Torodd Berstad, 1996:89, ISBN 82-7119-980-3, ISSN 0802-3271.
- "Estimation of structural parameters from response measurements on submerged
floating tunnels",
Rolf Magne Larssen, 1996:119, ISBN 82-471-0014-2, ISSN 0802-3271.
- "Numerical modelling of plain and reinforced concrete by damage mechanics",
Mario A. Polanco-Loria, 1997:20, ISBN 82-471-0049-5, ISSN 0802-3271.
- "Nonlinear random vibrations - numerical analysis by path integration methods",
Vibeke Moe, 1997:26, ISBN 82-471-0056-8, ISSN 0802-3271.

- “Numerical prediction of vortex-induced vibration by the finite element method”,
Joar Martin Dalheim, 1997:63, ISBN 82-471-0096-7, ISSN 0802-3271.
- “Time domain calculations of buffeting response for wind sensitive structures”,
Ketil Aas-Jakobsen, 1997:148, ISBN 82-471-0189-0, ISSN 0802-3271.
- "A numerical study of flow about fixed and flexibly mounted circular cylinders",
Trond Stokka Meling, 1998:48, ISBN 82-471-0244-7, ISSN 0802-3271.
- “Estimation of chloride penetration into concrete bridges in coastal areas”,
Per Egil Steen, 1998:89, ISBN 82-471-0290-0, ISSN 0802-3271.
- “Stress-resultant material models for reinforced concrete plates and shells”,
Jan Arve Øverli, 1998:95, ISBN 82-471-0297-8, ISSN 0802-3271.
- “Chloride binding in concrete. Effect of surrounding environment and concrete composition”,
Claus Kenneth Larsen, 1998:101, ISBN 82-471-0337-0, ISSN 0802-3271.
- “Rotational capacity of aluminium alloy beams”,
Lars A. Moen, 1999:1, ISBN 82-471-0365-6, ISSN 0802-3271.
- “Stretch Bending of Aluminium Extrusions”,
Arild H. Clausen, 1999:29, ISBN 82-471-0396-6, ISSN 0802-3271.
- “Aluminium and Steel Beams under Concentrated Loading”,
Tore Tryland, 1999:30, ISBN 82-471-0397-4, ISSN 0802-3271.
- "Engineering Models of Elastoplasticity and Fracture for Aluminium Alloys",
Odd-Geir Lademo, 1999:39, ISBN 82-471-0406-7, ISSN 0802-3271.
- "Kapasitet og duktilitet av dybelforbindelser i trekonstruksjoner",
Jan Siem, 1999:46, ISBN 82-471-0414-8, ISSN 0802-3271.
- “Etablering av distribuert ingeniørarbeid; Teknologiske og organisatoriske erfaringer fra en norsk ingeniørbedrift”,
Lars Line, 1999:52, ISBN 82-471-0420-2, ISSN 0802-3271.
- “Estimation of Earthquake-Induced Response”,
Símon Ólafsson, 1999:73, ISBN 82-471-0443-1, ISSN 0802-3271.
- “Coastal Concrete Bridges: Moisture State, Chloride Permeability and Aging Effects”
Ragnhild Holen Relling, 1999:74, ISBN 82-471-0445-8, ISSN 0802-3271.
- “Capacity Assessment of Titanium Pipes Subjected to Bending and External Pressure”,
Arve Bjørset, 1999:100, ISBN 82-471-0473-3, ISSN 0802-3271.

“Validation of Numerical Collapse Behaviour of Thin-Walled Corrugated Panels”,
Håvar Ilstad, 1999:101, ISBN 82-471-0474-1, ISSN 0802-3271.

“Strength and Ductility of Welded Structures in Aluminium Alloys”,
Mirosław Matusiak, 1999:113, ISBN 82-471-0487-3, ISSN 0802-3271.

“Thermal Dilation and Autogenous Deformation as Driving Forces to Self-Induced
Stresses in High Performance Concrete”,
Øyvind Bjøntegaard, 1999:121, ISBN 82-7984-002-8, ISSN 0802-3271.

“Some Aspects of Ski Base Sliding Friction and Ski Base Structure”,
Dag Anders Moldestad, 1999:137, ISBN 82-7984-019-2, ISSN 0802-3271.

"Electrode reactions and corrosion resistance for steel in mortar and concrete",
Roy Antonsen, 2000:10, ISBN 82-7984-030-3, ISSN 0802-3271.

"Hydro-Physical Conditions in Kelp Forests and the Effect on Wave Damping and
Dune Erosion. A case study on Laminaria Hyperborea",
Stig Magnar Løvås, 2000:28, ISBN 82-7984-050-8, ISSN 0802-3271.

"Random Vibration and the Path Integral Method",
Christian Skaug, 2000:39, ISBN 82-7984-061-3, ISSN 0802-3271.

"Buckling and geometrical nonlinear beam-type analyses of timber structures",
Trond Even Eggen, 2000:56, ISBN 82-7984-081-8, ISSN 0802-3271.

"Structural Crashworthiness of Aluminium Foam-Based Components",
Arve Grønsund Hanssen, 2000:76, ISBN 82-7984-102-4, ISSN 0809-103X.

“Measurements and simulations of the consolidation in first-year sea ice ridges, and
some aspects of mechanical behaviour”,
Knut V. Høyland, 2000:94, ISBN 82-7984-121-0, ISSN 0809-103X.

"Kinematics in Regular and Irregular Waves based on a Lagrangian Formulation",
Svein Helge Gjøesund, 2000-86, ISBN 82-7984-112-1, ISSN 0809-103X.

"Self-Induced Cracking Problems in Hardening Concrete Structures",
Daniela Bosnjak, 2000-121, ISBN 82-7984-151-2, ISSN 0809-103X.

"Ballistic Penetration and Perforation of Steel Plates",
Tore Børvik, 2000:124, ISBN 82-7984-154-7, ISSN 0809-103X.

"Freeze-Thaw resistance of Concrete. Effect of: Curing Conditions, Moisture Exchange
and Materials",
Terje Finnerup Rønning, 2001:14, ISBN 82-7984-165-2, ISSN 0809-103X

"Structural behaviour of post tensioned concrete structures. Flat slab. Slabs on ground",
Steinar Trygstad, 2001:52, ISBN 82-471-5314-9, ISSN 0809-103X.

"Slipforming of Vertical Concrete Structures. Friction between concrete and slipform panel",
Kjell Tore Fosså, 2001:61, ISBN 82-471-5325-4, ISSN 0809-103X.

"Some numerical methods for the simulation of laminar and turbulent incompressible flows",
Jens Holmen, 2002:6, ISBN 82-471-5396-3, ISSN 0809-103X.

"Improved Fatigue Performance of Threaded Drillstring Connections by Cold Rolling",
Steinar Kristoffersen, 2002:11, ISBN: 82-421-5402-1, ISSN 0809-103X.

"Deformations in Concrete Cantilever Bridges: Observations and Theoretical Modelling",
Peter F. Takács, 2002:23, ISBN 82-471-5415-3, ISSN 0809-103X.

"Stiffened aluminium plates subjected to impact loading",
Hilde Giæver Hildrum, 2002:69, ISBN 82-471-5467-6, ISSN 0809-103X.

"Full- and model scale study of wind effects on a medium-rise building in a built up area",
Jónas Thór Snæbjörnsson, 2002:95, ISBN82-471-5495-1, ISSN 0809-103X.

"Evaluation of Concepts for Loading of Hydrocarbons in Ice-infested water",
Arnor Jensen, 2002:114, ISBN 82-417-5506-0, ISSN 0809-103X.

"Numerical and Physical Modelling of Oil Spreading in Broken Ice",
Janne K. Økland Gjosteen, 2002:130, ISBN 82-471-5523-0, ISSN 0809-103X.

"Diagnosis and protection of corroding steel in concrete",
Franz Pruckner, 2002:140, ISBN 82-471-5555-4, ISSN 0809-103X.

"Tensile and Compressive Creep of Young Concrete: Testing and Modelling",
Dawood Atrushi, 2003:17, ISBN 82-471-5565-6, ISSN 0809-103X.

"Rheology of Particle Suspensions. Fresh Concrete, Mortar and Cement Paste with Various Types of Lignosulfonates",
Jon Elvar Wallevik, 2003:18, ISBN 82-471-5566-4, ISSN 0809-103X.

"Oblique Loading of Aluminium Crash Components",
Aase Reyes, 2003:15, ISBN 82-471-5562-1, ISSN 0809-103X.

"Utilization of Ethiopian Natural Pozzolans",
Surafel Ketema Desta, 2003:26, ISSN 82-471-5574-5, ISSN:0809-103X.

“Behaviour and strength prediction of reinforced concrete structures with discontinuity regions”, Helge Brå, 2004:11, ISBN 82-471-6222-9, ISSN 1503-8181.

“High-strength steel plates subjected to projectile impact. An experimental and numerical study”, Sumita Dey, 2004:38, ISBN 82-471-6282-2 (printed version), ISBN 82-471-6281-4 (electronic version), ISSN 1503-8181.

“Alkali-reactive and inert fillers in concrete. Rheology of fresh mixtures and expansive reactions.”

Bård M. Pedersen, 2004:92, ISBN 82-471-6401-9 (printed version), ISBN 82-471-6400-0 (electronic version), ISSN 1503-8181.

“On the Shear Capacity of Steel Girders with Large Web Openings”.

Nils Christian Hagen, 2005:9 ISBN 82-471-6878-2 (printed version), ISBN 82-471-6877-4 (electronic version), ISSN 1503-8181.

”Behaviour of aluminium extrusions subjected to axial loading”.

Østen Jensen, 2005:7, ISBN 82-471-6873-1 (printed version), ISBN 82-471-6872-3 (electronic version), ISSN 1503-8181.

”Thermal Aspects of corrosion of Steel in Concrete”.

Jan-Magnus Østvik, 2005:5, ISBN 82-471-6869-3 (printed version), ISBN 82-471-6868 (electronic version), ISSN 1503-8181.

”Mechanical and adaptive behaviour of bone in relation to hip replacement.” A study of bone remodelling and bone grafting.

Sébastien Muller, 2005:34, ISBN 82-471-6933-9 (printed version), ISBN 82-471-6932-0 (electronic version), ISSN 1503-8181.

“Analysis of geometrical nonlinearities with applications to timber structures”.

Lars Wollebæk, 2005:74, ISBN 82-471-7050-5 (printed version), ISBN 82-471-7019-1 (electronic version), ISSN 1503-8181.

“Pedestrian induced lateral vibrations of slender footbridges”.

Anders Rönquist, 2005:102, ISBN 82-471-7082-5 (printed version), ISBN 82-471-7081-7 (electronic version), ISSN 1503-8181.

“Initial Strength Development of Fly Ash and Limestone Blended Cements at Various Temperatures Predicted by Ultrasonic Pulse Velocity”.

Tom Ivar Fredvik, 2005:112, ISBN 82-471-7105-8 (printed version), ISBN 82-471-7103-1 (electronic version), ISSN 1503-8181.

“Behaviour and modelling of thin-walled cast components”.

Cato Dørum, 2005:128, ISBN 82-471-7140-6 (printed version), ISBN 82-471-7139-2 (electronic version), ISSN 1503-8181.

- “Behaviour and modelling of selfpiercing riveted connections”,
Raffaele Porcaro, 2005:165, ISBN 82-471-7219-4 (printed version), ISBN 82-471-7218-6 (electronic version), ISSN 1503-8181.
- ”Behaviour and Modelling of Aluminium Plates subjected to Compressive Load”,
Lars Rønning, 2005:154, ISBN 82-471-7169-1 (printed version), ISBN 82-471-7195-3 (electronic version), ISSN 1503-8181.
- ”Bumper beam-longitudinal system subjected to offset impact loading”,
Satyanarayana Kokkula, 2005:193, ISBN 82-471-7280-1 (printed version), ISBN 82-471-7279-8 (electronic version), ISSN 1503-8181.
- “Control of Chloride Penetration into Concrete Structures at Early Age”,
Guofei Liu, 2006:46, ISBN 82-471-7838-9 (printed version), ISBN 82-471-7837-0 (electronic version), ISSN 1503-8181.
- “Modelling of Welded Thin-Walled Aluminium Structures”,
Ting Wang, 2006:78, ISBN 82-471-7907-5 (printed version), ISBN 82-471-7906-7 (electronic version), ISSN 1503-8181.
- ”Time-variant reliability of dynamic systems by importance sampling and probabilistic analysis of ice loads”,
Anna Ivanova Olsen, 2006:139, ISBN 82-471-8041-3 (printed version), ISBN 82-471-8040-5 (electronic version), ISSN 1503-8181.
- “Fatigue life prediction of an aluminium alloy automotive component using finite element analysis of surface topography”,
Sigmund Kyrre Ås, 2006:25, ISBN 82-471-7791-9 (printed version), ISBN 82-471-7791-9 (electronic version), ISSN 1503-8181.
- ”Constitutive models of elastoplasticity and fracture for aluminium alloys under strain path change”,
Dasharatha Achani, 2006:76, ISBN 82-471-7903-2 (printed version), ISBN 82-471-7902-4 (electronic version), ISSN 1503-8181.
- “Simulations of 2D dynamic brittle fracture by the Element-free Galerkin method and linear fracture mechanics”,
Tommy Karlsson, 2006:125, ISBN 82-471-8011-1 (printed version), ISBN 82-471-8010-3 (electronic version), ISSN 1503-8181.
- “Penetration and Perforation of Granite Targets by Hard Projectiles”,
Chong Chiang Seah, 2006:188, ISBN 82-471-8150-9 (printed version), ISBN 82-471-8149-5 (electronic version), ISSN 1503-8181.

“Deformations, strain capacity and cracking of concrete in plastic and early hardening phases”,

Tor Arne Hammer, 2007:234, ISBN 978-82-471-5191-4 (printed version), ISBN 978-82-471-5207-2 (electronic version), ISSN 1503-8181.

“Crashworthiness of dual-phase high-strength steel: Material and Component behaviour”, Venkatapathi Tarigopula, 2007:230, ISBN 82-471-5076-4 (printed version), ISBN 82-471-5093-1 (electronic version), ISSN 1503-8181.

“Fibre reinforcement in load carrying concrete structures”,

Åse Lyslo Døssland, 2008:50, ISBN 978-82-471-6910-0 (printed version), ISBN 978-82-471-6924-7 (electronic version), ISSN 1503-8181.

“Low-velocity penetration of aluminium plates”,

Frode Grytten, 2008:46, ISBN 978-82-471-6826-4 (printed version), ISBN 978-82-471-6843-1 (electronic version), ISSN 1503-8181.

“Robustness studies of structures subjected to large deformations”,

Ørjan Fyllingen, 2008:24, ISBN 978-82-471-6339-9 (printed version), ISBN 978-82-471-6342-9 (electronic version), ISSN 1503-8181.

“Constitutive modelling of morsellised bone”,

Knut Birger Lunde, 2008:92, ISBN 978-82-471-7829-4 (printed version), ISBN 978-82-471-7832-4 (electronic version), ISSN 1503-8181.

“Experimental Investigations of Wind Loading on a Suspension Bridge Girder”,

Bjørn Isaksen, 2008:131, ISBN 978-82-471-8656-5 (printed version), ISBN 978-82-471-8673-2 (electronic version), ISSN 1503-8181.

“Cracking Risk of Concrete Structures in The Hardening Phase”,

Guomin Ji, 2008:198, ISBN 978-82-471-1079-9 (printed version), ISBN 978-82-471-1080-5 (electronic version), ISSN 1503-8181.

“Modelling and numerical analysis of the porcine and human mitral apparatus”,

Victorien Emile Prot, 2008:249, ISBN 978-82-471-1192-5 (printed version), ISBN 978-82-471-1193-2 (electronic version), ISSN 1503-8181.

“Strength analysis of net structures”,

Heidi Moe, 2009:48, ISBN 978-82-471-1468-1 (printed version), ISBN 978-82-471-1469-8 (electronic version), ISSN 1503-8181.

“Numerical analysis of ductile fracture in surface cracked shells”,

Espen Berg, 2009:80, ISBN 978-82-471-1537-4 (printed version), ISBN 978-82-471-1538-1 (electronic version), ISSN 1503-8181.

“Subject specific finite element analysis of bone – for evaluation of the healing of a leg lengthening and evaluation of femoral stem design”,

Sune Hansborg Pettersen, 2009:99, ISBN 978-82-471-1579-4 (printed version), ISBN 978-82-471-1580-0 (electronic version), ISSN 1503-8181.

“Evaluation of fracture parameters for notched multi-layered structures”,

Lingyun Shang, 2009:137, ISBN 978-82-471-1662-3 (printed version), ISBN 978-82-471-1663-0 (electronic version), ISSN 1503-8181.

“Modelling of Dynamic Material Behaviour and Fracture of Aluminium Alloys for Structural Applications”

Yan Chen, 2009:69, ISBN 978-82-471-1515-2 (printed version), ISBN 978-82 471-1516-9 (electronic version), ISSN 1503-8181.

“Nanomechanics of polymer and composite particles”

Jiaying He 2009:213, ISBN 978-82-471-1828-3 (printed version), ISBN 978-82-471-1829-0 (electronic version), ISSN 1503-8181.

“Mechanical properties of clear wood from Norway spruce”

Kristian Berbom Dahl 2009:250, ISBN 978-82-471-1911-2 (printed version) ISBN 978-82-471-1912-9 (electronic version), ISSN 1503-8181.

“Modeling of the degradation of TiB₂ mechanical properties by residual stresses and liquid Al penetration along grain boundaries”

Micol Pezzotta 2009:254, ISBN 978-82-471-1923-5 (printed version) ISBN 978-82-471-1924-2 (electronic version) ISSN 1503-8181.

“Effect of welding residual stress on fracture”

Xiabo Ren 2010:77, ISBN 978-82-471-2115-3 (printed version) ISBN 978-82-471-2116-0 (electronic version), ISSN 1503-8181.

“Pan-based carbon fiber as anode material in cathodic protection system for concrete structures”

Mahdi Chini 2010:122, ISBN 978-82-471-2210-5 (printed version) ISBN 978-82-471-2213-6 (electronic version), ISSN 1503-8181.

“Structural Behaviour of deteriorated and retrofitted concrete structures”

Irina Vasililjeva Sæther 2010:171, ISBN 978-82-471-2315-7 (printed version) ISBN 978-82-471-2316-4 (electronic version) ISSN 1503-8181.

“Prediction of local snow loads on roofs”

Vivian Meløysund 2010:247, ISBN 978-82-471-2490-1 (printed version) ISBN 978-82-471-2491-8 (electronic version) ISSN 1503-8181.

“Behaviour and modelling of polymers for crash applications”

Virgile Delhay 2010:251, ISBN 978-82-471-2501-4 (printed version) ISBN 978-82-471-2502-1 (electronic version) ISSN 1503-8181.

“Blended cement with reduced CO₂ emission – Utilizing the Fly Ash-Limestone Synergy”,
Klaartje De Weerd 2011:32, ISBN 978-82-471-2584-7 (printed version) ISBN 978-82-471-2584-4 (electronic version) ISSN 1503-8181.

“Chloride induced reinforcement corrosion in concrete” Concept of critical chloride content – methods and mechanisms.
Ueli Angst 2011:113, ISBN 978-82-471-2769-9 (printed version) ISBN 978-82-471-2763-6 (electronic version) ISSN 1503-8181.

“A thermo-electric-Mechanical study of the carbon anode and contact interface for Energy savings in the production of aluminium”.
Dag Herman Andersen 2011:157, ISBN 978-82-471-2859-6 (printed version) ISBN 978-82-471-2860-2 (electronic version) ISSN 1503-8181.

“Structural Capacity of Anchorage Ties in Masonry Veneer Walls Subjected to Earthquake”. The implications of Eurocode 8 and Eurocode 6 on a typical Norwegian veneer wall.
Ahmed Mohamed Yousry Hamed 2011:181, ISBN 978-82-471-2911-1 (printed version) ISBN 978-82-471-2912-8 (electronic ver.) ISSN 1503-8181.

“Work-hardening behaviour in age-hardenable Al-Zn-Mg(-Cu) alloys”.
Ida Westermann , 2011:247, ISBN 978-82-471-3056-8 (printed ver.) ISBN 978-82-471-3057-5 (electronic ver.) ISSN 1503-8181.

“Behaviour and modelling of selfpiercing riveted connections using aluminium rivets”.
Nguyen-Hieu Hoang, 2011:266, ISBN 978-82-471-3097-1 (printed ver.) ISBN 978-82-471-3099-5 (electronic ver.) ISSN 1503-8181.

“Fibre reinforced concrete”.
Sindre Sandbakk, 2011:297, ISBN 978-82-471-3167-1 (printed ver.) ISBN 978-82-471-3168-8 (electronic ver) ISSN 1503:8181.

“Dynamic behaviour of cablesupported bridges subjected to strong natural wind”.
Ole Andre Øiseth, 2011:315, ISBN 978-82-471-3209-8 (printed ver.) ISBN 978-82-471-3210-4 (electronic ver.) ISSN 1503-8181.

“Constitutive modeling of solargrade silicon materials”
Julien Cochar, 2011:307, ISBN 978-82-471-3189-3 (printed ver). ISBN 978-82-471-3190-9 (electronic ver.) ISSN 1503-8181.

“Constitutive behavior and fracture of shape memory alloys”
Jim Stian Olsen, 2012:57, ISBN 978-82-471-3382-8 (printed ver.) ISBN 978-82-471-3383-5 (electronic ver.) ISSN 1503-8181.

“Field measurements in mechanical testing using close-range photogrammetry and digital image analysis”

Egil Fagerholt, 2012:95, ISBN 978-82-471-3466-5 (printed ver.) ISBN 978-82-471-3467-2 (electronic ver.) ISSN 1503-8181.

“Towards a better understanding of the ultimate behaviour of lightweight aggregate concrete in compression and bending”,

Håvard Nedrelid, 2012:123, ISBN 978-82-471-3527-3 (printed ver.) ISBN 978-82-471-3528-0 (electronic ver.) ISSN 1503-8181.

“Numerical simulations of blood flow in the left side of the heart”

Sigrid Kaarstad Dahl, 2012:135, ISBN 978-82-471-3553-2 (printed ver.) ISBN 978-82-471-3555-6 (electronic ver.) ISSN 1503-8181.

“Moisture induced stresses in glulam”

Vanessa Angst-Nicollier, 2012:139, ISBN 978-82-471-3562-4 (printed ver.) ISBN 978-82-471-3563-1 (electronic ver.) ISSN 1503-8181.

“Biomechanical aspects of distraction osteogenesis”

Valentina La Russa, 2012:250, ISBN 978-82-471-3807-6 (printed ver.) ISBN 978-82-471-3808-3 (electronic ver.) ISSN 1503-8181.

“Ductile fracture in dual-phase steel. Theoretical, experimental and numerical study”

Gaute Gruben, 2012:257, ISBN 978-82-471-3822-9 (printed ver.) ISBN 978-82-471-3823-6 (electronic ver.) ISSN 1503-8181.

“Damping in Timber Structures”

Nathalie Labonnote, 2012:263, ISBN 978-82-471-3836-6 (printed ver.) ISBN 978-82-471-3837-3 (electronic ver.) ISSN 1503-8181.

“Biomechanical modeling of fetal veins: The umbilical vein and ductus venosus bifurcation”

Paul Roger Leinan, 2012:299, ISBN 978-82-471-3915-8 (printed ver.) ISBN 978-82-471-3916-5 (electronic ver.) ISSN 1503-8181.

“Large-Deformation behaviour of thermoplastics at various stress states”

Anne Serine Ognedal, 2012:298, ISBN 978-82-471-3913-4 (printed ver.) ISBN 978-82-471-3914-1 (electronic ver.) ISSN 1503-8181.

“Hardening accelerator for fly ash blended cement”

Kien Dinh Hoang, 2012:366, ISBN 978-82-471-4063-5 (printed ver.) ISBN 978-82-471-4064-2 (electronic ver.) ISSN 1503-8181.

“From molecular structure to mechanical properties”

Jianyang Wu, 2013:186, ISBN 978-82-471-4485-5 (printed ver.) ISBN 978-82-471-4486-2 (electronic ver.) ISSN 1503-8181.

- “Experimental and numerical study of hybrid concrete structures”
Linn Grepstad Nes, 2013:259, ISBN 978-82-471-4644-6 (printed ver.) ISBN 978-82-471-4645-3 (electronic ver.) ISSN 1503-8181.
- “Mechanics of ultra-thin multi crystalline silicon wafers”
Saber Saffar, 2013:199, ISBN 978-82-471-4511-1 (printed ver.) ISBN 978-82-471-4513-5 (electronic ver.) ISSN 1503-8181.
- “Through process modelling of welded aluminium structures”
Anizahyati Alisibramulisi, 2013:325, ISBN 978-82-471-4788-7 (printed ver.) ISBN 978-82-471-4789-4 (electronic ver.) ISSN 1503-8181.
- “Combined blast and fragment loading on steel plates”
Knut Gaarder Rakvåg, 2013:361, ISBN 978-82-471-4872-3 (printed ver.) ISBN 978-82-4873-0 (electronic ver.) ISSN 1503-8181.
- “Characterization and modelling of the anisotropic behaviour of high-strength aluminium alloy”
Marion Fourmeau, 2014:37, ISBN 978-82-326-0008-3 (printed ver.) ISBN 978-82-326-0009-0 (electronic ver.) ISSN 1503-8181.
- “Behaviour of threaded steel fasteners at elevated deformation rates”
Henning Fransplass, 2014:65, ISBN 978-82-326-0054-0 (printed ver.) ISBN 978-82-326-0055-7 (electronic ver.) ISSN 1503-8181.
- “Sedimentation and Bleeding”
Ya Peng, 2014:89, ISBN 978-82-326-0102-8 (printed ver.) ISBN 978-82-326-0103-5 (electric ver.) ISSN 1503-8181.
- “Impact against X65 offshore pipelines”
Martin Kristoffersen, 2014:362, ISBN 978-82-326-0636-8 (printed ver.) ISBN 978-82-326-0637-5 (electronic ver.) ISSN 1503-8181.
- “Formability of aluminium alloy subjected to prestrain by rolling”
Dmitry Vysochinskiy, 2014:363, ISBN 978-82-326-0638-2 (printed ver.) ISBN 978-82-326-0639-9 (electronic ver.) ISSN 1503-8181.
- “Experimental and numerical study of Yielding, Work-Hardening and anisotropy in textured AA6xxx alloys using crystal plasticity models”
Mikhail Khadyko, 2015:28, ISBN 978-82-326-0724-2 (printed ver.) ISBN 978-82-326-0725-9 (electronic ver.) ISSN 1503-8181.
- “Behaviour and Modelling of AA6xxx Aluminium Alloys Under a Wide Range of Temperatures and Strain Rates”
Vincent Vilamosa, 2015:63, ISBN 978-82-326-0786-0 (printed ver.) ISBN 978-82-326-0787-7 (electronic ver.) ISSN 1503-8181.

- “A Probabilistic Approach in Failure Modelling of Aluminium High Pressure Die-Castings”
Octavian Knoll, 2015:137, ISBN 978-82-326-0930-7 (printed ver.) ISBN 978-82-326-0931-4 (electronic ver.) ISSN 1503-8181.
- “Ice Abrasion on Marine Concrete Structures”
Egil Møen, 2015:189, ISBN 978-82-326-1034-1 (printed ver.) ISBN 978-82-326-1035-8 (electronic ver.) ISSN 1503-8181.
- “Fibre Orientation in Steel-Fibre-Reinforced Concrete”
Giedrius Zirgulis, 2015:229, ISBN 978-82-326-1114-0 (printed ver.) ISBN 978-82-326-1115-7 (electronic ver.) ISSN 1503-8181.
- “Effect of spatial variation and possible interference of localised corrosion on the residual capacity of a reinforced concrete beam”
Mohammad Mahdi Kioumars, 2015:282, ISBN 978-82-326-1220-8 (printed ver.) ISBN 978-82-1221-5 (electronic ver.) ISSN 1503-8181.
- “The role of concrete resistivity in chloride-induced macro-cell corrosion”
Karla Horbostel, 2015:324, ISBN 978-82-326-1304-5 (printed ver.) ISBN 978-82-326-1305-2 (electronic ver.) ISSN 1503-8181.
- “Flowable fibre-reinforced concrete for structural applications”
Elena Vidal Sarmiento, 2015:335, ISBN 978-82-326-1324-3 (printed ver.) ISBN 978-82-326-1325-0 (electronic ver.) ISSN 1503-8181.
- “Development of chushed sand for concrete production with microproportioning”
Rolands Cepuritis, 2016:19, ISBN 978-82-326-1382-3 (printed ver.) ISBN 978-82-326-1383-0 (electronic ver.) ISSN 1503-8181.
- “Withdrawal properties of threaded rods embedded in glued-laminated timber elements”
Haris Stamatopoulos, 2016:48, ISBN 978-82-326-1436-3 (printed ver.) ISBN 978-82-326-1437-0 (electronic ver.) ISSN 1503-8181.
- “An Experimental and numerical study of thermoplastics at large deformation”
Marius Andersen, 2016:191, ISBN 978-82-326-1720-3 (printed ver.) ISBN 978-82-326-1721-0 (electronic ver.) ISSN 1503-8181.
- “Modeling and Simulation of Ballistic Impact”
Jens Kristian Holmen, 2016:240, ISBN 978-82-326-1818-7 (printed ver.) ISBN 978-82-326-1819-4 (electronic ver.) ISSN 1503-8181.
- “Early age crack assessment of concrete structures”
Anja B. Estensen Klausen, 2016:256, ISBN 978-82-326-1850-7 (printed ver.) ISBN 978-82-326-1851-4 (electronic ver.) ISSN 1503-8181.

- “Uncertainty quantification and sensitivity analysis for cardiovascular models”
Vinzenz Gregor Eck, 2016:234, ISBN 978-82-326-1806-4 (printed ver.) ISBN 978-82-326-1807-1 (electronic ver.) ISSN 1503-8181.
- “Dynamic behaviour of existing and new railway catenary systems under Norwegian conditions”
Petter Røe Nåvik, 2016:298, ISBN 978-82-326-1935-1 (printed ver.) ISBN 978-82-326-1934-4 (electronic ver.) ISSN 1503-8181.
- “Mechanical behaviour of particle-filled elastomers at various temperatures”
Arne Iiseng, 2016:295, ISBN 978-82-326-1928-3 (printed ver.) ISBN 978-82-326-1929-0 (electronic ver.) ISSN 1503-8181.
- “Nanotechnology for Anti-Icing Application”
Zhiwei He, 2016:348, ISBN 978-82-326-2038-8 (printed ver.) ISBN 978-82-326-2019-5 (electronic ver.) ISSN 1503-8181.
- “Conduction Mechanisms in Conductive Adhesives with Metal-Coated Polymer Spheres”
Sigurd Rolland Pettersen, 2016:349, ISBN 978-326-2040-1 (printed ver.) ISBN 978-82-326-2041-8 (electronic ver.) ISSN 1503-8181.
- “The interaction between calcium lignosulfonate and cement”
Alessia Colombo, 2017:20, ISBN 978-82-326-2122-4 (printed ver.) ISBN 978-82-326-2123-1 (electronic ver.) ISSN 1503-8181.
- “Behaviour and Modelling of Flexible Structures Subjected to Blast Loading”
Vegard Aune, 2017:101, ISBN 978-82-326-2274-0 (printed ver.) ISBN 978-82-326-2275-7 (electronic ver.) ISSN 1503-8181.
- “Behaviour of steel connections under quasi-static and impact loading”
Erik Løhre Grimsmo, 2017:159, ISBN 978-82-326-2390-7 (printed ver.) ISBN 978-82-326-2391-4 (electronic ver.) ISSN 1503-8181.
- “An experimental and numerical study of cortical bone at the macro and Nano-scale”
Masoud Ramenzanzadehkoldeh, 2017:208, ISBN 978-82-326-2488-1 (printed ver.) ISBN 978-82-326-2489-8 (electronic ver.) ISSN 1503-8181.
- “Optoelectrical Properties of a Novel Organic Semiconductor: 6,13-Dichloropentacene”
Mao Wang, 2017:130, ISBN 978-82-326-2332-7 (printed ver.) ISBN 978-82-326-2333-4 (electronic ver.) ISSN 1503-8181.
- “Core-shell structured microgels and their behavior at oil and water interface”
Yi Gong, 2017:182, ISBN 978-82-326-2436-2 (printed ver.) ISBN 978-82-326-2437-9 (electronic ver.) ISSN 1503-8181.

- “Aspects of design of reinforced concrete structures using nonlinear finite element analyses”
Morten Engen, 2017:149, ISBN 978-82-326-2370-9 (printed ver.) ISBN 978-82-326-2371-6 (electronic ver.) ISSN 1503-8181.
- “Numerical studies on ductile failure of aluminium alloys”
Lars Edvard Dæhli, 2017:284, ISBN 978-82-326-2636-6 (printed ver.) ISBN 978-82-326-2637-3 (electronic ver.) ISSN 1503-8181.
- “Modelling and Assessment of Hydrogen Embrittlement in Steels and Nickel Alloys”
Haiyang Yu, 2017:278, ISBN 978-82-326-2624-3 (printed. ver.) ISBN 978-82-326-2625-0 (electronic ver.) ISSN 1503-8181.
- “Network arch timber bridges with light timber deck on transverse crossbeams”
Anna Weronika Ostrycharczyk, 2017:318, ISBN 978-82-326-2704-2 (printed ver.) ISBN 978-82-326-2705-9 (electronic ver.) ISSN 1503-8181.
- “Splicing of Large Glued Laminated Timber Elements by Use of Long Threaded Rods”
Martin Cepelka, 2017:320, ISBN 978-82-326-2708-0 (printed ver.) ISBN 978-82-326-2709-7 (electronic ver.) ISSN 1503-8181.
- “Thermomechanical behaviour of semi-crystalline polymers: experiments, modelling and simulation”
Joakim Johnsen, 2017:317, ISBN 978-82-326-2702-8 (printed ver.) ISBN 978-82-326-2703-5 (electronic ver.) ISSN 1503-8181.
- “Small-Scale Plasticity under Hydrogen Environment”
Kai Zhao, 2017:356, ISBN 978-82-326-2782-0 (printed ver.) ISBN 978-82-326-2783-7 (electronic er.) ISSN 1503-8181.
- “Risk and Reliability Based Calibration of Structural Design Codes”
Michele Baravalle, 2017:342, ISBN 978-82-326-2752-3 (printed ver.) ISBN 978-82-326-2753-0 (electronic ver.) ISSN 1503-8181.
- “Dynamic behaviour of floating bridges exposed to wave excitation”
Knut Andreas Kvåle, 2017:365, ISBN 978-82-326-2800-1 (printed ver.) ISBN 978-82-326-2801-8 (electronic ver.) ISSN 1503-8181.
- “Dolomite calcined clay composite cement – hydration and durability”
Alisa Lydia Machner, 2018:39, ISBN 978-82-326-2872-8 (printed ver.). ISBN 978-82-326-2873-5 (electronic ver.) ISSN 1503-8181.
- “Modelling of the self-excited forces for bridge decks subjected to random motions: an experimental study”
Bartosz Siedziako, 2018:52, ISBN 978-82-326-2896-4 (printed ver.). ISBN 978-82-326-2897-1 (electronic ver.) ISSN 1503-8181.

“A probabilistic-based methodology for evaluation of timber facade constructions”
Klodian Gradeci, 2018:69, ISBN 978-82-326-2928-2 (printed ver.) ISBN 978-82-326-2929-9 (electronic ver.) ISSN 1503-8181.

“Behaviour and modelling of flow-drill screw connections”
Johan Kolstø Sønstabø, 2018:73, ISBN 978-82-326-2936-7 (printed ver.) ISBN 978-82-326-2937-4 (electronic ver.) ISSN 1503-8181.

“Full-scale investigation of the effects of wind turbulence characteristics on dynamic behavior of long-span cable-supported bridges in complex terrain”
Aksel Fenerci, 2018 100, ISBN 9978-82-326-2990-9 (printed ver.) ISBN 978-82-326-2991-6 (electronic ver.) ISSN 1503-8181.

“Modeling and simulation of the soft palate for improved understanding of the obstructive sleep apnea syndrome”
Hongliang Liu, 2018:101, ISBN 978-82-326-2992-3 (printed ver.) ISBN 978-82-326-2993-0 (electronic ver.) ISSN 1503-8181.

“Long-term extreme response analysis of cable-supported bridges with floating pylons subjected to wind and wave loads”
Yuwang Xu, 2018:229, ISBN 978-82-326-3248-0 (printed ver.) ISBN 978-82-326-3249-7 (electronic ver.) ISSN 1503-8181.

“Reinforcement corrosion in carbonated fly ash concrete”
Andres Belda Revert, 2018:230, ISBN 978-82-326-3250-3 (printed ver.) ISBN 978-82-326-3251-0 (electronic ver.) ISSN 1503-8181.

“Direct finite element method for nonlinear earthquake analysis of concrete dams including dam-water-foundation rock interaction”
Arnkjell Løkke, 2018:252, ISBN 978-82-326-3294-7 (printed ver.) ISBN 978-82-326-3295-4 (electronic ver.) ISSN 1503-8181.

“Electromechanical characterization of metal-coated polymer spheres for conductive adhesives”
Molly Strimbeck Bazilchuk, 2018:295, ISBN 978-82-326-3380-7 (printed. ver.) ISBN 978-82-326-3381-4 (electrical ver.) ISSN 1503-8181.

“Determining the tensile properties of Artic materials and modelling their effects on fracture”
Shengwen Tu, 2018:269, ISBN 978-82-326-3328-9 (printed ver.) ISBN 978-82-326-3329-6 (electronic ver.) ISSN 1503-8181.

“Atomistic Insigh into Tranportation of Nanofluid in Ultra-confined Channel”
Xiao Wang, 2018:334, ISBN978-82-326-3456-9 (printed ver.) ISBN 978-82-326-3457-6 (electronic ver.) ISSN 1503-8181.

“An experimental and numerical study of the mechanical behaviour of short glass-fibre reinforced thermoplastics”.

Jens Petter Henrik Holmstrøm, 2019:79, ISBN 978-82-326-3760-7 (printed ver.) ISBN 978-82-326-3761-4 (electronic ver.) ISSN 1503-8181.

“Uncertainty quantification and sensitivity analysis informed modeling of physical systems”

Jacob Sturdy, 2019:115, ISBN 978-82-326-3828-4 (printed ver.) ISBN 978-82-326-3829-1 (electric ver.) ISSN 1503-8181.

“Load model of historic traffic for fatigue life estimation of Norwegian railway bridges”

Gunnstein T. Frøseth, 2019:73, ISBN 978-82-326-3748-5 (printed ver.) ISBN 978-82-326-3749-2 (electronic ver.) ISSN 1503-8181.

“Force identification and response estimation in floating and suspension bridges using measured dynamic response”

Øyvind Wiig Petersen, 2019:88, ISBN 978-82-326-3778-2 (printed ver.) ISBN 978-82-326-3779-9 (electronic ver.) ISSN 1503-8181.

“Consistent crack width calculation methods for reinforced concrete elements subjected to 1D and 2D stress states”

Reignard Tan, 2019:147, ISBN 978-82-326-3892-5 (printed ver.) ISBN 978-82-326-3893-2 (electronic ver.) ISSN 1503-8181.

“Nonlinear static and dynamic isogeometric analysis of slender spatial and beam type structures”

Siv Bente Raknes, 2019:181, ISBN 978-82-326-3958-8 (printed ver.) ISBN 978-82-326-3959-5 (electronic ver.) ISSN 1503-8181.

“Experimental study of concrete-ice abrasion and concrete surface topography modification”

Guzel Shamsutdinova, 2019:182, ISBN978-82-326-3960-1 (printed ver.) ISBN 978-82-326-3961-8 (electronic ver.) ISSN 1503-8181.

“Wind forces on bridge decks using state-of-the art FSI methods”

Tore Andreas Helgedagsrud, 2019:180, ISBN 978-82-326-3956-4 (printed ver.) ISBN 978-82-326-3957-1 (electronic ver.) ISSN 1503-8181.

“Numerical Study on Ductile-to-Brittle Transition of Steel and its Behavior under Residual Stresses”

Yang Li, 2019:227, ISBN 978-82-326-4050-8 (printed ver.) ISBN 978-82-326-4015-5 (electronic ver.) ISSN 1503-8181.

“Micromechanical modelling of ductile fracture in aluminium alloys”

Bjørn Håkon Frodal, 2019:253, ISBN 978-82-326-4102-4 (printed ver.) ISBN 978-82-326-4103-1 (electronic ver.) ISSN 1503-8181.

“Monolithic and laminated glass under extreme loading: Experiments, modelling and simulations”

Karoline Osnes, 2019:304, ISBN 978-82-326-4204-5 (printed ver.) ISBN 978-82-326-4205-2 (electronic ver.) ISSN 1503-8181.

“Plastic flow and fracture of isotropic and anisotropic 6000-series aluminium alloys: Experiments and numerical simulations “

Susanne Thomesen, 2019:312, ISBN 978-82-326-4220-5 (printed ver.), ISBN 978-82-326-4221-2 (electronic ver.) ISSN 1503-8181

“Stress-laminated timber decks in bridges”

Francesco Mirko Massaro, 2019:346, ISBN 978-82-326-4288-5 (printed ver.), ISBN 978-82-326-4289-2 (electronic ver.) ISSN 1503-8181

“Connections between steel and aluminium using adhesive bonding combined with self-piercing riveting: Testing, modelling and analysis”

Matthias Reil, 2019:319, ISBN 978-82-326-4234-2 (printed ver.), ISBN 978-82-326-4235-9 (electronic ver.) ISSN 1503-8181

“Designing Polymeric Icephobic Materials”

Yizhi Zhuo, 2019:345, ISBN 978-82-326-4286-1 (printed ver.), ISBN 978-82-326-4287-8 (electronic ver.) ISSN 1503-8181

“Fundamental Mechanisms of Ice Adhesion”

Rønneberg, Sigrid 2020:87, ISBN 978-82-326-4527-8 (printed version) ISBN 978-82-326-4524-5 (electronic version) ISSN 1503-8181

“Mechanical modeling of the polymeric coating on a subsea pipeline” Vestrum, Ole

2020:105, ISBN 978-82-326-4562-6 (printed version) ISBN 978-82-4563-3 (electronic version) ISSN 1503-8181

“Conceptual form-finding in structural engineering” Marcin Luczkowski 2020: “Self-assembled superstructures of magnetic nanoparticles: advanced nanofabrication and enhanced mechanical properties”

Verner Håkonsen 2020:271, ISBN 978-82-326-4890-0 (printed version) ISBN 978-82-326-4891-7 (electronic version) ISSN 1503-8181

“Micromechanical modelling of fracture in ductile alloys with applications to high-strength steel”

Sondre Bergo 2020:313, ISBN 978-82-326-4974-7 (printed version) ISBN 978-82-326-4975-4 (electronic version) ISSN 1503-8181

- “Fracture in wood of Norway spruce - Experimental and numerical study”
Katarzyna Ostapska 2020:314, ISBN 978-82-326-4976-1 (printed version) ISBN 978- 82-326-4977-8 (electronic version) ISSN 1503-8181
- “Dynamic anti-icing surfaces (DAIS)” Feng Wang 2020:330 ISBN 978-82-326-5006-4 (printed version) ISBN 978-82-326-5007-1 (electronic version) ISSN 1503-8181
- “«Multiaxial Fatigue analysis of offshore mooring chains, considering the effects of residual stresses and corrosion pits» Ershad P. Zarandi 2020:337 ISBN 978-82-326-5020-0 (printed version) ISBN 978-82-326-5021-7 (electronic version) ISSN 1503-8181
- “Production and documentation of frost durable high-volume fly ash concrete: air entrainment, cracking and scaling in performance testing” Andrei Shpak 2020:366 ISBN 978-82-326-5078-1 (printed version) ISBN 978-82-326-5079-8 (electronic version) ISSN 1503-8181
- “Physics-based and data-driven reduced-order blood flow models: Applications to coronary artery disease diagnostics” Fredrik Eikeland Fossan 2020:362 ISBN 978-82-326-5070-5 (printed version) ISBN 978-82-326-5071-2 (electronic version) ISSN 1503-8181
- “Multi-scale modelling and simulation of ductile failure in aluminium structures” Henrik Granum 2020:374 ISBN 978-82-326-5094-1 (printed version) ISBN 978-82-326-5095-8 (electronic version) ISSN 1503-8181
- “Testing and modelling of multi-material joints” Jon Fredrick Berntsen 2020:368 ISBN 978-82-326-5082-8 (printed version) ISBN 978-82-326-5083-5 ISSN 1503-8181
- “Heuristic models for wear prediction and dynamic-based condition monitoring techniques in pantograph-catenary interaction” Stefano Derosa 2020:381 ISBN 978-82-326-5108-5 (printed version) ISBN 978-82-326-5109-2 (electronic version) ISSN 1503-8181
- “Experimental and numerical study of dilation in mineral filled PVC” Sindre Nordmark Olufsen 2020:388 ISBN 978-82-326-5122-1 (printed version) ISBN 978-82-326-5123-8 (electronic version) ISSN 1503-8181
- “Residual stresses and dimensional deviation in metal additive manufacturing: prediction and mitigation methods” Li Sun 2020:411 ISBN 978-82-471-9600-7 (printed version) ISBN 978-82-471-9581-9 (electronic version) ISSN 1503-8181 (printed version) ISSN 2703-8084 (online version)

ISBN 978-82-471-9919-0 (printed ver.)
ISBN 978-82-471-9709-7 (electronic ver.)
ISSN 1503-8181 (printed ver.)
ISSN 2703-8084 (online ver.)



NTNU

Norwegian University of
Science and Technology